THE GEOLOGY AND GEOCHEMISTRY OF THE ARCHAEAN GRANITE-GREENSTONE TERRANE BETWEEN NELSPRUIT AND BUSHBUCKRIDGE, EASTERN TRANSVAAL

by

L.J. ROBB

A dissertation submitted to the Faculty of Science, University of the Witwatersrand, Johannesburg, for the Degree of Master of Science.

Johannesburg,
May, 1977.

FOR MY PARENTS

THE GEOLOGY AND GEOCHEMISTRY OF THE ARCHAEAN GRANITE-GREENSTONE TERRANE BETWEEN NELSPRUIT AND BUSHBUCKRIDGE, EASTERN TRANSVAAL

ABSTRACT

This study is concerned with an examination of the geology and geochemistry of the granitic terrane in the area between Nelspruit and Bushbuckridge, in the eastern Transvaal. This area, covering some 2500km^2, was mapped on a scale of 1:30 000 as well as being extensively sampled for the geochemical aspect of the study. In addition, the Barclay Vale Schist Belt, a small greenstone remnant occurring in the southwestern corner of the study area, was also mapped, on a scale of 1:10 000.

A brief description of the topography, climate and vegetation is presented as well as a summary of the previous work pertinent, both directly and indirectly, to the study area.

The geology of the Barclay Vale Schist Belt is described in detail in terms of the stratigraphic model obtained in the Barberton greenstone belt. The lithological succession in the Barclay Vale Schist Belt can be correlated with the "lower ultramafic unit" of the Onverwacht Group, Swaziland Supergroup.

The granitic terrane, which underlies most of the study area is comprised of six distinct granite types :-

(i) The Tonalite Gneisses and Migmatites.

(ii) The Nelspruit Migmatite and Gneiss Terrane.

(iii) The Nelspruit Porphyritic Granite

(iv) The Hebron Granodiorite

(v) The Cunning Moor Tonalite

(vi) The Mpageni Granite pluton

A description of each granite type is presented in terms of its field appearance, petrography and geochemical characteristics.

Geochronological work was carried out on three of the granite types mentioned above, namely the Nelspruit Porphyritic Granite, the Hebron Granodiorite and the Cunning Moor Tonalite. These preliminary results indicate that the Nelspruit Porphyritic Granite and the Hebron Granodiorite are broadly synchronous (approximately 3,2 b.y. old) whereas the Cunning Moor Tonalite is considerably younger than these two (2,8 b.y. old).

A semi-quantitative description of the relationships between topography and the chemical composition of granite types is presented by means of contour and polynomial trend surface maps. The contour maps indicate a broad correlation between the topography of the study area and the K_2O, Na_2O, Rb, Sr and Ba contents of the major granite types in the region. The polynomial trend surfaces indicate a roughly concentric or semi-concentric distribution of these elements over the study area.

The crystallization of the Nelspruit Porphyritic Granite is considered in terms of fractionation, a mechanism not commonly used to explain the formation of granitic bodies. The distribution of major and trace elements indicates that this granite cooled slowly allowing the crystallization of consecutive mineral phases to take place. It is envisaged that crystallization was initiated by an assemblage consisting of plagioclase and quartz with minor biotite, and that K-felspar was introduced on the liquidus only at an advanced stage of

crystallization.

A brief description is given of the post-granite geology of the study area. The field occurrence and geochemical analyses of mafic dykes and sills in the region are described. Suggestions regarding the tectonic implications of the dyke and sill distribution as well as the presence of large shear zones in the study area, are made.

Finally, the Archaean granitic terrane between Nelspruit and Bushbuckridge is described in terms of a model for the development of the sialic crust in this region. It is envisaged that early granites (emplaced prior to 3,2 b.y. ago) were, essentially mantle derived, whereas subsequent granites (emplaced later than 3,0 b.y. ago) were derived by reworking of pre-existing sialic crustal material.

TABLE OF CONTENTS

TABLE OF CONTENTS

CHAPTER 1

INTRODUCTION

CHAPTER 2

THE BARCLAY VALE SCHIST BELT

CHAPTER 3

THE GRANITES

CHAPTER 4

GEOCHEMICAL CONTOURING AND POLYNOMIAL TREND SURFACE ANALYSIS OF THE GRANITIC TERRANE BETWEEN NELSPRUIT AND BUSHBUCKRIDGE

CHAPTER 5

FRACTIONAL CRYSTALLIZATION IN THE NELSPRUIT PORPHYRITIC GRANITE AND THE EFFECTS ON ITS MAJOR AND TRACE ELEMENT GEOCHEMISTRY

CHAPTER 6

THE POST-GRANITE GEOLOGY OF THE AREA BETWEEN NELSPRUIT AND BUSHBUCKRIDGE

CHAPTER 1

INTRODUCTION

I. GENERAL STATEMENT

(a) Area of Investigation

This dissertation has been carried out under the auspices of the Geodynamics Project in South Africa and forms a contribution to that section of the project dealing with the evolution of the earth's crust on the cratons. In its broadest context the Geodynamics Project may be viewed as, " an international programme of res arch on the dynamics and dynamic history of the earth with emphasis on deep seated foundations of geological phenomena" (The Geodynamics Project in South Africa, 1975).

Participation of the Republic of South Africa in the Geodynamics Project has enabled a large number of earth scientists in this country to become involved in questions of fundamental importance, not only to South African geology, but to the global aspect of geological principles. In southern Africa this effort is subdivided into four sections :-

(i) The plate geodynamics of the Mesozoic and Cenozoic eras;

(ii) The geodynamics of Palaeozoic and Precambrian mobile belts;

(iii) The evolution of the earths crust on the cratons and,

(iv) a study of materials from the earth's mantle.

The working group concerned with the evolution of the earth's crust on the cratons has, as its study area, a strip of country in the eastern Transvaal (Figure I), which is largely underlain by granite with subordinate Archaean greenstone remnants. The Barberton Mountain Land itself,

has been the object of considerable study in the past, firstly, because of the early interest shown in it as a host to considerable mineral wealth and secondly because of the work done there as the result of the Upper Mantle Project (1964-1969). Since 1969 continued interest has been shown in the region by geologists associated with the Economic Geology Research Unit of the University of the Witwatersrand. Somewhat neglected in the overall picture of Archaean granite-greenstone evolution has been a detailed study of the granites that surround the Barberton greenstone belt, particularly to the north and west. The Geodynamics Project thus affords an ideal opportunity for earth scientists to study these granites in greater detail with a view to presenting a more balanced picture of Archaean crustal evolution.

The Geodynamics Project strip, outlined in Figure I, is being studied in detail in two areas: (i) The coordinator of the Barberton Geodynamics Project, Dr. C.R. Anhaeusser, is examining the southern portion of the study strip, particularly in the vicinity of Badplaas (Figure I). This area adjoins the southwestern extremity of the Barberton greenstone belt and consists of a complex assemblage of granites and mafic xenoliths. Detailed mapping of this complex granite-greenstone terrane is being undertaken in an attempt to define the geological relationships between granite and greenstone. (ii) The writer, for the purposes of this dissertation, was concerned with the northern portion of the study strip shown in hat hed ornamentation in Figure I. By contrast with the southern study region this area was mapped on a regional scale as it consists predominantly of granitic rock types and the main purpose of the investigation was aimed at a geochemical evaluation of the area.

(b) Aims of the Investigation

The aims and philosophy behind the work being

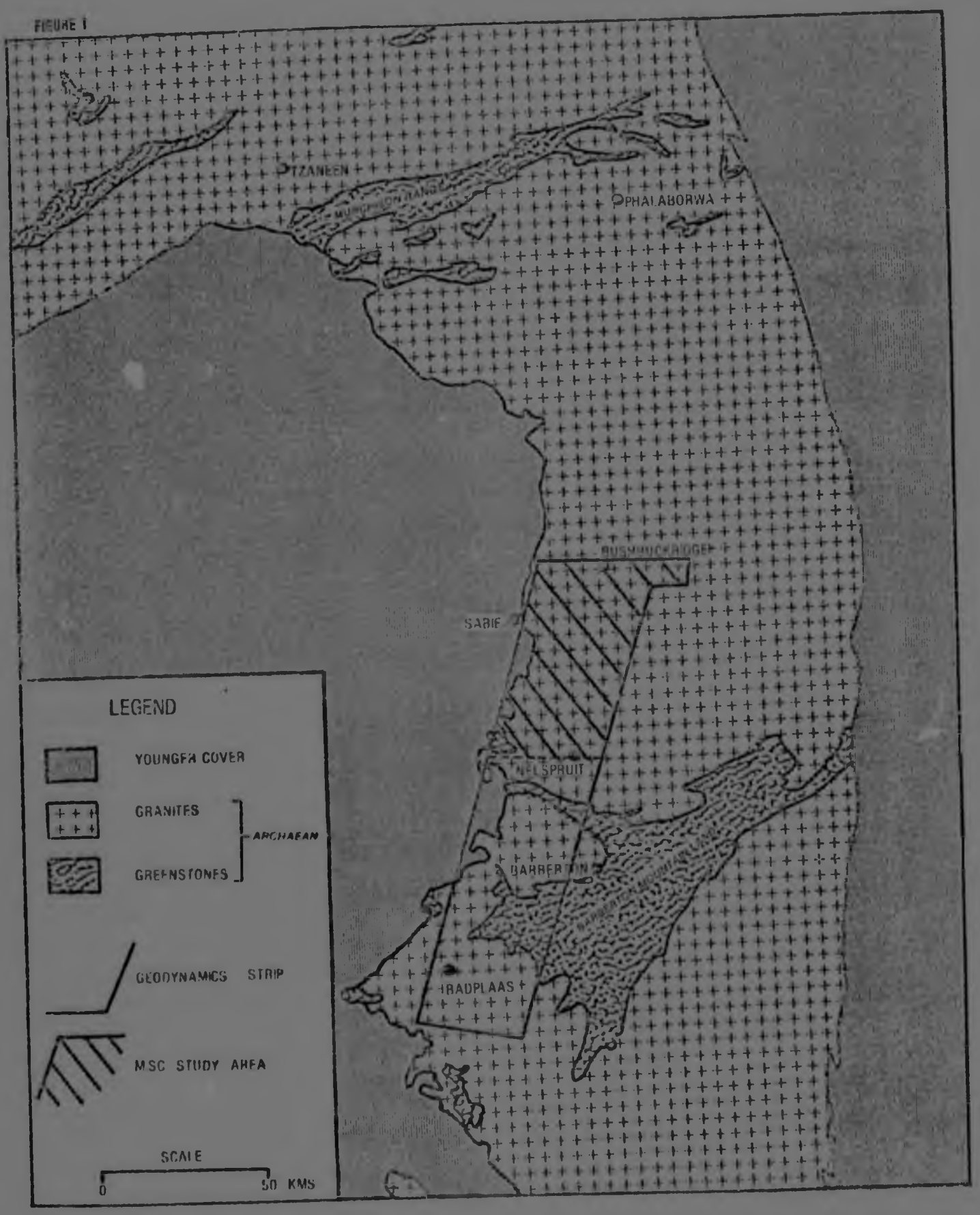

Figure 1. The Geodynamics Project area in the eastern Transvaal Lowveld. The hatched portion represents the study area dealt with in this dissertation.

carried out in the Barberton area for the Geodynamics Project is related to the current controversy regarding this, and other, Archaean granite-greenstone terranes. The controversy focuses attention on the origin, nature and subsequent evolution of the earth's primitive crust. Certain workers (Anhaeusser et al, 1969; Viljoen and Viljoen, 1969a, 1969d; Anhaeusser, 1973; Glikson, 1976a) have proposed models which involve the formation of an early simatic crust and the subsequent secular transformation thereof into one of sialic character. An opposing school of thought exists, however, which claims that the early crust was sialic in composition (Stowe, 1971; Lindley, 1973; Hunter, 1971a, 1974; Shaw, 1976). Useful resumés of this controversial state of affairs have been presented by Minnitt (1975), Anhaeusser (1975a) and Glikson (1976b).

The models presented by Anhaeusser (1973) and Hunter (1974), which provide opposing views on the nature and development of the Archaean crust in southern Africa were both formulated as the result of work carried out in and around the Barberton Mountain Land. Resolving the controversial state of knowledge in this area will require a detailed examination of granite-greenstone interaction, as well as an understanding of the nature and evolution of the processes involved in the accretion of the sialic crust. The work being undertaken in the southern portion of the study strip is designed to meet the first of these requirements whilst the area studied by the writer to the north, is designed to produce a contribution to the understanding of granites and their evolution. It is hoped that this two-fold approach will afford a clearer understanding of the mechanics behind the earth's early crustal development.

II. PHYSIOGRAPHY

(a) Relief

The most prominent relief feature of the area investigated by the writer is the north-south trending Transvaal Drakensberg Escarpment. This escarpment, which has an average altitude of approximately 1500m above mean sea level is made up of Proterozoic rocks of the Transvaal Supergroup. To the west of the study area the escarpment is formed by a thin, resistant capping of Black Reef Quartzite.

To the east of the escarpment the study area has been divided into two topographic sub-groups (Visser and Verwoerd, 1960). The western half has been termed "Middleveld" and is characterized by undulating hills and dome-shaped rocky platforms. Extending progressively eastwards towards the Kruger National Park, flatter and lower-lying country is encountered which is regarded as "Lowveld".

Representation of the topography of the region is presented in Figure 30 which is a computer drawn contour map of the spot heights of each of the sample localities in the study area. The differences between Middleveld and Lowveld are clearly demonstrated on this diagram by the 500m contour line. A further characteristic of the topography of the area is demonstrated in Figures 36, 37 and 38 which are, respectively, 1st, 2nd and 3rd degree polynomial trend surfaces of the topographic surface. In particular the 1st degree polynomial trend surface (Figure 36) shows the marked slope of land towards the east, trending away from the Transvaal Drakensberg Escarpment to the Lowveld of the Kruger National Park.

(b) Drainage

The drainage of the study area is influenced almost entirely by the Sabie and Crocodile river systems. Both these rivers rise on the escarpment and flow from west to east across the Middleveld and Lowveld (Figure 10).

The Crocodile River has a tortuous drainage course and, in geomorphological terms, can be described as existing

in a mature regime. Its two main tributaries in the study area are the Nelspruit and the Nsikazi Rivers, both of which flow in from the north (Figure 10). At Krokodilpoort the Crocodile River flows through a pronounced gorge where it bisects the Mpageni Granite pluton.

The Sabie River likewise occupies a mature regime for approximately 20km after dropping off the Transvaal Drakensberg Escarpment. However, as the river approaches the flatter and lower-lying country towards the Kruger National Park, its drainage course tends to straighten, particularly in the areas where prominent east-west trending dykes occur.

(c) Climate and Vegetation

Climatic and vegetation control in the study area is dependent largely on differences encountered in relief. Large areas of the Middleveld lie within the so-called "mist-belt", having an average annual rainfall in excess of 800mm, which renders these areas highly suitable for afforestation. The Lowveld areas have a lower average annual rainfall, usually approximately 600-700mm, and average temperatures are generally higher. Temperature data for three localities of differing relief across the region are presented in Table 1.

Table 1

AVERAGE DAILY TEMPERATURE (°C) FOR SOME LOCALITIES IN THE EASTERN TRANSVAAL
(after Visser and Verwoerd, 1960)

	Summer		Winter	
	Maximum	Minimum	Maximum	Minimum
SABIE (Escarpment)	26,2	15,3	20,7	-3,5
WHITE RIVER (Middleveld)	27,6	17,0	21,7	6,6
SKUKUZA (Lowveld)	32,3	19,4	25,5	5,8

Vegetation types in the study area are closely linked to the climatic zones. In the Middleveld the main vegetation type is forestry (mainly pine and gum) whereas the Lowveld is extensively grassed and sparsely wooded,principally with Acacia and Euphorbia type flora.

The Lowveld and Middleveld areas are also extensively cultivated, the area being one of considerable agricultural importance especially since the advent of irrigation. Tobacco, citrus, bananas, maize and vegetables form the main cash crops in the area, but a full range of sub-tropical fruits, including mangoes, avocado pears, and litchies, are also grown in the district.

III. SUMMARY OF PREVIOUS WORK RELATING TO THIS INVESTIGATION

This section discusses briefly the work that has been done in the past on Archaean granite-greenstone terranes, particularly in the eastern Transvaal. This discussion will deal mainly with granitic and associated rocks, as introductory remarks relating to greenstones will be presented in Chapter 2, which deals with the Barclay Vale Schist Belt.

(a) Very Early Work (for the period prior to 1942)

The first comprehensive account of granitic rocks in the eastern Transvaal stemmed from the work of Hall (1912) who described the rocks in and around the Murchison Range (Figure 1). Hall (1912) termed these granites the "Older Granite" to distinguish them from the granites of the Bushveld Igneous Complex or the Western Cape, and was thus the first to recognise the ancient nature of these rocks. Hall (1918) was also the first to attempt a sub-division of the so-called "Older Granite". In the area north of the Barberton Mountain Land he recognised a gneissic biotite-rich granite, well-

exposed in the vicinity of Nelspruit, and referred to it as the "Nelspruit Type". He also recognised a hornblende-bearing granite south of the Jamestown Hills which he termed the "De Kaap Valley Type". This granite was considered to be a separate, but possibly comagmatic, phase of the "Nelspruit Type" and the differences in texture and mineralogy between the two were attributed to extensive assimilation of mafic material by the former.

Du Toit (1926) used the name "Old Granite" for the granites of the eastern Transvaal and was the first investigator to suggest that these rocks formed part of a stable unit which he considered to be ".... the foundation rocks of South Africa" and which he termed the "Archaean Platform". It was as a result of the work of Du Toit that the granites of the eastern Transvaal came to be regarded as the "Basement" in the sense in which the term is used today.

Later work by van Eeden (1941) resulted in the "De Kaap Valley Type" being more specifically referred to as the "Kaap-graniet". Van Eeden concluded that the "Kaap-graniet" was distinctly older than the "Nelspruit Type" granite and suggested that it acted as a buttress against which rocks of the Swaziland Supergroup, in the Sheba Hills area, were folded during the emplacement of the "Nelspruit Type" granite. Van Eeden (1941) was also the first to report the presence of the "Mpageni Granite", a younger coarse-grained massive granite pluton which was clearly intrusive into the "Nelspruit Type" granite.

(b) Work Undertaken Between 1942 and 1960

During the period between 1942 and 1960 the main contributions of direct significance to the study area came from publications of the Geological Survey of South Africa.

Visser et al.(1956), now referred to van Eeden's "Kaap-graniet" as the "Kaap Valley Granite" and regarded this rock type as representing the acid phase of the "Jamestown Igneous Complex".

The "Nelspruit Type" granite and all associated granites of Post-Jamestown age were given a new name by these authors, that of "Archaean Granite and Gneiss". The reason for this change was to assign an age connotation to these rocks. The "Nelspruit Type" granite was also regarded by these authors, more specifically, as the "Nelspruit Granite".

Visser et al.(1956) also presented a detailed account of the Nelspruit and Mpageni Granites. The Nelspruit Granite, considered to be "... representative of the typical Archaean Granite of the Lowveld of the eastern Transvaal", was described as being characteristically medium-grained and biotite-rich, but coarse-grained and porphyritic in places. These authors described the primary structures within the Nelspruit Granite as "flow-layers" and "flow-lines" both varieties of which consist essentially of alternating bands of biotite-rich and biotite-free rock. The flow structures were attributed to compression during the emplacement of the granite. With regard to the origin of the Nelspruit Granite, Visser et al.(1956) maintained that it was not a primary magmatic derivative but the result of the progressive granitization of pre-existing, presumably mafic, rocks. They point out that various phases of the Nelspruit Granite are present in the Barberton area, ranging from shallow, marginal gneissose phases, exhibiting prominent flow structures and abundant mafic xenoliths, to deeper, massive phases, bearing almost no trace of the original intruded rock.

Visser et al.(1956) described the Mpageni Granite, which is situated approximately 20km due east of Nelspruit,

as a pale-reddish, very coarse-grained, massive rock. A sharp contact between the Mpageni and Nelspruit Granite on the southern side of the former body was reported. Here flow structures within the Nelspruit Granite were found to be clearly truncated by the more massive Mpageni Granite, indicating that the latter post-dates the former, more gneissic variety. These authors concluded that the Mpageni and Nelspruit Granites are comagmatic the latter being an autochthonous granite and the former, a late stage mobilizate, or para-autochthonous granite.

Visser and Verwoerd (1960) published a map (Sheet 22 - Geological Survey, South Africa) and accompanying explanation of the geology of the country north of Nelspruit. These investigators made some additional observations concerning both the Nelspruit and Mpageni Granites. In the area covered by Sheet 22, the Nelspruit Granite was described as exhibiting only slight variations in colour, texture, and mineral constituents, but distinct zones of schlieric (flow) textures were observed along the Sabie River Valley and in the southern portion of the mapped area (i.e. in the Nelspruit area). Mention was also made of a "hornblende-granite" outcropping in the vicinity of the farm Hebron 190 JT, and the presence of a continuous layer of sericitized granite occurring immediately below the Black Reef Quartzite. This sericitized granite was considered to be the result of paleo-weathering of the Archaean granites prior to the deposition of the Transvaal Supergroup.

Visser and Verwoerd (1960) also documented the presence of a large number of shear zones in the granite terrane north of Nelspruit, with predominantly north-northwest and north-northeast strike directions. They also examined the mineralogical and chemical changes associated with the process of mylonitization during formation of the shear zones and concluded that mylonitization is accompanied by increases in the alumina and potash and decreases in the silica and soda contents of the affected rocks.

With regard to the origin of the Nelspruit Granite, Visser and Verwoerd (1960) are in agreement with the suggestions made by Visser et al (1956). They reiterated that "... the observed facts are believed to point to progressive granitization of the older basement rocks, the internal structure of the Nelspruit Granite reflecting, at least in part, the bedding, fracture cleavage or schistocity of the deformed metamorphic formations".

(c) Recent Work (Undertaken up until 1975)

During the period between 1960 and 1975 major strides were made, not only in the understanding of greenstone belts, but also in the recognition and understanding of the various phases of granites that surround the Barberton Mountain Land. The impetus for this work was provided firstly as the result of the work carried out under the auspices of the Upper Mantle Project (1964-1969), and secondly as the result of the publications of workers affiliated with the Economic Geology Research Unit and the Swaziland Geological Survey, the latter being responsible for regional investigations of the Archaean granitic terrane southeast of the Barberton Mountain Land in Swaziland.

Viljoen (1963), working in the northern part of the Barberton greenstone belt regarded the Nelspruit Granite in a different light to Visser and Verwoerd (1960). Viljoen was of the opinion that the Nelspruit Granite (and migmatites) formed the basement upon which all the rocks of the Swaziland Supergroup were deposited and that mafic remnants in the Nelspruit Granite represented, in part, a pre-Swaziland Formation. Some of the amphibolitic 'rafts' were, however, described as being identical to amphibolites occurring at the base of the Onverwacht Group and these were regarded as being down-folded synclinal remnants of an originally more extensive sheet of overlying Onverwacht stratigraphy. Viljoen (1963) also described an intrusive pegmatitic phase into the

Nelspruit Granite, the origin of which was believed to be related to re-heating and mobilization of the latter.

Anhaeusser (1969) presented some new ideas on the granitic rocks surrounding the Barberton Mountain Land. Up until 1963 both Anhaeusser and Viljoen (1963) had considered that the highly migmatitic portions of the Nelspruit Granite might represent vestiges of an early crust that existed p. to the development of the typical greenstone belts. The reason for this suggestion was that the volcanic assemblag that comprised the lower portions of greenstone belts were considered to have developed on a relatively thin crust, the latter possibly being represented by sialic material.

Anhaeusser (1969) categorized the granitic rocks of shield areas in general, into three sub-divisions :- (i) complex migmatitic and gneissic terranes, (ii) circular or elliptic diapiric bodies, commonly sodic in character and (iii) potash-rich, coarse-grained, massive granites which interrupt all earlier formed trends and structures. He mentioned that parts of the Nelspruit Granite fall into the first category whereas the Kaap Valley Granite represents a classic example of the diapiric granite bodies of the second subdivision. Examples of the late potash-rich granites included the Mpageni Granite pluton and the Salisbury Kop Granite near Hectorspruit. The latter granite body was described by van Eeden and Marshall (1965). These granites, which fall into the third sub-division, were considered to possibly represent the only true magmatic granites in the shield areas. Aspects of Anhaeusser's (1969) granite classification are included in Figure 2, which is a compilation of the granitic rock types in the eastern half of the Kaapvaal Craton, modified by Hunter (1974).

Regarding the Archaean granitic terrane south of the Barberton Mountain Land it will be immediately noted, from Figure 2, that a greater variety of granite types appear to

exist to the south of the mountain land than to the north of it. This impression is erroneous and purely the result of there having been a greater amount of work carried out on the granites in Swaziland. Hunter (1973a) has provided the following classification of granite types which is based primarily on a detailed knowledge of the Archaean granite terrane in Swaziland :-

(a) The Ancient Gneiss Complex
(b) The Granodiorite Suite
(c) The Tonalite Gneiss domes
(d) The Nelspruit Gneisses and Migmatites
(e) The Homogenous Hood Granite
(f) The Granite Plutons

The categories (a) to (f) are listed in order of decreasing age. This classification accounts for all the subdivisions portrayed in Figure 2. It will be noted that the classification also included the Tonalite Gneiss domes and the Nelspruit Gneisses and Migmatites, units which are not encountered in Swaziland but are prominent in the areas just north and west of the Barberton Mountain Land. Two aspects regarding Hunter's (1973a) classification require clarification; (i) the Ancient Gneiss Complex is considered to be the basement upon which rocks of the greenstone assemblages (i.e. the Swaziland Supergroup) were deposited. All other granite types listed are regarded as being younger than the greenstone belts; (ii) generally the granitic rocks are found to become progressively enriched in potassium with decreasing age, a factor which Hunter considers to be concomittant with sialic crustal thickening and development.

Viljoen and Viljoen (1969b), working in the southwest and north of the Barberton Mountain Land, produced a similar looking granite classification, but which contains some significantly different features to those proposed by Hunter (1973a). Their classification was given as follows :-

(a) The Ancient Tonalitic Gneiss

(b) The Homogenous Hood Granite

(c) The Nelspruit Gneisses and Migmatites

(d) The Young Plutons.

In this classification the Granodiorite Suite is not recognized and the Ancient Gneiss Complex and Tonalitic Gneiss domes of Hunter (1973a) are considered as a single entity and referred to as the Ancient Tonalite Gneisses. These Ancient Tonalite Gneisses are, furthermore, considered to post-date and intrude the Swaziland Supergroup. Hence the opposing classifications of Hunter (1973a) and Viljoen and Viljoen (1969b) are in fact standpoints from which the opposing views regarding the nature of the earth's early crust, can be viewed. It is,therefore,pertinent to note that the controversial state of knowledge, previously alluded to, has been brought about largely as the result of geological investigations being carried out in two geographically distinct areas.

The classification of Viljoen and Viljoen (1969b) is similar to that of Hunter (1973a) in that it also implies a general increase in potash content and K_2O/Na_2O ratio as the granites get younger. In addition, these authors pointed out that an important relationship exists between granite type and topography in the Barberton region. The younger, more potassic, granites are considered to occupy higher terrain than older more sodic varieties. Cases in point are the Nelspruit Porphyritic Granite and the Homogenous Hood Granite, (Lochiel Granite - Hunter, 1974) which occupy elevated areas with respect to the flat, low-lying, Knap Valley Granite for example.

FIGURE 2

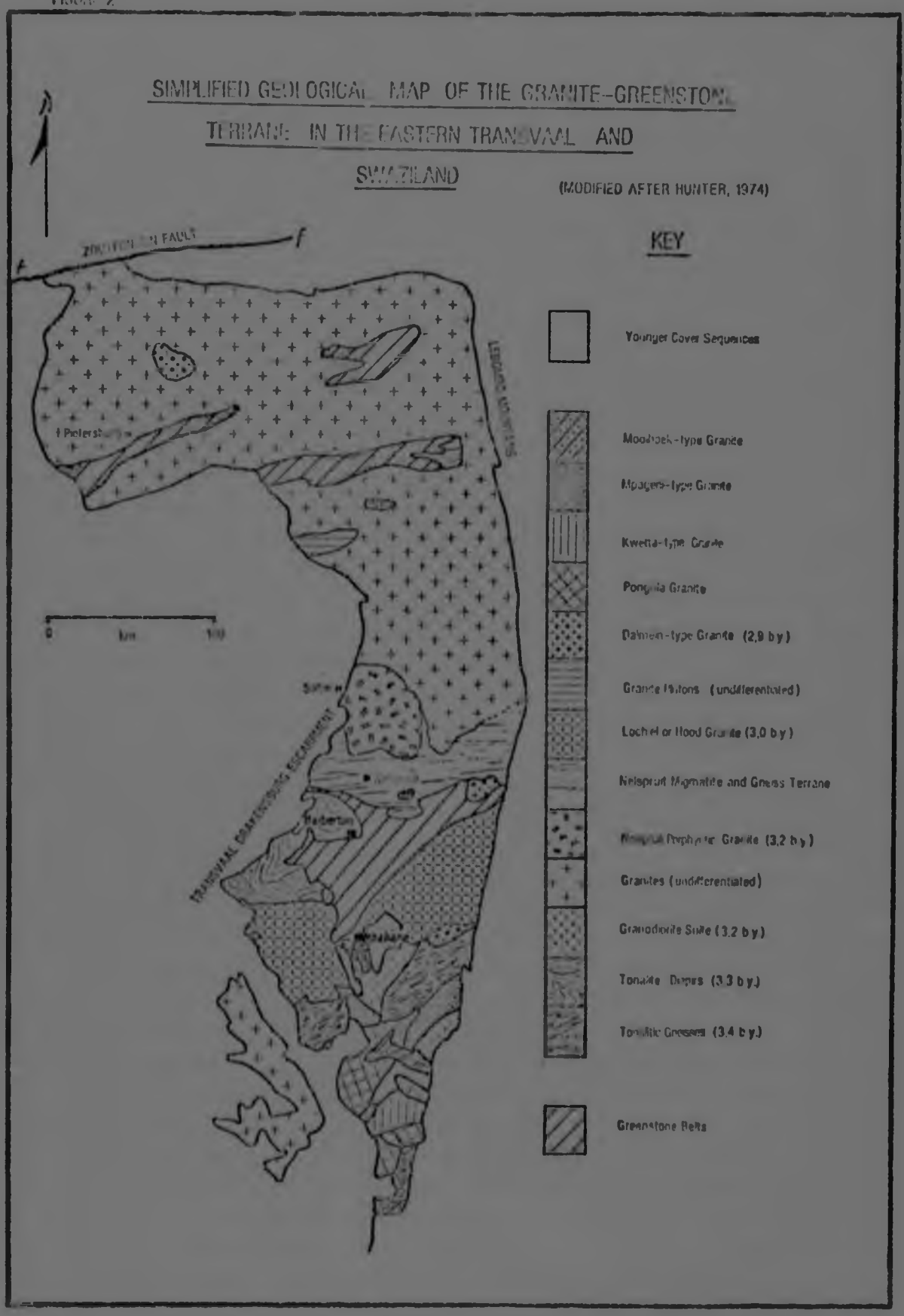
SIMPLIFIED GEOLOGICAL MAP OF THE GRANITE-GREENSTONE TERRANE IN THE EASTERN TRANSVAAL AND SWAZILAND
(MODIFIED AFTER HUNTER, 1974)
KEY
Younger Cover Sequences
Moodiek-type Granite
Mpageni-type Granite
Kwetla-type Granite
Pongola Granite
Dalmein-type Granite (2,9 by)
Granite Gneiss (undifferentiated)
Lochiel or Hood Granite (3,0 by)
Nelspruit Migmatite and Gneiss Terrane
Granites (undifferentiated)
Granodiorite Suite (3,2 by)
Tonalite Gneiss (3,3 by)
Greenstone Belts
0
km
100
TRANSVAAL ESCARPMENT

Viljoen and Viljoen (1969c) presented a concise summary of the geochemical evolution of the granitic rocks surrounding the Barberton Mountain Land. These authors considered the diapiric tonalite plutons, occurring in the southwest of the Mountain Land (Figure 2), to be the oldest granitic rocks in the area, and were of the opinion that Hunter's (1973a) Ancient Gneiss Complex in Swaziland possessed identical characteristics to the diapiric gneisses in the Transvaal. The origin of this tonalitic material is regarded as being linked to a major episode of differentiation within the earth's mantle subsequent to the extrusion of primitive mafic and ultramafic magmas which constitute the lower formations of the Onverwacht Group. The continuation of this major differentiation episode contributed to the subsequent addition to the crust, of more potash-rich granite phases. Viljoen and Viljoen (1969c) furthermore regarded potash metasomatism as being the primary mechanism in the formation of these subsequent phases. The resultant reconstituted material, is thought to be typified by the Nelspruit Gneisses and Migmatites. At a later stage small, transgressive granite plutons were introduced into the crust, and these were regarded as being possibly magmatic in origin.

Further detailed geological and geochemical investigations were carried out by Anhaeusser (1973b) on the Archaean granite and gneisses of the Johannesburg-Pretoria dome. Anhaeusser described a sequence of tonalitic gneisses, homogenous granodiorites, porphyritic granites, gneisses, and migmatites in an area that had previously been considered relatively homogenous. Recent geochronological work (C.R. Anhaeusser, verbal communication, 1976) on this granite dome has confirmed the suggestion made by Viljoen and Viljoen (1969b and c) that the Archaean basement granites became increasingly enriched in potash with decreasing age.

(d) <u>A Summary of Very Recent Work Pertinent to this Investigation</u>

Viljoen and Viljoen (1969c) presented a concise summary of the geochemical evolution of the granitic rocks surrounding the Barberton Mountain Land. These authors considered the diapiric tonalite plutons, occurring in the southwest of the Mountain Land (Figure 2), to be the oldest granitic rocks in the area, and were of the opinion that Hunter's (1973a) Ancient Gneiss Complex in Swaziland possessed identical characteristics to the diapiric gneisses in the Transvaal. The origin of this tonalitic material is regarded as being linked to a major episode of differentiation within the earth's mantle subsequent to the extrusion of primitive mafic and ultramafic magmas which constitute the lower formations of the Onverwacht Group. The continuation of this major differentiation episode contributed to the subsequent addition to the crust, of more potash-rich granite phases. Viljoen and Viljoen (1969c) furthermore regarded potash metasomatism as being the primary mechanism in the formation of these subsequent phases. The resultant reconstituted material, is thought to be typified by the Nelspruit Gneisses and Migmatites. At a later stage small, transgressive granite plutons were introduced into the crust, and these were regarded as being possibly magmatic in origin.

Further detailed geological and geochemical investigations were carried out by Anhaeusser (1973b) on the Archaean granite and gneisses of the Johannesburg-Pretoria dome. Anhaeusser described a sequence of tonalitic gneisses, homogenous granodiorites, porphyritic granites, gneisses, and migmatites in an area that had previously been considered relatively homogenous. Recent geochronological work (C.R. Anhaeusser, verbal communication, 1976) on this granite dome has confirmed the suggestion made by Viljoen and Viljoen (1969b and c) that the Archaean basement granites became increasingly enriched in potash with decreasing age.

(d) <u>A Summary of Very Recent Work Pertinent to this Investigation</u>

In recent years sophisticated geochemical modelling, mainly involving trace and rare-earth elements, has been applied to various granites in the Barberton region with a view to understanding the possible origins of these rocks. With the advent of accurate analytical techniques and a knowledge of the relevant crystal/liquid partition coefficients, it has become possible to produce realistic partial melting or fractional crystallization models for any granite type under investigation.

Condie and Hunter (1976) have produced trace element models for three groups of granites :- (i) the tonalite diapirs, (ii) The Dalmein-type plutons and the Hood Granite and, (iii) the Mpageni-type Plutons (see Figure 2). Rare-earth and large-ion lithophile element models suggest the following origins for these three granite types :-

(i) The tonalite diapirs (approximately 3,3 b.y. old) can be accounted for by a 10% partial melt of an eclogitic parent.

(ii) The Dalmein-type Plutons and Hood Granite (approximately 3,0 b.y.) are best derived from a 50% partial melt of a silicious garnet-bearing granulite.

(iii) The Mpageni-type Plutons (2,6-2,8 b.y.) can be derived by 70-80% fractional crystallization of a Dalmein-type magma.

As a result of these data Condie and Hunter (1976) proposed a "mantle-plume" model involving a pre-existing sialic crust and rifting tectonics to account for the granite-greenstone assemblage in the Barberton region.

Glikson (1976a) undertook similiar trace element studies on four granite sub-divisions from the Barberton Region:-

(i) albite porphyries from the lower ultramafic unit or the Onverwacht Group, (ii) the ancient tonalite diapirs, (iii) the Dalmein and Boesmanskop plutons (the latter being a small syenitic body south of the Barberton Mountain Land) and, (iv) the Nelspruit gneisses and migmatites and Homogenous Hood Granite. Glikson's data indicated that the albite porphyries had highly fractionated rare-earth element patterns indicating an equilibration with garnet and a concomittant high pressure origin. The ancient tonalites were thought to have been derived from the partial melting of an eclogite (c.p. Condie and Hunter, 1976), whereas the Dalmein and Boesmanskop plutons appear to have been derived from a lesser partial melt of an unspecified mafic parent. The Nelspruit gneisses and migmatites and the Homogenous Hood granite were thought to have been derived by partial melting of a tonalitic parent. With regard to the overall evolution of rocks from the Barberton region, Glikson (1976a) states that "The data lend support to models involving a secular transformation from an ensimatic to an ensialic tectonic environment..."

It is thus apparent that even the most recent geochemical work in the Barberton region has not resolved the controversial issues regarding the nature of the earth's earliest crust, and a consensus of opinion has still not been reached even though very similar geochemical techniques have been used to try and resolve them.

(e) Geochronological Investigations in the Barberton Region

Brief mention will be made here of some of the more important age determinations that are available from rocks in the Barberton region and surrounding areas. In an area where controversy exists concerning the nature of the earliest rocks, geochronology would appear to be the most useful tool the earth-scientist could resort to in attempting to solve this problem. However the commonly altered nature of many of the

critical rock types and the absence, in the past, of a detailed geochronological study programme has resulted in a poor understanding of the isotope geochemistry of the area.

Within the Swaziland Supergroup the oldest age yet obtained is 3,5 ± 0,2 b.y. for a komatiite from the lower Onverwacht Group (Jahn and Shih, 1974). A U-Pb age of 3,36 ± 0,1 b.y. is available for a quartz-porphyry from the Hooggenoeg Formation of the Onverwacht Group (Van Niekerk and Burger, 1969). In addition a Rb-Sr isochron age of 3,375 ± 0,02 b.y. is also available for the Middle Marker of the Onverwacht Group (Hurley et al., 1972).

In Swaziland the Ancient Gneiss Complex has been dated at 3,34 b.y. by the Rb-Sr method (Allsopp et al., 1969). This data makes this suite of rocks apparently younger than the lowermost formations of the Swaziland Supergroup. The Granodiorite Suite (Figure 2) has also been dated, by the Rb-Sr method, at 3,44 ± 0,3 b.y., however this isochron is unreliable (Allsopp et al., 1962).

Various dates for the ancient tonalite gneisses are available, ranging from 3,31 ± 0,04 b.y. to 3,22 ± 0.04 b.y. (Oosthuyzen, 1970). These dates indicate that the tonalite gneisses are younger than the lowermost formations of the Onverwacht Group.

The Nelspruit gneisses and migmatites, at one time thought to represent portions of the basement upon which the Swaziland Supergroup was deposited (Viljoen, 1963), have been dated both by U-Pb and Rb-Sr methods. The former method gave a date of 3,16 ± 0.05 b.y. (Oosthuyzen, 1970) whereas the latter method yielded an age of 2,992 ± 0,07 b.y. Clearly this terrane is younger than the tonalitic rocks to the south and evidence of considerable reworking is present from the initial $^{87}Sr/^{86}Sr$ ratio obtained from the Rb-Sr isochron (i.e. R_o = 0,7052 ± 0,0019, de Gasparis, 1967). The Lochiel

or Homogenous Hood Granite appears to have been emplaced contemporaneously with the Nelspruit gneisses and migmatites according to the U-Pb age of 3,075 ± 0,1 b.y. obtained by Oosthuyzen (1970).

The younger, transgressive granite plutons can be divided into two ages of emplacement, an older Dalmein-type pluton and a younger Mpageni-type pluton. The older type, for example the Dalmein plutor (3,19 ± 0,07 b.y.) and the Boesmanskop syenite pluton (3,13 ± 0,03 b.y. - Oosthuyzen, 1970) generally have ages in excess of 3,0 b.y. The younger plutons, for example the Mpageni pluton (2,81 ± 0,08 b.y. - Oosthuyzen, 1970) and the Mbabane pluton in Swaziland (2,55 ± 0,07 b.y. - Allsopp et al., 1962), on the other hand, generally have ages ranging between 2,8 - 2,5 b.y. These clearly represent the last phases in the development and consolidation of the Archaean granitic crust in this region.

IV. ACKNOWLEDGEMENTS

The author is indebted to Professor D.A. Pretorius for the opportunity to undertake this study at the Economic Geology Research Unit. This study was carried out under the auspices of the Geodynamics Project in South Africa and acknowledgement is made of the financial support received from the C.S.I.R. in this respect.

This dissertation was supervised by Dr. C.R. Anhaeusser and his continued assistance and advice during the last two years is very gratefully acknowledged. The author would also like to thank Mr. T.S. McCarthy and Mr. R.C.A. Minnitt for their help during this period.

The help offered by Miss J.R. Burkinshaw with regards to the various computer applications in this study is acknowledged. In this respect thanks are also due to

Mr. C. Guerin, Mr. F. Arnott and Mr. G. Gott.

Professor A. Goodwin and Mr. R. Fripp are thanked for contributions that they made during the field study. Professor A.J. Erlank is also thanked for reading a draft manuscript of Chapter 5.

The author wishes to express his gratitude to the Bantu Staff as well as Dr. C. Frick and Mr. R.C. Wallace of the Geological Survey, Pretoria, for their help in connection with the preparation and analysis of samples.

The interest shown by Professor H. Allsopp, Mrs. F. Barton, Dr. A.J. Burger and Mr. J. Fourie in the geochronological aspects of this study is also appreciated.

A particular word of thanks is due to Mrs. L. Tyler, Mr. N. Gomes and Mrs. H. Hudson for secretarial, drafting and photographic assistance received during the preparation of this dissertation. My gratitude to Mrs. D. Wentzel who typed the final draft of the thesis. A grateful word of thanks to my fiancée, Miss V. Tansley, for her help in the completion of this dissertation.

Finally the author would like to thank Mr. and Mrs. P. Thomas of White River for accommodation and companionship during the periods in the field.

CHAPTER 2

THE BARCLAY VALE SCHIST BELT

I. INTRODUCTION

The Barclay Vale Schist Belt is a small greenstone outlier approximately 40km northwest of the main mass of the Barberton greenstone belt. Because of its proximity to the latter, the Barclay Vale Schist Belt has, not surprisingly, a similiar lithology to that documented in portions of this greenstone belt. Thus a brief description of the stratigraphy of the Barberton greenstone belt, as well as other well documented Archaean remnants such as the Murchison and Pietersburg greenstone belts, will serve as a useful introduction to the geology of the Barclay Vale Schist Belt.

The Swaziland Supergroup, which comprises the Barberton greenstone belt, consists of a variety of igneous, volcanic and sedimentary rock types. These are divided into three groups which, in ascending order from the base of the succession, include :- (i) the Onverwacht Group which consists essentially of a succession of basic and ultrabasic lavas and is overlain by (ii) the Fig Tree Group and (iii) the Moodies Group. The latter two groups are comprised essentially of argillaceous and arenaceous sedimentary units and, because these rocks are not represented in the Barclay Vale Schist Belt, they will not be discussed further.

The Onverwacht Group, developed at the base of the Swaziland Supergroup, attains a thickness of approximately 15km in its type area, in the Komati River Valley, south of Barberton. This succession has been subdivided into six formations (Viljoen and Viljoen, 1969c). The lower three, the Sandspruit, Theespruit and Komati Formations, are referred to collectively as the Tjakastad Sub-Group or "lower ultramafic unit". The lower three formations are comprised of an abundance of mafic and ultramafic rocks represented by peridotitic and basaltic komatiites and high-Mg basalts. These distinctive rock types are characterized by high MgO and

low total alkali contents and high CaO/Al_2O_3 ratios. In addition a number of layered and differentiated ultramafic assemblages appear within the lower ultramafic unit. Minor rock types within this unit include soda-rich quartz-porphyry bodies, chemical sediments, calc-silicate rocks and banded iron formations. The ultramafic rocks in this assemblage, particularly where they occur as small xenolithic remnants, are commonly altered and may be represented in the form of talc, talc-chlorite and tremolite-actinolite schists, and serpentinites.

The lower ultramafic unit is terminated by a persistent chemical sedimentary unit known as the Middle Marker. Stratigraphically overlying this are developed the Hooggenoeg, Kromberg and Swartkoppie Formations which are known collectively as the Geluk Sub-Group or "mafic-to-felsic unit". These three formations consist of cyclically alternating mafic, intermediate and acid volcanics, including also a variety of pyroclastic rocks. Individual cycles commence with tholeiitic basalts which are in turn overlain by dacitic and rhyo-dacitic lavas. Commonly, individual cycles are capped by chert or ferruginous chert horizons (Viljoen and Viljoen, 1969g). Ultramafic rocks occur sporadically throughout this succession but are of minor volumetric importance. As in the lower ultramafic unit the rocks of the upper three formations of the Onverwacht Group are commonly altered and occur as talc, talc-chlorite and chlorite-actinolite.

Particular mention should be made of the layered and differentiated ultramafic assemblages that occur, particularly, in the lower ultramafic unit. These bodies usually consist of a sequence of dunites, harzburgites, peridotites, pyroxenites, gabbros and norites which may occur as cyclically repetitive units. These bodies generally occur on the northern flank of the Barberton

greenstone belt and are thought to represent intrusive sills emplaced very early in the history of the Onverwacht Group (Anhaeusser, 1969: 1976a).

Geologists working in other major greenstone belts in the northeastern Transvaal have documented a similiar stratigraphic succession to that outlined above for the Onverwacht Group. Grobler (1972) has described the lithology of the Mount Robert Volcanic Group of the Pietersburg Schist Belt. This succession consists of cycles of predominantly mafic and ultramafic metalavas with intercalated metasediments. These are, in turn, overlain by more metabasaltic and salic volcanic rock types. Pyroclastic rocks, as well as cherts, banded iron-formations and carbonates are also reported in this sequence. Grobler (1972) states in his conclusions that the Mount Robert Volcanic Group "... is the equivalent of the Onverwacht Group, or portions of it".

Minnitt (1975) working in the eastern extremity of the Murchison Greenstone Belt (Figure 1) reported that the basal stratigraphy of this Archaean assemblage consisted of a sequence of mafic and ultramafic metavolcanics together with interlayered quartz-sericite schists. This sequence is overlain by mafic and acid-to-intermediate tuffs and intercalated chemical sediments. Minnitt (1975) concluded that the stratigraphy of the eastern portion of the Murchison Greenstone Belt does not readily correlate with the model stratigraphic column obtained in the Barberton Greenstone Belt, but that the majority of the rock assemblages, although in places telescoped or incompletely developed, can best be correlated with the Onverwacht Group.

The nature of the environment in which the volcanic rocks of the Onverwacht Group and its correlatives were deposited, is readily discernible from characteristic field textures. Quench phenomena such as spinifex-textured lavas and pillow structures are ubiquitous throughout the areas in which these rocks occur. The majority of the rocks that

occur within the Onverwacht Group were, therefore, deposited in an aqueous environment (Anhaeusser, 1969; Viljoen and Viljoen, 1969a,g). Associated rocks, such as silicious schists, are thought to represent altered tuffs whereas the presence of carbonaceous chert horizons is indicative of biological activity in what must have been a primordial oceanic environment.

II. GENERAL GEOLOGICAL DESCRIPTION OF THE BARCLAY VALE SCHIST BELT

The Barclay Vale Schist Belt appears from beneath the Transvaal Drakensberg Escarpment at a point some 25km due west of Nelspruit. It covers an area of approximately 40km ^{2} and is dissected by the Crocodile River and one of its smaller tributaries. This greenstone remnant was mapped on a scale of 1:10 000 using enlarged aerial photographs and a reduced version of this map is reproduced in Figure 3. The exposure in the area is poor and as a result the detail on the map is scanty. A rectangular portion on the southern flank of the schist belt, on the farm Richmond 287JT, is comparatively well exposed and a detailed map of this area is reproduced in Figure 4.

As far as the writer is aware very little work has been carried out specifically on the Barclay Vale Schist Belt. Visser and Verwoerd (1960) provided a brief account of the geology of this area and although the basic structure of the schist belt is outlined on their accompanying map (Sheet 22 - Nelspruit), no detailed geology was recorded. These authors correlated the basic rocks of the schist belt with the so-called "Jamestown Igneous Complex", and the intercalated chemical sediments with the Fig Tree Group. The "Jamestown Igneous Complex', as originally defined, no longer exists according to more recent investigations in the Barberton region. Instead these predominantly mafic and ultramafic rocks are now regarded as constituting part of the lower Onverwacht Group (Anhaeusser, 1969; Viljoen and Viljoen, 1969e).

FIGURE 5

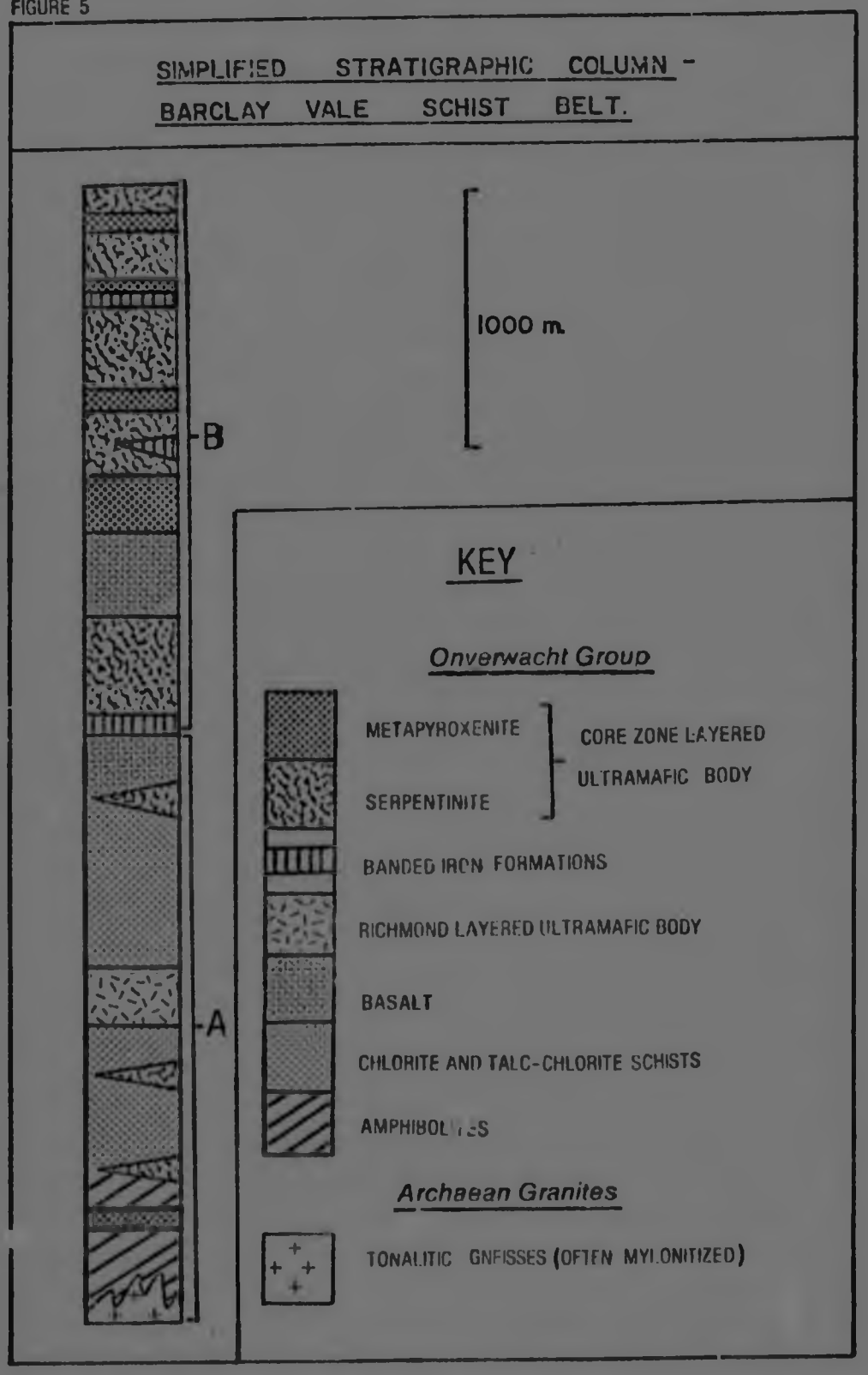

Figure 5. A simplified stratigraphic column of the Barclay Vale Schist Belt, eastern Transvaal.
A - Marginal areas - i.e. areas flanking the greenstone remnant, in close proximity to the Archaean granites.
B - Core Region - central fold structure comprising the Core Zone Layered Body.

The Barclay Vale Schist Belt is flanked in the east and south by granitic rocks, predominantly tonalitic in composition, and commonly mylonitized. (A detailed description of these granites will be given in Chapter 3). The schist belt is overlain to the west by rocks of the Transvaal Supergroup which form the prominent north-south trending Transvaal Drakensberg Escarpment (Figure 3). A number of mafic dykes intrude the Barclay Vale Schist Belt, the major ones being shown in Figure 3.

The geology of the schist belt can be divided into two broad subdivisions:- (a) the marginal areas and (b) the core region. These two subdivisions are illustrated in the simplified stratigraphic column of the Barclay Vale Schist Belt (Figure 5) and are designated A and B respectively.

(a) The Marginal Areas

The marginal areas of the schist belt (portion A of the stratigraphic column, Figure 5) consist essentially of a sequence of amphibolites overlain by chlorite and talc-chlorite schists. Volumetrically minor quantities of serpentinites, pyroxenites and cherts are also present. Portion A of the stratigraphic column is capped by a massive basaltic rock unit. The amphibolitic rocks are restricted to a prominent zone along the southern flank of the schist belt and are virtually absent in the remaining marginal areas (Figure 3). Elsewhere in this schist remnant, the greenstone contact zones consist predominantly of an alternating sequence of talc and talc-chlorite schists. The schistose nature of these rocks in fact characterizes the marginal or contact zones of the schist belt.

In addition to the above mentioned assemblages the marginal southern flank of the schist belt contains a small, linear, layered ultramafic body which is referred to as the "Richmond Layered Body" (Figure 4). Viljoen and Viljoen

(1970) have classified the differentiated ultramafic bodies that occur in the lower portions of the Onverwacht Group, into three varieties which they refer to as the Kaapmuiden-Type, the Stolzburg-Type and the Noordkaap-Type. The Richmond Layered Body most closely resembles the Kaapmuiden-Type which consists of an assemblage of dunite-peridotite-pyroxenite-gabbro-norite occurring as a differentiated succession. According to Viljoen and Viljoen (1970) this type of body commonly attains a thickness of over 600m and is usually represented by only one differentiated cycle, although the commencement of a second may occasionally be observed. The Richmond Layered Body differs from the typical Kaapmuiden-Type body by virtue of its small size. It does,however, consist of only a single differentiated cycle.

(b) The Core Region

The repetitive cyclical nature of the rock types occurring in the core region is illustrated in portion B of the simplified stratigraphic column of the Barclay Vale Schist Belt (Figure 5). Predominant rock types in this region are alternating layers of serpentinite and metapyroxenite (amphibolite) with occasional, prominently developed, layers of banded iron-formation. A single unit of basaltic lava, containing pillow structures, is also present in the core region.

The serpentinitic and metapyroxenitic rocks of the core region are considered to represent a layered ultramafic body, totally different to the Richmond Layered Body described above. The former layered ultramafic body, which is referred to as the "Core Zone Layered Body", and consists of alternating cycles of predominantly two rock types, has some affinity with the Stolzburg-Type of layered body described in the classification of Viljoen and Viljoen (1970). The Stolzburg-Type body is described as consisting of alternating zones of serpentinized dunites and orthopyroxenites and characterized

by the absence of clinopyroxenites, norites and gabbros. Anhaeusser (1976a)has demonstrated, however, that although the cyclically repetitive serpentinized dunites and orthopyroxenites are in fact predominent in the southwestern extension of the Stolzburg body, the entire body consists of a range of rock types which include gabbros and norites. Thus the classification scheme of Viljoen and Viljoen (1970) is not as simple as originally intended and the Core Zone Layered Body should in fact be correlated only with the southwestern portion of the Stolzburg Body.

The presence of h.atuses of chemical sedimentation within the Core Zone Layered Body,as well as the repetitive nature of the rock types,provides an indication that the ultramafic cycles involved were intruded as separate magma heaves probably in the form of intrusive sill-like bodies.

III. DETAILED GEOLOGICAL DESCRIPTION OF THE ROCK TYPES OCCURRING IN THE BARCLAY VALE SCHIST BELT

(a) THE MARGINAL AREAS

(i) Amphibolites

A pronounced zone of amphibolitic rock occurs along the southern flank of the schist belt (Figures 3 and 4). These amphibolites are manifest by two distinct textural types, the one variety is composed essentially of a massive black hornblende-bearing rock which occurs some distance from the granite contact whereas the other occurs as a banded rock near the granite contact (Figure 4). The latter variety of amphibolite, termed the "contact amphibolite",grades progressively into massive amphibolites away from the granite contact. The granite-amphibolite contact along the southern flank of the schist belt has been considerably influenced

by shearing as is evidenced by the mylonitic character of the tonalite gneisses in this region (see Chapter 3). It has been suggested (R. Fripp, personal communication, 1976) that the banded nature of the amphibolites near the contact may be due to the tectonic influence of shearing on the amphibolites. Highly attenuated structual features, similiar folding and crenulations are present in the contact amphibolites (Plate 1a, b and c) and there is no doubt that these are related to tectonic deformation. However, in thin section the layering in these rocks is seen to be composed essentially of alternating quartz-sericite and hornblende bands with minor magnetite in the latter, and evidence of a marked mylonitic fabric was not apparent. An alternative suggestion as to the origin of this compositional banding may be that it formed part of a bedded tuffaceous sequence which has been subsequently affected by structural deformation. Massive amphibolites further away from the granite contact would obviously not be tuffaceous in origin but may nevertheless be volcanic.

(ii) Serpentinites

Numerous discontinuous lenses and bands of serpentinite occur within the marginal areas of the Barclay Vale Schist Belt, particularly along its southern flank (Figure 3). In the field the serpentinite bodies are commonly foliated but are generally more massive than the highly schistose rocks that flank them. They occur as discontinuous, massive, lensoid bodies conformable with the surrounding stratigraphy probably as the result of acting as more competent resistors during the folding and tectonic disturbances in the schist belt.

In thin section the serpentinites consist predominantly of antigorite with lesser amounts of chrysotile, and

traces of magnetite, chlorite and talc. The rocks are generally very altered, even the pseudomorphic crystal outlines of olivine being no longer recognizable. In the absence of any primary mineralogy it is difficult to speculate on the origin of these rocks, geochemical considerations, however, suggest that they may have originally been dunitic or peridotitic.

(iii) Chlorite and Talc-Chlorite Schists

Assemblages of chlorite and talc-chlorite schists predominate in the marginal areas of the schist belt. These schistose rocks are generally highly altered and decomposed and are poorly exposed in the field. In only a few areas was it possible to distinguish the various chlorite and talc-chlorite schist units (Figure 4).

As is common in Archaean greenstone terranes the occurrence of chlorite and talc-chlorite schists reflects the typical greenschist metamorphism of the original volcanic pile. As one proceeds from the contact areas to the core of the Barclay Vale Schist Belt there is a noticeable decrease in the schistocity and degree of alteration of the schistose assemblages. At sample site T8-M.D.1 near the Crocodile River (Figure 3) the rocks are relatively massive and recognizable as a basaltic lava. The chlorite and talc-chlorite schists are likely therefore to represent the metamorphosed remnants of basaltic and possibly peridotitic lava flows.

In thin section the chlorite and talc-chlorite schists consist of chlorite, talc and altered, uralitized hornblende. Minor amounts of epidote, quartz and saussuritized plagioclase felspar also occur. This mineral assemblage may well be the result of the alteration of basalt and peridotite (or high Mg-basalt) lava flows such as have been described in the Komati River region in the southern portion of the Barberton greenstone belt (Viljoen and Viljoen, 1969a).

(iv) The Richmond Layered Body

The Richmond Layered Body was mapped in detail on a portion of the farm Richmond 287JT where it forms a prominent east-west trending ridge (Figure 4). This body has the form of an intrusive sill, conformable with the surrounding stratigraphy, and extending along strike for approximately 6km. It appears to be differentiated only at its widest point where it is approximately 150-200m wide (Figure 4).

The Richmond Layered Body, occurring as it does in the marginal areas of the Barclay Valley Schist Belt, has been considerably altered. Despite this alteration the differentiated character of the body is still recognizable. The base of the body consists of a poorly defined serpentinite layer in which the pseudomorphic outlines of olivine crystals are still recognizable. This basal serpentinite, possibly an original olivine cumulate (dunite) is virtually indistinguishable from the overlying serpentinite which forms the main part of the Richmond Body (Figure 4). The latter, now highly altered to antigorite, may originally have been a peridotite. Overlying the basal serpentinites is a prominent coarse-grained pyroxenitic layer, the latter consisting of disorientated, altered pyroxene grains. The pyroxene has been altered to an amphibole. The pyroxenite and underlying serpentinite layers exhibit a cross-cutting relationship in places along the strike length of the body (Figure 4). This feature may be related to complexities, such as convective disturbances, in the original differentiation process within the sill. The pyroxenite unit is overlain by amphibolite (altered gabbro) and the layered body is capped by a highly altered tremolite-actinolite schist. The tremolite-actinolite schist may not be part of the layered body as suggested by its conformable, juxtaposed position relative to it, and the differentiated sequence may in fact be capped by the altered gabbro.

(v) Additional Rock Types Occurring in the Marginal Areas of the Barclay Vale Schist Belt

(a) Banded and Fuchsitic Cherts : A number of banded chert horizons, some of them fuchsitic, occur within the marginal areas of the schist belt. The micaceous cherts have a distinctive green colour caused by the presence of chromium mica, fuchsite. These chemical sediments presumable represent periods of quiescence in the otherwise explosive volcanic and intrusive history of the greenstone belt.

(b) Tremolite Schists : A very distinctive, foliated and irregularly occurring tremolite schist outcrops in certain areas along the southern flank of the schist belt (Figure 4). In thin section the rock is so fine-grained as to appear almost monomineralic. The predominant constituent is considered to be tremolite and traces of an opaque oxide mineral, possibly magnetite, also occur.

(c) Rocks Displaying Carbonate Alteration: Certain rock types recorded on the detailed map of the southern flank of the Barclay Vale Schist Belt (Figure 4) have undergone considerable carbonate alteration. One of these is a mafic rock characterized by large (up to 1cm in diameter) calcareous nodules which give the rock a "pock-marked" appearance. The other carbonate altered rock has, as its predominant constituent, a fibrous mineral (possibly sillimanite?). Minnitt (1975) has described carbonated rocks from the eastern portion of the Murchison greenstone belt and concluded that carbonate alteration was essentially a metasomatic process. Carbonate alteration was considered to be related to the proximity of the altered rocks to a volcanic fissure through which carbonate-saturated solutions might readily pass. This idea readily accounts for the carbonate alteration in certain rocks, and the lack of it, in

similiar rocks nearby. Whitmore et al.(1946) noted the presence of chrome-mica (fuchsite) in zones of pervasive carbonate alteration. This feature may have some bearing on the origin of fuchsite in the banded cherts described above.

(d) Pyroxenite Dyke : An east-west trending pyroxenite dyke outcrops along the southern margins of the area mapped in detail (i.e. at sample locality T7-14, Figure 4). By comparison with the adjacent, altered, highly tectonized amphibolitic rocks, the pyroxenite appears massive and relatively little altered. In thin section the rock comprises of large (up to 5mm in length) subhedral blades of pyroxene, partially altered to tremolite. The pyroxenite has the appearance of a cumulate, as lesser amounts of intercumulus sphene, quartz and plagioclase also occur. Although this unit occurs conformably with the surrounding stratigraphy, its relatively unaltered nature and massive appearance sets it apart and it is considered to be a dyke. Its emplacement undoubtedly took place in the post-deformational history of this greenstone belt.

(b) THE CORE REGION

The core region of the Barclay Vale Schist Belt on the simplified stratigraphic column (portion B, Figure 5) is an assemblage consisting of banded iron-formations, basalts, metapyroxenites and serpentinites. On the map of the Barclay Vale Schist Belt (Figure 3) this assemblage occurs as a semi-concentric fold extending eastwards from beneath the Transvaal Drakensburg Escarpment.

(i) Banded Iron-Formations

Two continuous banded iron-formation units, and a number of smaller, discontinuous ones occur in the stratigraphy of the core-region (Figures 3 and 5). The

larger of the two continuous banded iron-formations forms the base of the lithological succession that constitutes the core region (Figure 5; Plate 1e). This banded iron-formation unit has, intermittently associated with it, a dark carbonaceous shale unit which was obviously deposited in the same quiescent period which allowed the original onset of chemical sedimentation to take place. In the northern part of the schist belt, near the Sudwala Cave road (Figure 3) this lower banded iron-formation becomes intensely brecciated (Plate 1f). This brecciation is probably related to later shearing and fracturing associated with the major north-south trending dyke that occurs in the western extremity of the Barclay Vale Schist Belt (Figure 3).

In thin section the banded iron-formations all consist of alternating bands of recrystallized chert and magnetite-hematite. The individual bands in this rock type vary from 1 to 10mm in thickness.

(ii) Basaltic Rocks.

A continuous layer within the core-region assemblage is constituted by rocks of basaltic composition which are characterized by pillow structures (Figure 3; Plate 1d). The basalts are generally massive in appearance but have undergone extensive alteration and appear to weather easily. Rocks in this unit are believed to be the untectonized equivalents of the chlorite schists developed elsewhere in the Barclay Vale Schist Belt. The presence of pillow structures in this unit indicate a subaqueous volcanic origin for this rock type. Although the occurrence of banded amphibolites in the marginal areas suggests that some of the rock types may have been deposited as mafic tuffs it is suggested that others, such as the chlorite and talc-chlorite schists may have had a subaqueous volcanic origin.

PLATE 1

A. Banded "contact amphibolites" from the marginal areas of the Barclay Vale Schist Belt on the farm Richmond 287 JT. The light bands consist of quartz and sericite and the dark bands contain mainly hornblende.

B. Inclusions of acidic material in the banded tuffaceous "contact amphibolite" sequence in the Barclay Vale Schist Belt. These inclusions may represent agglomeratic fragments in a pyroclastic succession.

C. Ptygmatically folded acidic veinlet in the banded "contact amphibolite", Barclay Vale Schist Belt. The deformation is possibly related to the shearing along the granite-greenstone contact.

D. Photograph of a weathered pillow structure in a basaltic lava from the core region of the Barclay Vale Schist Belt. Gas vesicles can be observed above the hammer handle.

E. Banded iron-formation from the core region of the Barclay Vale Schist Belt. The lighter bands consist of recrystallized chert whereas the darker ones are comprised predominantly of magnetite and hematite.

F. Photograph illustrating the effects of shearing and brecciation on the banded iron-formation displayed in Plate 1E. The shearing is apparently related to the emplacement of a large dyke in the area.

PLATE 1

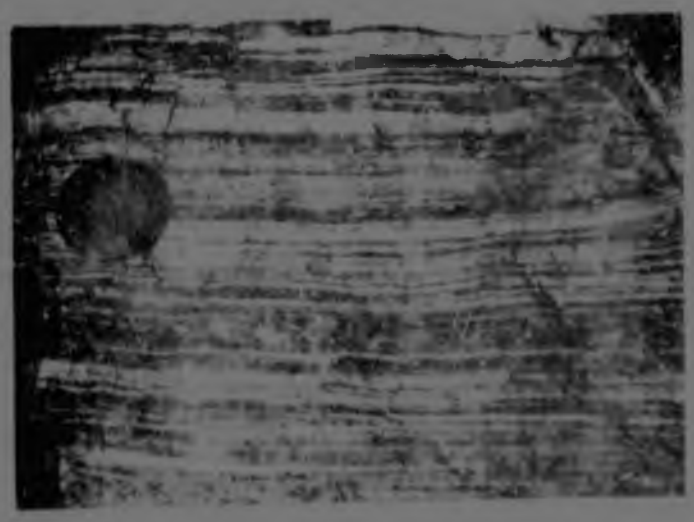

A

B

C

D

E

F

(iii) The Core Zone Layered Body

The alternating succession of serpentinitic and metapyroxenitic rocks that predominate the core region lithology is considered to represent a layered ultramafic differentiated body similiar to certain portions of the Stolzburg Body in the southwest of the Barberton greenstone belt (Viljoen and Viljoen, 1970; Anhaeusser, 1976a).

The serpentinites in the layered body are considerably more massive than those described from the marginal areas. In thin section their mineral assemblages are, however, similiar, with antigorite forming the predominant constituent. The pseudomorphic crystal outlines of olivine are commonly seen, the latter being enhanced by a rimming of magnetite grains, a by-product of the olivine-antigorite alteration process.

The metapyroxenites (amphibolites) are composed predominantly of tremolite, which is clearly the result of uralitization of pre-existing pyroxenes. The pseudomorphic outlines of these pyroxenes are still visible and the rock has the appearance of a pyroxenite in hand-specimen.

As mentioned, the Core Zone Layered Body consists of repetitive cycles of serpentinite and metapyroxenite. An integral part of this layered body, however, is the presence of banded iron-formations which may separate individual serpentinite and metapyroxenite layers or occur intraformationally within serpentinite layers (Figure 3). This is an indication that the layered body intruded in a sill-like fashion in an event which was probably represented by a number of magma heaves. It seems likely that the main process of differentiation may have taken place in the magma chamber, prior to intrusion. Geochemical considerations relating to differentiation

within the Core Zone Layered Body will be dealt with in a later section.

IV. SOME STRUCTURAL ASPECTS OF THE BARCLAY VALE SCHIST BELT

Although no detailed structural analysis was undertaken, either on the schist belt itself, or the surrounding tonalite gneisses, a number of foliation and schistocity measurements were recorded (Figure 3). Prominent in the area is the "wrap around" foliation of the tonalite gneisses with respect to the schistocity within the greenstone belt. The foliation in the tonalite gneisses is, in all cases, parallel to the fabric in directly adjacent greenstone material (Figure 3). This feature has been described by other workers recording the nature of tonalite gneiss-greenstone contacts in the Barberton region (Anhaeusser, 1969; Viljoen and Viljoen, 1969b). These authors attribute this phenomena to the diapiric intrusion of the greenstones by tonalitic granites which, together with subsequent granitization and contamination, eventually results in the imposition of a mineral lineation or fabric on the latter. Implicit in this process is the realization that the tonalites diapirically intrude the greenstones, and should the above theory prove correct, it follows that tonalite gneisses which surround the Barclay Vale Schist Belt must post-date the latter.

The overall structure of the schist belt is considered to be synformal, for a number of reasons. These include :-

(i) dip measurements recorded, particularly in the banded iron-formations of the folded core region, indicate a synclinal structure,

(ii) pillows in the interlayered volcanic basalt of the core region are orientated such that the top of the layer is towards the centre of the schist belt,

(iii) geochemical data on the serpentinites and metapyroxenites of the Core Zone Layered Body indicate a trend of increasing differentiation towards the centre of the schist belt (Figure 8), and

(iv) the trend of increasing differentiation in the Richmond Layered Body is also away from the margins of the schist belt (Figure 4).

The synformal nature of this schist belt remnant is in accordance with the structure of similiar schist belts elsewhere in southern African Archaean terranes (Anhaeusser, 1969; Viljoen and Viljoen, 1969e; Minnitt, 1975).

V MINERALIZATION IN THE BARCLAY VALE SCHIST BELT

Although no work was carried out in the Barclay Vale Schist Belt specifically with the aim of examining aspects of mineralization in the area, it was, however, noted during the course of mapping that numerous prospecting pits and trenches exist. Most of the excavations testify to the enthusiasm of the old-time gold prospector as well as persons interested in chrysotile asbestos fibre.

The basal serpentinites of the Richmond Layered Body are the site of numerous prospecting trenches and small adits where some gold is believed to have been extracted during the early years of this century (J. Greathead, personal communication, 1976). No details of tonnages or grades are available but judging from the size of the operation the amount of gold extracted appears to have been minimal. These trenches and adits are also the site of chrysotile asbestos mineralization. Traces of asbestos mineralization also occur scattered throughout the schist belt, particularly associated with the serpentinites and metapyroxenites of the Core Zone Layered Body. No mining of this fibre was ever undertaken.

VI. GEOCHEMICAL DATA FROM THE BARCLAY VALE SCHIST BELT

Although the majority of the rocks in the Barclay Vale Schist Belt, particularly in the marginal areas, have undergone considerable alteration, a number of localities, particularly in the core region contain rocks suitable for chemical analysis. Analyses of rocks from the Barclay Vale Schist Belt were all carried out (except where indicated) by the writer using the Geological Survey's E.X.A.M. unit in Pretoria. The statements made in Appendix 2, regarding the accuracy and precision of these analyses must be taken into account when comparing the Barclay Vale samples with analyses of similiar rock types in other greenstone belts in the eastern Transvaal.

Two diagrams, the first a plot of CaO v Al_2O_3 and the second a ternary Al_2O_3-CaO-MgO (ACM) plot were compiled for taxonomic purposes (Figures 6 and 7 respectively). On these diagrams both volcanic and cumulate-type samples are compared with similiar rock types from other greenstone belts in the eastern Transvaal. The compositions of two samples of metabasalt (T8-M.D.1, Figure 3 and T7-16, Figure 4) are compared with fields of Barberton-, Badplaas- and Geluk-Type basaltic komatiites as defined by Viljoen and Viljoen (1969a). Figures 6 and 7 show that both these samples (which are considered to be volcanic in origin) have close compositional affinities with the Barberton-Type basaltic komatiite. The whole rock compositions of samples T8-M.D.1 and T7-16 are presented in Table 3 where they are compared with an average Barberton-Type komatiite from the Murchison greenstone belt. These rock types are seen to have similiar compositions (Table 3).

Three samples of metapyroxenite are plotted on Figures 6 and 7. One of these, sample T7-4 (Figure 4), is a cumulate-textured metapyroxenite from the Richmond Layered

Figure 6. ACM diagram; comparison of samples from the Barclay Vale Schist Belt with average analyses from the Barberton greenstone belt.

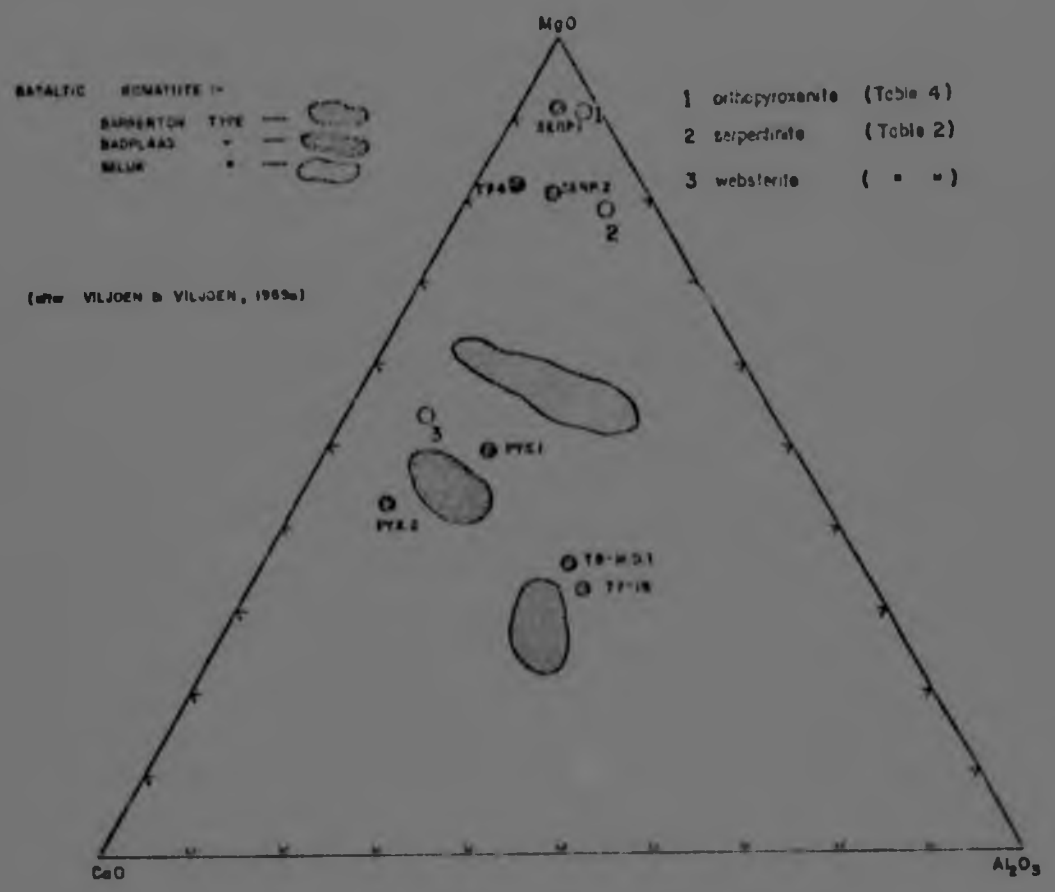

Figure 7. CaO v Al_2O_3 plot of samples from the Barclay Vale Schist Belt. Samples and symbols as in Figure 6.

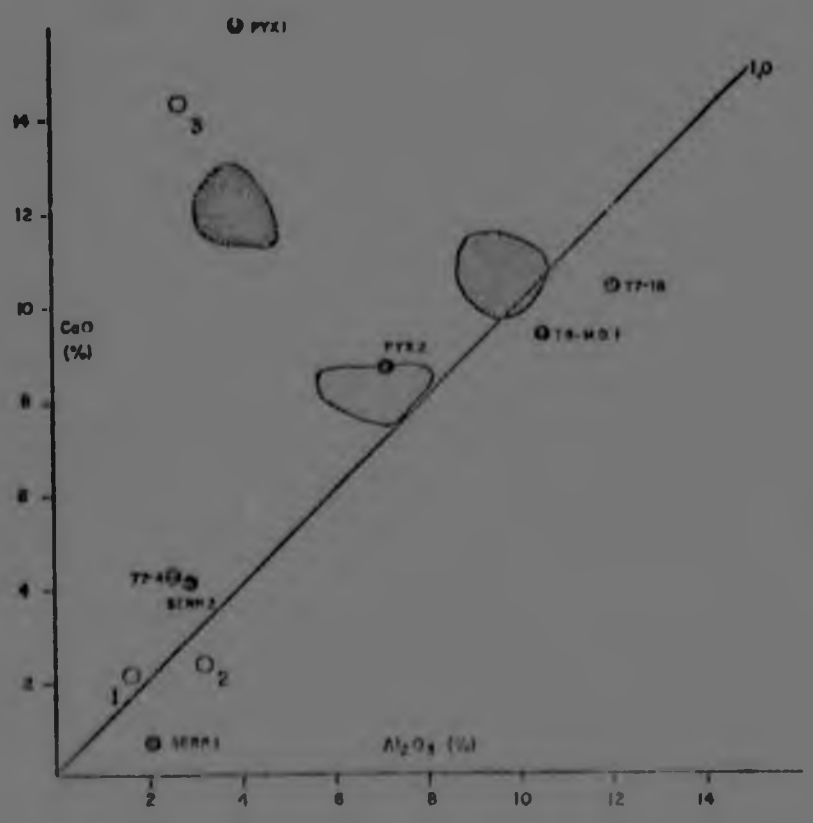

TABLE 2.

SERPENTINITES AND ALTERED PYROXENITES FROM THE C[illegible]E REGION OF THE BARCLAY VALE SCHIST BELT AND SIMILIAR ROCK-TYPES FROM OTHER GREENSTONE BELTS IN THE EASTERN TRANSVAAL

	1	2	3	4	5	6	7
	S.1	S.2	P.1	P.2			
SiO_2	39,3	42,3	49,5	52,9	40,4	44,1	53,22
TiO_2	0,19	0,29	0,39	0,48	0,13	0,11	0,08
Al_2O_3	1,8	2,7	3,9	7,0	3,2	3,85	3,01
Fe_2O_3	15,5	14,6	12,4	11,2	8,6	7,8	6,18
MnO	0,22	0,28	0,21	0,17	0,14	0,13	0,23
MgO	31,7	27,9	15,4	15,3	33,93	33,02	20,79
CaO	0,60	3,96	15,7	8,4	2,2	1,06	14,26
Na_2O	0,0	0,0	0,6	1,1	0,08	0,06	0,25
K_2O	0,07	0,06	0,07	0,04	0,02	0,08	0,06
P_2O_5	0,02	0,03	0,04	0,07	0,04	0,01	0,05
Cr_2O_3	0,12	0,18	0,03	0,11	-	-	-
L.O.I.	9,79	7,69	1,33	2,65	10,63	10,63	0,34
Ni(ppm)	1980	1570	350	280	-	-	-
TOTALS	98,71	99,99	99,57	99,42	99,37	99,85	98,47

Columns 1 and 2: Serpentinites - Barclay Vale Schist Belt.
Columns 3 and 4: Altered pyroxenites - Barclay Vale Schist Belt.
Column 5 : Average serpentinized peridotite-harzburgite (Anhaeusser, 1976a)
Column 6 : Serpentinite - Murchison Range (Minnitt, 1975)
Column 7 : Websterite - Koedoe Ultramafic Body (Viljoen and Viljoen, 1970).

(Columns 1 - 4 : Analysts - Bergstrom and Bakker).

Body, whilst the other two, samples P1 and P2 (Figure 3) are from metapyroxenites in the Core Zone Layered Body. Sample T7-4, from the Richmond body is seen to have a composition conforming closely to orthopyroxenites from the Stolzburg Layered Body, southwest of Barberton (Anhaeusser, 1976a). A comparision of the whole rock chemistry between sample T7-4 and the Stolzburg orthopyroxenites is presented in Table 4. Samples P1 and P2, from the Core Zone Layered Body, are seen to have compositions corresponding fairly closely to that of a clinopyroxenite (websterite) from the Koedoe Ultramafic Body described by Viljoen and Viljoen (1970), (Table 2). The ACM diagram (Figure 6) also exhibits the similiarity in composition between P1, P2 and the Koedoe body websterite, but because of significant differences in the CaO content of P1 and P2 (Table 2) the similiarities in composition are not reflected in Figure 7. The sample P2 appears to have a lower CaO value than the typical websterite, i.e. 8% as compared to approximately 14%.

The compositions of two serpentinites S1 and S2 (Figure 3) from the Core Zone Layered Body are also plotted on Figures 6 and 7. These compositions correspond closely with the compositions given for average serpentinized peridotites or harzburgites obtained from a variety of localities in the Barberton area (Anhaeusser, 1976a). Analyses of serpentinized peridotites and harzburgites from the Barberton region as well as a serpentinized ultramafic rock from the Murchison greenstone belt are listed in Table 2, for comparison with the samples S1 and S2 from the Core Zone Layered Body.

The analyses of samples of serpentinite and metapyroxenite from the Core Zone Layered Body have been plotted on a diagram which illustrates the variation in the composition of these samples with height in the stratigraphic column (Figure 8). This diagram attempts to establish the nature of differentiation within the Core Zone body. It is seen that with increasing height in the stratigraphic column SiO_2,

FIGURE 8

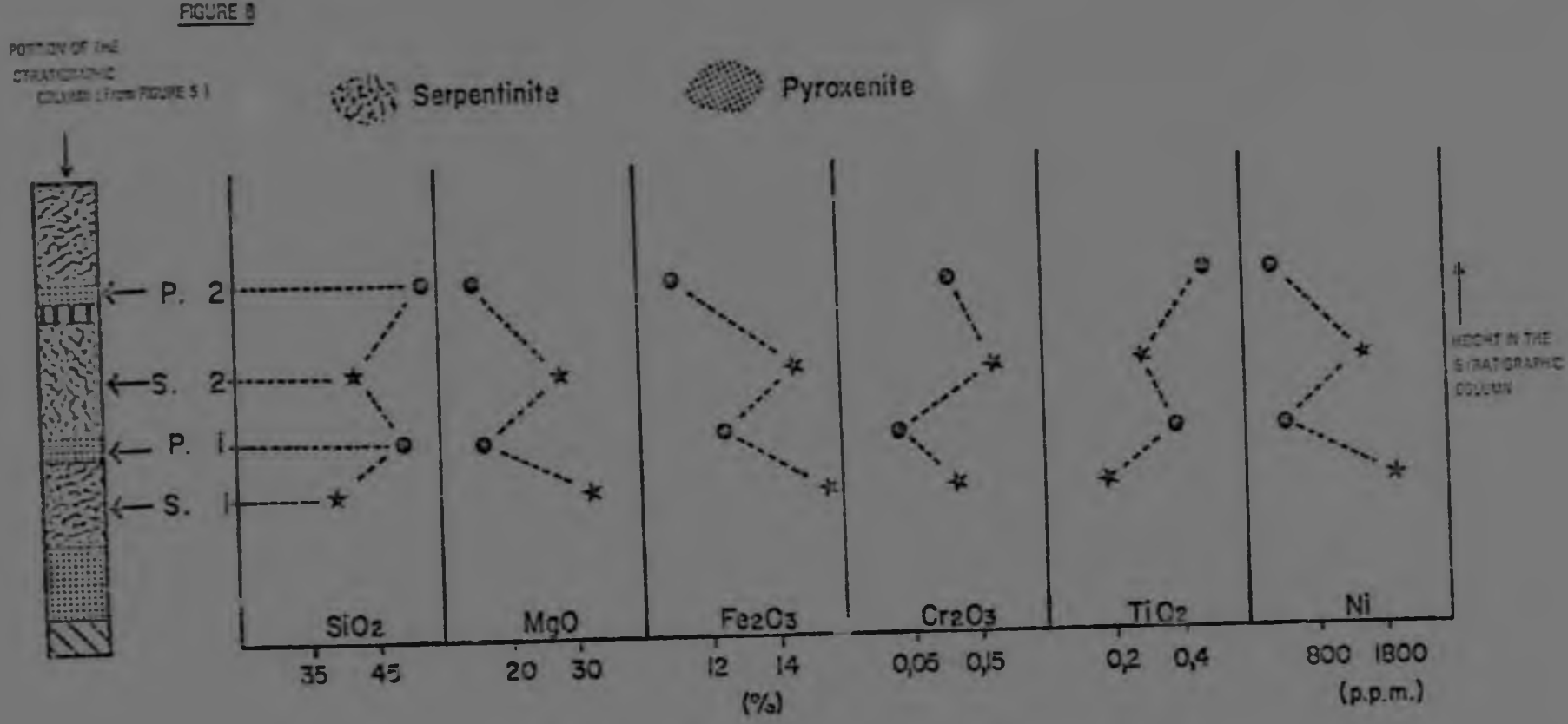

Figure 8. Diagram showing plots of various elements v stratigraphic height for four samples from the Core Zone Layered Body, Barclay Vale Schist Belt. Cyclically repetitive units of serpentinite (possibly originally dunite) and metapyroxenite show upward differentiation trends.

TABLE 3.

BASALT AND AMPHIBOLITE FROM THE BARCLAY VALE SCHIST BELT AND SIMILIAR ROCK TYPES FROM OTHER GREENSTONE BELTS IN THE EASTERN TRANSVAAL.

	1.	2.	3.	4.
	T8-M.D.1	T7-16		
SiO_2	50,65	51,43	53,75	52,88
TiO_2	0,75	0,69	0,87	0,48
Al_2O_3	10,26	11,76	10,02	7,56
Fe_2O_3	14,99	12,73	11,15	10,63
MnO	0,2	0,16	0,22	0,24
MgO	11,50	10,65	10,30	11,49
CaO	9,17	10,24	10,18	12,53
Na_2O	0,01	0,02	2,70	1,76
K_2O	0,24	0,38	0,47	0 05
P_2O_5	0,13	0,12	0,06	0,07
Cr_2O_3	0,04	0,07	-	-
L.O.I.	1,98	0,82	-	1,91
TOTALS	99,91	99,08	99,72	99,60

Column 1 : Pillowed basalt - Barclay Vale Schist Belt.
Column 2 : Amphibolite - Barclay Vale Schist Belt.
Column 3 : Average Barberton type basaltic komatiite, (Viljoen and Viljoen, 1969a).
Column 4 : Mafic lava (Barberton-type komatiite), Murchison Range (Minnitt, 1975).

(Columns 1 and 2 : Analyst - L.J. Robb, E.X.A.M. Unit)

TABLE 4.

PYROXENITE AND TREMOLITE SCHIST FROM THE FARM RICHMOND 287JT, BARCLAY VALE SCHIST BELT, AND SIMILIAR ROCK TYPES FROM OTHER GREENSTONE BELTS IN THE EASTERN TRANSVAAL.

	1		3	4
	T7-4	T7-9A		
SiO_2	51,95	51,69	52,94	50,32
TiO_2	0.01	0.09	0.08	0.09
Al_2O_3	2.49	2.75	1,50	5,08
Fe_2O_3	9,01	8,02	7,13	8,19
MnO	0,17	0,13	0,18	0,05
MgO	29,45	27,65	30,65	22,37
CaO	4,13	3,22	1,95	8,59
Na_2O	0,01	0,01	0,05	0,49
K_2O	0,01	0,01	0,09	0,01
P_2O_5	0,02	0,12	0,03	0,03
Cr_2O_3	0,53	0,42	-	-
L.O.I.	3,04	5,11	4,74	4,21
TOTALS	100,87	99,81	99,34	99,43

Column 1 : Altered pyroxenite - Barclay Vale Schist Belt.

Column 2 : Fine grained tremolite schist - Barclay Vale Schist Belt.

Column 3 : Orthopyroxenites - Stolzburg Layered Body (Anhaeusser, 1976a).

Column 4 : Tremolite-actinolite schist, Murchison Range (Minnitt, 1975).

Columns 1 and 2 : Analyst - L.J. Robb, (E.X.A.M. Unit)

Cr_2O_3 and TiO_2 increase in respective serpentinite and metapyroxenite layers whilst MgO, $Fe_2O_3$and Ni decrease. Hence younger intrusive phases (magma heaves) become successively more differentiated. The behaviour of Fe_2O_3 is, however, anomalous, in comparison to the behaviour of MgO. As differentiation increases the MgO content decreases and it is expected, because of MgO - FeO solid solution, that Fe_2O_3 should concomittantly increase. The Fe_2O_3 content however, clearly decreases with differentiation, the reason is unknown, but may possibly be related to analytical uncertainty.

Finally, purely for taxonomic purposes, mention is made of an analysis of a fine-grained tremolite schist (sample T7-9A, Figure 4) which was described in the section dealing with the geology of the marginal areas of the Barclay Vale Schist Belt. The sample, listed in Table 4, has a composition similiar to a tremolite-actinolite schist from the Murchison greenstone belt.

VII. SUMMARY AND CONCLUSIONS

The Barclay Vale Schist Belt may be divided into two subdivisions, each exhibiting distinct lithological characteristics :-

(i) The marginal areas consist of a sequence of amphibolites, chlorite and talc-chlorite schists with volumetrically minor amounts of serpentinite, pyroxenite and chert. The chlorite and talc-chlorite schists were probably originally basaltic and peridotitic flows of volcanic origin, similiar to those seen in the type area of the lower Onverwacht Group in the Barberton greenstone belt. Amphibolitic rocks in portions of the marginal areas may originally have been a banded tuffaceous sequence which has since undergone deformation as a result of their proximity to a highly sheared granite-greenstone contact. In addition to the extrusive succession of mafic and ultramafic volcanic rocks there is a small layered sill-like body (the Richmond Layered Body) which consists

of a differentiated sequence of serpentinites (possibly originally dunites or peridotites), metapyroxenites, amphibolites, and possibly tremolite-actinolite schist.

(ii) The core region of the Barclay Vale Schist remnant consists of cyclically alternating layers of serpentinite and metapyroxenite with continuous and discontinuous layers or lenses of banded iron-formation. The serpentinites and metapyroxenites represent a differentiated sequence (the Core Zone Layered Body) which has intruded the pre-existing rocks (banded iron-formations) in a sill-like fashion. It is likely that a number of separate magma heaves were responsible for the emplacement of the Core Zone body.

The rocks of the Barclay Vale Schist Belt can be correlated with the Lower Ultramafic Unit (or Tjakastad Sub-Group) of the Onverwacht Group, as outlined by Viljoen and Viljoen (1969e). This correlation is based on the following considerations :-

(i) The presence of large volumes of chlorite and talc-chlorite schists which probably represent highly altered mafic and ultramafic lavas (i.e. basalt and peridotite lava flows).

(ii) The presence, in basaltic rocks, of pillow structures indicating an extrusive, subaqueous origin for these rocks.

(iii) The presence of rocks with komatiitic affinities, a special characteristic of the lower Onverwacht assemblages.

(iv) The presence of chemical sediments in the form of banded iron-formations, cherts and, banded and fuchsitic cherts.

(v) The presence of intrusive, layered, differentiated ultramafic sill-like bodies.

CHAPTER 3

THE GRANITES

I. INTRODUCTION

(a) General Statement

This section gives a brief description of the techniques employed in producing the accompanying map of granite types and textures (Figure 10). Comprehensive photographic cover was available over the area in the form of 1:30 000 aerial photographs. All major geological features were recorded on the photographs and geological details pertaining to granite textures, structures, colour, the nature of inclusions and other related data, were recorded on specially prepared field data sheets. The map of granite types and textures (Figure 10) was compiled using the information from the 1:30 000 aerial photographs, together with that from the field data sheets. With the exception of discrete granite bodies, such as the Mpageni Granite and, to a lesser extent, the Hebron Granodiorite and the Cunning Moor Tonalite, contacts on this map are approximate and gradational. In certain areas shown in Figure 10, textural types are deliberately superimposed, for example in those areas where the Hebron Granodiorite occurs in bimodal association with the porphyritic granites. It will also be noted that porphyritic granites cover large areas, however their representation in Figure 10 is an oversimplification as they are characterized by considerable variations in the degree of phenocryst development.

(b) Chemical Analyses of the Granites

Approximately 76 full silicate analyses and over 200 partial analyses are referred to in this chapter. The full silicate analyses were all carried out by the writer using the energy-dispersive analytical equipment at the Geological Survey, Pretoria. The partial analyses (K_2O,

Na_2O, Rb, Sr and Ba) were undertaken, also by the writer, on the Philips X-ray fluorescence spectrometer in the Geology Department at the University of the Witwatersrand. A comprehensive account of the analytical procedures used in this dissertation is presented in Appendix 1.

(c) Granite Classification

In this dissertation the system of granite classification used is that devised by Harpum (1963). This simple scheme is based solely on K_2O/Na_2O ratios and its merits are found in its applicability to the range of rock types commonly found in Archaean granite terranes. The classification is presented in Figure 9, and is also summarized below :-

$K_2O/Na_2O < 0,6$ - Tonalite
$0,6 < K_2O/Na_2O < 1,0$ - Granodiorite
$1,0 < K_2O/Na_2O < 1,5$ - Adamellite
$K_2O/Na_2O > 1,5$ - Granite

One point requires clarification : the term "granite", where used on its own in the text, refers to the full range of rock types of granitic texture and affinity, whereas the term "granite (sensu stricto)" specifically implies that class of granitic rock with a K_2O/Na_2O ratio greater than 1,5.

In the various K_2O v Na_2O plots used in the text, portions of Harpum's granite classification scheme (Figure 9) are superimposed on the actual plots to provide an indication of the compositional range of the rock types being described.

(d) Brief Geological Description of the Granitic Terrane Between Nelspruit and Bushbuckridge

The various granite types and textures encountered

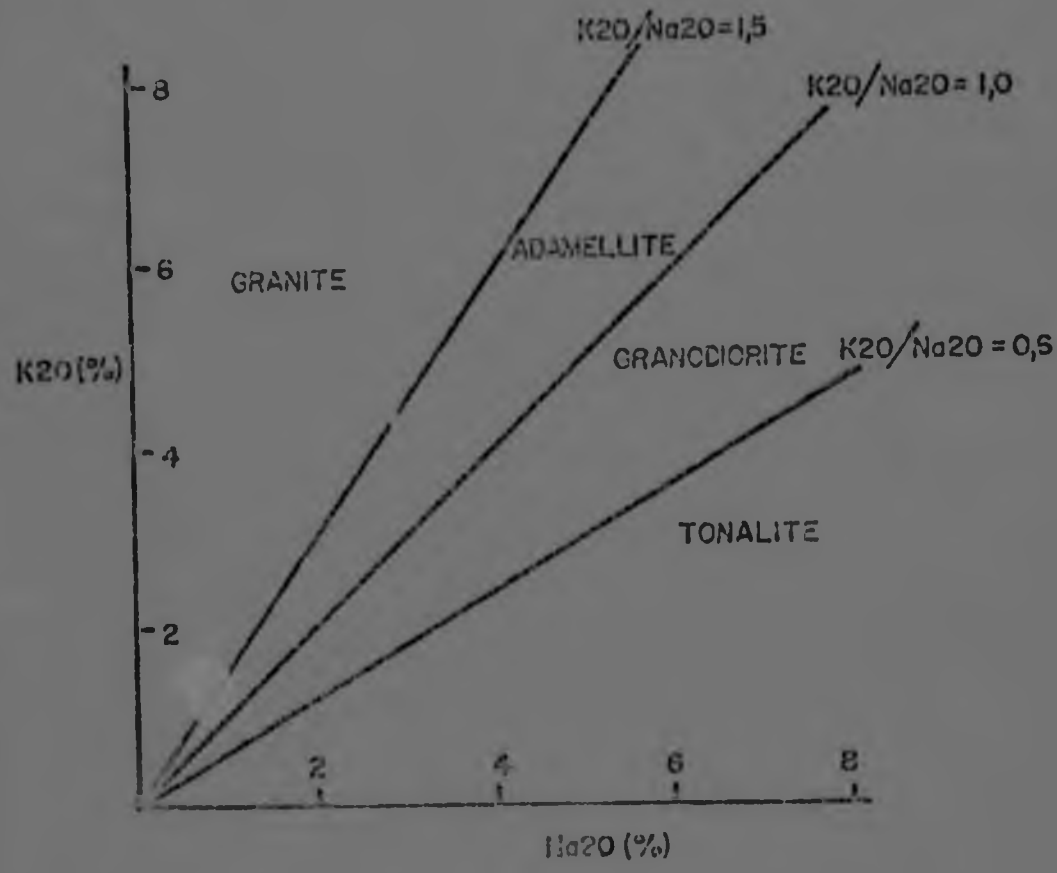

Figure 9. The classification of granitic rocks based on K_2O/Na_2O ratios (after Harpum, 1963).

in the area between Nelspruit and Bushbuckridge, are shown in Figure 10. Six varieties of granite are described in this area :-

(i) The Tonalite Gneisses and Migmatites are a complex, highly sheared, suite of rocks occurring in the immediate vicinity of greenstone remnants found in the area. The tonalite gneisses intrude the latter and migmatites are probably developed as the result of the interaction between tonalite and greenstone.

(ii) The Nelspruit Migmatite and Gneiss Terrane is generally more potassic than the Tonalite Gneisses and Migmatites and is best developed in the valleys of the Crocodile and Nsikazi Rivers in the south and east of the study area.

(iii) The Nelspruit Porphyritic Granite underlies the largest portion of the study area and consists of a massive, coarse-grained granite which is characterized by the ubiquitous development of medium-to-large microcline phenocrysts.

(iv) The Hebron Granodiorite forms a prominent pluton in the centre of the study area and intrudes the Nelspruit Porphyritic Granite.

(v) The Cunning Moor Tonalite occupies the very flat and low-lying terrane in the northeastern quadrant of the study area. It also post-dates the Nelspruit Porphyritic Granite.

(vi) The Mpageni Granite pluton is a coarse-grained potassic granite which intrudes the Nelspruit Migmatite and Gneiss Terrane in the southeast of the study area.

The impression may have been gained from Chapter 1, that the Archaean granitic terrane north of Nelspruit consists of a uniform rock-type which has been referred to previously as the "Nelspruit Gneisses and Migmatites". It can be seen from the break-down of granite types listed above, that this view is all too simplistic. Details of the nature of these various granite categories are presented in the following sections.

II. THE TONALITE GNEISSES AND MIGMATITES

(a) Field Description

The Tonalite Gneisses and Migmatites occur in two discrete areas (Figure 10). These areas include : (i) the southwestern corner of the study area where tonalite gneisses flank the Barclay Vale Schist Belt, and (ii) the southeastern corner of the area where tonalite gneisses are found north of the Ship Hill Layered Ultramafic Body near Kaapmuiden (Plate 2 a) . It is noticeable that the tonalite gneisses occur primarily in the immediate vicinity of greenstone remnants.

In the field the tonalites are almost invariably gneissic but in some areas migmatites are developed (Plate 2b and c). Where migmatites occur the contrast between light and dark bands is often very distinct and the impression may be gained that the darker, mafic portions have been intruded by the lighter, felsic component. It is conceivable therefore that these migmatites have formed as the result of the interaction between tonalitic material and pre-existing greenstone stratigraphy.

The tonalite gneisses themselves exhibit a pronounced mineral foliation which is invariably parallel to the schistocity of the adjacent greenstone remnants (Figure 3). This feature has been described previously by Anhaeusser (1969) and Viljoen and

Viljoen (1969b) and is discussed in Chapter 2.

The tonalite gneisses in both outcrop areas mentioned above are characterized by shearing and mylonitization, which considerably alters their texture and geochemical character (see later). Sheared tonalite gneisses have a friable texture in which "sweat" quartz veinlets and blebs are common.

The field relationships between the Tonalite Gneisses and Migmatites and the surrounding more potassic rocks are not clear (Figure 10). However, the transition takes place over a relatively short distance as the surrounding potassic material is considered to have intruded the preexisting tonalitic crust. These ideas are enlarged upon in Chapter 7.

(b) Petrography

The tonalites are generally pale-grey leuco-gneisses and are medium-to-fine grained, but may appear recrystallized in the vicinity of shear zones. They consist predominantly of plagioclase and quartz with lesser amounts of microcline and biotite. Much of the latter mineral has been chloritized. Plagioclase is, typically, poorly twinned but combinations of albite, pericline and Carlsbad twin varieties were observed. Twin lamellae are narrow when developed, indicating a composition range towards the sodic end of the plagioclase solid-solution series (Heinrich, 1965). Random sericitization of the plagioclase is also evident.

Quartz is characterized by extremely undulose extinction and exhibits sutured or crenulated boundaries. These recrystallization features are considered to be related to stress conditions associated with the shearing that has taken place in these rocks. Tonalite gneisses examined in the

vicinity of a shear zone, show extensive alteration to sericite. The effect of this sericite alteration is reflected in the K_2O content of these samples (6,6% K_2O - sample O-MONT, Table 23, Appendix 2). Workers in the Lewisian Complex of northwest Scotland (Beach and Fyfe, 1972; Beach, in press) and also in the Johannesburg-Pretoria Dome (Anhaeusser, 1973b) have described similiarly high potash contents in rocks associated with major shear zones. Beach and Fyfe (1972) attributed the high potash contents of these rocks to synkinematic metasomatic fluids. Further effects of mylonitization of these tonalite gneisses are discussed in the following section.

(c) Geochemistry

Full silicate analyses of eight samples of tonalite gneiss are presented in Table 5. This data, together with the data from the partial analyses carried out on the tonalite gneisses (Table 23, Appendix 2), is plotted on a K_2O v Na_2O diagram (Figure 12) and on a Rb v Sr diagram (Figure 13).

It is evident from Table 5 that three of the samples analysed may now no longer be regarded as tonalites, having high potash values (>3,0%) and K_2O/Na_2O ratios (>0,5). These three samples (I4, I5 and A65), were taken in the immediate vicinity of a sheared and mylonitized zone in the gneisses. The sheared and altered tonalites, together with the unaltered tonalite gneisses are plotted on a K_2O v Na_2O diagram (Figure 12). The former have K_2O/Na_2O ratios well outside the tonalite field indicating that mylonitization has a pronounced effect on the compositional characteristics of this rock type. The tonalite gneisses that have not undergone shearing all fall in or near the field of tonalite as defined in Harpum's classification scheme (Figure 12). The average composition of these tonalites (Table 5, Column 9) is very similiar to the composition of an average tonalite

TABLE 5

ANALYSES OF THE TONALITIC GNEISSES AND MIGMATITES AND AN AVERAGE TONALITIC GNEISS FROM THE ANCIENT GNEISS COMPLEX, SWAZILAND

	1	2	3	4	5	6	7	8	9	10
Sample	II	IIa	14*	15*	16	17	A62	A65*		
SiO_2	57,47	70,53	70,75	68,84	72,57	65,37	71,74	72,00	67,54	71,16
TiO_2	0,69	0,29	0,15	0,29	0,09	0,29	0,19	0,16	0,33	0,34
Al_2O_3	18,65	16,83	16,67	16,87	16,49	17,73	16,84	14,14	17,31	14,84
Fe_2O_3	6,42	2,33	1,39	2,75	0,94	3,18	1,76	1,39	2,93	2,29
MnO	0,11	0,06	0,06	0,08	0,04	0,08	0,04	0,04	0,07	0,02
MgO	5,29	0,43	0,52	0,07	0,51	1,64	1,19	0,77	1,81	0,95
CaO	4,40	2,72	1,57	1,63	2,29	2,55	0,82	1,62	2,88	3,18
Na_2O	4,71	3,98	4,35	4,11	4,13	3,82	4,76	5,37	4,36	4,82
K_2O	1,31	0,80	3,64	4,08	1,36	1,85	2,41	3,21	1,55	1,65
P_2O_5	0,01	0,01	0,01	0,01	0,01	0,01	0,01	0,01	0,01	0,12
L.O.I.	1,34	1,43	0,55	0,64	0,86	1,49	1,06	0,72	1,24	0,82
TOTALS	100,38	99,41	99,54	99,36	98,86	98,06	100,83	99,13	100,03	100,19
ppm										
Rb	123	62	96	172	52	51	81	94	74	-
Sr	402	342	297	213	366	442	132	401	337	-
Ba	703	288	360	571	219	213	494	492	383	-

* Tonalite gneisses altered by shearing and mylonitization.

Column 9 : Average of six tonalite gneisses, from various localities in the Nelspruit area.

Column 10 : Average tonalitic gneiss, Ancient Gneiss Complex, Swaziland (Hunter, 1973a)

Sample localities - see Figure 11.

Analyst : L.J. Robb

gneiss from the Ancient Gneiss Comples of Swaziland (Table 5, Column 10). Although similiar in composition it should be noted that the tonalites from the Ancient Gneiss Complex are considered to pre-date the Swaziland Supergroup (Hunter, 1973a), whereas the tonalite gneisses described in this section are considered to intrude the Barclay Vale Schist Belt (correlated with the lower Onverwacht Group, Chapter 2). This point will be enlarged upon in the following section.

The plot of Rb v Sr (Figure 13) shows a wide scatter of data similiar to that evident in the K_2O v Na_2O plot. The samples of sheared tonalite gneiss are characterized by somewhat higher Rb and lower Sr values than those samples unaffected by mylonitization. It appears that the process of mylonitization (possibly involving the transportation of various mobile ions by metasomatism, as suggested by Beach and Fyfe, 1972) results, not only in an increase in potash, but also in Rb content, with a concomittant decrease in the Sr content. In this respect Visser and Verwoerd (1960) have also described decreases in the soda and alumina content of rocks associated with major shear zones.

(d) Summary and Conclusions

(i) The tonalite gneisses and migmatites consist predominantly of gneissic rocks with minor occurrences of migmatites. An important feature, in the study area, is their close proximity to greenstone material.

(ii) These rocks are intensively sheared, a feature which is reflected in marked changes in texture and chemistry.

(iii) The relationship between the tonalite gneisses and migmatites and the more potassic Nelspruit

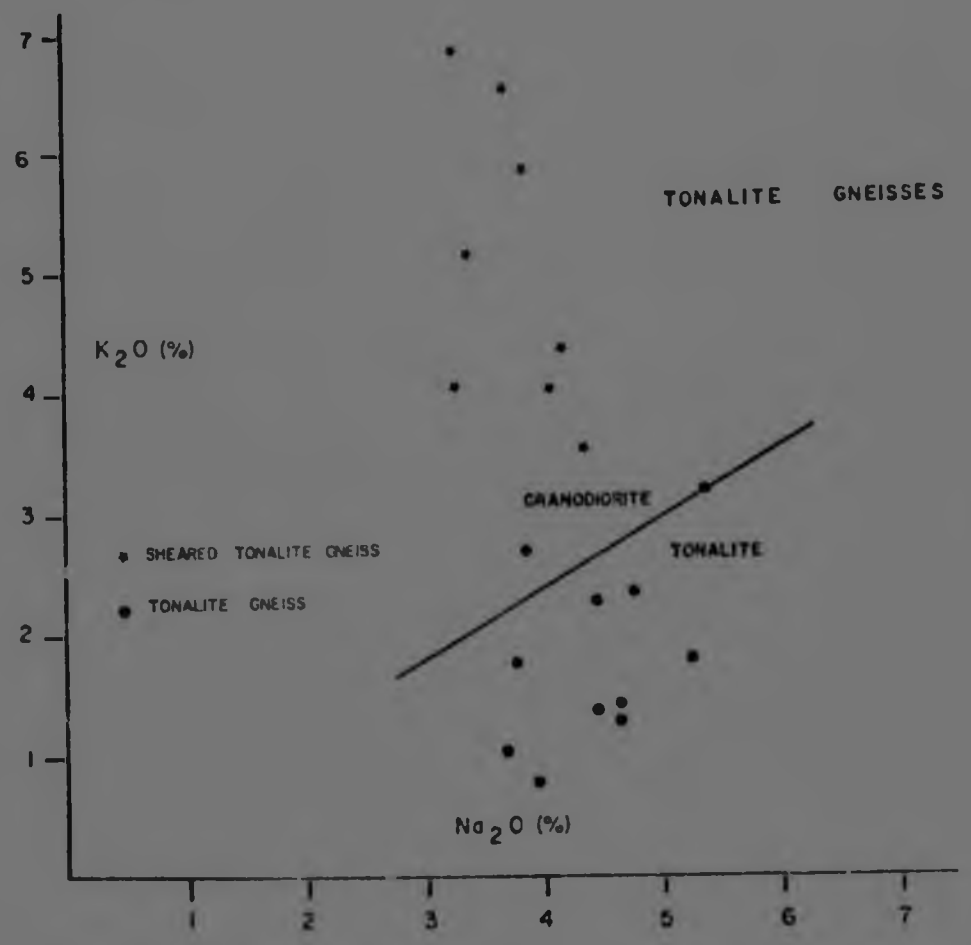

Figure 12. K_2O v Na_2O plot - Tonalite Gneisses and Migmatites. Circles represent tonalite gneiss, stars represent sheared tonalite gneiss.

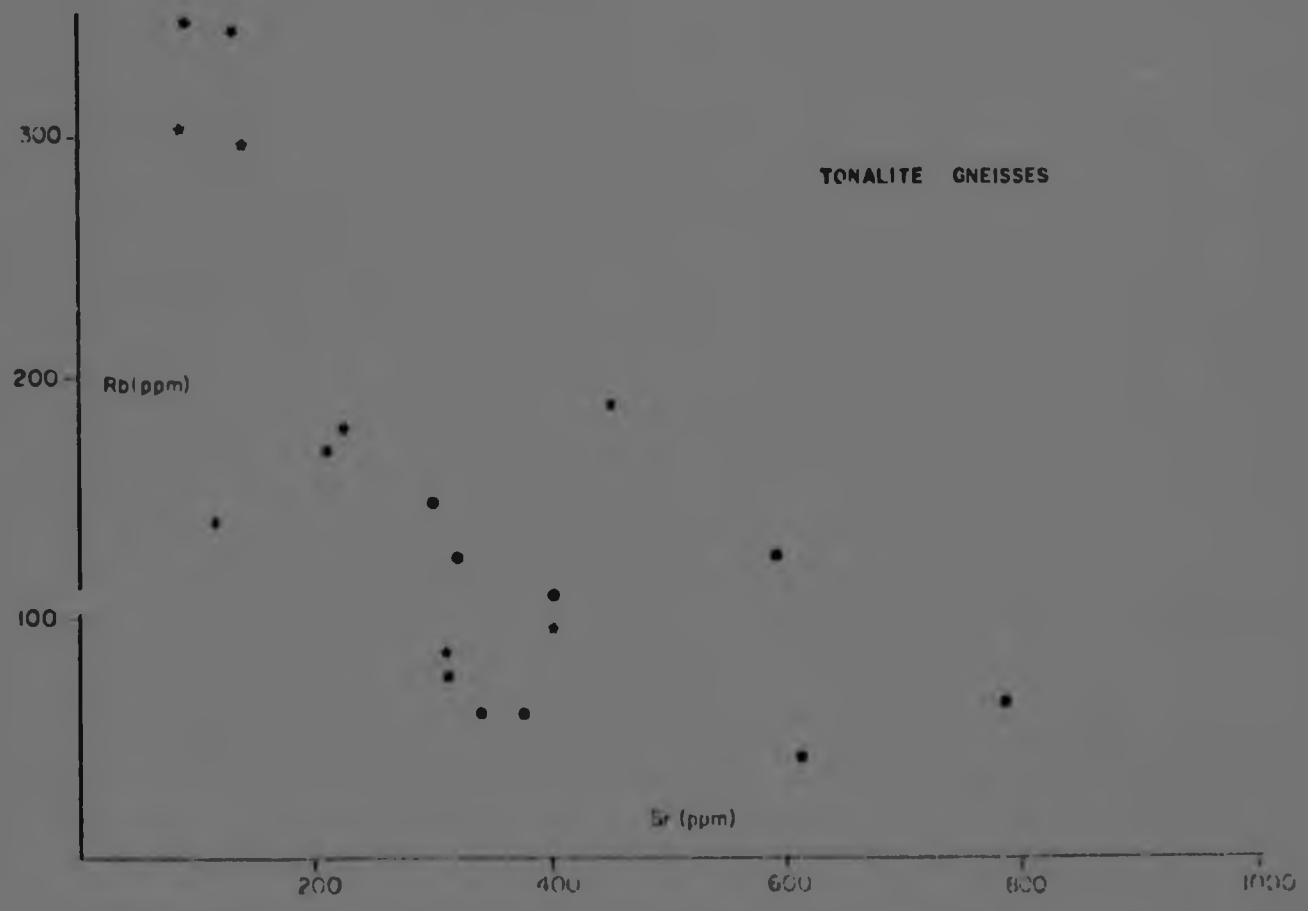

Figure 13. Rb v Sr plot - Tonalite Gneisses and Migmatites.

Migmatite and Gneiss Terrane is not clearly demonstrated, but in the light of previous work done on the Archaean granite terrane in the Barberton region (Chapter 1), the latter is considered to post-date the former. Geochronological work carried out in the Barberton region invariably suggests that the tonalitic rocks are older and thus represent earlier portions of the sialic crust, than their potassic counterparts in the same area (Anhaeusser, 1973a).

(iv) The Tonalite gneisses and migmatites are similiar in composition (Table 5) and texture to tonalite rocks of the Ancient Gneiss Complex in Swaziland. In Swaziland, Hunter (1973a) has described these rocks as being older than the Swaziland Supergroup, however the tonalite gneisses and migmatites in the study area are thought to intrude the Barclay Vale Schist Belt, the latter being correlated with the lower Onverwacht Group (Chapter 2). Whereas it is possible that the tonalite gneisses and migmatites are unrelated to rocks of the Ancient Gneiss Complex it is also not inconceivable that these differences may be the result of divergent opinions regarding the nature of the earth's earliest crust.

III. THE NELSPRUIT MIGMATITE AND GNEISS TERRANE

(a) General discussion on the origin of migmatites

Migmatites, and indeed granites themselves, have long been the subject of considerable controversy amongst earth scientists, particularly with regard to their origin and mode of formation. In the past a state of affairs, now referred to as the "granite controversy", existed, whereby

various schools of thought (French, Scandinavian, American) vied with each other to put forward a uniformitarian idea regarding the origin of granites and migmatites. The classic work by Read (1957) entitled "The Granite Controversy" was succint in outlining the arguments behind the various thoughts on granites, including suggestions that various granites may have widely differing origins.

One of the single most comprehensive reviews of migmatites was provided by Mehnert (1968) in his book "Migmatites and the Origin of Granitic Rocks". In this book the views of the classic workers on granitic rocks, (Erdmannsdorfer, Niggli, Schneiderhöhn, Michel-Levy and Holmquist) are combined, to provide a balanced account of both classic and recent ideas on the origins of granites and migmatites. Consequently three modes of formation of granitic (and related migmatitic) rocks are considered :-

(i) the magmatic formation of granite whereby the rock forms by crystallization from pristine mantle derived liquid,

(ii) the anatectic formation of granite whereby the original granitic liquid is derived by the melting of a pre-existing rock type,

(iii) the metasomatic formation of granite which involves the in situ changing of a pre-existing rock type by the infiltration of granite-forming fluids or "ichor".

Migmatitic rocks, defined essentially as "mixed rocks" composed of felsic and mafic portions, can be genetically classified in a different way :-

(i) migmatites of venitic origin are formed by partial anatexis of a parent rock with differentiation processes causing the separation between light and

dark bands,

(ii) migmatites of arteritic origin are formed when felsic material is intruded as a liquid of completely foreign origin, into a mafic parent.

A combination of these two schemes indicates that venitic migmatites are anatectically formed granitic rocks whereas arteritic migmatites are essentially magmatic (or perhaps metasomatic) in origin. It is therefore, particularly difficult to distinguish between migmatites of different origins without a detailed knowledge of the chemistry of the whole rock system.

(b) Migmatite terminology used in this dissertation

An important result of the 21st International Geological Congress held in Copenhagen, in 1960, was the definition of uniform terminology regarding migmatites. This terminology, which has been adopted by Mehnert (1968) has limitations in that certain of the terms have genetic implications. "In order to obtain an acceptable nomenclature of migmatites it is expedient to separate descriptive terms from those with a genetic content" (Mehnert, 1968).

As only a purely descriptive terminology was required for the purposes of this dissertation an abbreviated form of Mehnert's (1968) migmatite terminology was adopted. The few terms, described below, were found to be adequate in describing the various migmatitic and gneissic rocks encountered in the study area :-

PALEOSOME : Predominently mafic (melanocratic) portion of the migmatite.

LEUCOSOME : Predominently felsic (leucocratic) portion of the migmatite.

SCHOLLEN : A migmatite where fragments of paleosome are "floating" within homogenous leucosome.

STROMATIC : A migmatite in which paleosome and neosome form distinct layers or bands. Gneisses are a diffuse form of a stromatic textured migmatite.

FOLDED : A stromatic or gneissic textured migmatite where folding or buckling occurs.

SCHLIEREN : A highly diffuse migmatite characterized by light and dark streaks which are often contorted.

(c) Field description

Large areas between Nelspruit and Bushbuckridge are underlain by granitic rocks which exhibit gneissic textures and are commonly migmatitic. The Nelspruit Migmatite and Gneiss Terrane (Figure 10) is distinct from the tonalite gneisses and migmatites previously described both chemically and texturally, as will be seen from the following description. The Nelspruit migmatites and gneisses occur in three distinct zones in the study area :-

(i) a southern belt located along the Crocodile River valley,

(ii) an eastern belt situated along the Nsikazi River valley bordering the Kruger National Park and,

(iii) an east-west trending belt largely occupying the Sabie River valley.

In addition, isolated occurrences of migmatites and gneissic textured rocks exist throughout the study area (Figure 10).

A large variety of migmatites are seen in the field and some of the main textural types are illustrated in Plate 2 (d,e and f) and Plate 3 (a and b). No distinction is made between the terms "migmatite" and "gneiss"; this is deliberate as these two textural types are considered to be gradational and, as indicated above in the section on migmatite terminology, a gneiss is considered as a diffuse (granitized?) stromatic

PLATE 2

A. Typical terrain underlain by the Tonalite Gneisses and Migmatites north of Kaapmuiden. In the background to the northwest, the hilly terrain is underlain by the more potassic Nelspruit Migmatite and Gneiss Terrane.

B. Tonalite Gneisses and Migmatites east of the Barclay Vale Schist Belt, at sample locality Il (Figure 11). The dark, mafic material represents a relic fold apparently intruded (in a lit-par-lit fashion) by tonalitic material.

C. Tonalite Gneisses and Migmatites east of the Barclay Vale Schist Belt. The mafic material again showing apparent lit-par-lit intrusion by tonalitic material.

D. Layered or stromatic structure in migmatites from the Nelspruit Migmatite and Gneiss Terrane, from an area approximately 5km south of White River.

E. Mafic rafts or xenoliths in migmatites from the Nelspruit Migmatite and Gneiss Terrane. Locality, approximately 3km north of Hazy View.

F. Folded migmatites in the Nelspruit Migmatite and Gneiss Terrane approximately 20km north of Kaapmuiden.

PLATE 2

A

B

C

D

E

F

textured migmatite.

Two unusual textural features, which may have some bearing on the genetic aspect of migmatite development, occur within the Nelspruit Migmatite and Gneiss Terrane :-

(i) in the Sabie River valley, near Hazy View (Figure 10) there is an occurrence of migmatite xenoliths (Plate 3 c and d) This outcrop consists essentially of a schollen textured migmatite where the"rafted' material is in itself, also a migmatite. The interpretation placed on the textures in this exposure suggest that a pre-existing stromatic migmatite has been intruded by a more potassic granitic magma. Plate 3e, from this outcrop, shows two distinct types of leucosome, with A appearing tonalitic in composition and veins B, appearing similiar to the surrounding, intrusive, more potassic granite. The indication is, therefore, that the second,schollen migmatite, is arteritic in origin, having developed later in the sequence of events. The stromatic migmatite rafts may be related to the Tonalite Gneisses and Migmatites described previously.

(ii) in the Crocodile River valley, 1km west of Nelspruit, large biotite xenoliths were noted, the latter being extensively pervaded by large (2-3cm long) euhedral microcline phenocrysts which are aligned parallel to the schistocity in the xenolith (Plate 4a). The surrounding granite is also extensively porphyritic and it appears that locally induced metasomatism may have been responsible for transporting K-felspar-rich fluids along planes of greatest penetrability (i.e. parallel to the schistocity) in the xenolith. This unusual occurrence of biotite xenolith is perhaps an indication of the complex interaction of processes that have been involved in the development of the migmatite and gneiss terrane and surrounding granites.

(d) A Note on the Significance of Relief within the Nelspruit Migmatite and Gneiss Terrane

As mentioned briefly in Chapter 1, previous workers (Viljoen and Viljoen, 1969b; Hunter, 1973a) have noted the correlation between granite type (in particular the potash content of the granite) and topography in the Barberton region. In the study area it is no coincidence that the major portion of the Nelspruit Migmatite and Gneiss Terrane occurs in three major river valleys which are generally low-lying with respect to the Nelspruit Porphyritic Granite. The relationship between the Nelspruit Porphyritic Granite and the migmatite and gneiss terrane is analogous to that which exists between the Hood Granite (forming the Lochiel Plateau) and the low-lying Ancient Tonalites of Swaziland (Viljoen and Viljoen, 1969b). In the latter case the Hood Granite is thought to overlie the Ancient Tonalites as a sheet or a hood. In the north of the Barberton Mountain Land, however, it is the Nelspruit Porphyritic Granite which occupies the higher lying terrane and the migmatites and gneisses which occupy the lower lying areas. A quantitative assessment of the relationship between topography and granite type (the latter based mainly on chemistry) is given in Chapter 4.

(e) The Suggested Relationship between the Nelspruit Migmatite and Gneiss Terrane and the Nelspruit Porphyritic Granite

The Nelspruit migmatites and gneisses and the Nelspruit Porphyritic Granite are considered to be co-genetic. Although geochemical considerations confirm this, the impression is gained principally from field observations. In Figure 10 the Nelspruit Migmatite and Gneiss Terrane is shown as having a superimposed porphyritic texture with some areas even having intensely porphyritic textures. In many instances it is only possible to distinguish the Nelspruit migmatites and gneisses from the Nelspruit Porphyritic Granite by subtle schlieric or gneissic textures as both may exhibit the characteristic porphyritic texture. In short, therefore, it is envisaged that the migmatites and gneisses formed as the result of the interaction between the Nelspruit Porphyritic

PLATE 3

A. Mafic xenoliths and schlieren in migmatites from the Nelspruit Migmatite and Gneiss Terrane. Locality, approximately 15km west of Nelspruit.

B. Layered migmatites showing the distinction between the lighter coloured leucosome and the darker, more mafic, paleosome. Locality, Nelspruit Migmatite and Gneiss Terrane, approximately 25km north of Kaapmuiden.

C. Xenolith of layered migmatite surrounded by homogenous granitic material. Locality, sample site E8 (Figure 11) approximately 3km north of Hazy View.

D. Xenolith of layered migmatite surrounded by homogenous granitic material. Locality, sample site E8, approximately 3km north of Hazy View.

E. A close up view of part of a migmatite xenolith at sample locality E8 (Figure 11). The leucosomes marked A are tonalitic in composition and are related to the original migmatitic rock. The leucosomes marked B are more potassic in composition and are considered to be related to the surrounding granitic material.

F. A photograph of an aplite vein with a marginal coarse-grained pegmatitic phase. Locality, sample site A31 (Figure 11), south of the Nyamazaneni African Township.

PLATE 3

A

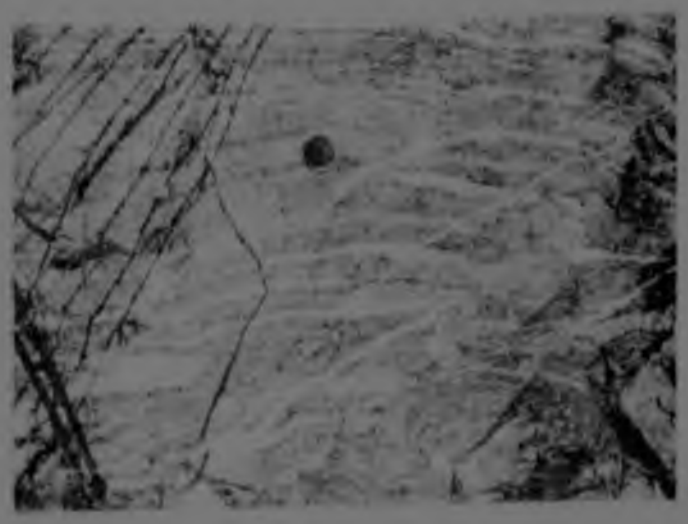

B

C

D

E

F

Granite and pre-existing crustal material (possibly similiar to the Tonalite Gneisses and Migmatites previously described), and in this sense, are co-genetic with the porphyritic granite.

(f) Petrography

The petrographic description of the migmatites and gneisses is divided into two sections, the first describing the leucosome of the migmatites and the second describing the paleosome.

(i) Leucosomes

The leucosomes consist predominantly of plagioclase, quartz and microcline with subordinate amounts of biotite. Minor amounts of muscovite, apatite and rutile may also be present. Two features characterize the leucosomes of the migmatites and gneisses, firstly the often marked, preferred orientation of the biotites and secondly the sutured quartz grain boundaries (Plate 4b). These textural characteristics suggest that tectonic stress has played a role in the history of development of these rocks.

An unusual feature, occasionally observed in the leucosomes, is the presence of poikilitic plagioclase. Some of the larger plagioclase grains were found to contain inclusions of an earlier plagioclase phase as well as biotite and quartz. No explanation is offered for this phenomenon, but it serves to indicate the complex petrogenesis involved in the formation of the migmatitic rocks in the area.

Random sericitization of the plagioclase is evident and myrmekitic micro-textures are present at plagioclase-microcline interfaces. The occasional microcline phenocrysts that are present are invariably markedly poikilitic and contain inclusions of plagioclase, quartz and biotite. This feature is indicative of the late formation of microcline in the rock.

(ii) Paleosomes

The mineralogy of the paleosomes was found to be more variable than that of the leucosomes. Biotite, plagioclase and quartz generally formed the main constituents but in some cases hornblende forms the main mafic component. Subordinate amounts of muscovite, microcline and epidote may be present as well as trace amounts of sphene, rutile, apatite and opaque oxides (often identified as pyrite in hand-specimen).

Paleosomes contain variable amounts of mafic minerals. This is thought to directly reflect the degree of granitization that the paleosome has undergone. Furthermore, the nature of the mafic mineral in the paleosome (i.e. biotite or hornblende) is a reflection either of the original composition of the parent mafic rock or, a further manifestation of the degree of granitization that the paleosome may have undergone. The principles behind granitization or assimilation (Nockolds, 1933) are particularly complicated and require detailed geochemical and thermodynamical work, and as a result are not considered in this dissertation.

(g) Geochemistry

This section deals with two topics :- (i) the general geochemical characteristics of the migmatites and gneisses and, (ii) a section on the origin and mode of formation of the migmatites and gneisses.

(i) Geochemical characteristics of the Nelspruit Migmatite and Gneiss Terrane

Full silicate analyses of samples from the migmatite and gneiss terrane are listed in Tables 6, 7 and 8, whereas partial analyses are presented in Table 24, Appendix 2. This data is diagrammatically represented in K_2O v Na_2O (Figure 14) and Rb v Sr (Figure 15) plots. The K_2O v Na_2O plot shows a wide range in compositions - in fact a continuum exists from tonalitic to granitic (sensu stricto) compositions. This

TABLE 6

ANALYSES OF SAMPLES FROM THE NELSPRUIT MIGMATITE AND GNEISS TERRANE

Samples	A23(i)	A23(ii)	D28A	E4B	E8B	B28	C22	C35	A46
SiO_2	64,32	68,38	64,12	67,69	68,80	72,98	71,76	69,94	62,87
TiO_2	0,50	0,14	0,53	0,3	0,36	0,13	0,21	0,24	0,51
Al_2O_3	17,98	16,63	18,33	17,17	16,43	14,31	14,42	15,85	18,66
Fe_2O_3	4,18	1,33	3,33	2,28	2,65	1,35	1,41	1,81	3,88
MnO	0,09	0,03	0,07	0,05	0,04	0,04	0,04	0,05	0,09
MgO	0,87	0,53	0,28	0,98	1,44	1,18	1,92	0,98	2,26
CaO	2,63	1,50	2,63	1,89	2,74	1,38	1,36	1,79	3,98
Na_2O	4,07	3,12	4,75	4,18	4,64	4,38	2,64	3,39	3,67
K_2O	3,84	6,52	3,88	4,93	1,70	4,32	6,53	4,36	1,82
P_2O_5	0,01	0,01	0,06	0,01	0,01	0,01	0,20	0,01	0,28
L.O.I.	0,41	0,67	0,70	0,67	0,61	0,50	0,31	0,48	0,73
TOTALS	98,91	98,85	98,73	100,18	99,47	99,38	100,80	98,90	98,67
ppm									
Rb	157	189	90	106	35	127	122	169	49
Sr	376	444	420	563	602	314	311	216	865
Ba	988	939	443	1362	248	348	1234	4[illegible]	459

A23(i) : Mafic portion of migmatite (i.e. paleosome).

A23(ii) : Felsic portion of migmatite (i.e. leucosome).

Sample localities - Figure 11.

Analyst : L.J. Robb

Figure 14. K_2O v Na_2O plot - Nelspruit Migmatite and Gneiss Terrane.

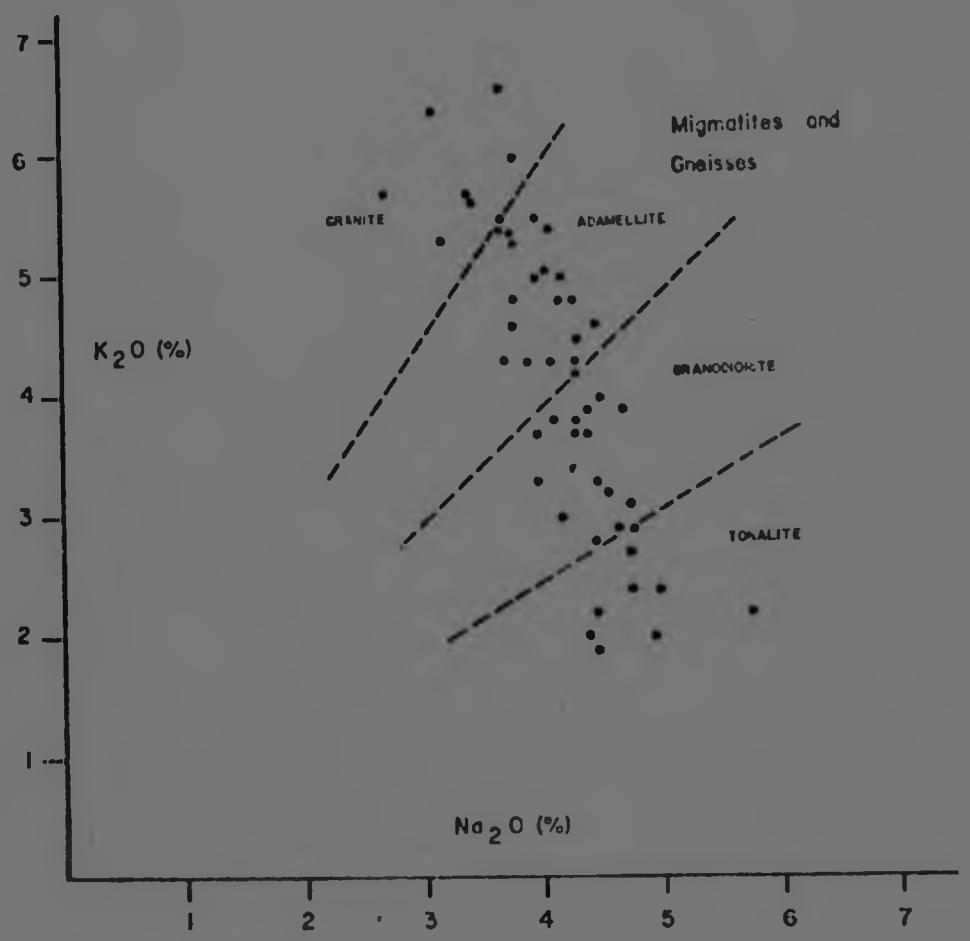

Figure 15. Rb v Sr plot - Nelspruit Migmatite and Gneiss Terrane.

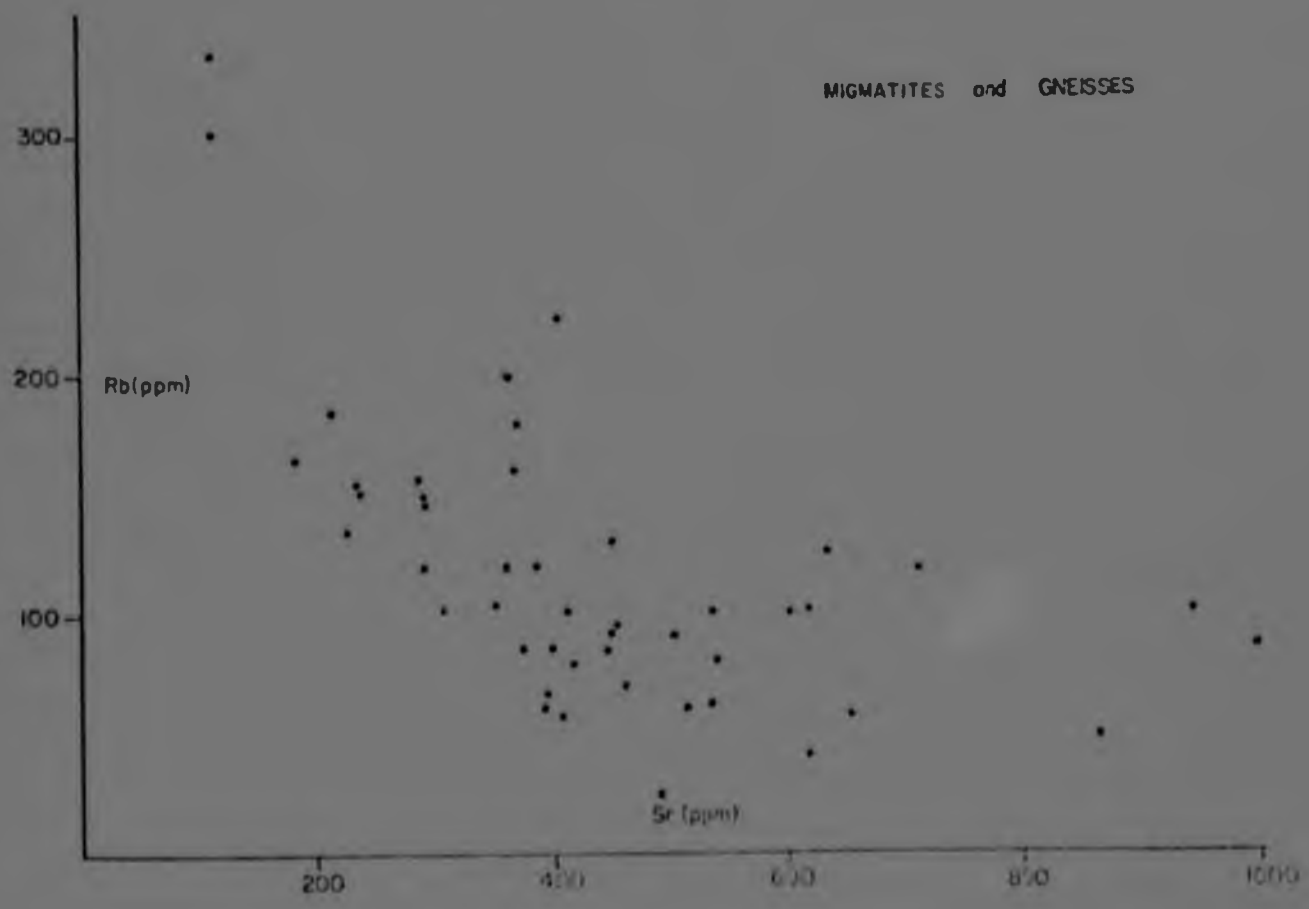

spread is thought to be related to two factors :- firstly, sampling inconsistencies (i.e. unless a very large sample is taken it is difficult to obtain a representative sample of a rock such as a migmatite) and secondly, to the actual nature of the migmatites themselves. Migmatites that have undergone variable degrees of reworking and granitization are likely to exhibit different major element contents. In view of the close genetic link suggested between the Nelspruit migmatites and gneisses and the potassic Nelspruit Porphyritic Granite, it is likely that the migmatites plotting in the fields of adamellite and granite (sensu stricto) will have undergone a greater degree of homogenization and granitization than those plotting in the fields of granodiorite and tonalite.

Figure 15 exhibits an antipathetic relationship between Rb and Sr. The spread in this data is probably related to the same factors that caused the spread in the K_2O v Na_2O plot (see above).

Data from the full silicate analyses of a variety of granite types have been plotted on Quartz-Albite-Orthoclase (Qtz-Ab-Or) and Alkali-FeO-MgO (AFM) ternary plots(Figures 16 and 17). The petrologic functions used here are listed in Table 28, Appendix 2. It is clear from both these diagrams that the composition field of the Nelspruit Porphyritic Granite overlaps, to a certain extent, with that from the Nelspruit Migmatite and Gneiss Terrane. This is an indication that, from a geochemical standpoint, these two rock assemblages are similiar, and furthermore supports the suggestion made previously that they may be co-genetic. Also plotted on the AFM ternary diagram (Figure 17) are samples of mafic xenoliths from the migmatite and gneiss terrane. It is clear from the diagram that the wide variation in the chemical content of these mafic rock types, mentioned in the section on petrography, is a prominent characteristic of the migmatites and gneisses. This chemical disparity is more clearly illustrated by examining full silicate analyses of mafic xenoliths (Table 7) from the migmatite and gneiss terrane. Considerable variations in the silica, total iron, magnesium, sodium and potassium contents of these samples exist, again reflecting variations in the degree of assimilation that these mafic remnants have undergone.

TABLE 7

ANALYSES OF MAFIC XENOLITHS FROM THE NELSPRUIT MIGMATITE AND GNEISS TERRANE

Samples	E4C	C23B	C22B	C25B	B16A	E26A	H10A
SiO_2	48,99	61,34	62,37	48,12	52,76	53,22	62,24
TiO_2	1,18	0,92	1,03	3,10	1,16	1,21	0,84
Al_2O_3	13,35	16,62	16,36	12,24	11,76	13,64	13,31
Fe_2O_3	9,48	4,76	5,20	18,29	11,62	12,25	5,57
MnO	0,15	0,10	0,10	0,17	0,22	0,17	0,12
MgO	8,20	3,27	2,27	7,36	11,24	7,42	5,64
CaO	8,35	3,63	3,80	5,52	7,15	5,09	3,53
Na_2O	6,71	5,28	5,79	0,24	0,30	5,03	4,78
K_2O	2,52	2,77	2,45	4,57	3,29	0,74	1,99
P_2O_5	1,41	0,44	0,32	1,22	0,95	0,45	0,53
L.O.I.	0,45	0,49	0,38	0,25	0,60	2,29	0,41
TOTALS	100,81	99,61	100,07	101,21	100,05	101,51	98,97
ppm							
Rb	63	157	109	93	63	28	99
Sr	1277	453	402	264	763	512	385
Ba	1503	753	881	1623	831	161	211

Sample localities - Figure 11

Analyst · L.J. Robb

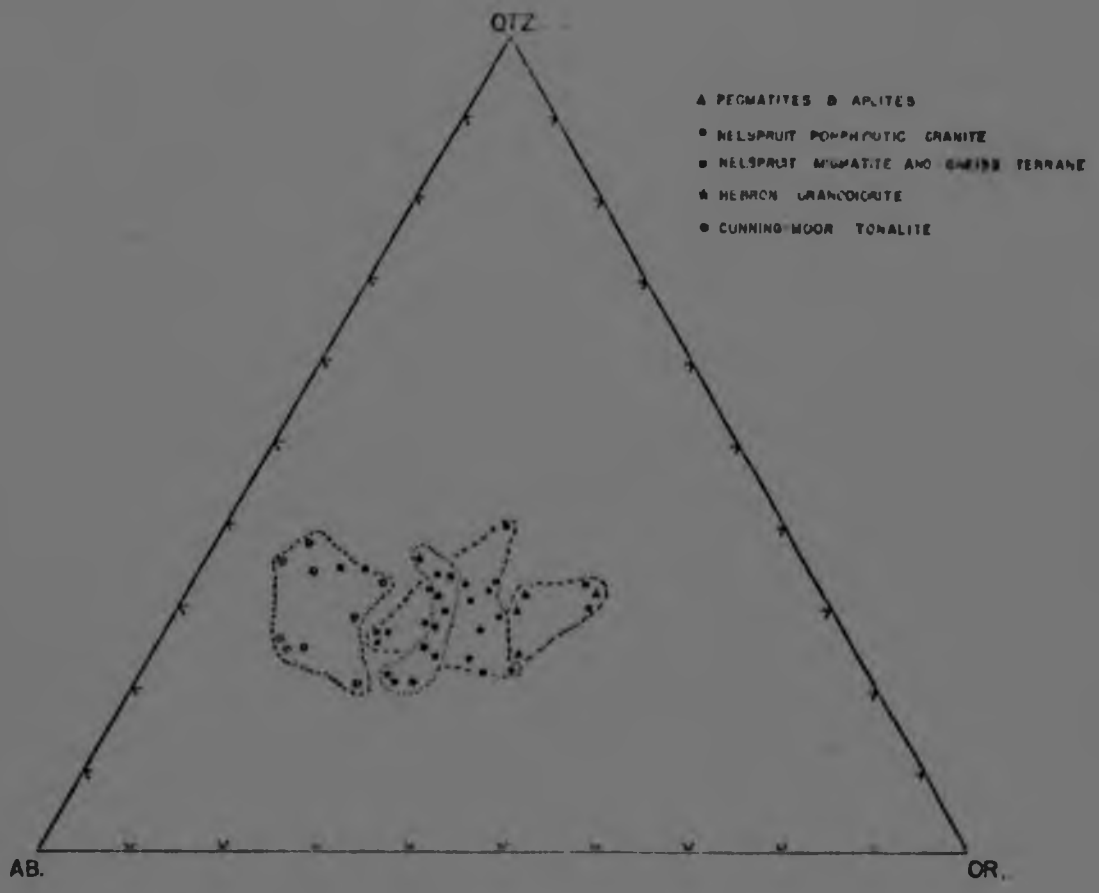

Figure 16. Quartz-Albite-Orthoclase plot -- Various granite types in the study area.

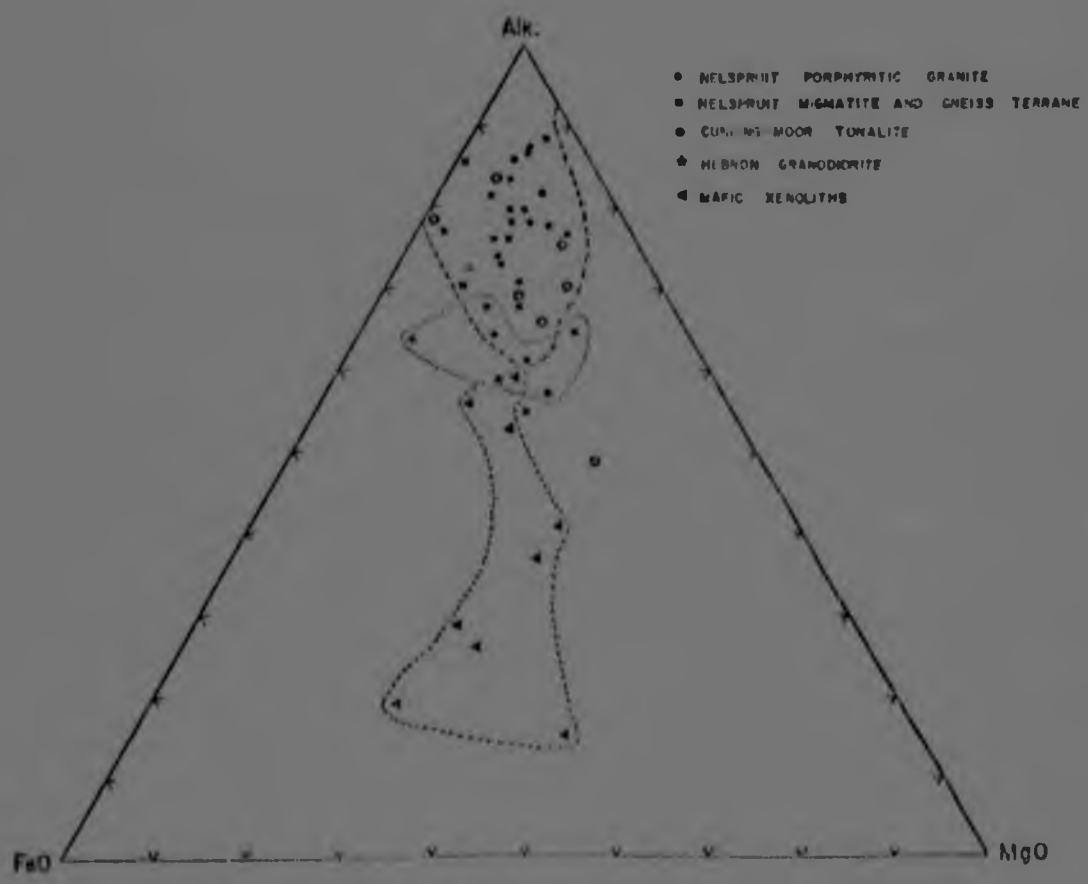

Figure 17. Total Alkalis-FeO-MgO plot - various granite types in the study area.

(ii) The origin and mode of formation of the migmatite and gneiss terrane

The question of the origin and mode of formation of migmatites and gneisses is a complicated and little studied one. It requires a detailed knowledge of the migmatite terrane in the field, as well as a thorough geochemical (and geochronological) understanding,before any ideas as to the origin of these complex mixed rocks is likely to be obtained. Furthermore, it is believed that a number of interacting processes are responsible for the formation of migmatite terranes and hence a unique solution to the problem may not be possible.

Detailed studies have been made in the past concerning the origin of migmatitic rocks. Lowman (1965) studied migmatites in Gilpin County, Colorado and arrived at the conclusion that the leucosomes of these particular migmatites were non-anatectic in origin. This conclusion was largely based on the fact that modal analyses of the leucosomes did not plot in the region of the "thermal minima" in the hydrous quartz-albite-orthoclase system; i.e. that portion of the system where incipient partial melt fractions are likely to plot.

White (1966), on the other hand, studying the migmatites from the Palmer region of South Australia concluded that the migmatites in this area were venitic in origin, forming as a result of metamorphic differentiation. Regional considerations as well as the equilibrium distribution of Ba and Rb in coexisting biotite and K-felspars within the migmatites, were responsible for this conclusion.

With respect to the Nelspruit Migmatite and Gneiss Terrane, no detailed geochemical studies have yet been undertaken, however, certain regional observations concerning this terrane have been made. Viljoen and Viljoen (1969c) have described this migmatite and gneiss terrane as being, "... strongly indicative of a major episode of wide-spread potash

metasomatism, partial mobilization (anatexis) as well as local palingenesis, plasticization and granite and pegmatite intrusion". Furthermore these authors state, with regard to migmatite formation, that "...although in some cases it would appear that these complex mixed rocks have formed by anatectic mobilization in situ, much of the evidence from large migmatite terrains strongly supports an origin related to widespread K-metasomatism with or without granite addition.."

For the purposes of this dissertation an attempt has been made to quantify the existing, somewhat inconclusive, ideas on the origins of the Nelspruit Migmatite and Gneiss Terrane. It must be stressed at the outset that the conclusions, derived from the mass balance experiment described below, are based on analyses carried out on a single sample, and may not represent the mode of formation of the entire migmatite and gneiss terrane in the study area.

The sample selected for detailed analysis (B24-for locality see Figure 11) is illustrated in Plate 4c. In this photograph A represents the paleosome, B the leucosome and C appears to be a mixture of the two. The sample was split into its three components (A, B and C) and each was analysed for major and trace elements (Table 8). This data is plotted on a Quartz-ΣFelspar-ΣMafics ternary plot (Figure 18a) together with data from a similiar experiment carried out by Mehnert (1968). These two sets of data will be discussed individually :-

(a) Mehnert's mass balance experiment :-

Mehnert analysed the various portions of a migmatite sampled in the Black Forest region, Germany. This migmatite sample was divided into a paleosome, a leucosome and a third portion, termed a melanosome, which is the mafic-rich rim associated with the leucosome. These three components are plotted on the Quartz-ΣFelspar-ΣMafics diagram (Figure 18a)

Figure 18. Mass balance experiment on migmatite separates from sample B24.

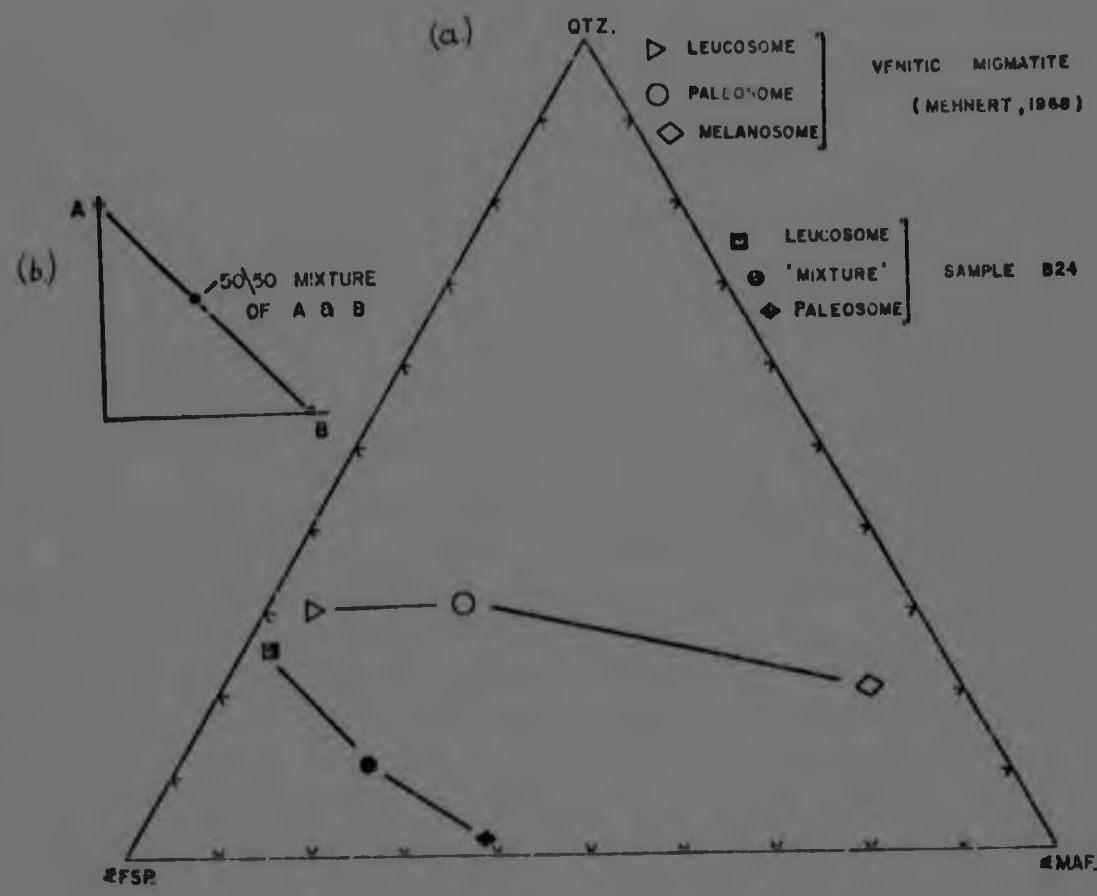

Figure 19. The positions of migmatite leucosomes from the study area in relation to the field of thermal minima in the system Qtz-Ab-Or.

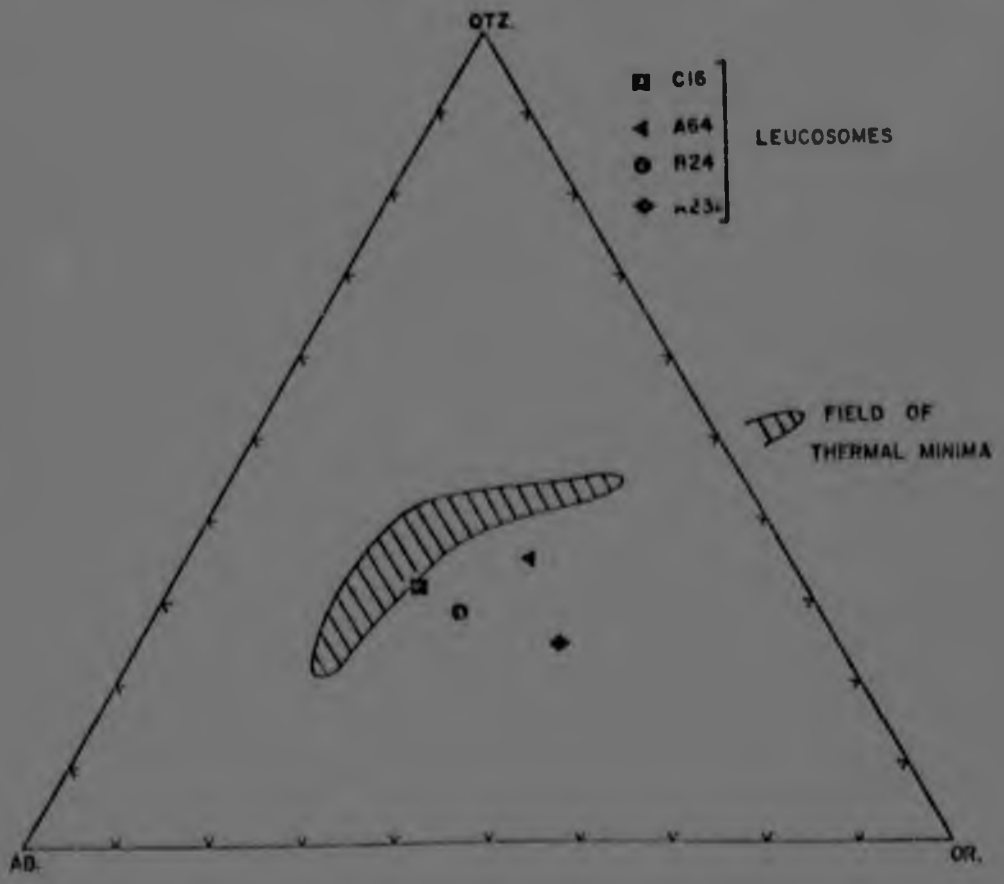

where it is seen that the three points lie approximately on a straight line with the paleosome (the inferred parent rock) lying between the leucosome and melanosome. The indication here is that the two end members (the leucosome and melanosome) are the result of anatectic differentiation of the parent rock. Furthermore, Mehnert (1968) indicated that the composition of the leucosome corresponds closely to the position of minimum melting in the granite system. Clearly, the experiment indicates that the Black Forest migmatite is venitic in origin and the result of in situ metamorphic differentiation.

(b) Mass balance experiment on sample B24 from the Nelspruit area :-

The components of the migmatite sample B24, plot in different positions relative to those of Mehnert's migmatite on the ternary plot in Figure 18a. In this case the paleosome and leucosome of B24 form the end-members of an approximately straight line, and the "mixture" lies approximately half-way between these two points. The position of these points is analogous to the simple mixing diagram indicated in Figure 18b, where a 50/50 mixture of two pure products A and B will lie on a straight line exactly half way between these two points. The implication for the Nelspruit migmatite is, therefore, that the paleosome (A) was intruded by the leucosome (B) and partial assimilation has taken place, to yield the resultant "mixture" (C). This implies an arteritic origin for this particular migmatite. To further substantiate this suggestion, the composition of the B24 leucosome was plotted on a Quartz-Albite-Orthoclase diagram (Figure 19) together with the leucosomes of three other migmatite samples (Tables 6 and 8). It is apparent that these leucosomes do not plot within the field of thermal minima, or minimum melting points, in the granite system and are not likely to have been formed by partial anatexis as was the case with Mehnert's leucosome. The fact that this feature applies to all four leucosome samples analysed from the Nelspruit Migmatite and Gneiss terrane is perhaps indicative that the arteritic origin suggested for the B24 migmatite may, in fact, represent a

TABLE 8

ANALYSES OF MIGMATITE SEPARATES FROM THE NELSPRUIT MIGMATITE AND GNEISS TERRANE

	1	2	3	4	5	6	7
Samples	B24(1)	B24(2)	B24(3)	A64(1)	A64(2)	C16(1)	C16(2)
SiO_2	71,50	60,98	49,74	74,50	66,57	71,30	62,26
TiO2	0,14	0,76	2,09	0,12	0,54	0,29	0,87
Al_2O_3	16,98	14,95	13,12	13,85	15,82	15,17	17,11
Fe_2O_3	1,30	6,44	15,19	0,29	2,89	2,09	4,37
MnO	0,03	0,15	0,25	0,02	0,06	0,06	0,07
MgO	0,01	3,58	7,70	0,01	1,79	0,02	2,90
CaO	1,49	4,15	3,34	1,18	2,25	1,94	2,77
Na_2O	4,15	4,66	2,34	3,03	5,05	4,30	6,16
K_2O	4,79	2,42	5,51	5,73	3,05	3,59	3,19
P_2O_5	0,01	0,54	0,93	0,05	0,14	0,01	0,12
L.O.I.	0,66	0,30	0,66	0,67	0,65	0,53	0,73
TOTALS	101,04	99,33	100,80	99,40	98,82	99,30	100,56
ppm							
Rb	368	193	180	102	72	105	115
Sr	200	465	398	776	813	467	407
Ba	348	415	684	1794	1032	810	1018

B24(1) - leucosome
B24(2) - 'mixture'
B24(3) - paleosome
A64(1) - leucosome
A64(2) - paleosome
C16(1) - leucosome
C16(2) - paleosome

Sample localities - Figure 11

Analyst : L.J. Robb

widespread mode of formation in this migmatite terrane.

It must be stressed again that the conclusion reached in the above experiment does not necessarily apply to the entire Nelspruit Migmatite and Gneiss Terrane, and the writer is convinced that migmatite formation involves the complex interaction of a variety of processes, of which the arteritic origin suggested above, may represent only one of several possible mechanisms.

(h) Summary and Conclusions

(i) The Nelspruit Migmatite and Gneiss Terrane consists of a complex suite of mixed rocks which exhibit a variety of textural types. This suite of rocks occupies essentially low-lying terrain, the latter generally coinciding with the three major river valleys in the area.

(ii) General field observations, including the presence of textures described as "migmatite xenoliths" described from the area near Hazy View, as well as the mass balance experiment, suggest that the predominant mode of formation of the migmatite and gneiss terrane involved the addition of foreign granitic material to an environment consisting of pre-existing mafic material. This does not preclude the possibility that some granitic component (possibly tonalitic in composition) was also present in the region prior to the influx of later potassic phases.

(iii) The similarity of certain characteristic properties of the Nelspruit Porphyritic Granite (i.e. its potassic and porphyritic nature) with those of the Nelspruit migmatites and gneisses suggest that the intrusion of the porphyritic granite may have

largely been responsible for the formation of the migmatite terrane.

(iv) It is of interest, at this stage, to speculate on the possible nature of the crust in the area, prior to the intrusion of the Nelspruit Porphyritic Granite and the generation of the migmatites and gneisses. The presence of tonalite gneisses (the latter possibly similiar to the ancient tonalites in the Barberton and Swaziland regions) in the area flanking the Barclay Vale Schist Belt provides an important clue as to the nature of events preceding the advent of the porphyritic granite intrusion. I is suggested, particularly in view of the knowledge available from the remainder of the Archaean terrane in the Barberton region (Chapter 1), that an assemblage of tonalite gneisses and migmatites, as well as remnant greenstone belts, formed the crust prior to the intrusion of the Nelspruit Porphyritic Granite. The generation of the Nelspruit migmatites and gneisses, in the areas peripheral to this intrusive granite, was concomittant with the emplacement of the porphyritic granite.

IV. THE NELSPRUIT PORPHYRITIC GRANITE

(a) Field Description

Most of the Archaean granitic terrane between Nelspruit and Boshbuckridge is underlain by the Nelspruit Porphyritic Granite. This is a massive, coarse-grained, grey-to-pink granite characterized by the almost ubiquitous presence of large microcline megacrysts.

The extent of the Nelspruit Porphyritic Granite is shown in Figure 10, which also illustrates the distribution of the textural types that were recognized within the granite.

Three grades of porphyritic granite are recognized :-

(i) an intensely porphyritic granite where the microcline megacrysts are large (up to 30mm in length) and euhedral. On average the megacrysts occupy more than 25% of the volume of the rock (Plate 4d).

(ii) a moderate-to-slightly porphyritic granite which occupies most of the Nelspruit Porphyritic Granite terrane. Megacrysts are euhedral to subhedral in shape, and not as prominently developed as in the intensely porphyritic granite variety.

(iii) granites in which few, if any, microcline megacrysts occur. This textural variety was seen only in a small area approximately 8km south of White River (Figure 10).

The best developed occurrence of intensely porphyritic granite is located in an arc-chaped belt immediately south of White River. Areas of intense phenocryst development also occur within the Nelspruit migmatites and gneisses. The presence of these megacrysts, as pointed out earlier, may suggest a co-genetic relationship between the migmatites and gneisses and the porphyritic granite.

Mention has already been made in this chapter regarding the significance of topography in the Archaean granitic terrane of the Barberton region. The fact that the Nelspruit Porphyritic Granite generally occupies higher-lying country-side than the migmatite and gneiss terrane has been alluded to. Typical characteristics of the former hilly terrain, are illustrated in Plate 4e and f. Comparison of these two photographs with Plate 8b, which shows the flat nature of the terrain underlain by the Cunning Moor Tonalite in the northeast of the map area, demonstrates the contrasting topographic character of areas underlain by different granite types. It is likely that the coarser-grained granites are less susceptible to erosion and degradation than sodic granites. Other sodic

PLATE 4

A. Large, dark, biotite xenolith containing numerous large poikilitic microcline phenocrysts aligned parallel to the schistose fabric of the xenolith. This occurrence is considered to represent an example of locally induced K-metasomatism. The photograph was taken in the Nelspruit Migmatite and Gneiss Terrane, 1 km west of Nelspruit.

B. Photomicrograph of a typical gneissic-textured rock from the Nelspruit Migmatite and Gneiss Terrane, showing the crenulated quartz boundaries which indicate that the rock has undergone deformation, Sample A39, Magnification 20X.

C. Sample of migmatite (B24) used in the mass balance experiment. A-paleosome; B-leucosome; C-a mixture of paleosome and leucosome.

D. Intensely porphyritic granite with large disorientated microcline phenocrysts. Locality, sample site B20 (Figure 11) west of White River.

E. Typical Nelspruit Porphyritic Granite terrane showing "whaleback" outcrop development. Locality, approximately 10km west of White River.

F. View of Nelspruit Porphyritic Granite terrane showing the hilly nature of the region underlain by this rock type. Locality, approximately 10km east of White River.

PLATE 1

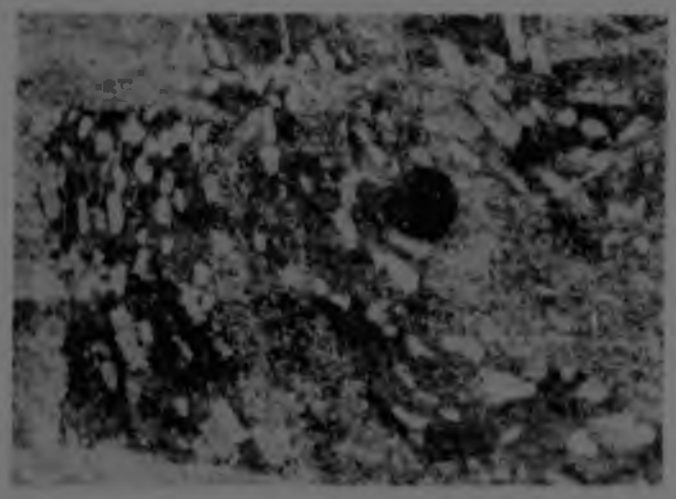

A

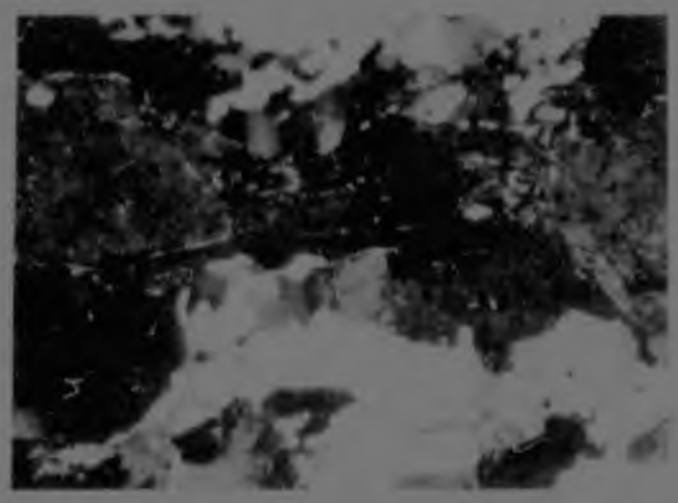

B

C

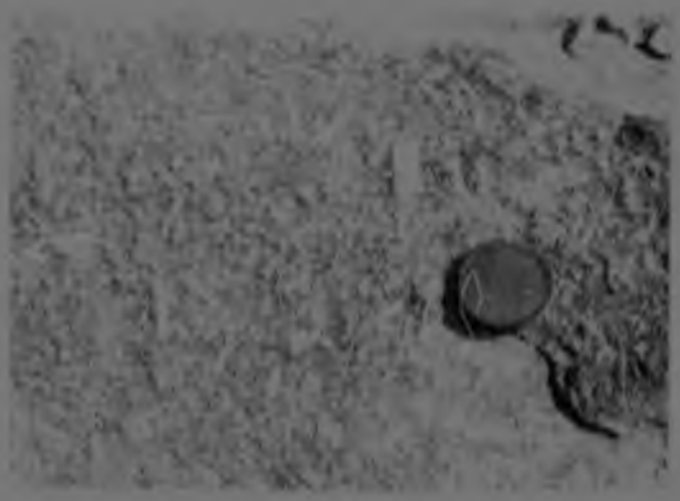

D

E

F

granites such as the Kaap Valley diapir and the Nelshoogte and Theespruit tonalitic plutons have similiar flat and low-lying topographic characteristics.

(b) Petrography

The Nelspruit Porphyritic Granite can be described as having a bimodal texture consisting of large microcline megacrysts (10-30mm in length) set in a medium-to-coarse ground mass of quartz, plagioclase and biotite. In general the porphyritic granite consists predominantly of microcline microperthite, plagioclase and quartz with minor amounts of biotite and muscovite. Trace amounts of zircon, rutile and apatite are also present.

Plagioclase grains are commonly zoned and sericitized - preferential sericitization of calcic cores is common. Plagioclase twin-lamellae are usually narrow indicating a composition towards the sodium end of the solid-solution series. Larger grains of plagioclase occasionally contain inclusions of smaller grains of the same mineral, a feature possibly indicative of two episodes of plagioclase crystallization.

The microcline megacrysts are clearly late formed phenomena and exhibit well-defined poikilitic (or poikiloblastic?) textures. Inclusions of quartz, plagioclase and biotite are all found within the microcline. Plate 5a shows plagioclase and quartz inclusions in a large microcline megacryst.

In Plate 5a it can be seen that the plagioclase grain boundaries are highly corroded, this effect possibly being due to the reaction between plagioclase and later formed microcline. This reaction is also manifest in other forms; Plate 5b, for example, shows a plagioclase grain in contact with a microcline megacryst, the former exhibiting a prominent reaction rim within which a reversal in the extinction of twin lamellae has taken place. Plate 5c shows the development of myrmekitic textures at the interface between a plagioclase and microcline grain. Phenomena such as those

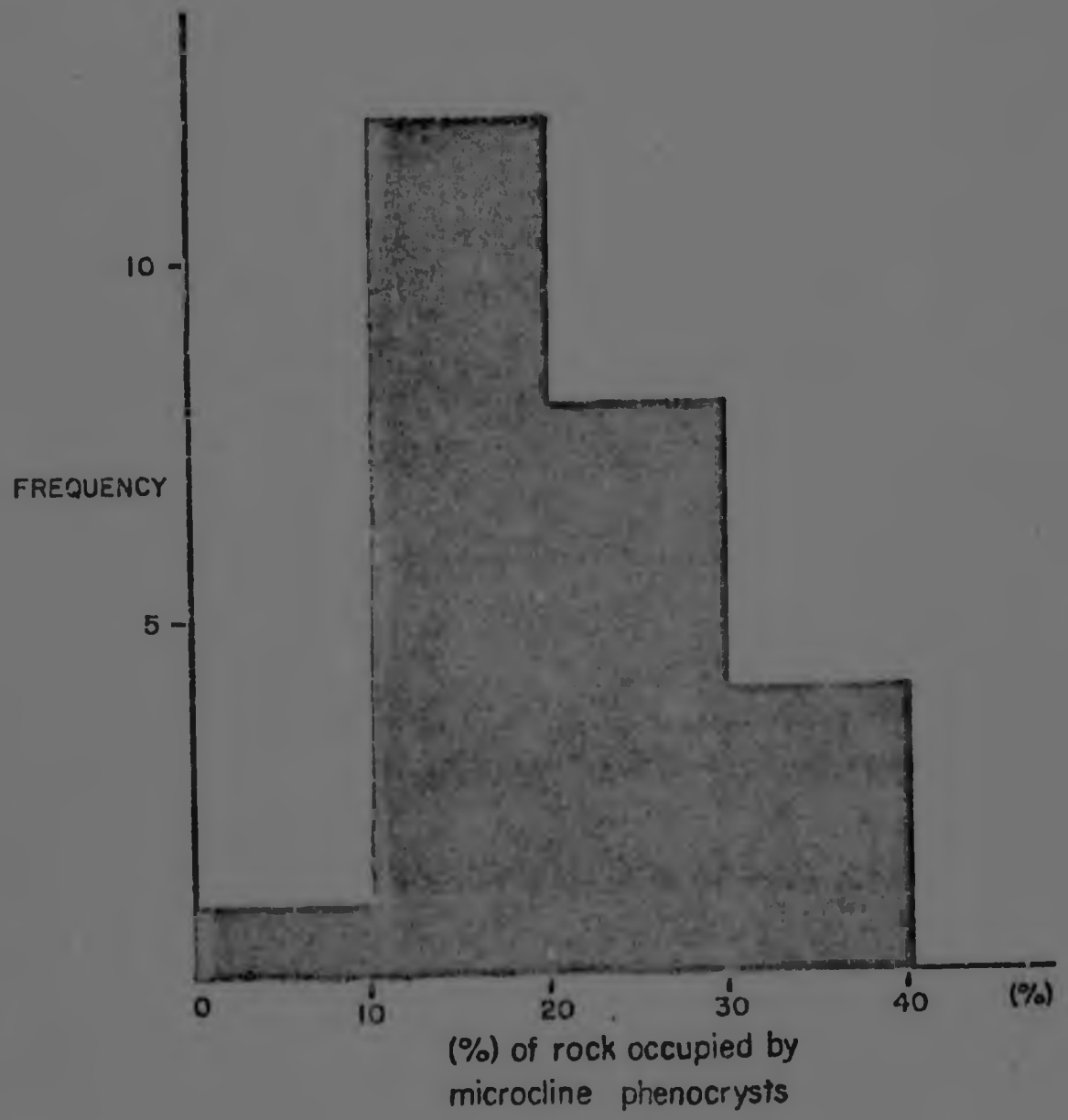

Figure 22. Histogram illustrating the relative proportions of rock occupied by microcline phenocrysts in the Nelspruit Porphyritic Granite.

described above have been recorded previously and Augustithis (1973) has stated that, "... the reaction margins of myrmekitized plagioclases are of petrogenetic significance in support of a later K-felspar crystallization". The question regarding the origin of the microcline megacrysts in the porphyritic granite (i.e. whether the megacrysts should be described as phenocrysts or porphyroblasts) is discussed in detail in a subsequent section.

In concluding this section on the petrography of the porphyritic granite consideration will be given to the volume of rock occupied by the microcline megacrysts. An estimation of the volumes occupied by megacrysts was carried out by measuring, with a planimeter, the areas of megacryst outlines on a randomly sliced sample of porphyritic granite, and comparing this with the total area of the sliced section. This procedure was carried out on 26 samples of porphyritic granite and the results are summarized in the histogram shown in Figure 22. The actual range in phenocryst volumes is from 9,4% to 39,0% but the data is positively skewed because the majority of porphyritic granites have between 10% and 30% of their volumes occupied by microcline megacrysts.

(c) Aplites, Pegmatites and Quartz-Felspar Porphyry Dykes

It is applicable at this stage to briefly describe the geology and geochemistry of aplites, pegmatites and quartz-felspar porphyry dykes that occur within the Nelspruit granitic terrane. The distinctive chemistry that characterizes both the aplites and the pegmatites is illustrated in a quartz-albite-orthoclase ternary plot (Figure 16) where the high potash values of these rocks (Table 9) serve to distinguish them from other granite types.

(i) Pegmatites

Pegmatites occur as veins and dykelets throughout the study area. They are typically very coarse-grained and consist predominantly of microcline, quartz and biotite

with lesser amounts of muscovite and plagioclase. Chemically, they are characterized by high silica, potash and rubidium contents and low Sr and Ba contents (Table 9). These trace element characteristics clearly indicate the fractionated, late phase nature of the pegmatites, by comparison with most of the samples from the porphyritic granite.

(ii) Aplites

Like the pegmatites, aplites also occur as veins and dykelets throughout the study area. They are generally pink, medium-grained, equigranular rocks and consist predominantly of microcline and quartz with lesser amounts of plagioclase, muscovite, biotite and rutile. In the field they are occasionally rimmed by coarser-grained pegmatitic material (Plate 3f). This relationship has been described previously in the literature by San Miguel (1969) who attributes the pegmatite-aplite assemblage to post-magmatic metamorphism and metasomatism. He suggested that the aplites formed by recrystallization (due to stress) of a parent granitic rock with subsequent metasomatic activity causing marginal pegmatitic replacement. The writer prefers to view aplites as part of the magmatic process of granite emplacement and suggests that the coarser-grained pegmatitic margins occasionally exhibited by the aplites may be due to the migration of volatile phases towards the edges of these veins.

The aplites have a similiar major element chemistry to the pegmatites and demonstrate the same high silica and potash contents. The rubidium content of the aplites is also similiar to that of the pegmatites (Table 9) but strontium, and particularly barium, values are notably higher. This increase in Sr and Ba is probably related to the presence of minerals in the aplite into which strontium and barium are readily partitioned (fo example strontium is strongly partitioned into plagioclase).

PLATE 5

A. Photomicrograph of a poikilitic microcline phenocryst in the Nelspruit Porphyritic Granite. The boundaries of plagioclase and quartz inclusions are eroded by virtue of reaction with the surrounding microcline. Sample B1, Magnification 20X.

B. Photomicrograph showing a zone of reaction between plagioclase and later-formed microcline where partial reversal in the extinction of the twin lamellae has taken place. Sample B1, Magnification 50X.

C. Photomicrograph showing a zone of reaction between plagioclase (on the right) and a later-formed microcline phenocryst, where quartz exsolution (myrmekitization) has taken place. Sample B1, Magnification 20X.

D. A typical shear zone in the Nelspruit Porphyritic Granite. Note the positive relief which commonly characterizes these features. The whitish rock type is a quartz-rich mylonite. Locality, 15km northwest of White River.

E. Striations or slickensides on a vertical surface within a typical shear zone. The attitude of these slickensides indicates the predominantly horizontal component of movement (i.e. shearing) with only a small component of vertical movement.

PLATE 5

A

B

C

D

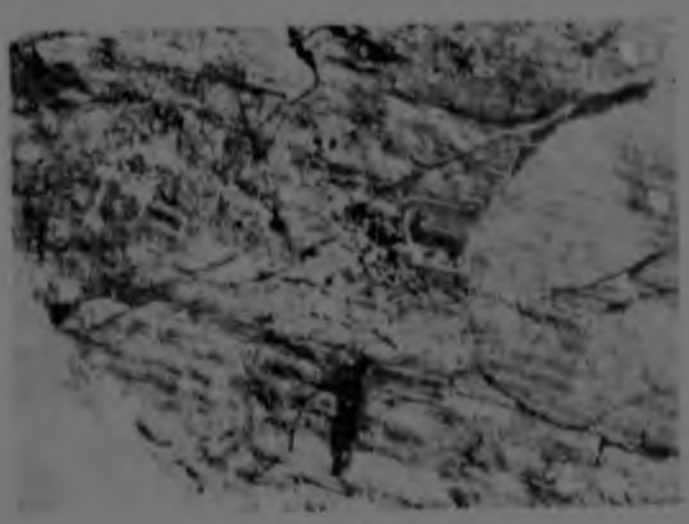

E

(iii) Quartz-Felspar Porphyry Dykes

Only two such dykes each only one to two kilometres long, occur in the study area, outcropping in the southeastern portion of the region(Figure 60) These dykes have a distinct bimodal texture, consisting of a fine-grained matrix within which occur medium-fine grained (1-2mm long) phenocrysts of quartz and plagioclase. Quartz, plagioclase, muscovite, sericite and microcline form the main constituents of the rock.

Geochemically these dykes have a high silica content (Table 9) but otherwise major element compositions are similiar to that of an average granite. The trace element composition of the dykes are, however, anomalous, as they show very high rubidium and extremely low strontium and barium contents. Judging from their trace element chemistry it is suggested that these rocks may represent the product of a highly fractionated granitic magma, or alternately,a low degree of partial melt of a granitic parent.

(d) Geochemistry

In addition to outlining the broad chemical characteristics of the Nelspruit Porphyritic Granite the following section deals with the complex problem of the origin and mode of formation of the large microcline megacrysts that characterize this granite. The origin of these megacrysts (i.e. whether they are related to the magmatic events associated with the actual emplacement of the granite, or whether they are the result of later metasomatic or metamorphic events) is critical to an evaluation of the origin of the granite as a whole.

(i) Broad geochemical characteristics of the porphyritic granite

A great deal of new chemical data is available on

TABLE 9

SAMPLES OF PEGMATITES, APLITES AND A QUARTZ-FELSPAR PORPHYRY DYKE FROM THE STUDY AREA

	A17	A28A	A31B	A28	A38A
SiO_2	70,94	71,92	74,25	72,35	74,01
TiO_2	0.10	0.09	0.01	0.01	0.01
Al_2O_3	16,02	15,00	13,79	15,86	13,99
Fe_2O_3	1,17	1,22	0,12	0,64	0,32
MnO	0,04	0,03	0,02	0,03	0,14
MgO	0,01	0,22	0,01	0,01	0,01
CaO	0,66	1,01	1,12	0,60	0,57
Na_2O	2,61	3,61	3,58	4,16	3,85
K_2O	6,54	5,44	5,55	6,14	4,86
P_2O_5	0,01	0,01	0,01	0,01	0,01
L.O.I.	0,78	0,77	0,38	0,40	0,64
TOTALS	98,87	99,31	98,81	100,19	98,40
ppm					
Rb	289	198	205	305	668
Sr	100	178	86	66	30
Ba	184	578	44	34	17

A17 - aplite vein
A28A - aplite vein
A31B - pegmatite vein
A28 - pegmati vein
A38A - quartz-felspar porphyry dyke

Sample localities - see Figure 11

Analyst : L.J. Robb

the Nelspruit Porphyritic Granite. Eighteen full silicate analyses are presented in Table 10 as well as a large number of partial analyses which are listed in Table 25, Appendix 2.

Examination of Table 10 shows considerable variation in the composition of the Nelspruit Porphyritic Granite, reflected in the K_2O/Na_2O ratios, and the values of silica, alumina and iron. These significant differences, well above those expected from analytical discrepancies, indicate a range in the chemical composition of this granite. When the chemical data from Table 10, in addition to the data from the partial analyses (Table 25), is plotted on a K_2O v Na_2O variation diagram (Figure 23) a considerable spread in compositions is seen. In fact, a continuum from tonalite through to granite (sensu stricto) is portrayed. Thus although textures and field relationships suggest a single granite type, it is evident that compositionally, this granite is highly variable. A plot of Rb v Sr for the Nelspruit Porphyritic Granite (Figure 24) also indicates considerable variation in the trace element composition of this granite. On this diagram it is possible to discern two populations of data which are discussed below (best-fit lines have been plotted through these two sets of data in Figure 24 allowing the two populations to be more clearly evident) :- (i) a high Rb population which exhibits a wide variation in Sr content (ii) a low Rb population which exhibits a more restricted variation in its Sr content. Closer examination of these two populations shows them to be related to distinctive textural sub-types within the Nelspruit Porphyritic Granite. The high Rb population generally coincides with samples that have been described as intensely porphyritic and the low Rb population appears to be coincident with the moderate-to-slightly porphyritic granite.

The considerable variation in the composition of the Nelspruit Porphyritic Granite is a topic which has been

Figure 23. K_2O v Na_2O plot - Nelspruit Porphyritic Granite.

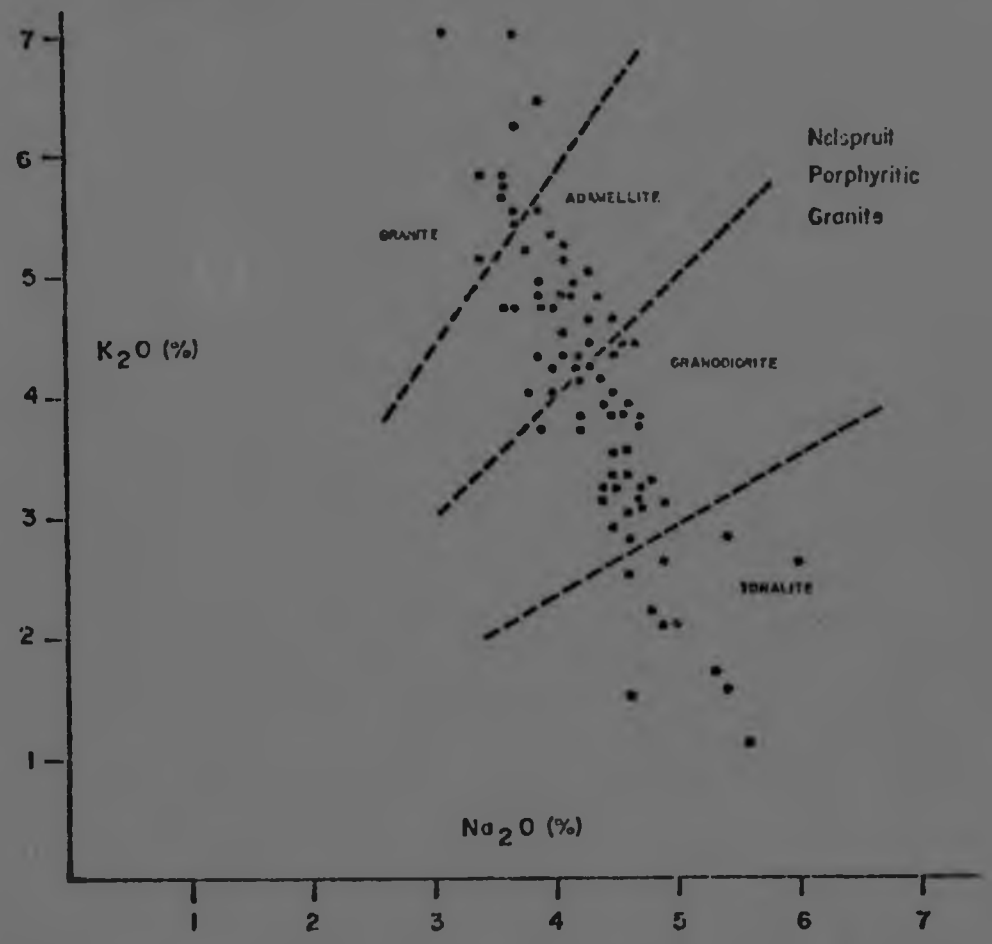

Figure 24. Rb v Sr plot - Nelspruit Porphyritic Granite : the possibility that two populations of data exist is enhanced by regression lines through them (m= slope : c = intercept).

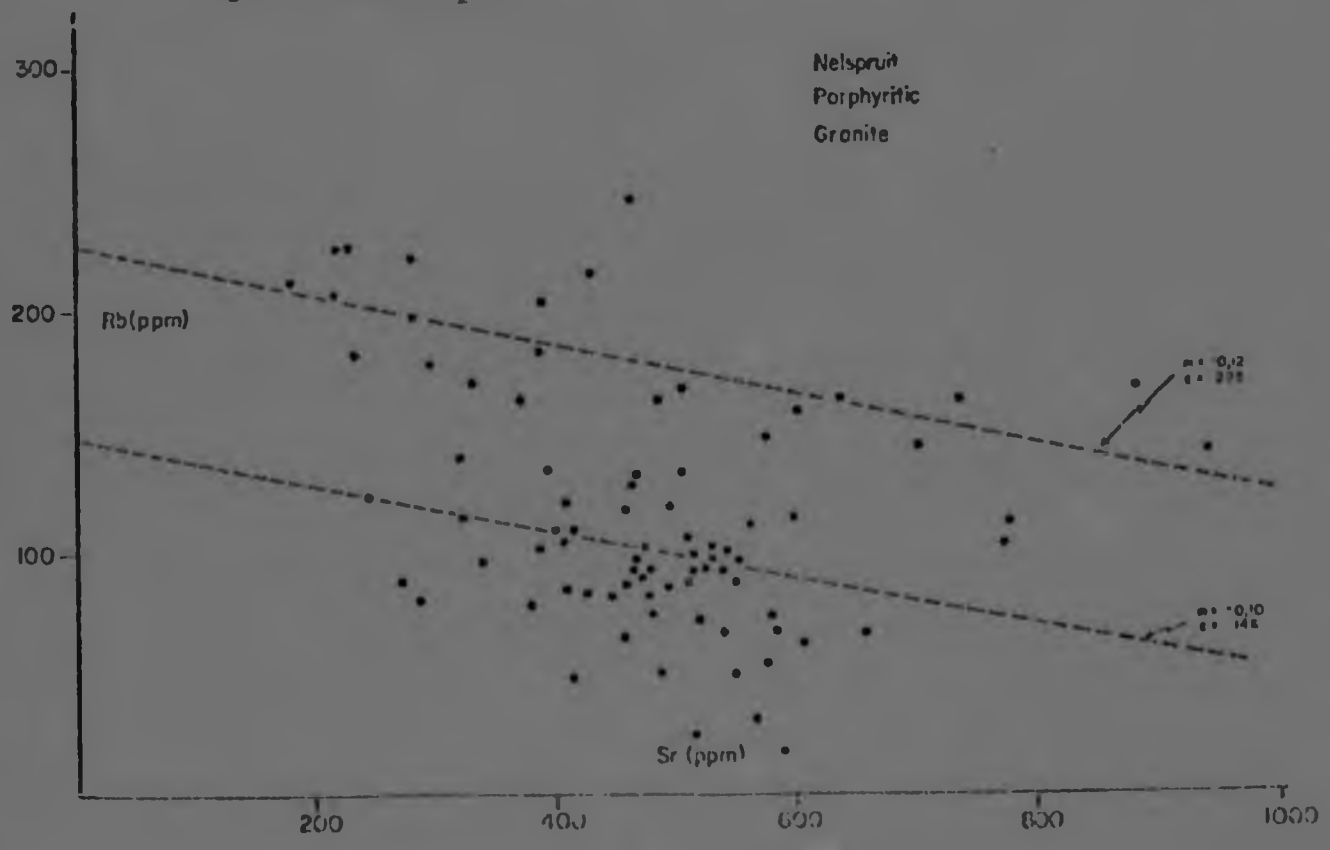

TABLE 10

ANALYSES OF THE NELSPRUIT PORPHYRITIC GRANITE

	A1	B26	B1	G8	P78	B7	C39	E1	A8M	E4	E1V	CDA	E8	E8.1	M6	A3	B344	L23
SiO_2	70,72	71,63	65,1[illegible]	64,92	72,99	68,30	71,65	71,53	[illegible]	[illegible]	[illegible]	[illegible]	69,19	68,62	71,03	66,69	67,58	69,55
TiO_2	0.21	0,30	0,54	0.48	0.10	0,35	0,15	0,36	[illegible]	[illegible]	[illegible]	[illegible]	0,25	0,32	0,21	0.59	0,62	0.26
Al_2O_3	14,17	12,35	15.05	15,96	14,74	15,11	15,6[illegible]	13,73	[illegible]	15,33	[illegible]	[illegible]	17,50	15,18	15,31	16,85	16,12	16,48
Fe_2O_3	2,01	2,67	3,47	3,53	0,77	2,54	1,32	1,68	[illegible]	[illegible]	[illegible]	[illegible]	1,97	2,59	1,44	2,86	3,43	1,37
MnO	0.06	0.06	0,07	0,07	0,03	[illegible]	0,04	0,04	[illegible]	[illegible]	[illegible]	[illegible]	0,04	0.06	0,04	0,09	0,04	0,04
MgO	1,09	0,9[illegible]	2,31	1,54	0.70	1,53	0,60	<0,01	[illegible]	[illegible]	[illegible]	[illegible]	0,33	[illegible],56	0,63	1,19	0,89	1,01
CaO	1,68	1,74	2,33	2,55	1,35	2,37	1.86	2,22	[illegible]	[illegible]	[illegible]	[illegible]	2,62	2,91	1,43	1,86	1,50	1,37
Na_2O	4,41	4,44	4,20	3,40	3,72	3,65	3.97	5.38	[illegible]	[illegible]	[illegible]	[illegible]	4,51	5.53	4,03	3,62	4,12	2,12
K_2O	4.00	4,19	2,46	3,51	4,75	4,23	3,70	2,81	[illegible]	[illegible]	[illegible]	[illegible]	1,47	0,31	5,06	6,39	4,85	3,96
P_2O_5	<0,01	0,11	<0,01	0,10	<0,01	0,14	<0,01	<0,01	[illegible]	[illegible]	[illegible]	[illegible]	<0,01	<0,01	0,17	0,04	<0,01	<0,01
L.O.I.	0,72	0,53	0,45	0,45	0,55	0,34	0,37	0,39	[illegible]	[illegible]	[illegible]	[illegible]	0,28	0,69	0,37	0,36	0,52	0,37
TOTAL	98,79	99,13	[illegible]	98,45	[illegible]	[illegible]	[illegible]	[illegible]	[illegible]	99,29	[illegible]	[illegible]	[illegible]	[illegible]	[illegible]	[illegible]	[illegible]	[illegible]
ppm																		
Rb	121	112	112	244	83	140	83	56	141	50	90	130	57	53	110	218	159	101
Sr	333	351	774	483	425	632	481	455	284	574	427	255	572	531	343	435	330	474
Ba	725	858	1141	739	805	1285	659	703	370	675	800	622	842	406	822	1113	421	715

Sample localities - Figure 11

Analyst : L.J. Robb

examined in detail, and Chapter 5 has been devoted entirely towards a more complete discussion of this problem. Briefly, however, it is suggested that the compositional variation exhibited by this granite is the result of fractionation of successive mineral phases in the granite system, a process which can be closely modelled by considering the partitioning of trace elements into these minerals.

(ii) The origin and mode of formation of the microcline megacrysts in the Nelspruit Porphyritic Granite

A number of techniques, including full silicate analysis, microprobe scans and triclinicity measurements were used to assess the nature of the microcline megacrysts that characterize the porphyritic granite. These are described in turn, below, and an attempt is made at the end of the section to explain the mode of formation of the microcline.

A. Full silicate analyses of microcline megacrysts

Microcline megacrysts from four samples of Nelspruit Porphyritic Granite were extracted and analysed for major and trace elements (Table 11). Three of the samples (E4, F5 and D3) were microcline megacrysts from the porphyritic granite whereas one (B25) was a microcline megacryst extracted from a mafic (biotite-rich) xenolith within porphyritic granite (see Plate 4a). All four microcline megacrysts have very similiar compositions and variations in iron and magnesium are a reflection of the amount of included biotite in the megacryst. The trace element compositions of the microcline megacrysts are variable, particularly with respect to Sr and Ba. There is, for example, an order of magnitude difference in the Ba content of the microcline megacrysts from samples B25 and F5 (Table 11). A possible explanation for this is that the megacrysts may have formed in such a way that the laws governing the partitioning of trace elements into various mineral phases could not have applied (i.e. the megacrysts

Figure 25. A portion of a microprobe trace across a microcline phenocryst from the Nelspruit Porphyritic Granite (Sample A32). The trace shows the distribution of potassium and sodium across the phenocryst. Sharp "kicks" are due to the presence of microperthitic stringers.

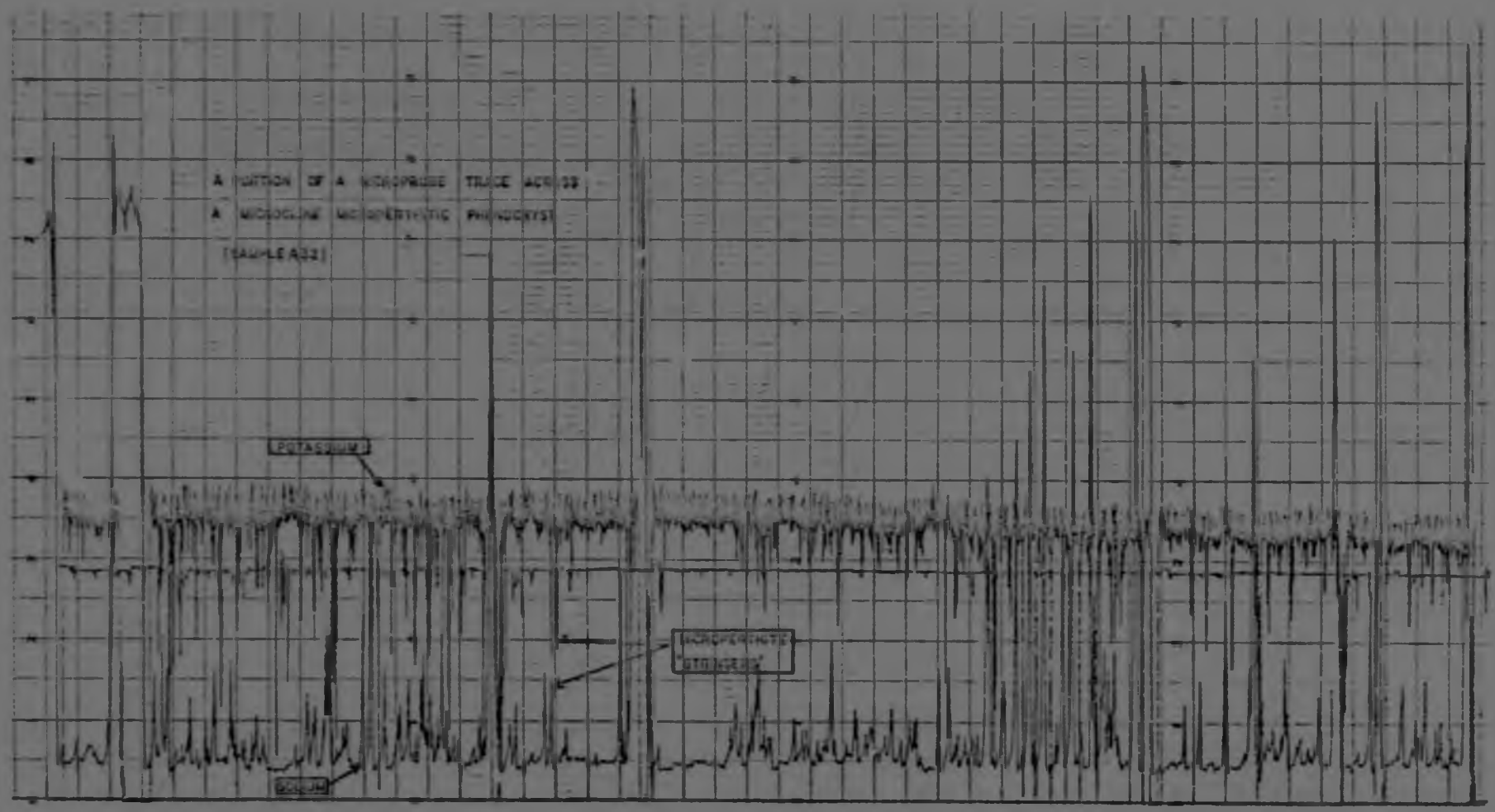

may have formed out of equilibrium with the remaining mineral phases in the system).

B. Electron microprobe scans across microcline megacrysts

Polished thin sections of two microcline megacrysts (Samples A32 and B25) were prepared for electron microprobe analysis to establish the nature of any zoning that might be present. The scans were carried out on a JEOL JXA-5OA Electron Probe Micro-analyser by Mr. R.C. Wallace at the Geological Survey, Pretoria. (The instrument was run at 15KV with a specimen current of 0,03/*amps, the electron beam had a diameter of 2/*). The megacrysts were qualitatively analysed for K, Na, Ca and Ba, the results being summarized below :-

(a) Potassium showed no variation in concentration along a traverse across the megacrysts except at exsolution lamellae (perthite) where sharp decreases were detected (Figure 25).

(b) Sodium showed no variation except for sharp increases where the beam crossed exsolution lamellae (Figure 25).

(c) Barium showed no variation except for slight sharp decreases where exsolution lamellae were intersected.

(d) Calcium, like Ba, showed no variation across the megacrysts except for sharp increases where exsolution lamellae were intersected.

A portion of a potassium and sodium microprobe scan, for a microcline megacryst from sample A32, is illustrated in Figure 25 and the constant nature of these concentrations (except for variations at microperthite lamellae) is clearly evident. Excluding the microperthite, the microcline megacrysts

TABLE 11

ANALYSES OF MICROCLINE MEGACRYSTS FROM SAMPLES OF THE NELSPRUIT PORPHYRITIC GRANITE

	Microcline Megacrysts from :-			
	B25	E4	F5	D3
SiO_2	63,20	65,17	63,91	64,64
TiO_2	0,32	0,25	0,01	0,13
Al_2O_3	19,63	18,54	19,63	19,67
Fe_2O_3	0,72	1,37	0,01	0,62
MnO	0,03	0,02	0,01	0,02
MgO	0,46	0,03	0,31	0,07
CaO	0,48	0,77	0,01	0,54
Na_2O	2,59	2,73	2,18	2,20
K_2O	11,24	10,49	12,82	11,34
P_2O_5	0,01	0,01	0,01	0,06
L.O.I.	n.d.	n.d.	n.d.	n.d.
TOT. S	98,88	99,37	98,84	99,30
ppm				
Rb	169	182	372	281
Sr	1083	669	315	569
Ba	5790	3119	522	2619

Sample localities - Figure 11

Analyst : L.J. Robb

have a homogenous composition showing no traces of zoning whatsoever. The behaviour of potassium, sodium, barium, and calcium at the sites of exsolution lamellae indicates a composition resembling that of plagioclase felspar.

C. Triclinicity measurements on the microcline megacrysts

A knowledge of the crystal structure (triclinicity) of K-felspar can be useful in understanding the nature and origin of this mineral. K-felspar is a complex mineral and its polymorphs have different crystal structures. These polymorphs may also evolve through different structural states, depending on the processes affecting its formation. A brief explanation of the theory behind triclinicity measurements is given :-

K-felspar ($KAlSi_3O_8$) has a number of polymorphs -

SANIDINE - is the high temperature polymorph with a monoclinic structure, and consists of disordered Si and Al atoms.

ORTHOCLASE and ADULARIA- have a crystal structure intermediate between monoclinic and triclinic.

MICROCLINE - is the low temperature polymorph with a triclinic structure and consists of ordered Si and Al atoms.

The triclinicity of a K-felspar crystal is the deviation of the α and γ lattice angles from the theoretically perfect 90°.00'. This deviation is reflected in the separation of, for example, the 131 and $1\bar{3}1$ peaks in a diffraction trace. Goldsmith and Laves (1954) defined triclinicity (Δ) quantitatively using the following expression :-

$$\Delta = 12{,}5\ (d131 - d1\bar{3}1)$$

The values of triclinicity are thus defined as lying between 0 and 1, where 0 indicates a perfectly monoclinic crystal and 1 a perfectly triclinic crystal.

TABLE 12

THE RESULTS OF TRICLINICITY MEASUREMENTS ON SIX MICROCLINE MEGACRYSTS FROM THE NELSPRUIT PORPHYRITIC GRANITE

Sample	2θ	θ	sinθ	d	d131-d1$\bar{3}$1	Δ
C46	131 29,28 1$\bar{3}$1 30,02	14,64 15,01	0,2527 0,2588	3,047 2,975	0,072	0,90
D34	131 29,38 1$\bar{3}$1 30,12	14,6 15,0	0,2535 0,2599	3,037 2,963	0,074	0,93
E4	131 29,44 1$\bar{3}$1 30,14	14,72 15,07	0,2541 0,2599	3,030 2,963	0,067	0,84
F5	131 29,50 1$\bar{3}$1 30,28	14,75 15,14	0,2546 0,2611	3,023 2,949	0,075	0,94
D25	131 29,55 131 30,12	14,77 15,06	0,2549 0,2599	3,021 2,963	0,058	0,74
B25	131 29,45 131 30,15	14,72 15,07	0,2541 0,2599	3,030 2,963	0,067	0,84
					Average = 0,86	

Where Δ = Triclinicity

Sample localities - see Figure 11

The value of Δ is thought to be useful, with regard to the petrogenesis of a K-felspar crystal, in the following way :- A primary microcline, for example, which crystallized directly into the triclinic state will very likely have high values of Δ, ie. approaching 1. A microcline that has formed from the inversion of a higher temperature polymorph, such as orthoclase or sanidine, may, however, be expected to retain certain aspects of its monoclinic parentage and hence have values of Δ intermediate between 0 and 1.

Microcline megacrysts from six random samples of the porphyritic granite were extracted, pulverized to -200 mesh, set in a slide and mounted on a Phillips X-ray Diffractometer. Radiation was CuKα induced through a Ni filter, the scanning speed was $0{,}125^{o}.2\theta.\ min^{-1}$ and the chart speed was $1600mm.hr^{-1}$. The results that were obtained for these samples are presented in Table 12. Triclinicity ranged from 0,74 to 0,94 with an average figure of 0,86. The results indicate that most of the microcline megacrysts have a strong triclinic structure but there is suggestion of a degree of intermediate character to some of their geometries.

The interpretation of triclinicity results is often open to differences of opinion and frequently a unique solution is not possible. As a result it is necessary to consider other factors which may be of importance to the question as well as to bear in mind the conclusions reached by other workers who have measured triclinicities. A brief summary of some of the interpretations attached to K-felspars which have been subjected to triclinicity measurements is given below :-

(i) Kolbe (1966) demonstrated that an inverse relationship exists between the triclinicity and albite content of K-felspars in the Cape Granite. He also indicated that high triclinicities were derived from K-felspars that had suffered post-magmatic deformation and subsequent hydrothermal alteration.

(ii) Heier (1957) suggested that post-magmatic hydrothermal solutions were responsible for converting monoclinic K-felspars to triclinic microclines.

(iii) Dietrich (1962) concluded that the higher triclinicities obtained with increasing differentiation in the Boulder Batholith, Colorado, was a consequence of an increase in the volatile content and resulting lower temperature of crystallization.

(iv) Goldsmith and Laves (1954) have indicated that the cross-hatched twinning, often characteristic of microclines, is the result of their evolution from a monoclinic to a triclinic state. Consequently microclines that crystallize directly into the triclinic state cannot exhibit cross-hatched twinning.

(v) Hunter (1973b) obtained high triclinicity values for K-felspars from the Hood Granite and the late granite plutons of Swaziland. These K-felspars were all found to be replacing plagioclase. The lack of intermediate triclinicity values was regarded as indicative of the pristine nature of the K-felspars and, hence, not the result of a temperature dependent inversion. This, and other considerations, indicated to Hunter that the crystallization of these granites took place under passive hydrothermal conditions. In contrast to Kolbe (1966), Hunter further suggested that the presence of perthite does not markedly affect the triclinicity values of highly ordered microclines.

It is clear from the resumé above, which indicates the differences in interpretation given to similiar values of triclinicity (compare Dietrich, 1962 with Hunter, 1973b), that conclusions regarding either the K-felspars or the

granite as a whole, are made by considering all the evidence available and are not based solely on triclinicity measurements. The following section deals with the possible mode of formation of the microcline megacrysts in the porphyritic granite and attempts to take into consideration all the available data.

D. Suggestions as to the origin and mode of formation of the microcline megacrysts in the Nelspruit Porphyritic Granite

The most important characteristics of the microcline megacrysts, which occur ubiquitously throughout the Nelspruit Porphyritic Granite, can be summarized as follows :- (i) the megacrysts are all microcline microperthites which exhibit distinct cross-hatched twinning, (ii) from petrographic evidence it is clear that they have all formed late in the crystallization history of the rock, (iii) they are poikilitic in texture containing inclusions of quartz, biotite and plagioclase, (iv) the microclines are compositionally homogenous with respect to major elements, however, their trace element contents (Rb, Sr and Ba) are highly variable, (v) the microcline megacrysts show no signs of zoning and, (vi) they are characterized by moderately high to intermediate values of triclinicity.

Megacrysts, similiar to those described in the study area, are commonly regarded as being metasomatic in origin (Stone and Austin, 1961; Booth, 1968). This appears to be a feasible suggestion for the microcline megacrysts of the porphyritic granite, particularly when considering such features as the large microcline " dents de cheval" contained within the biotite xenolith, illustrated in Plate 4a. Although the latter feature appears to be metasomatic in origin it is difficult to visualize this process having been effective over the entire area occupied by the porphyritic granite. Little is known about the movement and behaviour of potash-rich

fluids and the question of their source remains a problem. Furthermore, Booth (1968), describing metasomatic K-felspars from the Cornubian Granite in England, emphasizes their zoned nature, a feature not in keeping with the results of the microprobe scans described above. While not discounting localized metasomatic effects, the large areal exten of the porphyritic granite (Figure 10) and the obscure nature of potash-rich metasomatic fluids is taken as indicating that metasomatism was not the mechanism that resulted in the formation of the microcline megacrysts.

The tendency towards intermediate values of triclinicity and the ubiquitous cross-hatched twinning that occurs in the microcline suggest, in the light of work by Goldsmith and Laves (1954), that the microcline has had a complex petrogenetic history involving the temperature-dependent inversion from a monoclinic polymorph such as sanidine or orthoclase. It is likely, therefore, that the formation of microcline may have been an "in situ" process involving the accumulation and recrystallization of pre-existing, probably higher temperature, K-felspar. This may have been a much later metamorphic process (i.e. the microclines may have formed by "porphyroblastesis", akin to the growth of metamorphic minerals in the solid state) or it may have been linked with the final stages of crystallization of the rock (i.e. a process still associated with the igneous history of the rock).

Parslow (1971) described poikilitic microcline megacrysts containing inclusions of biotite, plagioclase and quartz from the Cairnsmore of Fleet Granite in southwest Scotland. In discussing the problem of the origin of these megacrysts Parslow stated that, "... in a simple temperature controlled crystallization sequence the microcline would still, even if late stage, be expected to exhibit a distribution of the type described for the micas and presumably be intersticial in nature. Since this is not the case some factor must have

influenced the later stages of consolidation". The factor that Parslow refers to is a regional stress field which manifests itself in the late stages of crystallization of the granite, as it attains an essentially solid character. It was this stress that was probably responsible for the mobilization and recrystallization of the microclines. These would subsequently be termed "phenocrysts" as their formation is incorporated in the igneous history of the rock.

The lack of field evidence for a later metamorphic overprint indicates that the microcline megacrysts of the Nelspruit Porphyritic Granite, like those of the Cairnsmore of Fleet Granite, formed by mobilization and recrystallization of pre-existing K-felspar during an event that is likely to have been related to the igneous history of the rock. The megacrysts are therefore described as phenocrysts (rather than porphyroblasts) and hence the term "porphyritic granite". No evidence exists in the area north of Nelspruit for a regional stress field (i.e. which might manifest itself in a preferential alignment of microcline phenocrysts) such as the one that was present in the Cairnsmore of Fleet Granite, and it is suggested that the mobilization and recrystallization of pre-existing K-felspar in the study area must have taken place in response to thermal effects. The exact nature of these effects in unknown, but it is possible that more than one period of intrusion of the porphyritic granite was involved, these intrusions resulting in re-heating of the partially solidified pre-cursor granites.

(e) Summary and Conclusions

(i) The Nelspruit Porphyritic Granite underlies most of the study area and generally occupies high lying and hilly terrain.

(ii) In the field, three textural sub-types of the porphyritic granite are recognizable, firstly an

intensely porphyritic granite, secondly, a moderate-to-slightly porphyritic granite (characterizing most of the porphyritic granite) and, thirdly, granite which exhibits few, if any, phenocrysts. No distinct geological contacts are recognizable between any of these sub-types and all are considered co-magmatic.

(iii) The Nelspruit Porphyritic Granite exhibits a wide range in major and trace element compositions, a factor considered to be related to fractionation within this granite and which will be dealt with in detail in Chapter 5.

(iv) The microcline phenocrysts which characterize the porphyritic granite are considered to have formed by the in situ mobilization and recrystallization of pre-existing K-felspar. This event is considered to have taken place within the igneous history of the granite, probably in response to thermal effects, the nature of which are obscure .

(v) The suggestions regarding the mode of formation of the microcline phenocrysts, together with the geochronological evidence presented later, and the trace element modelling described in Chapter 5, indicate that the porphyritic granite is magmatic in character (i.e. rather than anatectic or metasomatic). This opinion differs from that offered by Viljoen and Viljoen (1969c) who suggested that metasomatism was the principal mechanism for the formation of the potash-rich granites (i.e. the Nelspruit Migmatites and Gneisses) to the north of the Barberton Mountain Land (see Chapter 1).

(vi) As mentioned previously, the Nelspruit Migmatite and Gneiss Terrane and the Nelspruit Porphyritic Granite are considered to be co-genetic. The generally

higher lying nature of the latter granitic assemblage with respect to the former, suggests that it may have a sheet-like character, effectively overlying the migmatite and gneiss terrane. An analogous situation exists between the Hood Granite and the underlying Ancient Gneiss Complex as described in Swaziland by Hunter (1973a).

V. THE CUNNING MOOR TONALITE

(a) Field Description

The Cunning Moor Tonalite occupies very distinctive flat, low-lying countryside in the northeastern portion of the study area (Figure 10). The nature of this terrain is clearly illustrated in Plate 8b.

Outcrops within the area underlain by the Cunning Moor Tonalite are poor and restricted to isolated small domes and river exposures. For this reason the field relationships between the tonalites, the porphyritic granite and the migmatites and gneisses are obscure. At one outcrop (sample locality F5 - Figure 11) there is a suggestion of a contact between a porphyritic textured granite and the Cunning Moor Tonalite. This particular outcrop (Plate 6a) shows a vein of tonalitic material intruding a porphyritic textured granite. This isolated example cannot, however, be considered as conclusive evidence of the relationship between the Cunning Moor Tonalite and the Nelspruit Porphyritic Granite .

In the field the Cunning Moor Tonalite is generally homogenous, but, particularly on the margins of this body, it appears foliated and commonly contains mafic xenoliths (Plate 6c). In the southern portion of the Cunning Moor Tonalite the foliation is approximately parallel to the

inferred contact between the latter and the migmatites and gneisses. Pegmatites and aplites occur within the Cunning Moor Tonalite (Plate 6b), but their occurrence is not nearly as common as in the migmatite and gneiss terrane, or in the porphyritic granite.

Although the field relationships are inconclusive the Cunning Moor Tonalite is considered younger than both the adjacent migmatite and gneiss terrane and the Nelspruit Porphyritic Granite. This conclusion is supported by Rb-Sr whole rock dating carried out on both the Nelspruit Porphyritic Granite and the Cunning Moor Tonalite, the results of which will be more fully discussed in a later section.

(b) Petrography

The Cunning Moor Tonalite is a grey, massive, medium-to-coarse-grained rock, generally exhibiting an equigranular texture save for the occasional development of microcline phenocrysts. The rock consists predominently of plagioclase and quartz with lesser amounts of biotite, microcline and sphene. Trace amounts of rutile, zircon, apatite and muscovite were also noted.

Plagioclase is generally characterized by poor twinning and is often zoned as evidenced by the preferential sericitization of calcic cores. Microcline has a markedly interstitial character in the rock and is poikilitic, containing inclusions of plagioclase, quartz and biotite. The interstitial nature of the microcline (Plate 6d) is very similiar in appearance to that of an intercumulus phase in a mafic cumulate rock.

Sphene occurs in greater than accessory amounts in this rock type, as large (up to 3mm in length) euhedral, poikilitic grains. Quartz and plagioclase are commonly included within the sphene (Plate 6e) indicating its late formation in the crystallization history of the rock. The

PLATE 6

A. Photograph of a possible zone of contact between the Cunning Moor Tonalite and a porphyritic phase of the Nelspruit Migmatite and Gneiss Terrane. A vein of tonalitic material (fine grained, centre) intrudes the porphyritic-textured granite.

B. Two phases of aplitic veins intruding the Cunning Moor Tonalite at sample locality F14, east of Hazy View.

C. Dark mafic xenoliths in a railway cutting in the Cunning Moor Tonalite, near its contact with the Nelspruit Migmatite and Gneiss Terrane. Locality, 3km east of sample site E13 (Figure 11), east of Hazy View.

D. Photomicrograph illustrating the intersticial nature of microcline in the Cunning Moor Tonalite, emphasizing its late crystallization in the cooling history of this rock. Sample F14 (east of Hazy View), Magnification 20X.

E. Photomicrograph of a large grain of sphene occurring in the Cunning Moor Tonalite. The sphene contains inclusions of quartz and plagioclase, and formed late in the crystallization history of the Cunning Moor Tonalite. Sample F14, Magnification 20X.

PLATE 6

A

B

C

D

E

sphene is also zoned and twinned in some cases.

(c) Geochemistry

Nine fresh samples of the Cunning Moor Tonalite were selected for major and trace element analysis. The results (Table 13) substantiate the statement made concerning the homogeneity of this rock type and similiar compositions are seen to exist over large areas. Apart from the distinct textural differences described, the Cunning Moor Tonalite differs from the bulk of the Nelspruit Porphyritic Granite by its higher sodium and calcium and lower potash and rubidium contents (compare Table 13 with Table 10).

When the data from Table 13, together with that from the partial analyses of the Cunning Moor Tonalite (Table 26, Appendix 2), is plotted on a K_2O v Na_2O plot (Figure 26), a spread of compositions is observed. Over half the samples are, however, strictly tonalitic in composition, with the majority of the remainder falling into the granodioritic field. There is, therefore, adequate justification for calling the body a tonalite and the actual spread in composition may be related to the effects of fractionation as was suggested for the Nelspruit Porphyritic Granite (see Chapter 5).

The data was also plotted on a Rb v Sr plot (Figure 27) and the expected antipathetic relationship between these two trace elements (as determined by their respective bulk partition coefficients - see Chapter 5) is again apparent. If Figure 27 is compared with Figure 24 (the Rb v Sr plot for the Nelspruit Porphyritic Granite) the generally lower Rb content of the Cunning Moor Tonalite is noticeable.

It is conceivable that the Cunning Moor Tonalite may represent a co-genetic phase of the Nelspruit Porphyritic Granite. Geochemically colinear trends (with respect to the K_2O v Na_2O and Rb v Sr plots between the two types) tend to support

Figure 26. K_2O v Na_2O plot - Cunning Moor Tonalite.

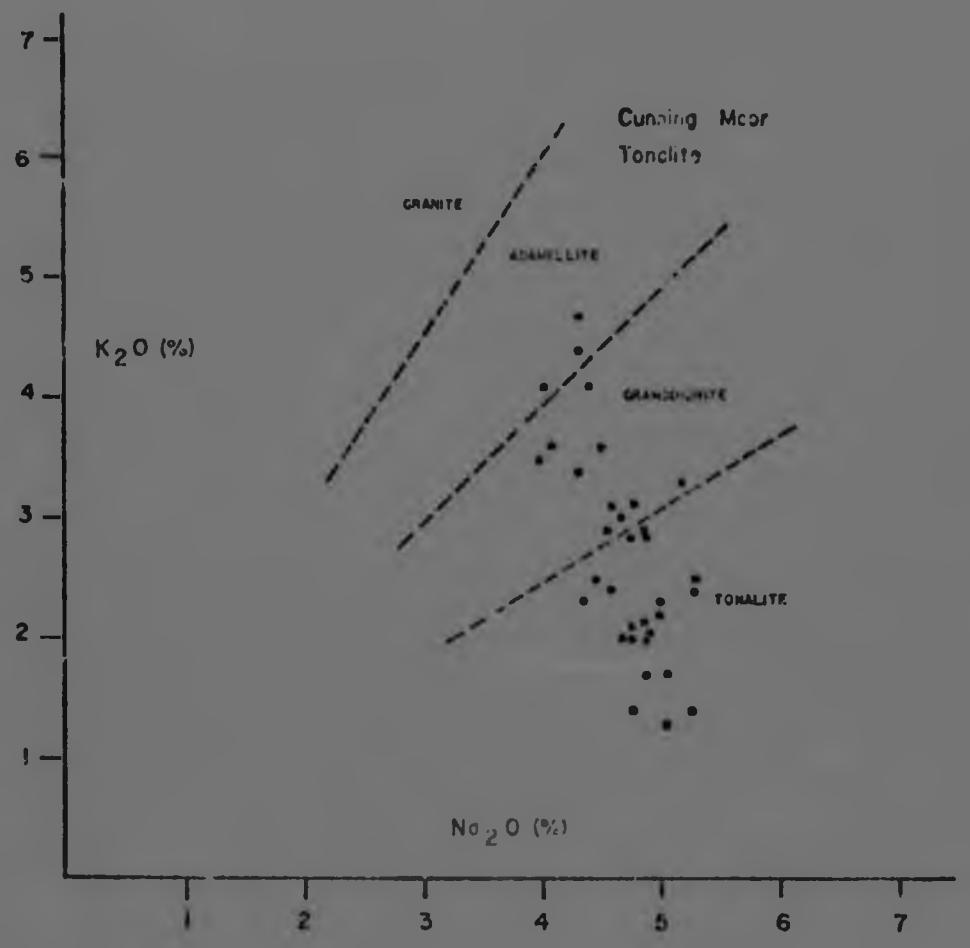

Figure 27. Rb v Sr plot - Cunning Moor Tonalite.

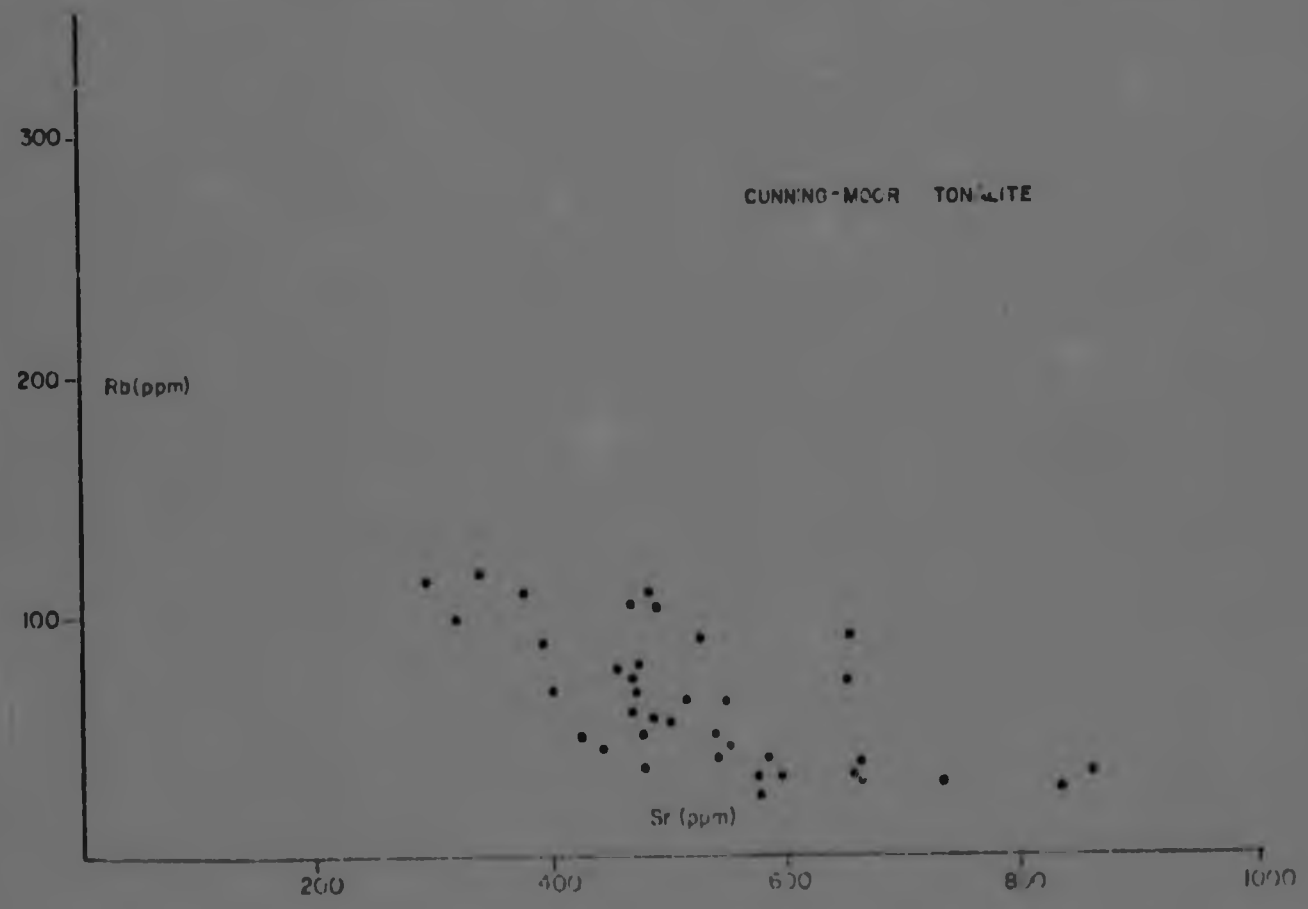

TABLE 13

SELECTED SAMPLES FROM THE CUNNING MOOR TONALITE

Samples	F12	F1	F8	F14	F21	F20	E25	E21A	G12
SiO_2	70,29	69,02	67,63	69,40	69,86	65,13	69,92	69,64	69,83
TiO_2	0,35	0,23	0,48	0,33	0,31	0,46	0,22	0,24	0,59
Al_2O_3	15,81	16,33	16,34	15,51	15,23	16,14	14,29	16,70	18,84
Fe_2O_3	2,80	1,78	2,81	2,53	1,93	3,23	1,72	1,91	3,98
MnO	0,06	0,04	0,07	0,07	0,06	0,08	0,05	0,03	0,09
MgO	0,01	1,95	1,53	1,89	0,47	3,47	1,89	1,59	1,68
CaO	3,02	2,03	3,29	2,96	2,41	2,83	2,19	,16	3,55
Na_2O	5,30	4,25	5,51	4,77	5,92	4,12	5,61	4,38	4,98
K_2O	1,05	2,74	1,56	1,55	2,84	1,09	3,50	3,35	1,52
P_2O_5	0,01	0,01	0,01	0,15	0,01	0,02	0,01	0,01	0,01
L.O.I.	0,24	0,45	0,41	0,30	0,40	0,70	0,68	0,43	0,46
TOTALS	98,93	98,83	99,66	97,35	98,91	99,45	100,[illegible]	100,63	99,47
ppm									
Rb	35	89	42	33	45	41	79	104	91
Sr	573	392	542	573	549	583	468	493	525
Ba	160	497	153	309	735	153	937	711	192

Sample localities - Figure 11

Analyst : L.J. Robb

this contention. However the strontium isotope data available from both the porphyritic granite and the tonalite indicates markedly different intial $^{87}Sr/^{86}Sr$ ratios and hence dispels any suggestions of a co-genetic link between the two (the isotope results are presented in a later section). The initial $^{87}Sr/^{86}Sr$ ratio for the Cunning Moor Tonalite is considerably higher than that for the Nelspruit Porphyritic Granite and this, coupled with its known younger isotopic age, suggests that the former may be the result of re-working (i.e. a partial melt product) of the latter. Such a suggestion would require confirmation using techniques such as rare-earth element modelling to determine the degree of partial melting involved and the feasibility thereof,with respect to the trace element composition of the resultant product.

(d) Summary and Conclusions

(i) The Cunning Moor Tonalite occupies a distinctive outcrop area characterized by very flat and low-lying terrain in the northeastern portion of the study area.

(ii) The Cunning Moor Tonalite is compositionally more homogenous than the Nelspruit Porphyritic Granite and is predominantly tonalitic. The variations in composition observed may be related to fractionation, a mechanism considered to be very pronounced in the porphyritic granite (Chapter 5) but probably not as marked in the tonalite.

(iii) Although geochemically colinear trends suggest that the Cunning Moor Tonalite and the Nelspruit Porphyritic Granite may be co-genetic, isotope data clearly indicates that this is not the case. Instead the suggestion is made that the former may be a partial melt product of the latter but the means to test this are beyond the scope of this dissertation.

(iv) Within the framework of what is currently known regarding the evolution of the Archaean granitic rocks in the Barberton region (see Chapter 1) the isotopic age of the Cunning Moor Tonalite (i.e. 2,844 ± 0,027 b.y. - see later) isolates it as being anomalous with respect to other tonalites in the region. It is, in fact, the youngest tonalite known in the Archaean terrane of the Barberton region and also the only one known to post-date rocks more potassic than itself.

VI. THE HEBRON GRANODIORITE

(a) Field Description

The Hebron Granodiorite is totally dissimiliar to any other granitic rock type in the study area. It is blue-grey in colour, massive, medium-grained with an equigranular texture, and is generally devoid of megacrysts.

In the field the Hebron Granodiorite outcrops in two distinctive ways :-

(i) It occurs as a unimodal body occupying an area of approximately 50 km^2 to the north-northwest of White River, in the vicinity of the Hebron Forest Reserve (Figure 10). This outcrop area is termed unimodal as the granodiorite occurs to the exclusion of all other rock types except later mafic intrusives. The nature of the outcrop area is illustrated in Plate 7a. The actual outcrop in this region is relatively poor and no unequivocal contact with the surrounding porphyritic granite could be located.

(ii) Outside the actual outcrop area of this body the Hebron Granodiorite occurs as veins and dykelets within the Nelspruit Porphyritic Granite. The areas of this bimodal association are illustrated in Figure 10, which shows a number of large, discrete, areas which exhibit this relationship. In

PLATE 7

A. A large hill comprised mainly of the Hebron Granodiorite in its unimodal outcrop area in the vicinity of the Hebron Forest Reserve, 20km north-northwest of White River.

B. An occurrence of Hebron Granodiorite in one of its bimodal outcrop areas. A vein of medium-fine grained Hebron Granodiorite intrudes and rafts off a portion of the coarse-grained Nelspruit Porphyritic Granite. Locality, sample site C39, west of Hazy View.

C. Photograph showing the distinctive polygonal weathered appearance of the Hebron Granodiorite. Locality, sample site C40, west of Hazy View.

D. A photomicrograph showing the broadly equigranular texture of the Hebron Granodiorite. The main mineral consituents in the rock are plagioclase, quartz and biotite. Sample C13, Magnification 20X.

E. A photograph of the Mpageni Granite pluton, taken in the Crocodile River gorge approximately 20km east of Nelspruit.

PLATE 7

A

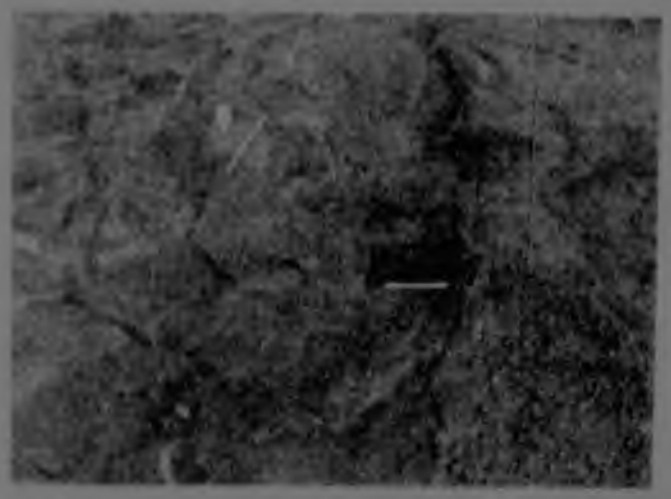

B

C

D

E

these bimodal areas, veins and dykelets of material identical to that of the actual Hebron Granodiorite body clearly intrude and often "raft off" the porphyritic granite (Plate 7b). The indications, from the bimodal outcrop areas, are that the Hebron Granodiorite post-dates the Nelspruit Porphyritic Granite.

The two modes of occurrence of the Hebron Granodiorite provide something of an unusual geological feature. It is suggested that the unimodal area may represent the focus of intrusion of the Hebron body whereas the bimodal areas appear to have suffered only from localized intrusive veining which accompanied the main intrusive event.

Wherever it occurs in the field the Hebron Granodiorite has a distinctive appearance and is characterized by polygonal cracks on the weathered surfaces of the rock (Plate 7c).

(b) Petrography

The Hebron Granodiorite consists predominantly of plagioclase and quartz with minor amounts of biotite, microcline and muscovite. Accessory amounts of sphene, apatite and rutile also occur. The equigranular texture of this rock is a prominent feature, and is illustrated in Plate 7d.

Under the microscope little difference is apparent between the granodiorites from the unimodal area and those from the bimodal areas. This is particularly important in view of the fact that veins of Hebron Granodiorite occurring in the bimodal areas may sometimes be mistaken for aplite veins. Aplites, however, contai- significant amounts of microcline and very little biotite, two features which clearly distinguish them from the Hebron Granodiorite (the latter can contain in excess of 10 percent of biotite and usually has only minor amounts of microcline).

TABLE 14

SAMPLES OF THE HEBRON GRANODIORITE FROM BOTH UNIMODAL AND BIMODAL OUTCROP AREAS

Sample	C13	C14	C49	C48	D25A	G2	C39A	D10	E1A
SiO_2	65,23	66,88	70,21	70,30	67,01	66,95	69,65	64,22	68,87
TiO_2	0,68	0,75	0,30	0,07	0,45	0,47	0,18	0,65	0,27
Al_2O_3	16,90	13,93	14,61	16,87	17,36	15,49	16,95	14,83	15,50
Fe_2O_3	3,92	4,75	2,11	0,72	3,34	2,58	1,55	4,27	2,21
MnO	0,07	0,06	0,06	0,02	0,05	0,05	0,06	0,06	0,05
MgO	1,39	2,14	2,48	0,01	0,59	2,87	0,83	3,21	1,93
CaO	2,46	2,57	1,82	0,61	3,26	2,39	2,22	3,04	3,31
Na_2O	4,10	3,61	3,63	3,41	4,97	4,70	3,88	4,20	5,47
K_2O	3,68	3,48	3,68	6,06	1,01	3,41	3,11	3,59	0,61
P_2O_5	0,06	0,20	0,05	0,01	0,01	0,12	0,01	0,50	0,03
L.O.I.	0,57	1,19	0,61	0,53	0,69	0,04	0,48	0,66	0,57
TOTALS	99,05	99,57	99,56	98,59	98,65	99,67	98,92	99,24	98,83
ppm									
Rb	85	100	146	211	82	77	93	109	31
Sr	350	340	388	142	593	812	393	355	553
Ba	879	709	670	434	226	1264	546	746	149

Analyst : L.J. Robb

Samples C13, C14, C49 and C48 - Hebron Granodiorite from the unimodal outcrop area in the vicinity of the Hebron Forest Reserve.

Samples D25A, G2, C39A, D10 and E1A - Hebron Granodiorite from the bimodal outcrop areas.

Sample localities - Figure 11

A petrographic characteristic of all the Hebron Granodiorite samples examined is the apparent presence of two generations of plagioclase. Larger plagioclase grains were found to contain inclusions of smaller plagioclase grains. The former are commonly zoned, a feature reflected in the preferential sericitization of the calcium-rich cores of these grains. Another common petrographic feature is the formation of myrmekitic textures in the reaction zones between plagioclase and microcline grains.

(c) Geochemistry

A total of nine samples of Hebron Granodiorite were analysed for major and trace elements (Table 14). Four of these samples were selected from the unimodal outcrop area whereas the remainder were obtained from various bimodal outcrop areas.

A comparison of the four samples from the unimodal area with the five samples from bimodal areas (Table 14) shows that there are no significant or systematic chemical differences between the two types. Chemical variations within the two sub-types are, in fact, as pronounced as the variations between them. The possibility that veins of Hebron Granodiorite from the bimodal areas may be aplites can also be discounted, as is shown when comparing the chemistry of the aplites (Table 9) with that of the Hebron Granodiorite (Table 14). It is evident that the aplites have significantly higher potash and rubidium contents, and lower magnesium, iron and strontium contents than the granodiorites.

Apart from its textural distinction, the Hebron Granodiorite is also, in some respects, chemically distinctive. This is emphasized in an Alkalis-FeO-MgO (AFM) ternary plot (Figure 17) where it is seen that the latter is generally more mafic than the majority of samples from the other granite types in the study area (with the exception of the mafic xenoliths which consist of considerably more MgO and FeO than typical granitoid rocks). This is a reflection of the high biotite content (approximately 10%) that characterizes the Hebron Granodiorite.

Figure 28. K_2O v Na_2O plot - Hebron Granodiorite.

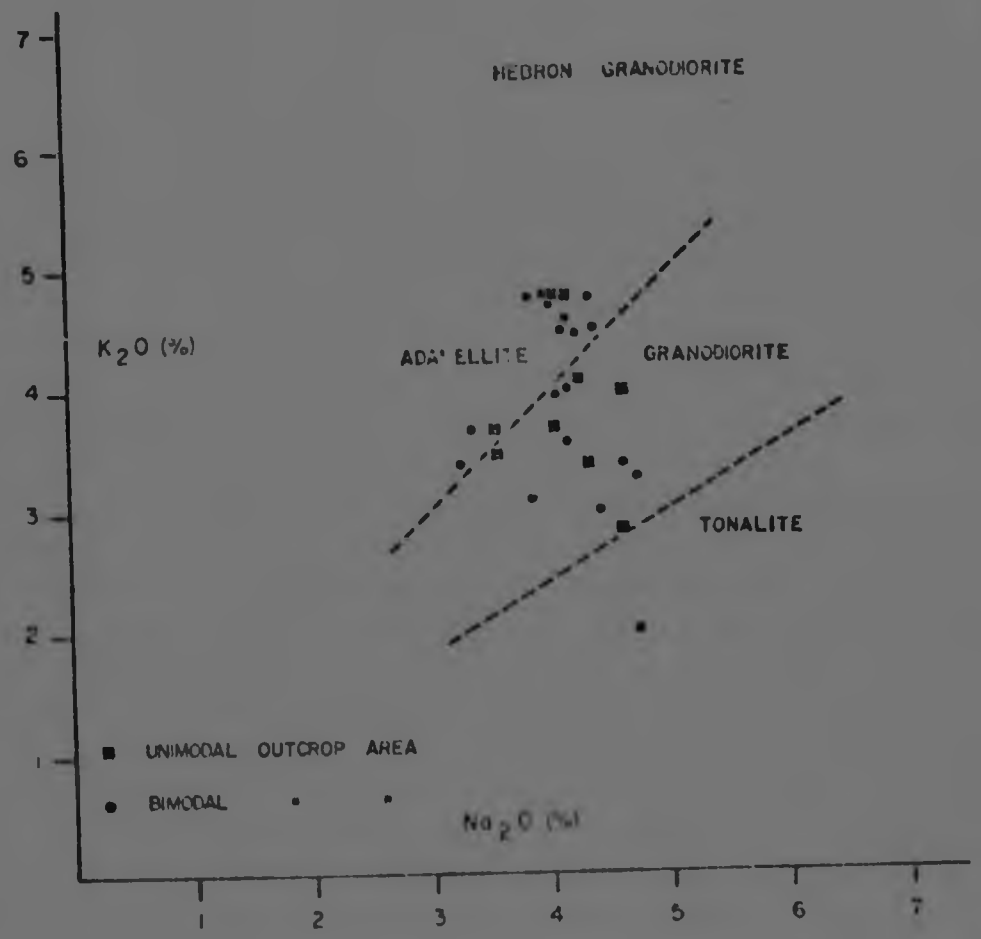

Figure 29. Rb v Sr plot - Hebron Granodiorite.

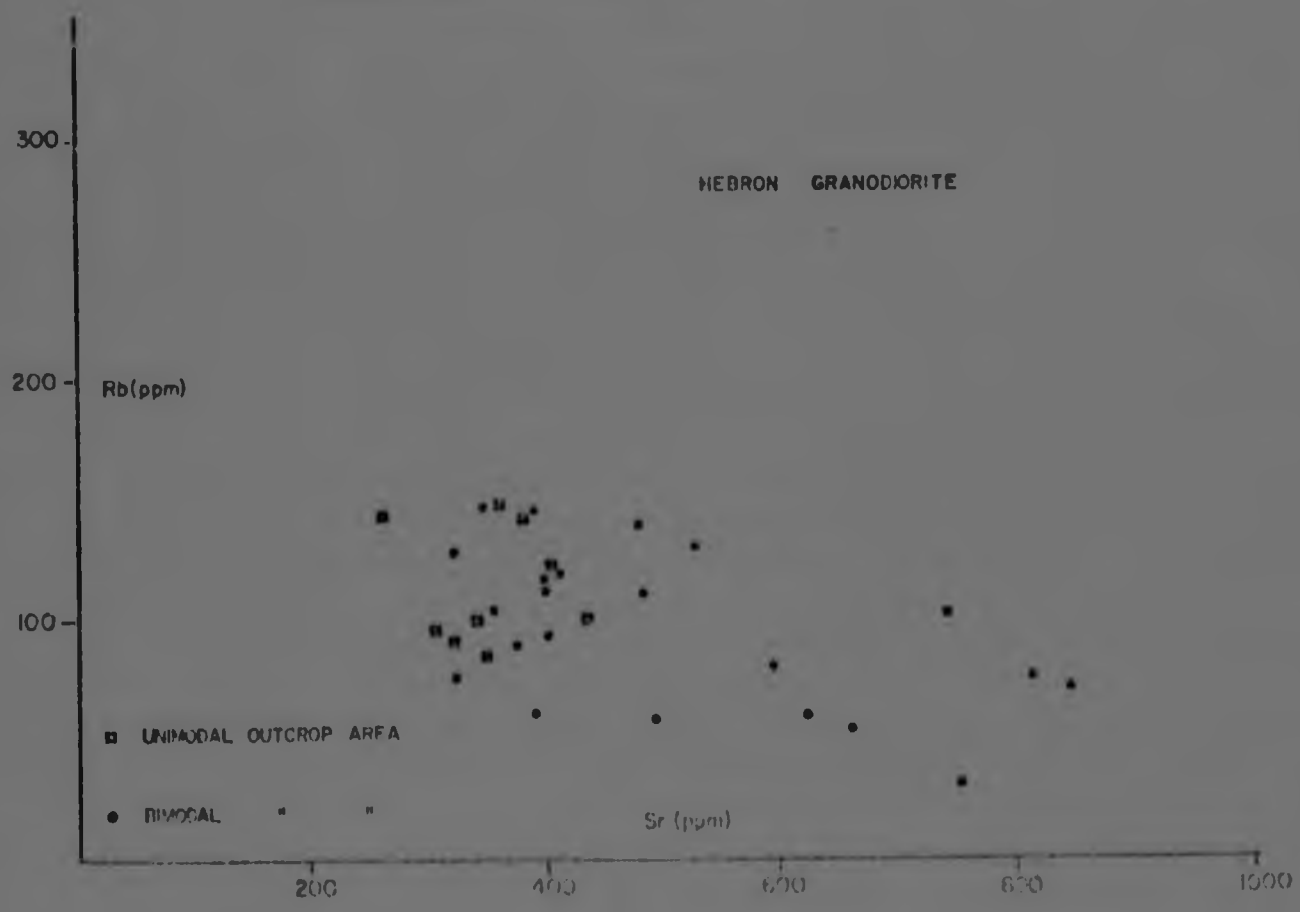

The data shown in Table 14, in addition to data from the partial analyses of the Hebron Granodiorite (Table 27, Appendix 2) has been plotted on K_2O v Na_2O and Rb v Sr plots (Figures 28 and 29 respectively). A distinction is made on these diagrams between samples from the unimodal outcrop area and those from the bimodal outcrop areas. On the K_2O v Na_2O diagram both these sets of data plot within the field of granodiorite, or close to it, in the adamellite field. By comparison with the wide range in compositions exhibited by the Nelspruit Porphyritic Granite this distribution is comparatively well clustered. The Hebron Granodiorite is, therefore, more homogenous in composition than the porphyritic granites and the migmatites and gneisses described earlier. The K_2O v Na_2O plot also emphasizes the lack of any compositional distinction between the granodiorites of the unimodal and bimodal areas.

The Rb v Sr plot (Figure 29) illustrates the same broad antipathetic relationship between these two elements that has been exhibited in the other granite types of the study area. Most of the samples tend to cluster in the vicinity of 100 ppm Rb and 400 ppm Sr, with only a few of the remaining samples making up the scatter in the diagram. This again reflects the essentially homogenous nature of this rock type. It will also be noted that all the samples from the unimodal outcrop area fall within the main cluster of points on this plot. This is to be expected as samples of the granodiorite from the bimodal areas are more likely to have diverse chemical characteristics than those from the unimodal area, which probably represents the focus of the intrusion of this granitic body. Samples from the bimodal outcrop areas may also be more fractionated than those from the unimodal outcrop area.

Both U-Pb and Rb-Sr isotope data is available on the Hebron Granodiorite and this information will be presented later. The Rb-Sr isochron for the granodiorite indicates an age slightly older than that obtained for the Nelspruit

Porphyritic Granite, a factor not compatible with the observed field relationships. However, the isochron has a large error margin and there is some overlap between these ages. The initial $^{87}Sr/^{86}Sr$ ratio for the Hebron Granodiorite is very low (R_o = 0,7007 ± 0,0005) suggesting an uncontaminated mantle origin for this rock.

(d) Summary and Conclusions

(i) In the field the Hebron Granodiorite outcrops in two distinct forms :- firstly it occupies a urimodal outcrop area which probably represents the focal point of the intrusion of this body and, secondly, it occurs as veins within the Nelspruit Porphyritic Granite in discrete areas which have suffered only localized effects of this intrusion.

(ii) The Hebron Granodiorite is characterized by homogeneity with respect to its major and trace element chemistry. It appears that the effects of fractionation, which have been mentioned previously in connection with the Nelspruit Porphyritic Granite, and which are responsible for significant variations in major and trace element chemistry, may not have played a significant role in the crystallization of this rock type.

(iii) Isotopic evidence suggests that the intrusion of the Hebron Granodiorite is related to an uncontaminated mantle source and very closely linked, time-wise, to the Nelspruit Porphyritic Granite. Field relationships indicate that the former post-dates the latter.

VII. THE MPAGENI GRANITE

(a) General Description

The Mpageni Granite occupies a small (approximately

6km^2), discrete, pluton-like body in the southeastern corner of the study area (Figure 10). It's rugged nature, emphasized by the Crocodile River which laterally bisects it, is illustrated in Plate 7e.

The Mpageni Granite, which is cross-cut by numerous post-Transvaal Supergroup mafic dykes, is considered to be the youngest granite in the study area. It's cross-cutting relationship with the surrounding Nelspruit Migmatite and Gneiss Terrane, as well as isotopic data, place this granite into the category of "Younger Plutons" in the regional classification of the granites of the Barberton region as outlined by Viljoen and Viljoen (1969b). These authors regard the "Younger Plutons" as being the final granitic event responsible for the consolidation of the early Archaean granitic crust (see Chapter 1).

For the purpose of this dissertation no detailed work was undertaken on the Mpageni Granite as a considerable amount of data is already available regarding this body. A summary of the existing state of knowledge concerning this granite pluton is presented below.

(b) A summary of some of the more important work carried out on the Mpageni Granite

Visser et al.(1956) were the first to describe the intrusive nature of the Mpageni Granite, based on the cross-cutting relationship between the foliation in the so-called "Nelspruit Granite" and the massive textured Mpageni Granite. These authors also referred to the presence of syenitic and quartz-syenitic rocks intimately associated with the latter. They concluded their description of the Mpageni Granite by suggesting that it was a co-magmatic phase of the Nelspruit Granite (i.e.co-magmatic with the porphyritic migmatites and gneisses that surround the pluton).

Visser and Verwoerd (1960) furnished a petrographic description of the Mpageni Granite as well as providing a full

TABLE 15

MAJOR ELEMENT ANALYSIS OF A SAMPLE FROM THE MPAGENI GRANITE

SiO_2	71,50
TiO_2	0,19
Al_2O_3	14,22
Fe_2O_3	1,32
FeO	0,99
MnO	0,05
MgO	1,11
CaO	1,51
Na_2O	4,27
K_2O	4,99
P_2O_5	0,08
S	0,04
H_2O^+	0,40
H_2O^-	0,05
TOTAL	100,72

Sample from the Mpageni Granite pluton at Gorge Siding (Visser and Verwoerd, 1960).

silicate analysis of the latter (Table 15). The granite is described as consisting predominantly of plagioclase, orthoclase, microcline, quartz and biotite with accessory amounts of fluorspar, apatite, zircon and tourmaline. Texturally, the granite is described as being massive and slightly porphyritic with patches of gneissose material which, "... can be ascribed to assimilation of older rock"(Visser and Verwoerd, 1960). The full silicate analysis listed in Table 15 indicates a typical granitic composition, the K_2O/Na_2O ratio of 1,17, reflecting more specifically, an adamellitic composition, after the classification of Harpum (1963).

A number of isotopic studies have been carried out on the Mpageni Granite and ages have been obtained by both Rb-Sr and U-Pb methods. De Gasparis (1967) obtained an isochron which yielded an age of 2,55 ± 0,09 b.y. with an initial $^{87}Sr/^{86}Sr$ ratio of 0,7065 ± 0,0016. This age is considerably younger an the figure of 2,99 ± 0,09 b.y. obtained by De Gasparis for the age of the surrounding Nelspruit Migmatite and Gneiss Terrane and confirms the geological observations that the Mpageni Granite intrudes the latter. The high value of the initial $^{87}Sr/^{86}Sr$ ratio suggests an origin related to reworking of crustal material. Oosthuyzen (1970) produced a U-Pb mineral age for the Mpageni Pluton of 2,81 ± 0,08 b.y. This is an older age than indicated by the Rb-Sr method but nevertheless still indicates that this granite post-dates the surrounding migmatites and gneisses.

The question of the origin of the Mpageni Pluton has been dealt with in some detail by Condie and Hunter (1976). This is a question of some importance as the answers relating to work of this nature are likely to reflect the modes of origin of all the "Younger Plutons" that occur in the Barberton region. Insight into the mechanisms that prevailed during the late stages of consolidation of the Archaean granite crust are thus available. Condie and Hunter (1976) carried out trace and rare-earth element modelling on data from a number of

samples from the Mpageni Pluton. They concluded that this granite formed as the result of 70-80% fractional crystallization of a granodioritic magma similiar in composition to the Dalmein Pluton in the southwest of the Barberton Mountain Land. This conclusion is also compatible with the high $^{87}Sr/^{86}Sr$ ratio obtained by De Gasparis (1967). Whereas the older tonalitic rocks in the region (such as the Dalmein Pluton) are considered to have formed by the partial melting of mantle-derived basaltic material (Condie and Hunter, 1976), younger more potassic events in the formation of the granitic crust are apparently related to the reworking of existing crustal material Thus mantle-derived material was probably rare or non-existent in the closing stages of the consolidation of the earth's early crust.

VIII. A BRIEF ACCOUNT OF THE PRELIMINARY GEOCHRONOLOGICAL WORK CARRIED OUT IN THE STUDY AREA

(a) Introduction

The geochronological work presented in this section was carried out as part of the involvement of a number of universities and scientific institutions in the South African Geodynamics Project. The U-Pb work was carried out at the National Physical Research Laboratory of the C.S.I.R., Pretoria, under the supervision of Dr. A.J. Burger. The Rb-Sr work was carried out at the Bernard Price Institute of Geophysics at the University of the Witwatersrand, by Mrs. E. Barton, under the supervision of Professor H.L. Allsopp.

Three rock types in the study area were dated, i.e. the Nelspruit Porphyritic Granite, the Cunning Moor Tonalite and the Hebron Granodiorite. All three types were subjected to Rb-Sr and U-Pb dating procedures. The results of this work (as yet unpublished) are presented and discussed below with the kind permission of the geochronologists involved.

(b) Results

The results of the geochronological work carried out in the area during 1976, are summarized in Table 16. It is important to note that considerable discrepancies exist between the Rb-Sr and U-Pb data and thus the data, in its present form, is in need of refinement. As a result, the age relationships suggested by this data will not be considered in any great detail, nor will any genetic considerations be based solely on parameters such as initial $^{87}Sr/^{86}Sr$ ratios.

(i) The Rb-Sr results :-

The error margins obtained on the Rb-Sr isochrons are all acceptable, the least reliable being that obtained for the Hebron Granodiorite, which represents a ± 2,1% error. The data suggests that the Hebron Granodiorite is slightly older than the Nelspruit Porphyritic Granite, a factor not compatible with the geological evidence. There is overlap, however, between the error margins of these two isochrons and, in this light, the writer remains of the opinion that the granodiorite post-dates the porphyritic granite. Nevertheless it appears that these two events were virtually synchronous. The Cunning Moor Tonalite, on the other hand, is seen to be significantly younger than either of the other two granite types (Table 16).

With regard to the initial $^{87}Sr/^{86}Sr$ ratios, both the Hebron Granodiorite and the Nelspruit Porphyritic Granite have low R_o values suggesting uncontaminated magmatic origins possibly related to mantle or lower crustal sources. The Cunning Moor Tonalite has a much higher R_o value suggesting an origin related to reworking of pre-existing crustal material.

(ii) The U-Pb results :-

The ages resulting from the U-Pb method are highly discordant, a factor which casts doubt as to their reliability.

TABLE 16

COMPARISON OF GEOCHRONOLOGICAL RESULTS OBTAINED BY RB-SR AND U-PB METHODS

Granite Type	Method	Number of samples analysed	Age (b.y.)	R_O
Cunning Moor Tonalite	Rb-Sr	6 point isochron	2,844 (±0,027)	0,7034 (±0,0001)
Nelspruit Porphyritic Granite	Rb-Sr	6 point isochron	3,205 (±0,049)	0,7016 (±0,0004)
Hebron Granodiorite	Rb-Sr	5 point isochron	3,28 (±0,068)	0,7007 (±0,0005)
Nelspruit Porphyritic Granite	U-Pb	3 random zircon analyses + 2 size fractions on discordant lines.	2,84	not applicable
Hebron Granodiorite and Cunning Moor Tonalite	U-Pb	2 random zircon analyses. 1 random zircon analysis + 2 size fractions (both types on a single discordant line)	2,99	not applicable

Notes : (i) b.y. - 1 billion years = 1000 million years

(ii) R_O - Initial $^{87}Sr/^{86}Sr$ ratio

(iii) Rb-Sr per kind permission of Mrs. E. Barton
U-Pb per kind permission of Dr. A.J. Burger.

The U-Pb isotope ratios were analysed from random-sized zircons as well as from size-fraction zircons, and both the resultant ages (Table 16) were obtained from well-defined discordant lines passing through the origin of the concordia plot. This factor implies that the lead-loss that caused discordancy in in these ages took place in very recent times. The U-Pb ages are, however, significantly different to those ages obtained by the Rb-Sr method. The Hebron Granodiorite and the Cunning Moor Tonalite give an identical age which is older than the age obtained for the Nelspruit Porphyritic Granite (Table 16). Whereas this is the case with regards the Hebron Granodiorite, the Rb-Sr method clearly indicates that the Cunning Moor Tonalite is significantly younger than the porphyritic granite. The largest discrepancy, however, concerns the absolute age of the Nelspruit Porphyritic Granite where the U-Pb age for the latter is seen to be 0,365 b.y. younger than that obtained by the Rb-Sr method. The two methods are therefore producing discrepancies, not only with respect to the relative ages of the three granite types, but also with respect to their absolute ages. From the point of view of the geological control, the writer considers that the results of the Rb-Sr method, although not entirely compatible, fit the observed facts far better than do the results obtained by the U-Pb method.

(c) Some points regarding the discrepancies in the geochronological results

The geochronological data, in its present state, is of little assistance in helping to unravel the question of the relative ages of the three granite types in the study area, nor can it provide any quantitative data concerning the origins of these granites. The accuracy and precision of the data has, therefore, to be improved upon and two possibilities exist :-

(i) Additional samples can be collected to increase the number of points on the Rb-Sr isochrons and the U-Pb

discordant lines. This process, however, involves considerable additional expense and in the case of the Rb-Sr isochrons, which all have medium-to-small error margins, may not significantly improve their accuracy and precision.

(ii) In the case of the U-Pb method careful selection of existing zircon size-fractions may significantly improve the state of the existing data. It is likely that this suggestion will be carried out in the near future and that the existing discrepancies may be resolved.

At present, however, these geochronological results are of little use and the reasons behind these significant discrepancies remain unknown.

IX. SUMMARY AND CONCLUSIONS

This chapter has dealt with a detailed geological and geochemical description of the six granite types that have been defined in the study area. The development of these Archaean granites in this area is seen as a complex sequence of events spanning approximately 700 million years of the earth's early geological history. As a conclusion a brief summary of the main events and processes that have resulted in the formation of this portion of the Archaean granitic basement, is presented :-

(a) Assuming that the earth's primordial crust consisted of a mafic-to-ultramafic assemblage similiar to that observed in the Barclay Vale Schist Belt and the Onverwacht Group of the Barberton Greenstone Belt, then the first granitic material to appear on the earth's crust was tonalitic or trondhjemitic in composition. In the study area this material is

manifest as the Tonalite Gneisses and Migmatites, and now occurs over limited outcrop areas in close proximity to the greenstone remnants. The introduction of this tonalitic material was a widespread event, as is evidenced by the nature of the granite terrane to the south of the Barberton Mountain Land which is characterized by a complex assemblage of greenstone remnants, migmatites and tonalite and trondhjemite gneisses (C.R. Anhaeusser, personal communication, 1976). According to the dating of other tonalitic gneisses and migmatites, particularly to the south of the Barberton Mountain Land (Allsopp et al, 1969; Oosthuyzen, 1970) this event probably took place between 3,3 and 3,4 b.y. ago.

(b) Approximately 3,2 b.y. ago the widespread introduction of a potassic granite took place in a well-defined high-lying area to the north of the Barberton Mountain Land. This intrusive event considerably altered the nature of the pre-existing tonalite-greenstone crust, its principal effect being one of homogenization. This granitic magma, occupying a large area, is thought to have cooled slowly, allowing the fractionation of successive mineral phases to take place - a feature reflected in the trace element distributions. Complicated physicochemical interactions, possibly related to repeated pulses of magmatism, resulted in the formation of late-phase microcline phenocrysts by the mobilization and recrystallization of existing K-felspar. Areas marginal to the Nelspruit Porphyritic Granite, and which are lower-lying, topographically than the latter, were not subjected to the full impetus of the process of homogenization that characterized the focal regions, and are underlain by gneissic and migmatitic textured rocks. These migmatites and gneisses are, as a result, thought to be predominantly arteritic in origin.

(c) Almost synchronous with the event that produced the Nelspruit Porphyritic Granite and the Nelspruit Migmatite and Gneiss Terrane, was the intrusion of the Hebron Granodiorite. This body, probably lower-crust or mantle derived (according to the initial $^{87}Sr/^{86}Sr$ ratios), occurs predominantly in one area to the north-northwest of White River, but also appears disseminated over a much wider area as veins intruding the porphyritic granite.

(d) Approximately 2,8 b.y. ago the Cunning Moor Tonalite was emplaced in the northeastern corner of the study area. This body, probably the result of reworking of pre-existing felsic or intermediate crustal material (by virtue of a high initial $^{87}Sr/^{86}Sr$ ratio), represents the youngest body of tonalite in the Barberton region and the only one to post-date granitic material more potassic than itself.

(e) The final event in the formation of the granitic crust in the study area was the emplacement of the potassic Mpageni Granite pluton. This event took place between 2,8 and 2,55 b.y. ago (De Gasparis, 1967; Oosthuyzen, 1970) as the result of the fractional crystallization of a granodioritic magma (Condie and Hunter, 1976).

CHAPTER 4

GEOCHEMICAL CONTOURING AND POLYNOMIAL TREND SURFACE ANALYSIS OF THE GRANITIC TERRANE BETWEEN NELSPRUIT AND BUSHBUCKRIDGE

I. INTRODUCTION TO THEORY AND TECHNIQUES

(a) Logistics

One of the objects of this study was to obtain an indication of the regional distribution of certain elements in the Archaean granitic terrane between Nelspruit and Bushbuckridge. Specifically for this purpose, a large number of samples (approximately 300) were collected from the entire area. The distribution of sample localities is illustrated in Figure 11; although the sampling could not be carried out on a regular grid pattern, the sample distribution and density is even throughout the area.

Of the samples collected 76 were subjected to full major element analysis as well as analysis for certain trace elements (i.e. Rb, Sr and Ba). The remaining samples (just over 200 in number) were partially analysed for K_2O, Na_2O, Rb, Sr and Ba. The major element analyses have all been listed in Chapter 3 (Tables 5 - 14) whereas the partial analyses are presented in Appendix 2 (Tables 23-27). The variables that were contoured are the elements K_2O, Na_2O, Rb, Sr and Ba. In addition the spot heights in the area were also contoured, to provide a topographic map of the region. The spot height data was obtained by reading off the altitude values at each sample locality, from the 1:50 000 topographical sheets.

The contouring and polynomial trend surface analyses were all calculated and plotted by computer. The calculations were carried out on the IBM 370 computer at the University of the Witwatersrand, and the plotting was done on a CALCOMP plotter attachment. All handling and processing of data, with

respect to the computer application, was carried out by Miss J.R. Burkinshaw of the Economic Geology Research Unit.

The distribution of the geochemical data is portrayed in two ways in this chapter. The first involved standard data contouring whereas the second involved polynomial trend surface analysis :-

(b) Data Contouring

Contouring of data on the IBM 370 computer is carried out using the standard contouring package GPCP (General Purpose Contouring Programme). Contouring within the framework of GPCP involves the use of three variables; two of these are independent variables (the X and Y coordinates of the sample locality) while the third, a dependent variable, is a specific value attributable to the sample locality (e.g. K_2O, Rb, Ba). The X and Y coordinates were calculated by overlaying a rectangular grid on the 1:150 000 map of the sample localities (Figure 11). Geochemical values attributable to specific sample localities were obtained from the Tables mentioned above. The scale of the contour map was designed to coincide exactly with that of the 1:150 000 geological map of the area (compare Figure 10 with Figures 30-35). It will be noted in Figures 30-50 that GPCP contains an option which allows certain areas, with no data points, to be omitted from consideration in the calculations. Areas coinciding with the Kruger National Park, the Transvaal Drakensberg Escarpment, as well as the granitic terrane south of Nelspruit have been blanked out on all the contour maps and trend surfaces.

(c) Polynomial Trend Surface Analysis

(i) The calculation of polynomial trend surfaces on the University of the Witwatersrand's computer :-

The purpose of polynomial trend surface analysis in

geology is to objectively separate out the regional trends in a set of data from complex local fluctuations. This has been carried out mainly with respect to geochemical data by numerous workers including Whitten (1961), Parslow (1971), Anhaeusser (1973b) and Davis (1973). Davis (1973) has stated that "Trend analysis is the geology profession's name for a mathematical method of separating map data into two components - that of a regional nature, and local fluctuations".

Polynomial trend surface analysis is,therefore, a smoothing technique based on the fitting of successive orders of polynomial expressions to data sets, starting from a simple linear and moving through successively more complex curvilinear surfaces. For example, the first degree polynomial surface is expressed in terms of the general equation for a planar surface in geometric space :-

$$y = b_o + b_1x_1 + b_2x_2$$

The second order polynomial surface is expressed in terms of a parabolic surface and includes squared and cross-product terms :-

$$y = b_o + b_1x_1 + b_2x_2 + b_3x_1^2 + b_4x_2^2 + b_5x_1x_2$$

Similiarly, the third degree polynomial is expressed in terms of a hyperbolic surface and includes a cubed term and cross-products. Successively higher order surfaces involve raising the terms to higher powers with the result that higher order trend surfaces become more complex and begin to approach the shape of the standard contour surface.

The standard GPCP, mentioned above, usually contains an option which allows it to calculate the polynomial coefficients and plot the various regression surfaces. However, in the University of the Witwatersrand's version of this package this

option was not available and a special technique was devised by Miss Burkinshaw to obtain these surfaces on the CALCOMP plotter.

In the first instance, the polynomial coefficients were derived from the raw data by feeding the latter into a standard statistical package programme SPSS (Statistical Package for the Social Sciences). The resultant coefficients were then read into a special programme (written by Mr. G. Gott of the University's Computer Centre) which calculated the values of the polynomial trend surface at each intersection of the standard rectangular grid that GPCP uses to plot contour lines. The third and final stage in the production of the polynomial trend surface was simply the plotting of contours by the GPCP using the values at each grid point calculated by the above programme. The polynomial trend surfaces (Figures 36 -50) are presented in this dissertation as scaled down versions of the original 1:150 000 plots drafted onto a base map of the study area.

(ii) The Significance of Polynomial Regression Surfaces

It is advisable, prior to discussing the geological implications of the various polynomial regression surfaces, to consider their validity and significance. Davis (1973) has stressed that "... polynomial functions are used for geological trend analysis merely as a matter of convenience." Of even greater importance, he adds, the "Use of polynomials in no way intimates a belief that geologic processes are polynomial functions."

It is important to realize, when considering Figures 36-50, that only the broadest regional geochemical trends are being portrayed and the validity of the trend is severely limited by the confines of the area within which the samples were collected. Any genetic interpretations that may result from polynomial trend surfaces should only be made bearing

these limitations in mind.

Table 17 summarizes the results of certain significance tests carried out on the various polynomial trend surfaces as they were computed. It will be noted that all surfaces were significant at the 1 per cent level with the exception of the third degree Na_2O surface and all the Ba surfaces. It will also be noted, however, that with the exception of the altitude surfaces, all the polynomial trend surfaces have very low correlation coefficients. This appears to be a characteristic of other geochemical trend surfaces (Anhaeusser, 1973b) and is most likely related to the effects of strong local fluctuations in the data which, in turn, are related to the complexities of granite petrogenesis and trace element partitioning. The fact that none of the Ba surfaces are significant at the 1 per cent level is problematical. It may be that whereas Rb and Sr behave in accordance with the partitioning laws that govern their distribution, Ba does not appear to behave as conservatively and its distribution tends to fluctuate somewhat randomly. It will be noted that the contour surface for Ba (Figure 35) exhibits a considerable range of values which contribute towards the insignificant Ba trend surfaces.

II. DESCRIPTION AND GEOLOGICAL IMPLICATIONS OF THE VARIOUS CONTOUR MAPS

(a) Data Contouring

The contour maps for topography (metres), K_2O (%), Na_2O (%), Rb (ppm), Sr (ppm) and Ba (ppm), are presented in Figures 30-35 respectively.* All sample localities, and the specific values attached to each locality, are shown on these maps.

(i) Topography

This contour map represents only an approximation of

* (On these maps the red colour indicates high values and the blue colour indicates low values)

TABLE 17

F TESTS AND CORRELATION COEFFICIENTS RELATING TO THE VARIOUS POLYNOMIAL TREND SURFACES

VARIABLE	DEGREE OF EQUATION	F VALUE	SIGNIFICANT AT:-	R^2
Altitude (metres)	1^o	177,113	α = 0,01	0,607
	2^o	90,276	α = 0,01	0,666
	3^o	78,856	α = 0,01	0,762
K_2O (%)	1^o	9,603	α = 0,01	0,083
	2^o	11,853	α = 0,01	0,222
	3^o	8,506	α = 0,01	0,273
Na_2O (%)	1^o	6,072	α = 0,01	0,069
	2^o	3,050	α = 0,01	0,087
	3^o	1,767	not significant	0,092
Rb (ppm)	1^o	15,622	α = 0,01	0,163
	2^o	7,438	α = 0,01	0,191
	3^o	5,231	α = 0,01	0,235
Sr (ppm)	1^o	13,686	α = 0,01	0,147
	2^o	6,581	α = 0,01	0,174
	3^o	4,332	α = 0,01	0,200
Ba (ppm)	1^o	0,694	not significant	0,008
	2^o	1,355	not significant	0,041
	3^o	0,926	not significant	0,051

α - denotes the level of significance.
F VALUE - that value derived from the F TEST.
R^2 - a correlation coefficient between the data and the theoretical surface.

the actual topographic surface in the area between Nelspruit and Bushbuckridge as the control points are limited to the spot heights of each sample locality. This map has been included in this section to illustrate the extent of the correlation between topography and the various geochemical parameters measured. The relationship between topography and granite composition in the Barberton region has been described by Viljoen and Viljoen (1969c) and has been referred to earlier in Chapters 1 and 3. These authors have noted the positive correlation between high-lying areas and granites of potassic composition.

Figure 30 shows that the western half of the study area is underlain by terrain of elevation greater than 800m above mean sea level (a.m.s.l.) whereas the eastern half has an elevation less than 800m a.m.s.l. and which extends down to as low as 350m a.m.s.l. The northeastern quadrant of the map is also clearly less rugged than the remainder of the area to the south and west.

Comparison of the topographical contour map with Figure 31, which illustrates the K_2O distribution in the study area, shows a good correlation between the terrain occupying an elevation of greater than 800m and the areas of high K_2O values (i.e. $>$ 4-5% K_2O). Similiarly the contour maps showing the distribution of Rb and Ba (Figures 33 and 35) show a positive correlation between high Rb and Ba concentrations and high-lying areas.

An inverse relationship exists between the Na_2O and Sr distributions (Figures 32 and 34 respectively) and topography. The lower-lying areas ($<$ 800m a.m.s.l.), particularly in the northwest of the study area, are generally characterized by higher values of Na_2O and Sr than the higher-lying areas in the remainder of the region.

These contour maps, therefore, offer a clear

quantitative indication that topography and granite composition in the study area, are related. Clearly, high potash (and concomitantly high Rb) areas appear to be more resistant to weathering than those areas underlain by granites of a sodic composition.

(ii) Potassium (K_2O)

The K_2O contour map (Figure 31) is characterized by isolated patches of high K_2O concentration (generally in excess of 5% K_2O) in the main mass of the granitic terrane, and a prominent low K_2O area in the northeastern quadrant of the map area. This distribution pattern becomes particularly meaningful when this map is compared with the geological map of the study area (Figure 10). The areas of high potash concentrations correspond closely, in the majority of cases, to those areas underlain by intensely porphyritic granite. This relationship is to be expected as a granite containing numerous large microcline phenocrysts will naturally have a higher potash content than a granite containing a lesser number of such phenocrysts. The prominent area of low K_2O values (generally $< 3\%$ K_2O) in the northeast corresponds with the outcrop area of the Cunning Moor Tonalite (compare Figure 31 and Figure 10).

(iii) Rubidium (Rb)

The distribution of rubidium (Figure 33) is complementary to that of K_2O (Figure 31). High Rb values (>130 ppm Rb) generally correspond with the area underlain by the Nelspruit Porphyritic Granite whereas lower values (<130 ppm Rb) correspond with the Cunning Moor Tonalite.

A careful examination of the rubidium contour map provides an indication of a vaguely concentric distribution pattern over the area. In addition to the low Rb values over the Cunning Moor Tonalite, low values (<100 ppm Rb) also occur in a long narrow strip along the western margin of

of the study area. Generally speaking, therefore, the higher Rb values occur in the core region of the map. This aspect will be enlarged upon in the discussion on the trend surface analyses.

(iv) Sodium (Na_2O)

The contour map of Na_2O is shown in Figure 32 and again illustrates the nature of the local fluctuations which characterize all the contour maps. A comparison of the Na_2O distribution (Figure 32) and the K_2O distribution (Figure 31) shows these two to be inversely related. The area underlain by the Cunning Moor Tonalite is characterized by high Na_2O granites ($>4,5\%$ Na_2O) whereas most of the porphyritic granites possess intermediate-to-low values of Na_2O ($< 4,5\%$ Na_2O).

(v) Strontium (Sr)

The contour map of strontium (Figure 34) illustrates a random distribution of this element by comparison with the K_2O and Rb distributions. The distribution of Sr is, to a certain extent, inverse to that of Rb as the area underlain by the Cunning Moor Tonalite is one of relatively high Sr values (>550 ppm Sr). The random distribution of Sr values in the porphyritic granite can be accounted for by referring to Figure 24, (Chapter 3), which is a plot of Rb v Sr for the Nelspruit Porphyritic Granite. This diagram, it will be recalled, discloses two distinct populations of data, one of them being characterized by high Rb and Sr values. The significance of these two populations is dealt with in detail in Chapter 5 which describes the effects of fractionation on the porphyritic granite. The process of fractionation and the resulting variation in Sr values are responsible for the random distribution of Sr values in the main granite mass of the study area.

(v) Barium (Ba)

The contour map of barium concentrations (Figure 35)

is characterized by large fluctuations in the distribution of this element, a factor which cannot be readily ascribed to the known geological pattern. Generally, however, the area underlain by the Cunning Moor Tonalite has lower values of barium than the area underlain by the porphyritic granite. Thus a broad positive correlation exists between Ba, K_2O and Rb. A comparison of the Ba distribution (Figure 35) with Figure 10 (the geological map of the region) illustrates the fact that areas of high Ba concentrations coincide approximately with areas of intense phenocryst development. The latter areas are characterized by porphyritic granite containing up to 35 per cent of their volume as large microcline phenocrysts. Thus, when considering the high partition coefficient of Ba into K-felspar (i.e. 6,0 - see Table 18), the observed distribution of Ba is not surprising.

The strong component of local fluctuation in the Ba distribution, illustrated in Figure 35, has been discussed previously with respect to the significance of the polynomial trend surfaces and is thought to be reflected in the low 'F' values and correlation coefficients obtained for the Ba surfaces (Table 17).

(b) Polynomial Trend Surfaces

(i) Altitude

The 1st, 2nd and 3rd degree polynomial trend surfaces of the topographical data are presented in Figures 36, 37 and 38 respectively. Polynomial trend surfaces of altitude were constructed in an attempt to confirm the relationship between topography and granite composition, mentioned previously. It was hoped that low order polynomial regression surfaces for altitude would directly (or inversely, depending on the element under consideration) reflect the surfaces of the elements whose distribution over the study area is known. However, a comparison of the altitude regression surfaces with equivalent

surfaces for these elements (Figures 39-50) shows no direct similiarity. The reason for this is the strong regional easterly slope of the terrain away from the north-south trending Transvaal Drakensberg Escarpment towards the low-lying regions of the Kruger National Park and Moçambique. This regional trend is clearly evident in the first degree regression surface (Figure 36) and strong components of this trend prevail through 2nd and 3rd degree surfaces (Figures 37 and 38). It is evident that comparisons between topography and granite composition are far more meaningful when considering the actual contour maps of the data and not the polynomial trend surfaces.

(ii) K_2O, Na_2O, Rb, Sr and Ba

Various polynomial regression surfaces for the distribution of these elements are presented in Figures 39-50. No surface greater than the third degree surface was presented because of the generally observed decrease in the statistical significance of successively higher order surfaces (Table 17). For this reason also, the 3rd degree Na_2O surface was not presented, and only one Ba surface (the 2nd degree surface) has been included.

A. The 1st degree polynomial regression surfaces :- The first degree regression surfaces for K_2O, Na_2O, Rb and Sr (Figures 39, 42, 44 and 47 respectively) behave in a complementary fashion with respect to each other. K_2O and Rb, which are geochemically diadochic show decreases in concentration from the southwest to the northeast whereas Na_2O and Sr, also diadochic, show increases in the same direction. This marked regional trend is due primarily to the influence of the Cunning Moor Tonalite in the northeastern portion of the area.

B. The 2nd degree polynomial regression surfaces :- The second degree regression surfaces for K_2O, Na_2O, Rb, Sr and Ba (Figures 40, 43, 45, 48 and 50 respectively) show basic

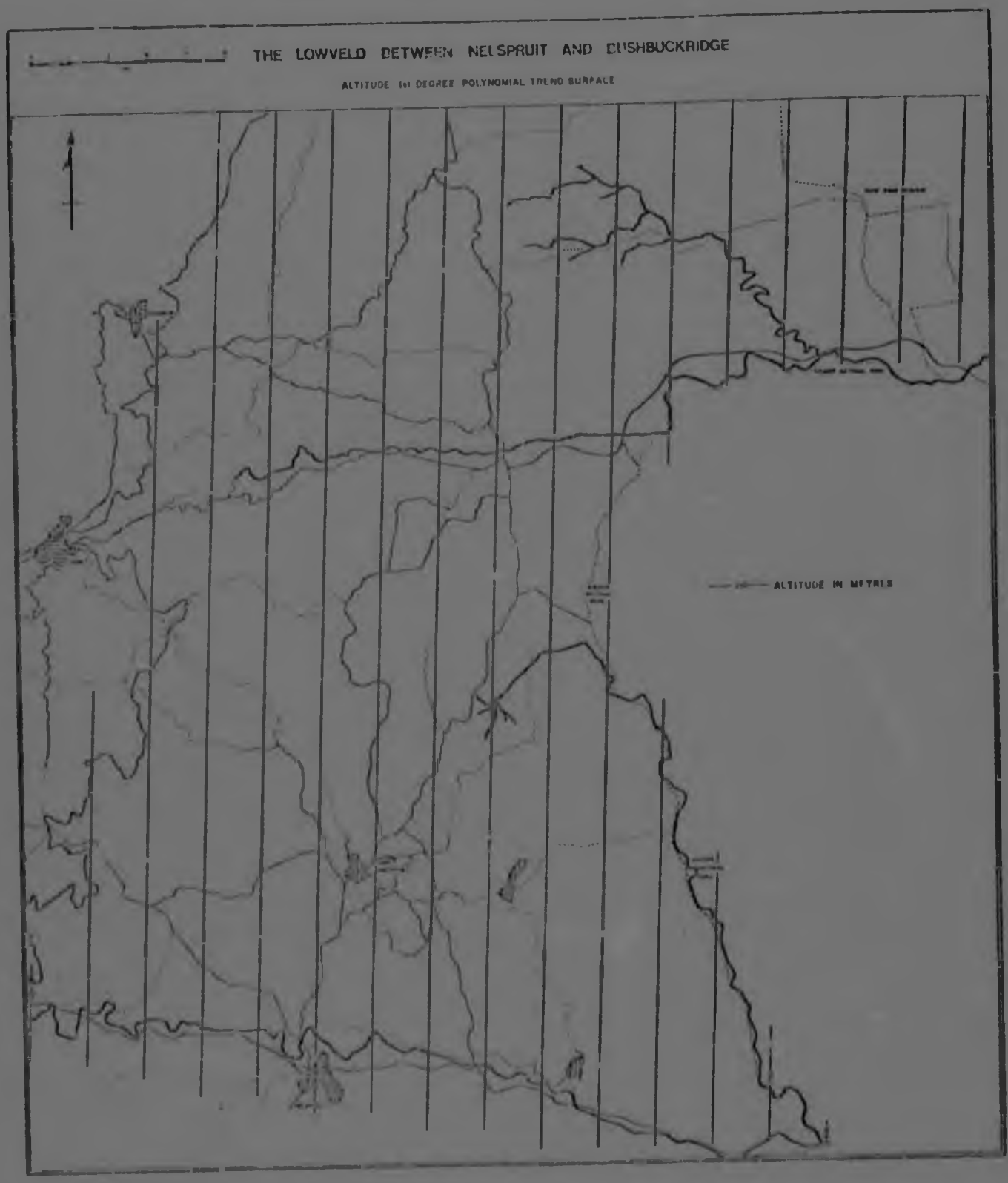

Figure 36. 1st degree polynomial trend surface map of altitude.

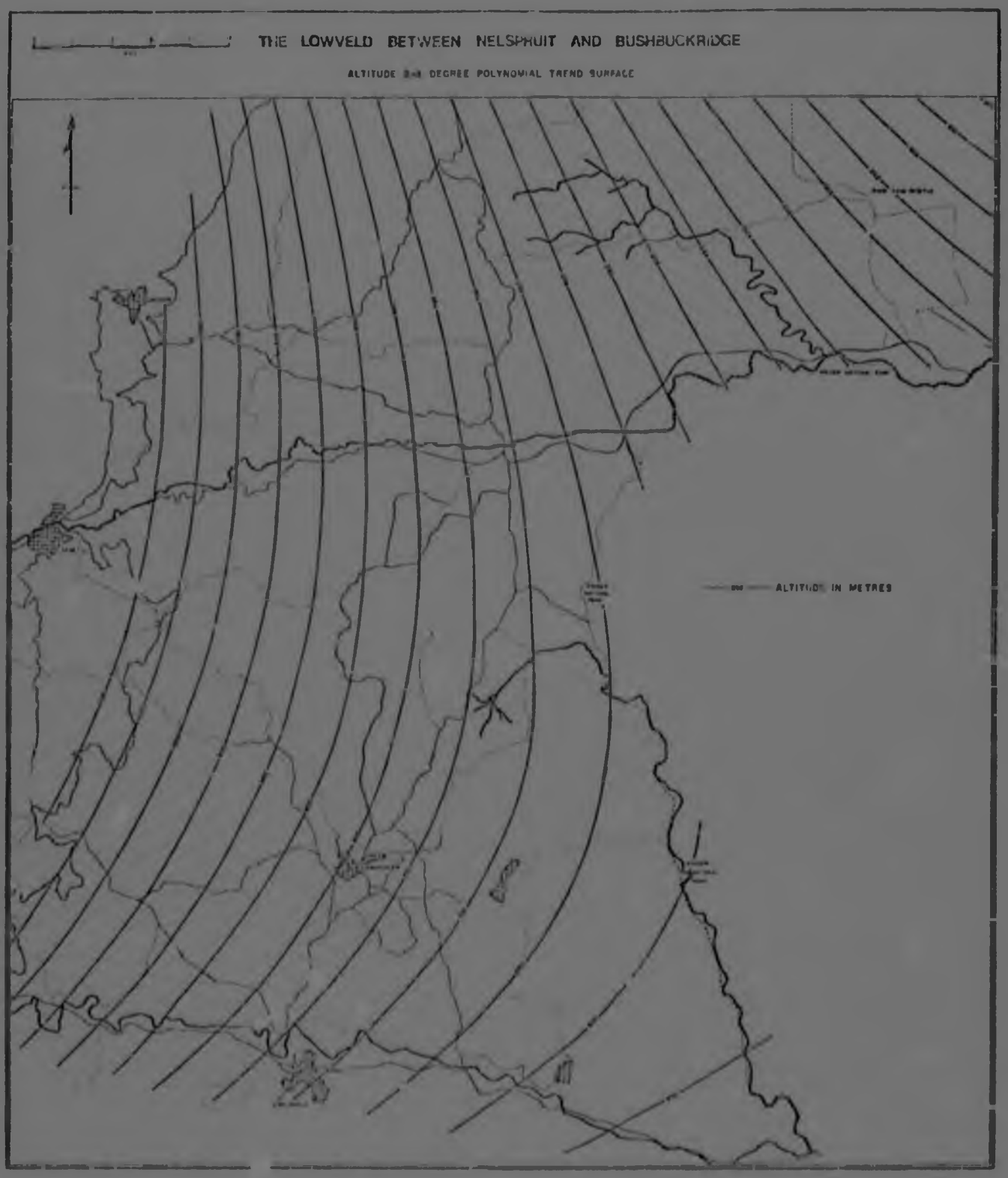

Figure 37. 2nd degree polynomial trend surface map of altitude.

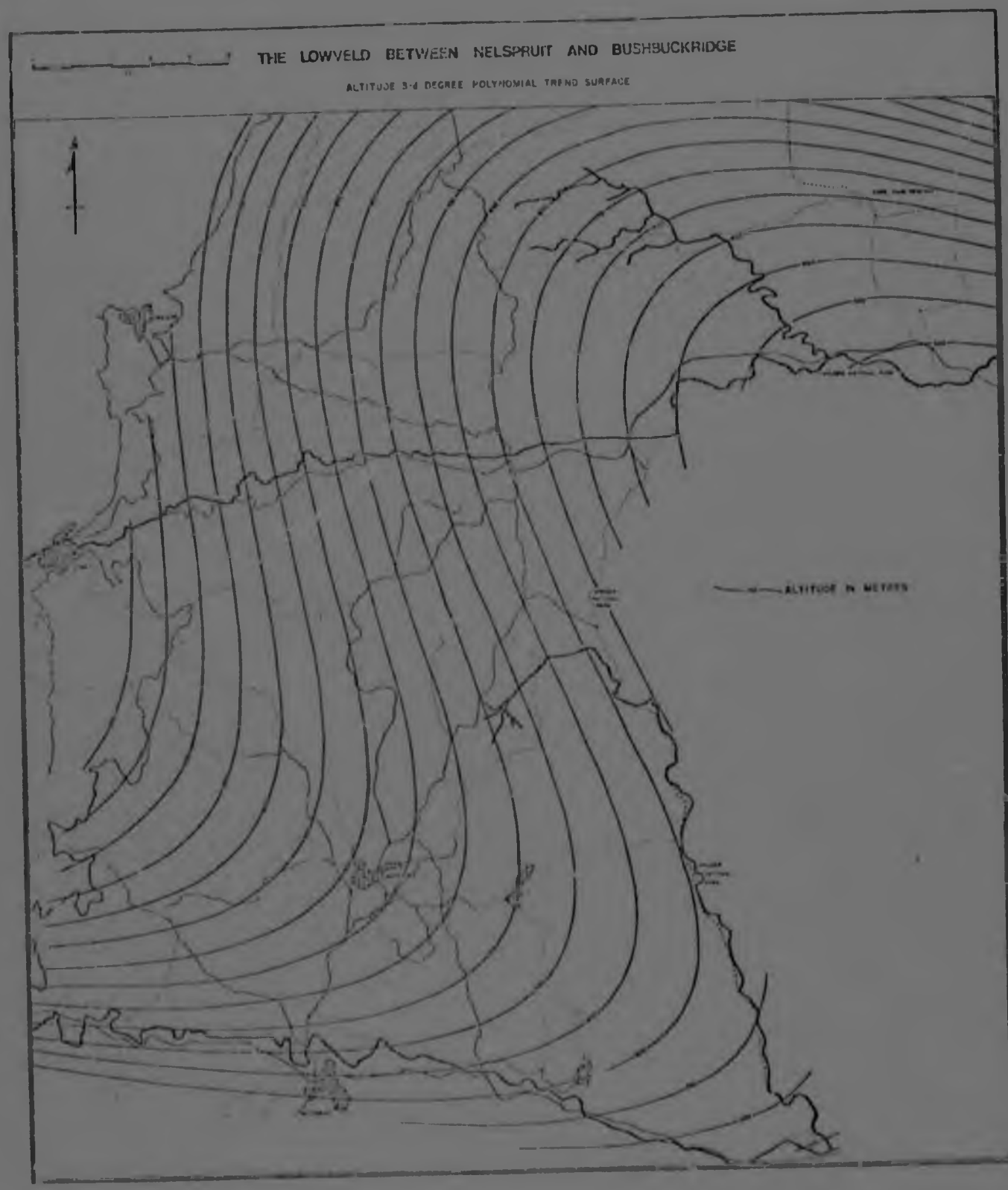

Figure 38. 3rd degree polynomial trend surface map of altitude.

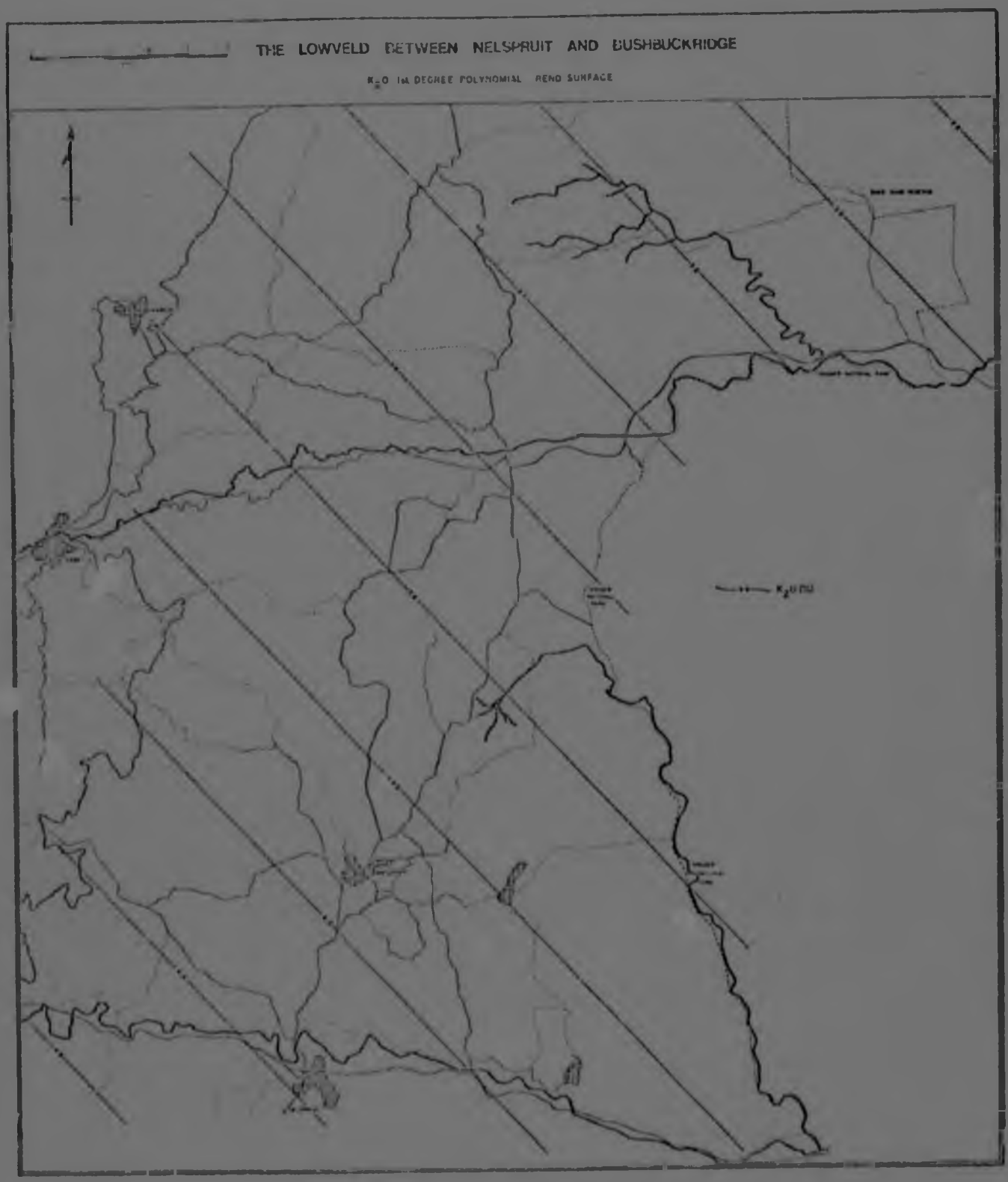

Figure 39. 1st degree polynomial trend surface map of K_2O.

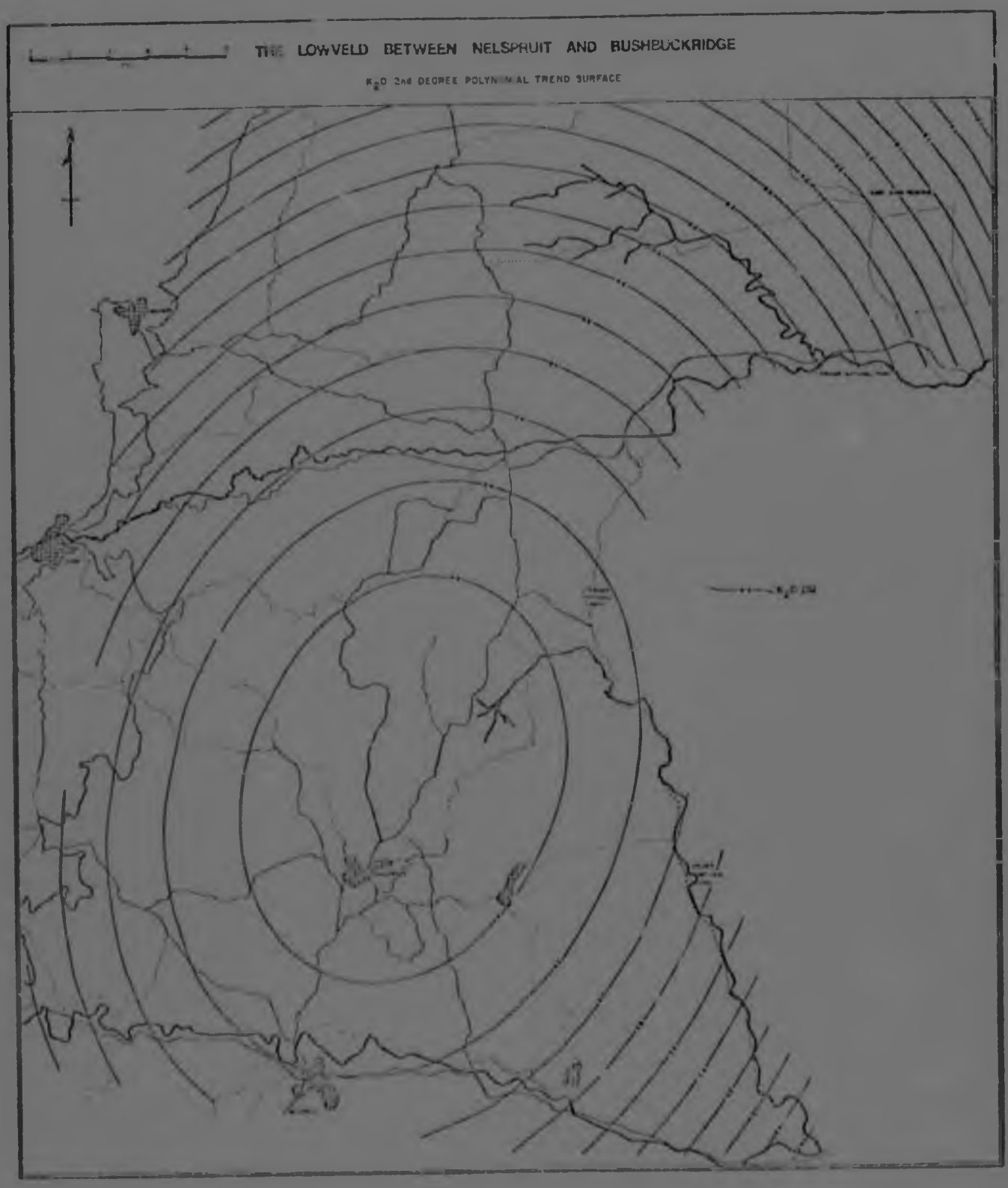

Figure 40. 2nd degree polynomial trend surface map of K_2O.

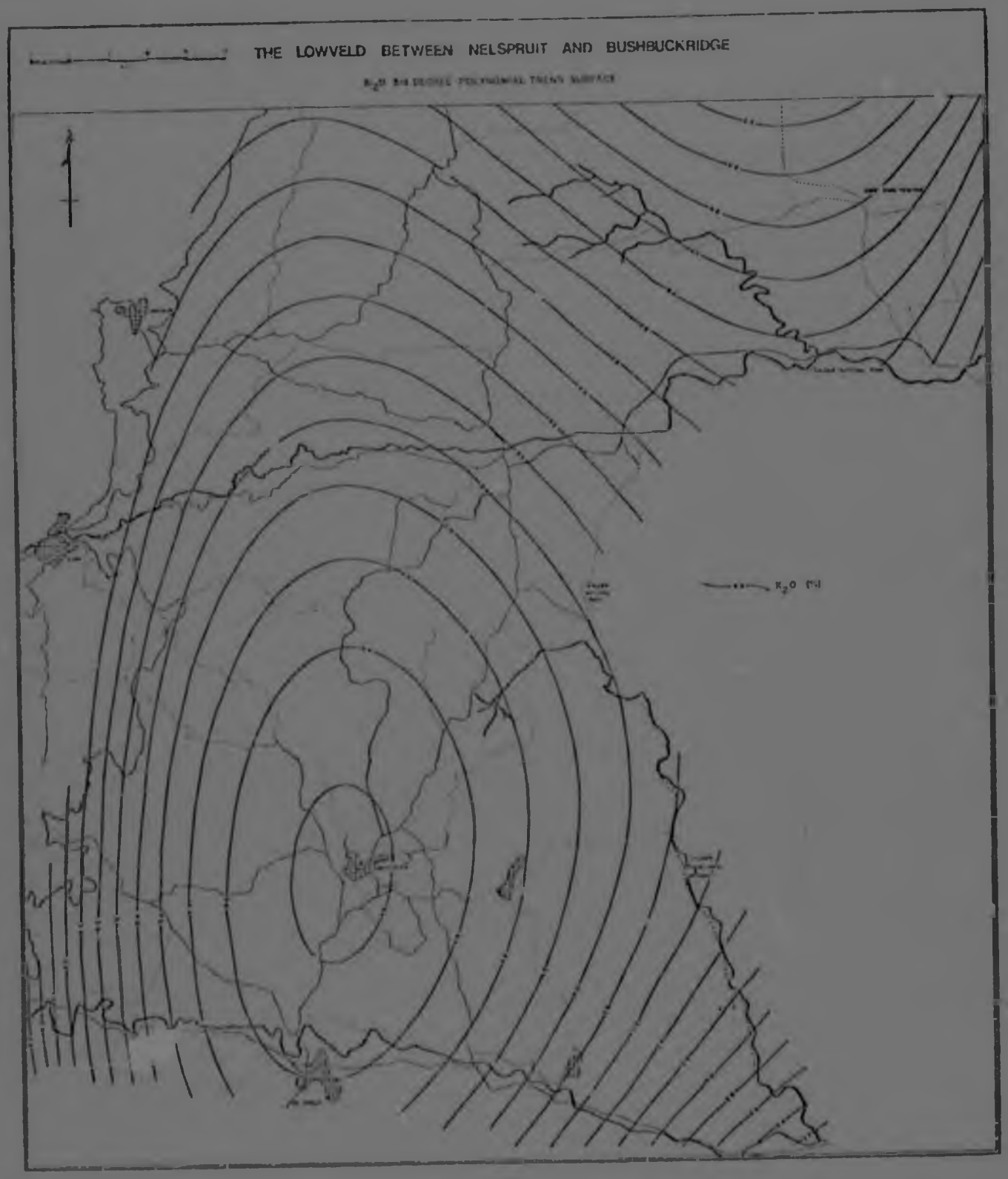

Figure 41. 3rd degree polynomial trend surface map of K_2O.

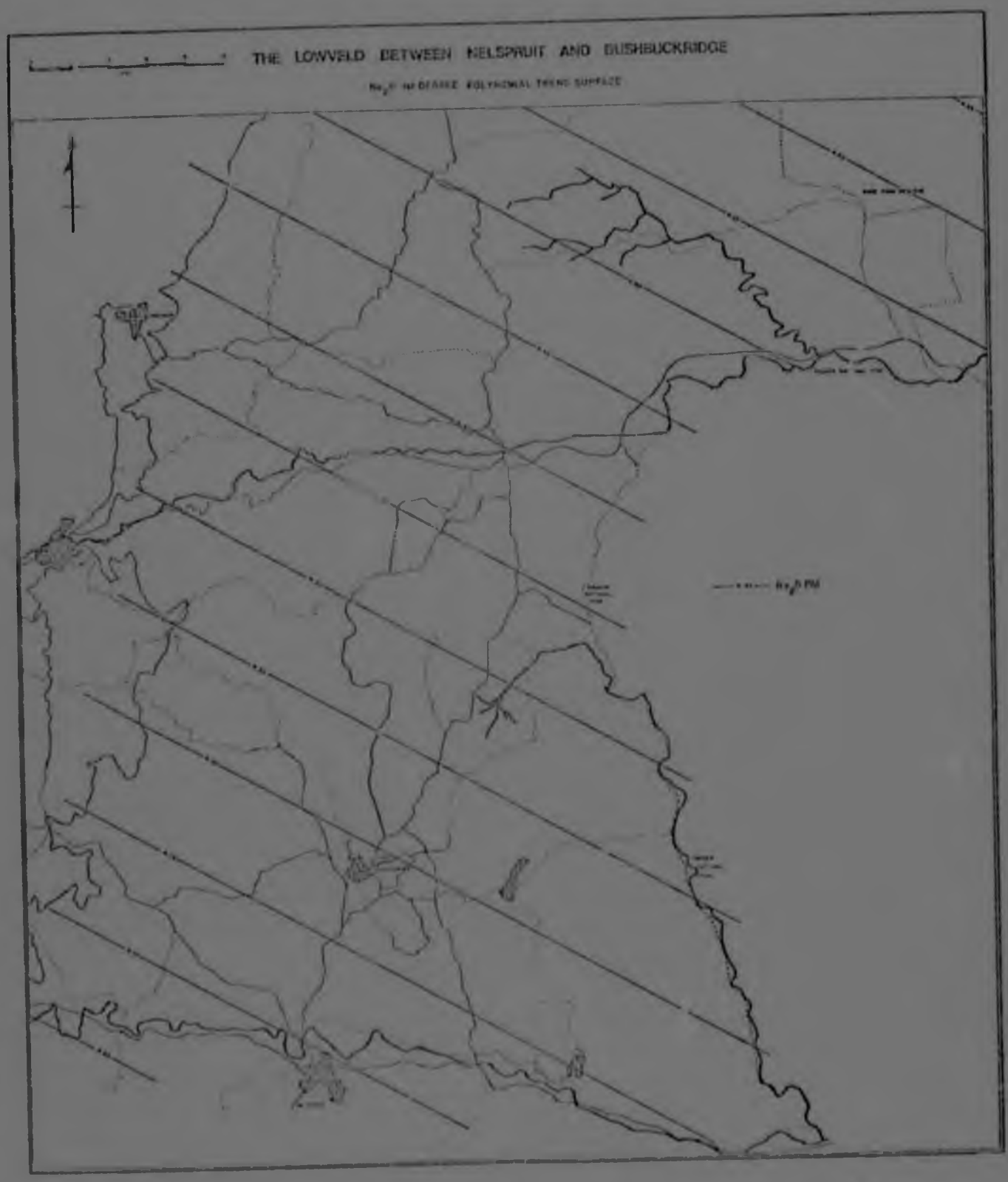

Figure 42. 1st degree polynomial trend surface map of Na_2O.

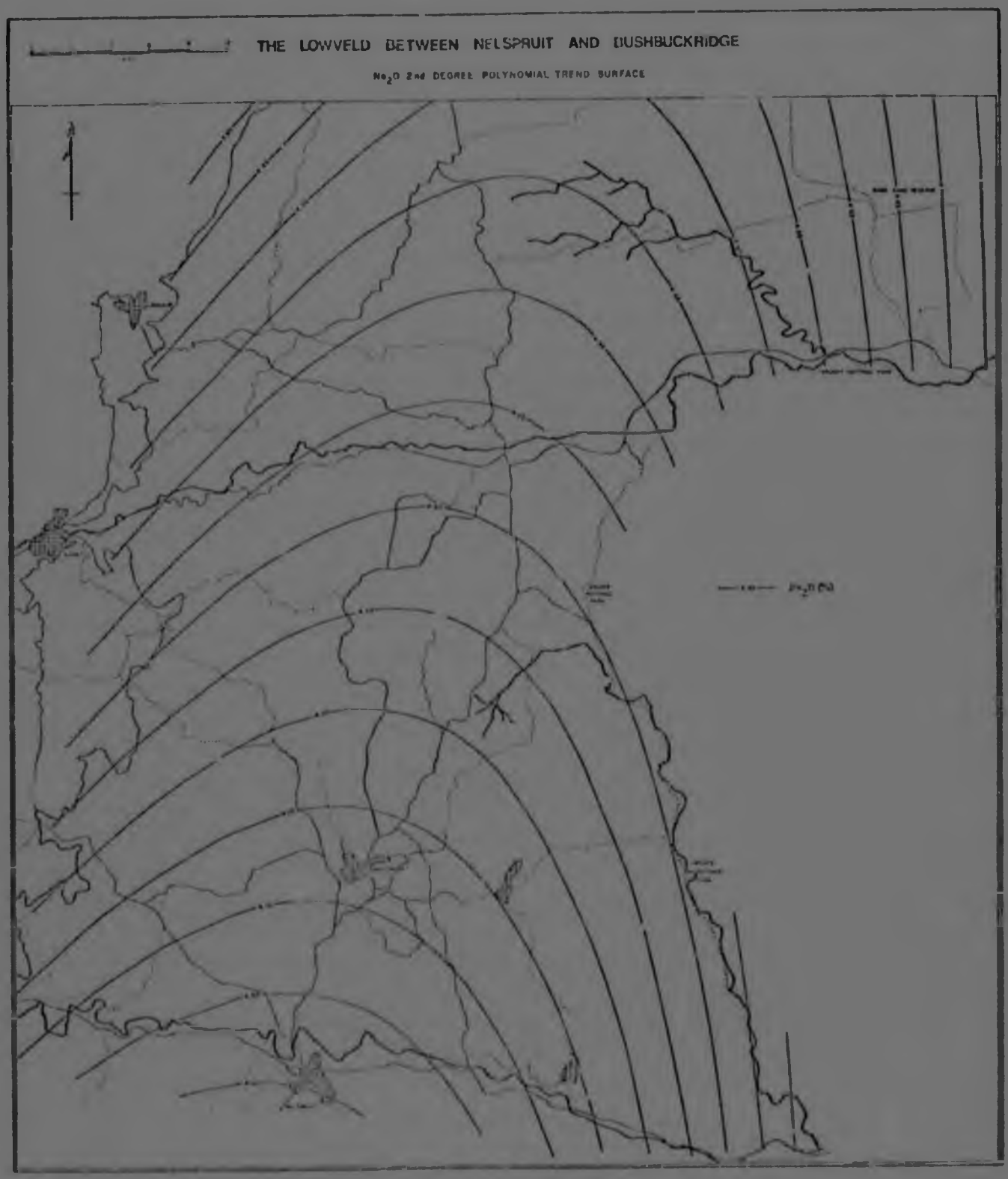

Figure 43. 2nd degree polynomial trend surface map of Na_2O.

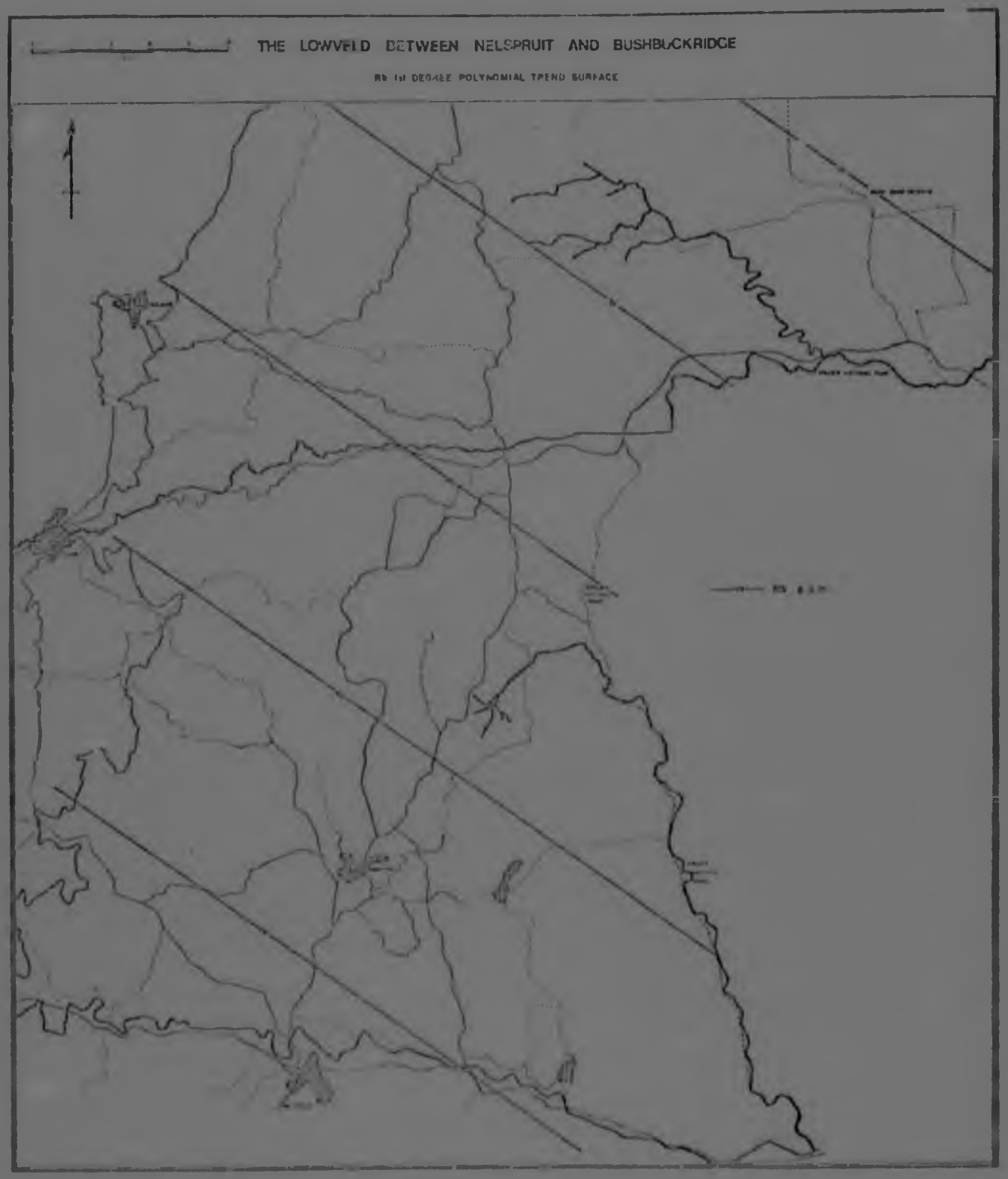

Figure 44. 1st degree polynomial trend surface map of Rb.

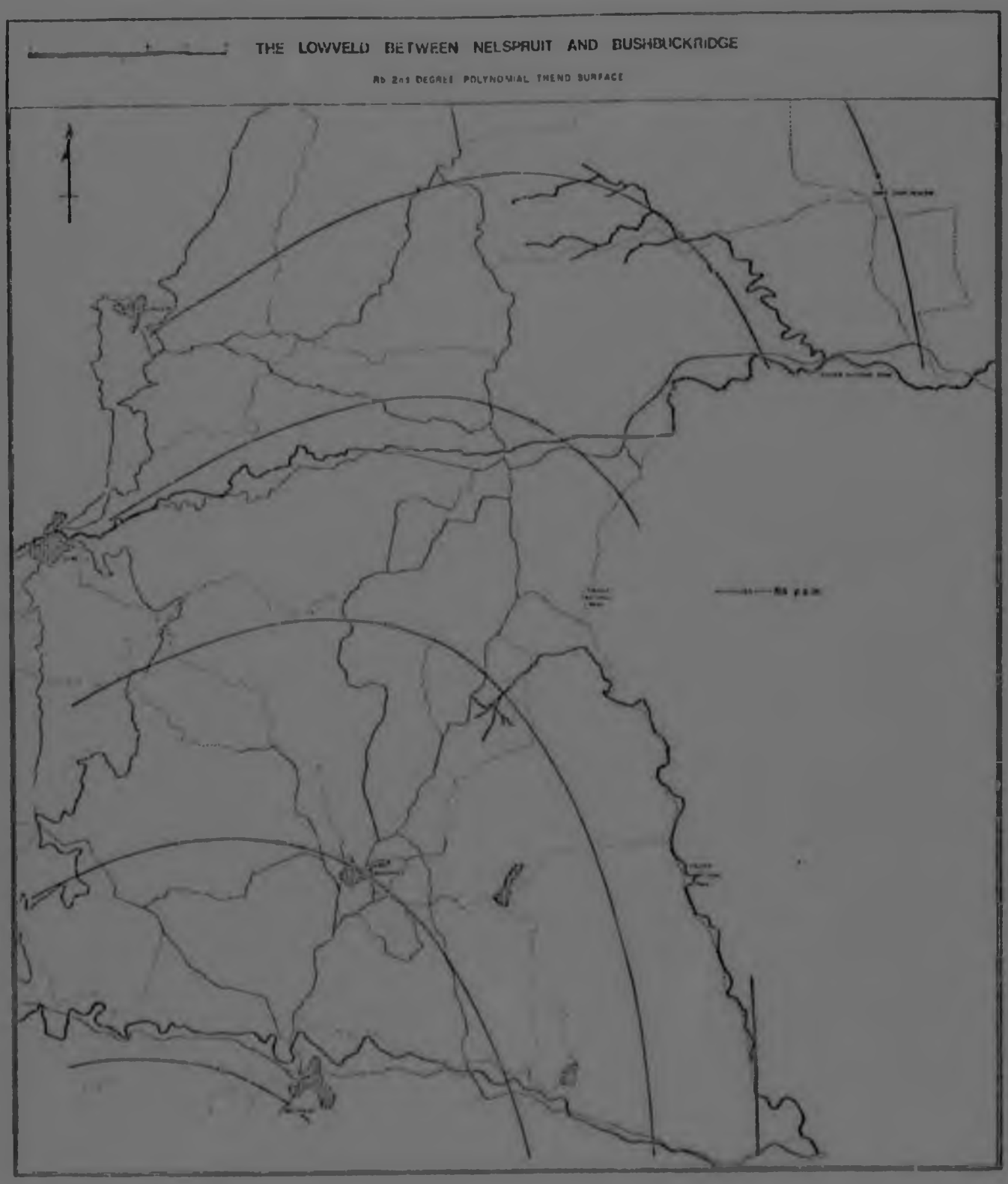

Figure 45. 2nd degree polynomial trend surface map of Rb.

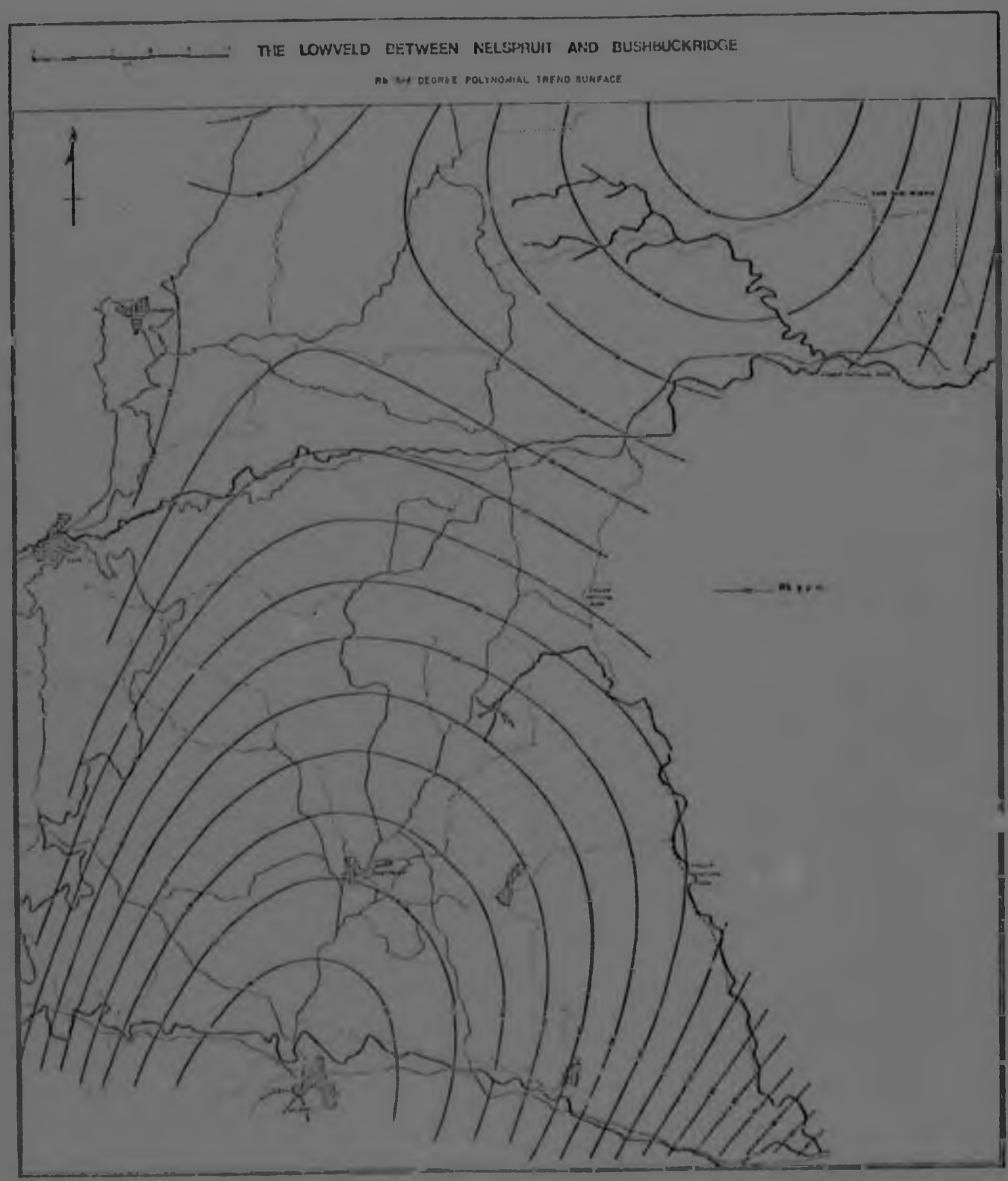

Figure 46. 3rd degree polynomial trend surface map of Rb.

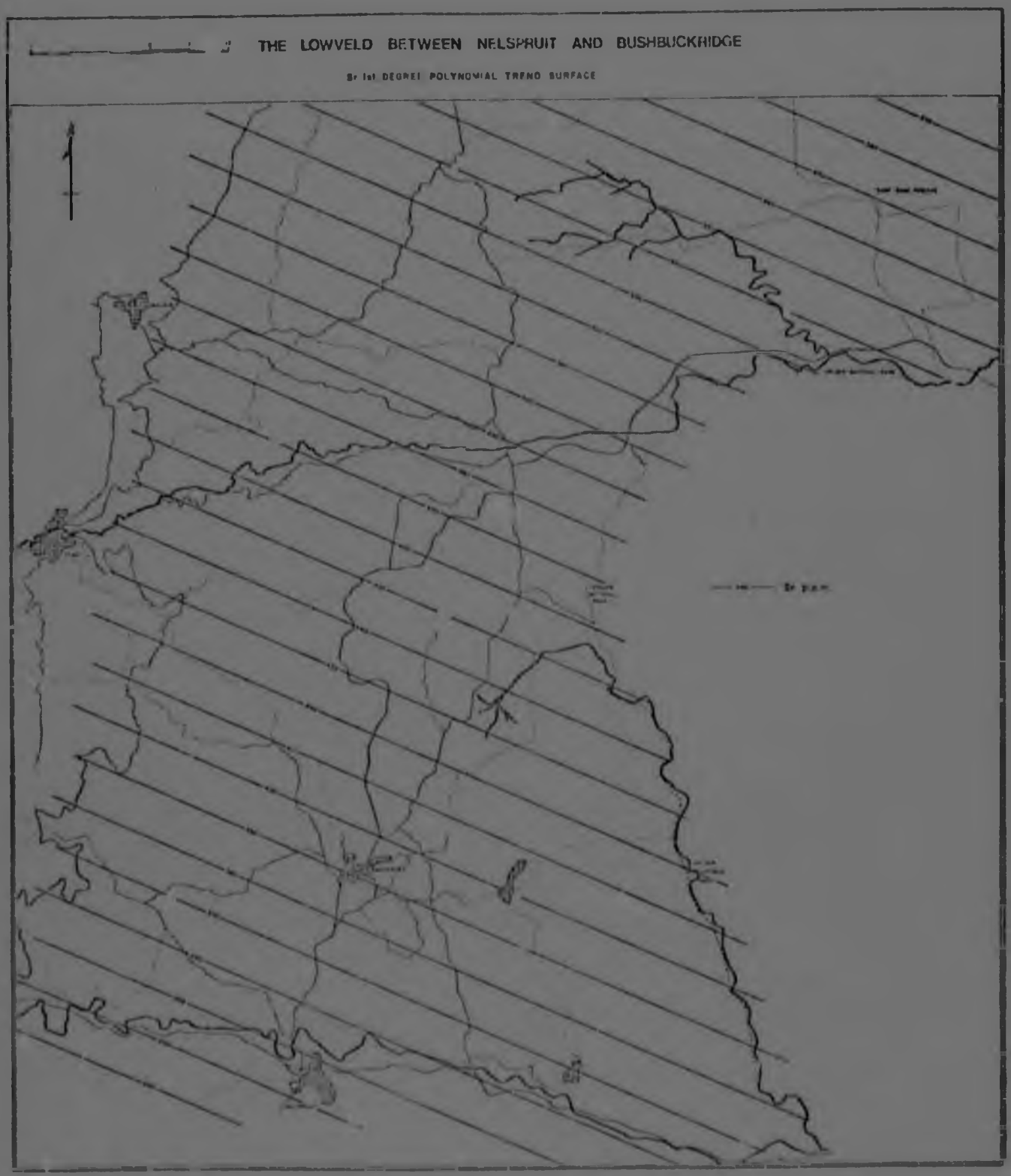

Figure 47. 1st degree polynomial trend surface map of Sr.

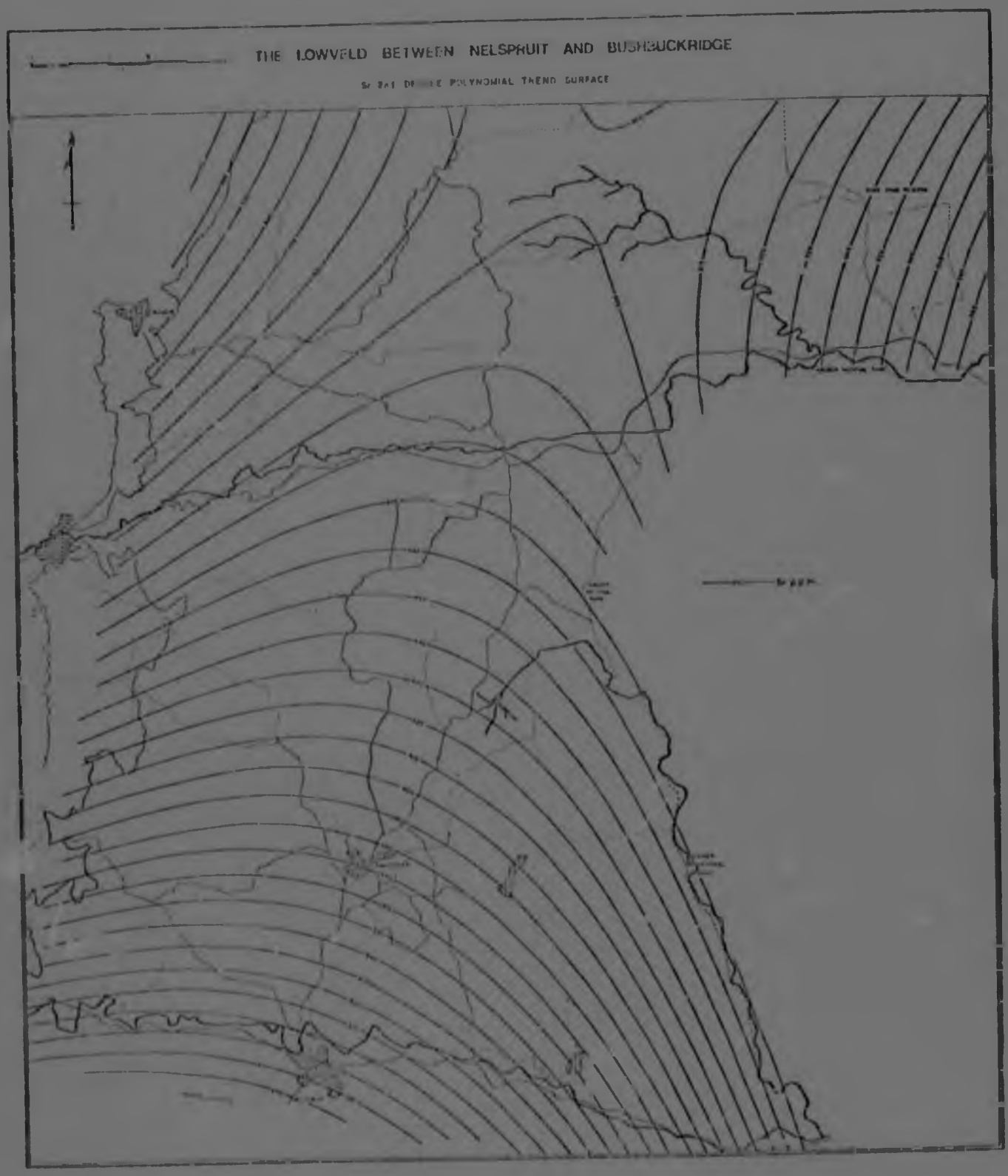

Figure 48. 2nd degree polynomial trend surface map of Sr.

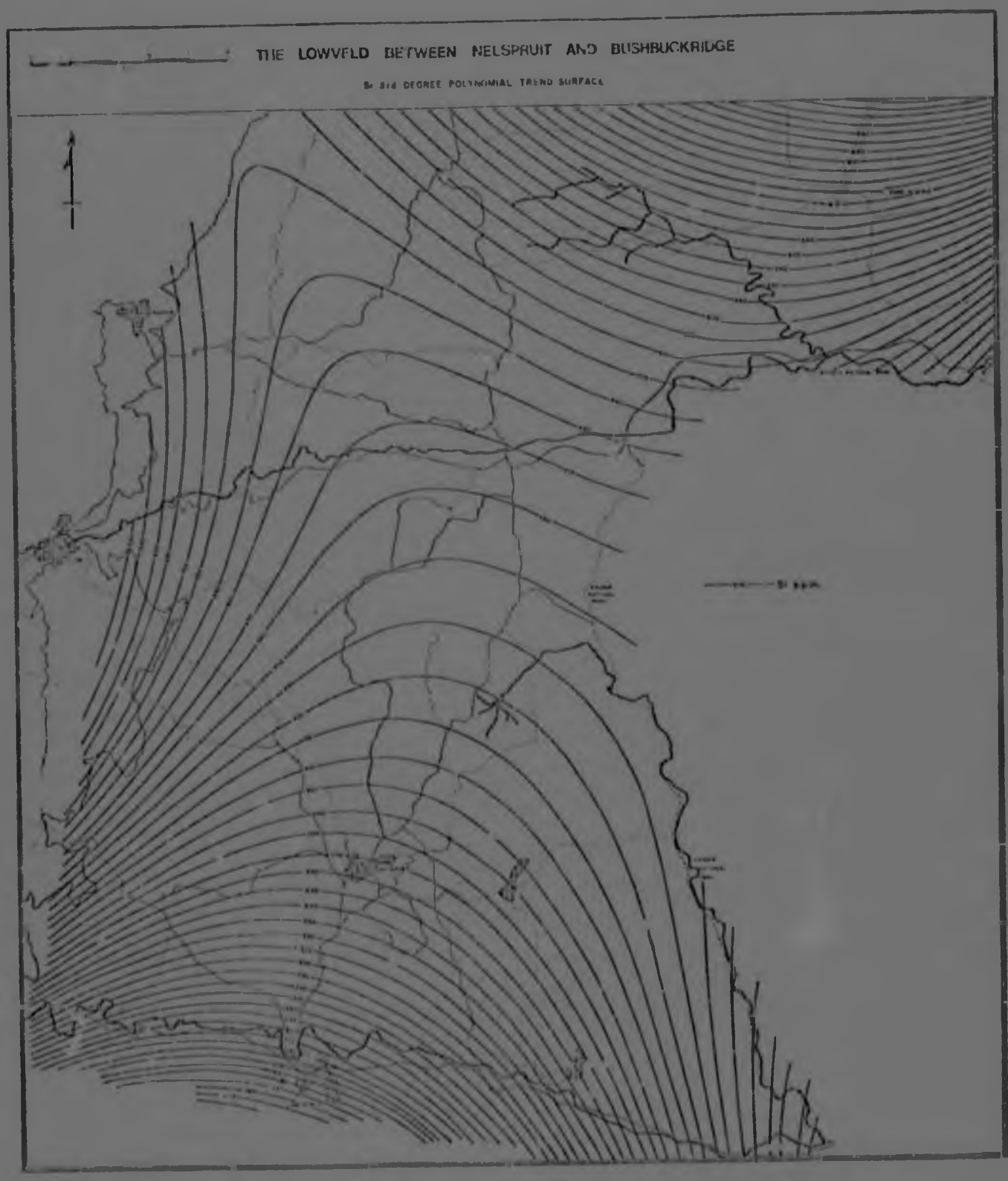

Figure 49. 3rd degree polynomial trend surface map of Sr.

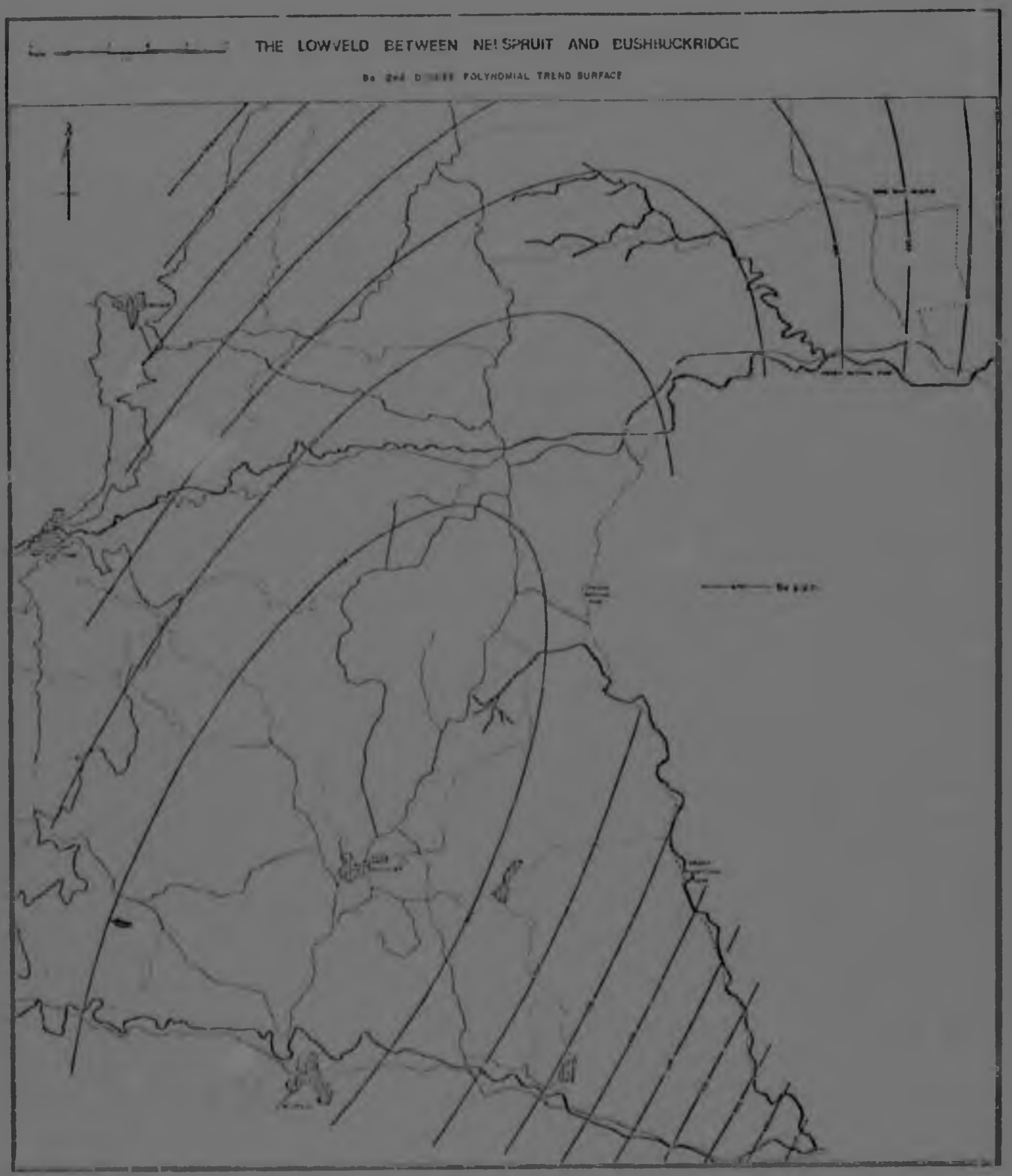

Figure 50. 2nd degree polynomial trend surface map of Ba.

differences in their configuration but are all characterized by a tendency towards a concentric or semi-concentric pattern. Prominent in this respect are the 2nd degree surfaces of K_2O and Ba which show high concentrations in a well-defined core region in the centre of the study area (Figures 40 and 50). The complementary behaviour of Ba and K_2O, as mentioned before, is not surprising when one considers the high partition coefficient of Ba into K-felspar (i.e. 6,0 - see Table 18). The 2nd degree surfaces for Na_2O, Rb and Sr largely reflect the trends exhibited by the 1st degree surfaces but with a marked semi-concentric curvilinearity.

c. The 3rd degree polynomial regression surfaces:- The 3rd degree regression surfaces for K_2O, Rb and Sr (Figures 41, 46 and 49 respectively) are again characterized by a concentric pattern in the case of K_2O and semi-concentric patterns in the case of Rb and Sr. Of particular importance in the third degree surfaces is the isolation of the area underlain by the Cunning Moor Tonalite away from the concentric and semi-concentric patterns that characterize the remainder of the area underlain by porphyritic granite. This statistical technique can, therefore, clearly differentiate between granites of differing chemical character. The differentiation of these two areas is in keeping with the Rb-Sr isotope data which suggests that the Cunning Moor Tonalite is significantly younger than the Nelspruit Porphyritic Granite (Chapter 3).

The implications of the concentric and semi-concentric element distribution patterns that characterize the second and third degree polynomial regression surfaces are particularly significant in the light of the conclusions that have been derived regarding the crystallization mode of the Nelspruit Porphyritic Granite. This information is discussed in detail in Chapter 5 where it is shown that this porphyritic granite has undergone fractional crystallization, the latter process resulting in distinctive major and trace element behaviour. The full significance of the concentric and semi-concentric trend

surface patterns will therefore be discussed in Chapter 5. It is interesting to note at this stage, however, that similiar concentric geochemical distribution patterns have been described by Wolhuter (1973) for the Opemisca Lake granite pluton in Quebec, Canada. This distribution pattern has been ascribed to the effects of differen[illegible]tion in the interior of this pluton.

CHAPTER 5

FRACTIONAL CRYSTALLIZATION IN THE NELSPRUIT PORPHYRITIC GRANITE AND THE EFFECTS ON ITS MAJOR AND TRACE ELEMENT GEOCHEMISTRY

I. INTRODUCTION

Implicit in the understanding of most mafic and ultramafic igneous rocks has been the concept of fractional crystallization, the latter involving the segregation of solids and residual melts. Such a crystallization mode has a marked effect on the mineralogy and major and trace element chemistry of such rocks.

Igneous petrologists have been reticent in applying such a mechanism to the crystallization of granitic rocks and, certainly, igneous sedimentary structures, indicative of fractional crystallization, are uncommon in the latter rocks. Petrographic evidence suggestive of cumulus-intercumulus relationships are also not normally observed in granites and the majority of workers assume that they have a "liquid" character, formed essentially by equilibrium crystallization. A number of authors have, in the past, described differentiated granites (Emeleus, 1963; Kolbe, 1966; Wolhuter, 1973; Smith, 1974, 1975; Taylor, 1976). In particular, McCarthy and Hasty (1976) have examined the consequences of fractional crystallization on the distribution of trace elements in granites.

The textural recognition of fractionated granites (or cumulate granites) is rare because, as McCarthy and Hasty have pointed out, the precipitation of crystals from an intercumulus melt derived from a parent magma of composition approaching that of the thermal minimum in the granite system would have the same mineralogical characteristics as that of the cumulate assemblage. The character of such intercumulus precipitates may further be masked by adcumulate effects or

by exsolution phenomena. However, the behaviour of trace elements, such as Rb, Sr and Ba, which partition themselves strictly into various mineral phases, provides a means by which possible fractional crystallization processes in a granite may be detected. The distribution of trace elements, whose partition coefficients are known, can be accurately modelled and then compared with empirical data to confirm or reject the possibility of fractionation having taken place in a particular granite. This procedure is described in detail in this chapter, with particular emphasis on the Nelspruit Porphyritic Granite which forms the main granite type in the study area.

II. THEORETICAL ASPECTS RELATED TO TRACE ELEMENT MODELLING

For theoretical considerations the crystallization of a magma may be thought of as occurring in three different ways :-

(i) By assuming that the crystallization of solid phases in the liquid takes place under perfect equilibrium conditions i.e. the crystals are at all times in equilibrium with the liquid from which they formed. In this instance, the resulting solid will have exactly the same composition as the parent liquid.

(ii) By assuming that perfect fractional crystallization takes place, i.e. that crystals obey the Rayleigh Law. This implies that crystals grow in isolation from the liquid from which they were derived. Mathematical equations for the distribution of trace elements obeying the Rayleigh Law have been given by Neumann et al. (1954) and Greenland (1970).

(iii) By assuming a mode intermediate between that of perfect equilibrium and perfect fractional crystallization, namely that of incremental equilibrium

crystallization. In this situation a crystal grows in equilibrium with the liquid from which it forms for a period of time before being subsequently isolated from that liquid. Mathematical equations for the distribution of trace elements obeying this mode of crystallization are presented by McCarthy and Hasty (1976).

In this exercise trace elements were considered to behave according to the Rayleigh Law (i.e. perfect fractional crystallization was taking place) and the modelling procedure was carried out using the equations derived by Neumann et al. (1954) :-

The distribution of trace elements between solid and liquid phases is given by the following equations:-

$$\frac{Cl}{Co} = (1-f)^{(D-1)}$$

and

$$\frac{Cs}{Co} = D.(1-f)^{(D-1)}$$

where :-

- Cl - Concentration of a trace element in the liquid phase
- Cs - Concentration of a trace element in the solid phase
- Co - Initial concentration of the trace element
- D - Solid/Liquid partition coefficient
- f - The mass fraction of solids produced

The calculation of the bulk partition coefficient (i.e. the partition coefficient of a trace element into an assemblage consisting of more than one mineral phase) is given by :-

$$D_{bulk} = \sum_{i=1}^{n} Wi.Di$$

where :-

Wi - weight fraction of the ith mineral
Di - the partition coefficient of an element between the liquid and the ith mineral

A prerequisite for trace element modelling procedures is a knowledge of the crystal/liquid partition coefficient of the relevant trace elements into various minerals. The partition coefficients used in this excercise are presented in Table 18, below.

TABLE 18

CRYSTAL/LIQUID PARTITION COEFFICIENTS USED IN THE TRACE ELEMENT MODELLING

	Quartz	Plagioclase	K-felspar	Biotite
Rb	0,0001	0,04	0,80	3,0
Sr	0,0001	3,35	3,60	0,4
Ba	0,0001	0,40	6,0	6,0

(after McCarthy and Hasty, 1976).

The actual calculation of the distribution of the trace elements during fractional crystallization was carried out on the University of the Witwatersrand's IBM 370 computer using a simple programme written by the author. This programme calculates the trace element concentrations at various increments of fractional crystallization (i.e. 0%, 10%, 20%, 30%, etc.) in both the solid and liquid phases. These results may then be plotted on relevant binary diagrams (e.g. Figure 51a and b).

III. THE TRACE ELEMENT MODEL

The trace element model is based essentially on the distribution of Rb, Sr and Ba in the Nelspruit Porphyritic Granite. The object of this model is to attempt to predict the crystallization process in the latter granite. The crystallization of a granite can be considered simplistically in terms of a Quartz-Albite-Orthoclase (Qtz-Ab-Or) ternary diagram such as that in Figure 52. In this diagram the cotectic lines at two different water pressures ($P.H_2O$ = 0,5Kb and $P.H_2O$ = 3,0Kb) are given and also the Qtz-Ab-Or ratios of 86% of 1190 granitic samples (after Winkler and von Platen, 1961). In addition, the average Qtz-Ab-Or ratio of 15 samples of Nelspruit Porphyritic G anite is also provided (from data presented in Table 10, Chapter 3). If one considers a granitic magma of this average composition which lies within the stability field of albite, then the first mineral to crystallize will be plagioclase. The composition of successive residual liquids will change towards the plagioclase-quartz cotectic, until, when this phase boundary is reached, quartz crystallizes together with plagioclase in approximately equal proportions. Successive residual liquids will now change in composition towards the thermal minimum on this diagram, which is the common point of all three mineral phases. When this point is reached K-felspar will start to crystallize together with plagioclase and quartz, again in approximately equal proportions. If mineral phases, which crystallized early in this process, are effectively separated from those that crystallized later on, then fractional crystallization is taking place. In a granite which is cooling very slowly it is conceivable that crystallization will commence from the margins and progress inwards towards the core of the magma chamber. It is also possible therefore, that the margins of the magma chamber solidified during the time that only plagioclase (or plagioclase + quartz perhaps) was crystallizing, and that K-felspar was only introduced as a cumulus phase towards the centre of the magma chamber,in

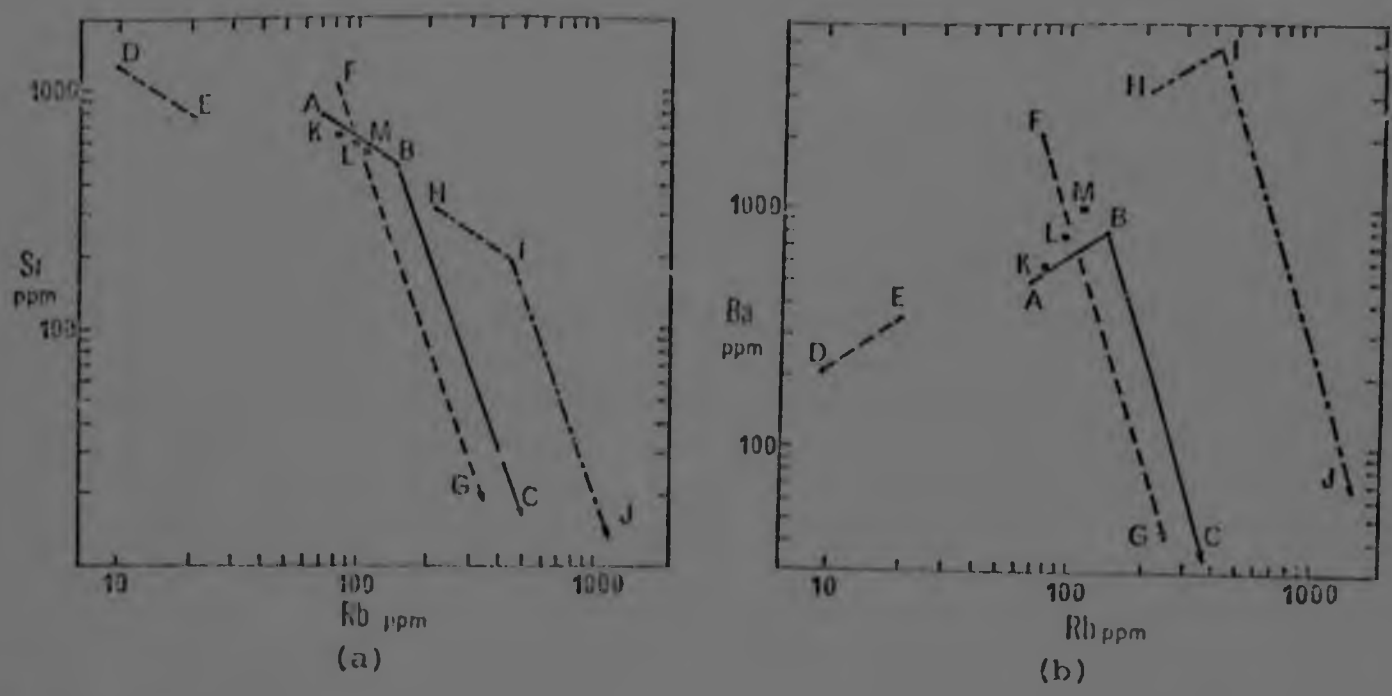

Figure 51. Diagrams showing the effect of fractional crystallization on the Ba, Sr and Rb contents of a granitic melt. Initial melt is at A. From this melt, 47 per cent plagioclase, 49 per cent quartz and 4 per cent biotite are fractionally removed, causing the liquid to move towards B. The composition of the solid phase lies along DE. At B, which represents 55% crystallization of melt A, the liquidus mineralogy changes to 32 per cent plagioclase, 28 per cent quartz, 30 per cent K-felspar and 10 per cent biotite. The liquid composition now changes towards C, and the fractionally separated solid compositions lie along FG. HI represents the compositions of biotite in equilibrium with melts along AB, and IJ, biotites in equilibrium with melts along BC. K is the composition of a 50-50 mix of E and B; L represents a 5% addition of biotite I to K, and M represents a 10% addition of biotite I to K.

the late stages of crystallization. Such a crystallization history would markedly affect the regional distribution of trace elements partitioning into the various mineral phases.

The trace element model that is considered in this section involves two distinct stages of crystallization. The first involves the fractionation of plagioclase + quartz ±biotite (biotite is not represented in the Qtz-Ab-Or system but is an integral part of granite petrogenesis and plays an important role in the partitioning of trace elements), whereas the second involves the fractionation of plagioclase + quartz + biotite + K-felspar. The distribution of Rb, Sr and Ba during the two stages of crystallization has been calculated and is presented in the form of Rb v Sr and Rb v Ba plots in Figure 51a and b. In the case where plagioclase + quartz + biotite are fractionating (in the model the proportions selected were 47% plagioclase, 49% quartz and 4% biotite - these modal proportions were chosen purely for the sake of convenience in modelling), the change in concentration of trace elements in the liquid phase is given by the line AB, whereas the change in the solid phase is given by DE (Figure 51a and b). It is seen that Ba and Rb are partitioned into the melt and hence their abundance increases with fractionation, but that of Sr decreases, as this element is strongly partitioned into plagioclase (Table 18).

As mentioned previously the fractionation of plagioclase + quartz (+ biotite) will continue until the K-felspar phase volume is reached, whereupon a potash felspar, in addition to the former minerals, will commence to crystallize. In the model (Figure 51) point B (which represents 55% crystallization of liquid A) is taken to be the point where K-felspar is introduced as a cumulus phase. This has an immediate effect on the distribution of the trace elements in question, as is seen in the change in the slope of the trends.

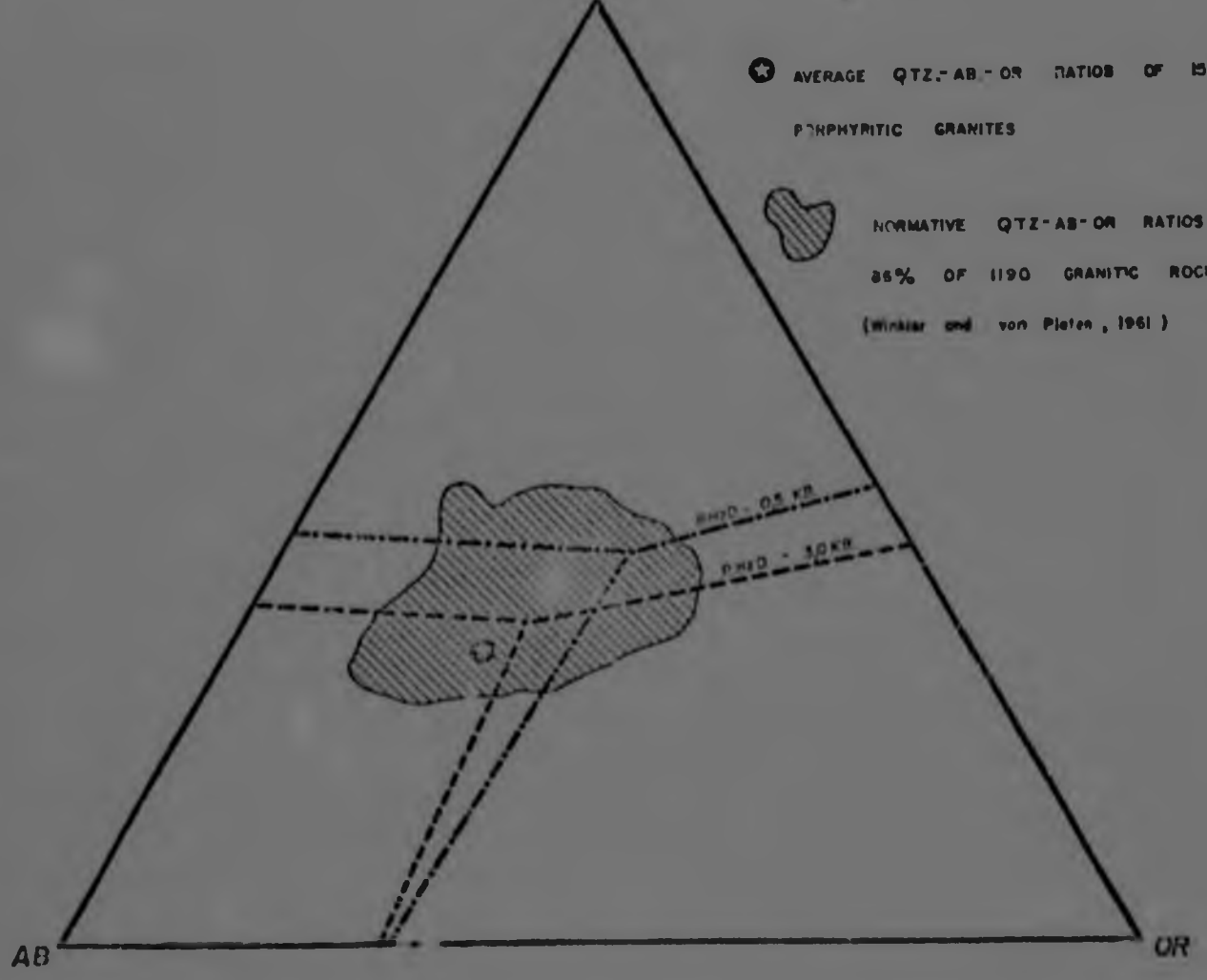

Figure 52. The system Quartz-Albite-Orthoclase showing the stability fields at (i) P_{H_2O} = 0,5 Kb (ii) P_{H_2O} = 3,0 Kb. The average compositional field for 86% of 1190 granitic rocks is included on the diagram as an indication of the compositional range of granites.

During this stage of crystallization (where the proportion of minerals used is now 32% plagioclase, 28% quartz, 10% biotite and 30% K-felspar) the melt changes composition along DC. The first solid containing cumulus K-felspar has a composition F and subsequent solids lie along FG. It is evident that Ba is now actively removed from the melt as it is strongly partitioned into K-felspar (Table 18). Sr likewise, is more strongly removed from the melt than previously, because of the greater quantity of felspars in the cumulus assemblage. Thus the two stages of crystallization are represented by distinctly different slopes in the model.

The two pertinent points which characterize the suggested two-stage crystallization process of this hypothetical granite are (i) the increase of Ba and decrease of Sr in both solid and residual liquid with increasing fractionation in the plagioclase + quartz + biotite crystallization stage, and (ii) the marked change in the distribution of the trace elements (i.e. the change in slope of the trends) that occurs when K-felspar is introduced as a cumulus phase in the latter stages of crystallization.

IV. THE APPLICATION OF THE TRACE ELEMENT MODEL TO THE NELSPRUIT PORPHYRITIC GRANITE

The Nelspruit Porphyritic Granite was described in detail in Chapter 3 where it was mentioned that although microcline phenocrysts are a ubiquitous characteristic of this rock type their development is variable. The wide variation in composition (i.e. K_2O/Na_2O ratios) exhibited by this granite was also described.

In an attempt to statistically define the existence of sub-types within the porphyritic granite, a cluster analysis of 92 samples of the porphyritic granite was undertaken on the basis of the variables K_2O, Na_2O, Rb, Sr and Ba. The dendogram illustrating the results of this cluster analysis is shown in Figure 53. This diagram illustrates the presence of four clusters, the intercepts of which are indicated by the

FIGURE 53

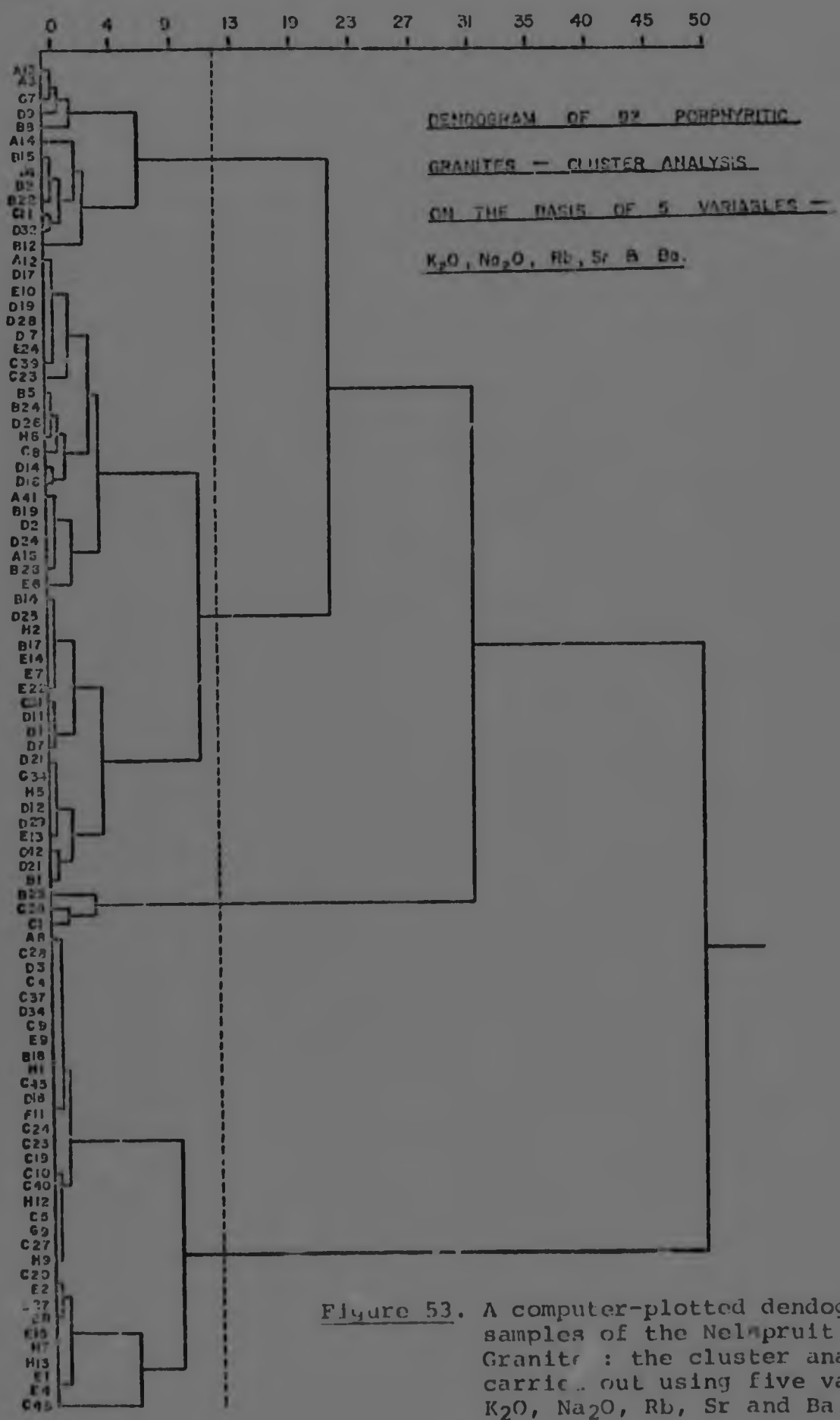

Figure 53. A computer-plotted dendogram of 92 samples of the Nelspruit Porphyritic Granite : the cluster analysis was carried out using five variables, K_2O, Na_2O, Rb, Sr and Ba.

vertical dashed line. The topmost cluster is characterized by granites of high K_2O, Rb and Ba concentrations, whereas the lowermost cluster consists of granites rich in Na_2O and Sr. The two central clusters have compositions intermediate between these extremes. It should be noted, however, that one of the intermediate clusters contains only three samples which, on closer examination, have not only high K_2O concentrations, but also anomalously high Sr values (N.B. an examination of Figure 24, Chapter 3, shows a few samples in the high K_2O and Rb population which have high Sr values). Because of this, it is felt that this small cluster would fit, more appropriately, into the topmost cluster which consists of high K_2O and Rb granites. As a result, essentially only two clusters occur in this diagram, the upper, smaller, cluster consisting of high K_2O, Rb and Ba granites and the lower, larger, cluster consisting of intermediate to high values of Na_2O and Sr. If these two groups are plotted separately on Rb v Sr and Rb v Ba diagrams, the resultant trace element distribution trends appear very similiar to the model trends described above (compare Figure 54a and b with Figure 51a and b).

The implication of this feature is that a two stage crystallization process, similiar to that described above, may have taken place within the Nelspruit Porphyritic Granite. It appears as though the majority of samples fall on trends, the slopes of which coincide with the model slopes for plagioclase + quartz + biotite fractionation. It will be noted in this trend that Sr decreases and Ba increases in concentration with fractionation, as predicted by the models. The minority of samples (open circles, Figure 54a and b), however, exhibit trends with markedly different slopes to those of the first trend, and which coincide with the plagioclase + quartz + biotite + K-felspar trend illustrated in the model (Figure 51). The latter trend appears, however, to have been influenced by the introduction of K-felspar as a cumulus phase in the crystallization sequence of the granite.

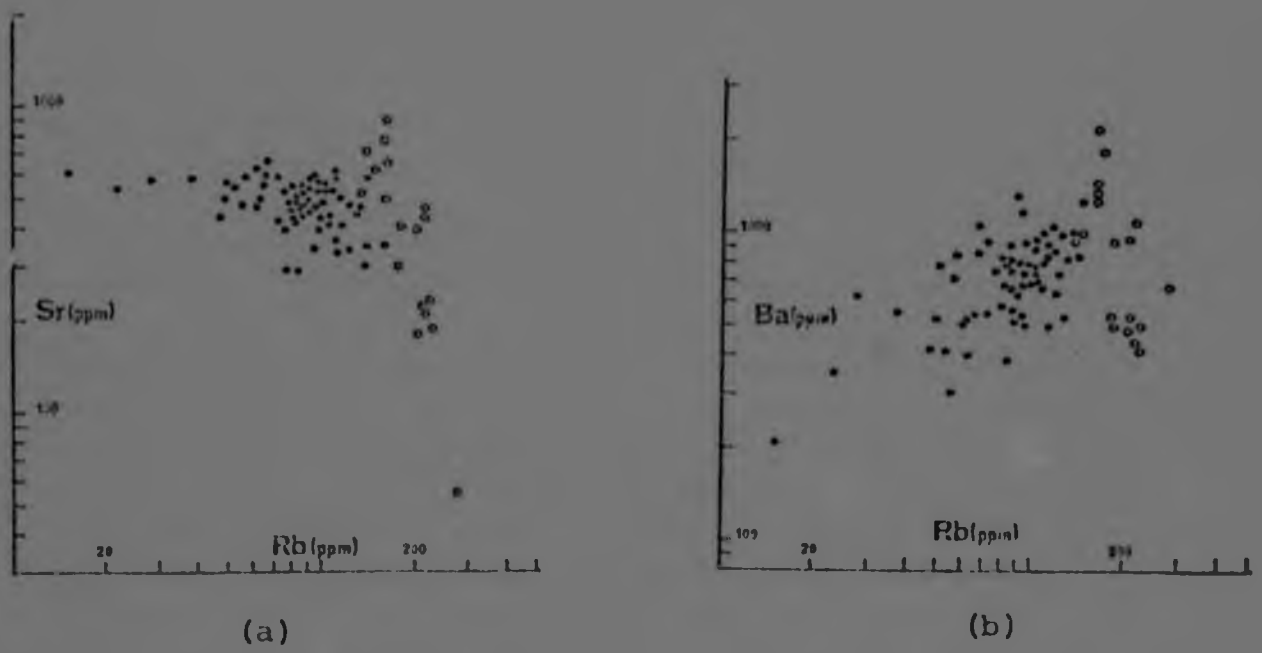

Figure 54. Plots of Rb v Sr and Rb v Ba for the Nelspruit Porphyritic Granite. The different symbols denote two varieties of granite. The closed symbols represent granites considered to have formed by plagioclase + quartz + biotite fractionation whereas the open symbols represent granites believed to have formed by plagioclase + quartz + biotite + K-felspar fractionation.

It will be noted that the empirical data exhibits a fairly wide scatter of points within the individual trends. This effect is considered to be related to the presence of intercumulus liquid and is an important consideration in the crystallization of these rocks.

(a) The effects of intercumulus liquid on the crystallization of the Nelspruit Porphyritic Granite

As McCarthy and Hasty (1976) have pointed out, the perfect separation of cumulus crystals from a melt is unlikely, and the presence of trapped intercumulus melt may be anticipated. This will result in the composition of solids lying between the pure melt and pure cumulate trends (i.e. between lines AB and DE in Figure 51) as the solids attain a partially "liquid" character in the presence of intercumulus melt. Actual solid compositions within the two trends will, thus, lie scattered in the parallelogram space enclosed by ABED and FBCG respectively (Figure 51).

The presence of intercumulus liquid will have a marked effect on the alkali contents of rocks forming in the plagioclase + quartz + biotite fractionation branch. It is obvious that the Na_2O content of this cumulus assemblage will be similiar to that of the melt so that variation in the amount of trapped intercumulus melt will have a negligible effect on the Na_2O content. By contrast the K_2O content of this cumulus assemblage will be considerably lower than that of the melt (there being no K-felspar in this assemblage) and will not vary with fractionation. The K_2O content of the melt will become residually enriched with progressive fractionation of K_2O-poor cumulus phases.

The interrelationships between trace elements and K_2O content for plagioclase + quartz + biotite fractionation in a mixed cumulus-intercumulus assemblage (i.e. a whole rock)

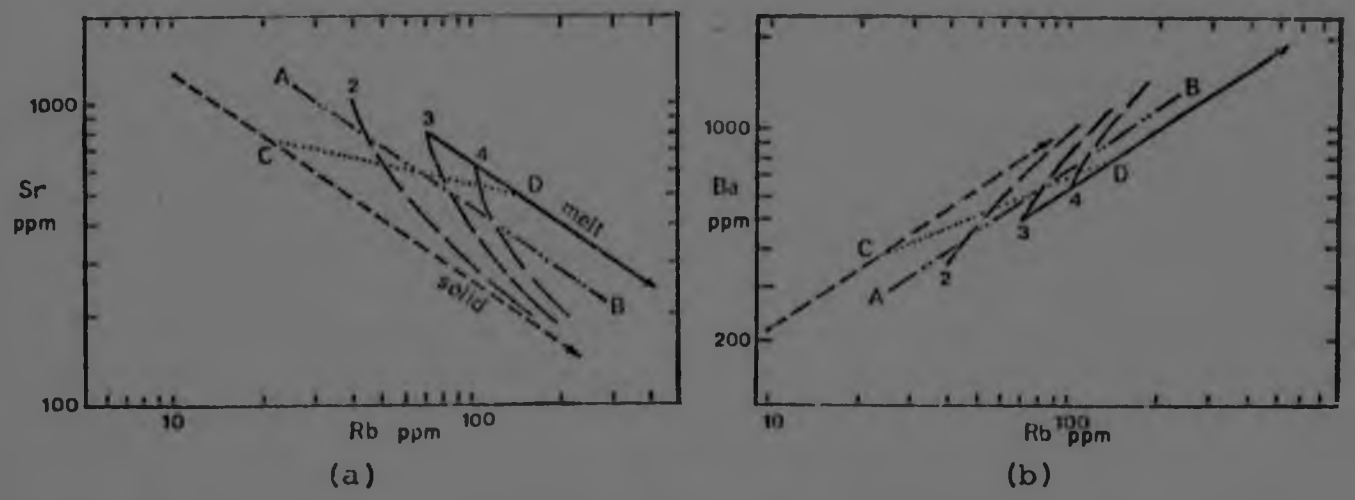

Figure 55. Diagrams showing the relationship between the degree of fractionation and the K_2O content in rocks undergoing plagioclase + quartz + biotite fractionation. The Rb v Sr and Rb v Ba curves for this fractionation trend are reproduced from Figure 51. It is assumed that the initial melt contained 3% K_2O and that the separating solid phase contained a constant 1% K_2O (i.e. exsolved K_2O in the plagioclase lattice). Lines of constant K_2O content (i.e. 2, 3 and 4% K_2O) for mixed cumulus-intercumulus assemblages have been calculated and are shown (long dashes). The change in the K_2O content of a mixture containing 25% intercumulus melt is shown by the intersection of the lines 2, 3 and 4 (%K_2O) with the line AB. The line CD is the locus of compositions of mixed assemblages which may form at 55% solidification of the original magma (i.e.the point in the model where it is assumed that a plagioclase + quartz + biotite + K-felspar assemblage starts to crystallize).

are portrayed in Figure 55a and b. In this figure, the Rb, Sr and Ba distribution curves for plagioclase + quartz + biotite fractionation are taken from Figure 51. Assuming the initial magma contained some 3% K_2O (i.e. point A, Figure 51) and that the cumulus assemblage contained only 1% K_2O (i.e. K_2O in solid solution with the plagioclase), then a line of constant 3% K_2O may be drawn in. Similiarly lines of constant 2% K_2O, 4% K_2O, etc., may also be drawn in (Figure 55). The positions of these lines are calculated by considering the proportionate decreases in K_2O content with decreasing amounts of intercumulus liquid (i.e. K_2O contents will decrease towards the pure cumulate trend. The line AB (Figure 55) represents the compositions containing 25% intercumulus melt. It is seen that a rock containing this amount of intercumulus liquid and which contains 3% K_2O will be considerably less fractionated than one containing a smaller amount of intercumulus liquid (i.e. with a composition closer to that of the pure solid). Therefore, because of an increasing K_2O content in the liquid, brought about by an increase in fractionation, it follows that the more fractionated the system, the less intercumulus liquid is necessary to produce a given K_2O content in a mixed assemblage. With respect to the real situation, as intercumulus liquid is always likely to be present in a fractionating system, an increase in K_2O should be observed along a fractionation trend. Figure 56a and b represents plots of the empirical data for the plagioclase + quartz + biotite fractionation trend (from Figure 54) in which the samples have been ranked according to their K_2O values. In Figure 56 samples with less than 3% K_2O (dots) occur on the left, and samples with greater than 4% K_2O (solid squares) occur on the right, indicating a general increase in the K_2O content with increased fractionation. This must indicate, therefore, the presence of significant amounts of intercumulus liquid. Variations in the amount of intercumulus liquid contribute towards the observed scatter in the empirical data. It will also be noted that the theoretical trace element distribution trends (Figure 55) are somewhat steeper than the

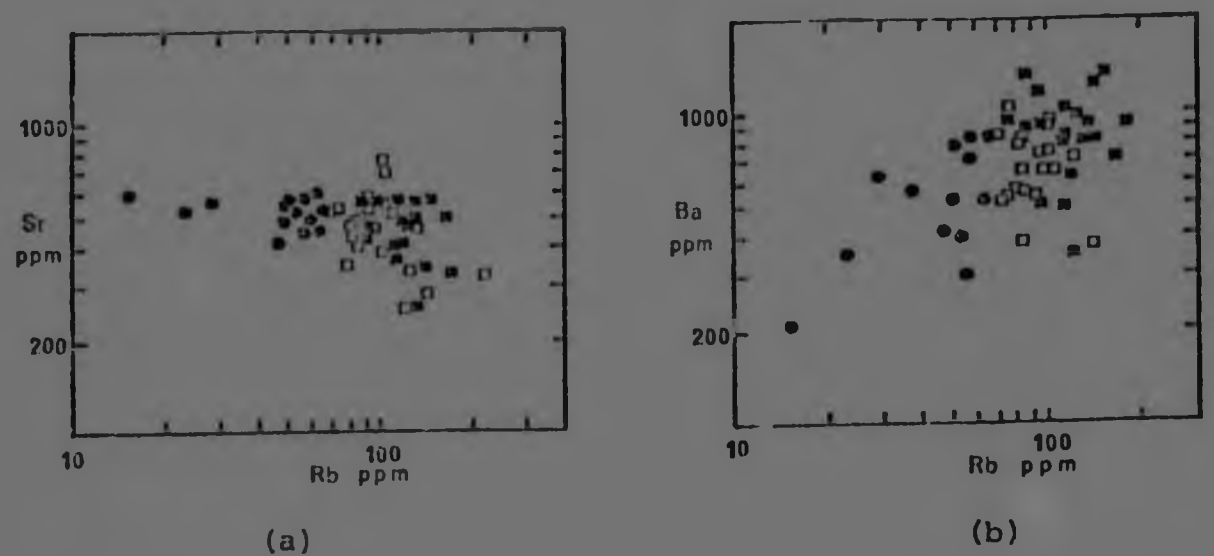

Figure 56. Diagrams showing the relationship between the Rb v Sr and Rb v Ba trends, and the K_2O content in rocks of the Nelspruit Porphyritic Granite which are thought to have formed as the result of plagioclase + quartz + biotite fractionation. Dots denote samples with less than 3% K_2O, open squares, 3 - 4% K_2O and closed squares, greater than 4% K_2O.

general trend observed in the empirical data (Figure 56). However, the line CD in Figure 55 represents the locus of compositions of mixed cumulus/intercumulus assemblages which have formed after 55% crystallization of the magma. The slope of this line (i.e. CD) more closely resembles the slope of the empirical data in Figure 56, the latter being somewhat less steep than predicted for the plagioclase + quartz + biotite fractionation trend in the theoretical model (Figure 51 and 55).

It is important to note when considering rocks that have formed within the plagioclase + quartz + biotite fractionation trend that the presence of intercumulus liquid implies the presence of intercumulus K-felspar in the resulting rock. In the natural state rocks that are considered to have formed within this fractionation trend all contain K-felspar. This K felspar must, however, be regarded as being intercumulus in character and therefore has no effect on the distribution of trace elements in the rock (i.e. in trace element modelling the intercumulus melt component is considered to have crystallized in isolation from the surrounding cumulus constituents).

In addition, it should be noted that the effect of intercumulus liquid, particularly with respect to K_2O contents, is minimal when considering the plagioclase + quartz + biotite + K-felspar fractionation trend, as liquid and solid compositions are likely to be very similiar.

Parameters commonly used in the detection of fractionation in igneous rocks are the K/Rb and K/Ba ratios. According to the discussion above, the Nelspruit Porphyritic Granite should also reflect fractionated K/Ba and K/Rb ratios. Furthermore, the effects of intercumulus liquid on the plagioclase + quartz + biotite fractionation trend should also be observed using these ratios. The empirical K/Rb v K_2O and K/Ba v K_2O plots (Figure 57) exhibit a very wide

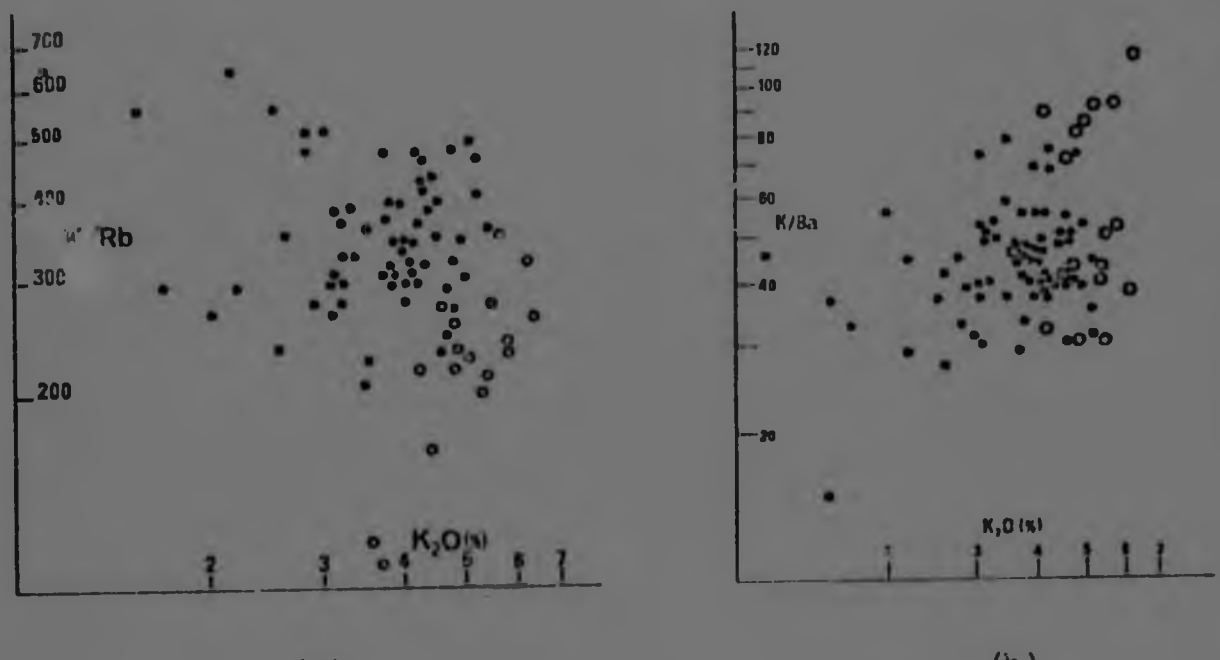

(a) (b)

Figure 57. Plots of K/Rb v K_2O and K/Ba v K_2O for the Nelspruit Porphyritic Granite. The different symbols denote two varieties of granite. The closed symbols represent granites considered to have formed by plagioclase + quartz + biotite fractionation whereas the open symbols represent granite thought to have formed by plagioclase + quartz + biotite + K-felspar fractionation.

scatter of data points. The points conforming to the model plagioclase + quartz + biotite fractionation trend are seen to fall to the left of those of the plagioclase + quartz + biotite + K-felspar trend. The theoretical distributions of the K/Rb and K/Ba ratios, conforming to the crystallization sequence described in the trace element model (Figure 51), are presented in Figure 58. In Figure 58a, point A represents a melt having a K/Rb ratio of 350 and a K_2O content of 3%. The cumulus assemblage is again assumed to contain a constant 1% K_2O (due to solid solution of K_2O in plagioclase). The first solid to separate lies at point D. With progressive crystallization the melt changes composition from A to B while the cumulate moves towards E. Also shown are the changes in composition of mixed cumulus/intercumulus assemblages containing 10%, 20% and 40% trapped intercumulus liquid. It is evident, from this figure, that variations in the amount of intercumulus liquid will result in a wide scatter in the data although a general decrease in K/Rb with increasing K_2O (i.e. increasing fractionation) should be discernible. The empirical data (Figure 57a) shows a wide scatter in the K/Rb ratios of the plagioclase + quartz + biotite fractionation trend.

At point B (Figure 58a), which represents approximately 55% crystallization, K-felspar becomes a cumulus phase accompanied by a slight increase in the biotite content. A distinct change in the K/Rb distribution occurs and, with continued fractionation, leads to a significant drop in K/Rb in both melt and solid. The melt changes in composition from B to C maintaining a fairly constant (but slightly decreasing) value of K_2O, around 5%. The first K-felspar-bearing solid to separate from melt B lies at F, with a K_2O content of approximately 6%. Successive solids change in composition towards G. The minimal effects of the presence of intercumulus liquid on the plagioclase + quartz + biotite + K-felspar fractionation trend is depicted by the line NP in both Figures 58a and 58b. This line represents an assemblage

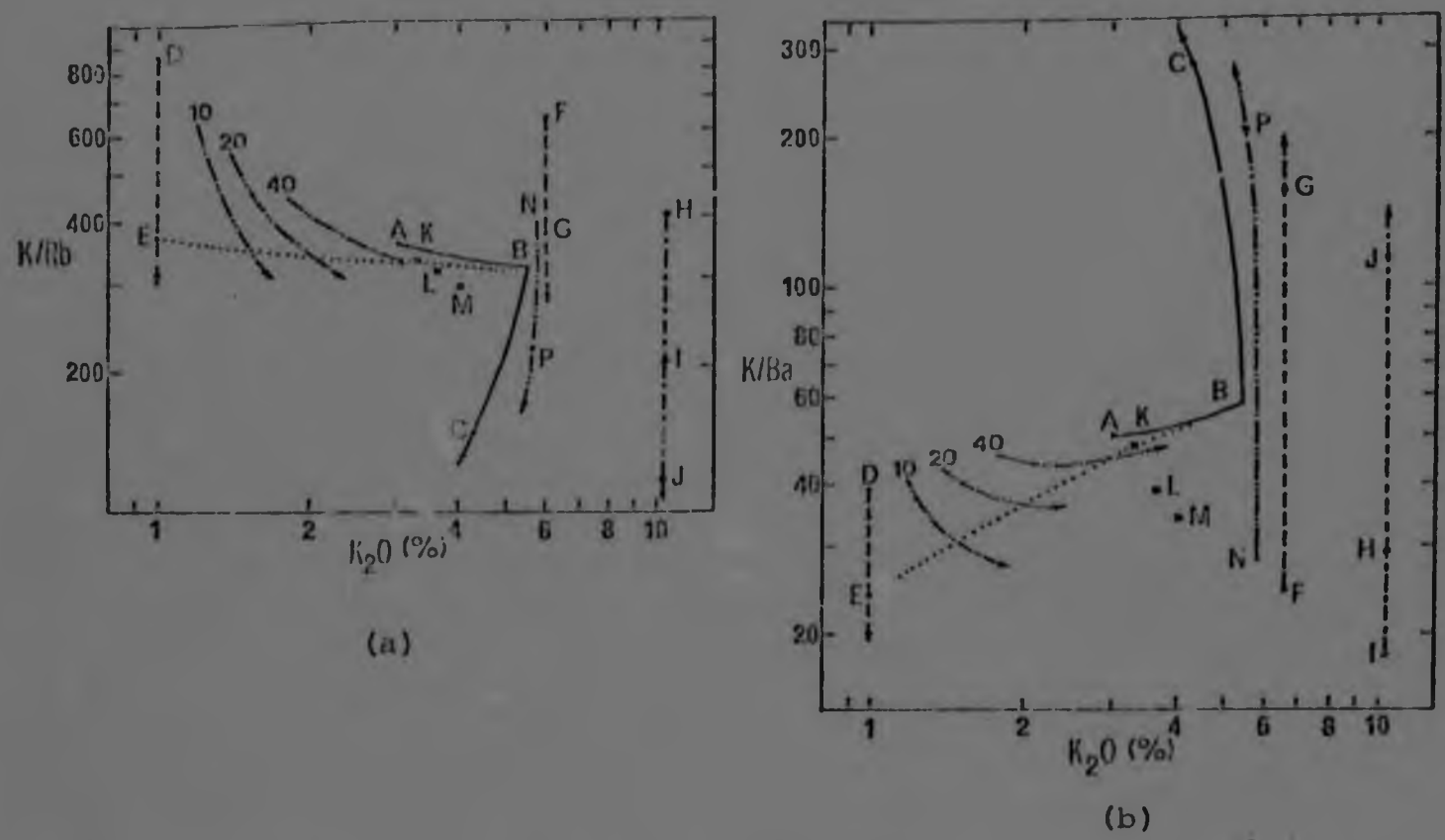

Figure 58. Diagrams illustrating the theoretical relationships between K/Rb, K/Ba and K_2O contents during the fractional crystallization involved in the model (Figure 51). Initial magma composition is at A. This melt fractionates plagioclase (47%), quartz (49%) and biotite (4%). The first solid formed is assumed to contain 1% K_2O and lies at D. Subsequent solids lie along DE. The melt evolves along AB. The loci of composition of mixed cumulus-intercumulus assemblages containing 10%, 20% and 40% intercumulus melt are shown. Curve EB is the locus of mixed assemblages which may form at 55% crystallization of melt A. At B, cumulus mineralogy changes to plagioclase (32%), K-feldspar (30%), quartz (28%) and biotite (10%). The first solid lies at F, and subsequent solids lie along FG. The melt evolves towards C. NP is the locus of compositions containing 20% intercumulus melt. Biotites in equilibrium with melts along AB lie along HI (assuming a constant 10,5% K_2O in the biotite), while biotites in equilibrium with melts BC lie along IJ. K is a 50-50 mix of melt B and cumulate E, and L represents a mixture of 5% biotite I with K; M represents a mixture of 10% biotite I with K.

containing 20% intercumulus melt, and is little removed from the line FG (i.e. the line representing the change in pure solid compositions). It will be seen from the empirical data (Figure 57a) that the samples conforming to the plagioclase + quartz + biotite + K-felspar fractionation trend exhibit limited scatter and a well-defined trend involving a rapid decrease in K/Rb ratio with fractionation. The limited scatter in this trend is undoubtedly related to the limited effects of intercumulus melt on the plagioclase + quartz + biotite + K-felspar trend.

The distribution of the K/Ba ratio during the two fractionation trends is analogous to that of the K/Rb ratio except that the K/Ba ratio increases markedly during the plagioclase + quartz + biotite +K-felspar trend. The same comments (relating to the effects of intercumulus liquid) made regarding the K/Rb ratio, can be made ab the K/Ba ratio. In this case, fractionation from melt A of plagioclase + quartz + biotite causes the melt to increase in K/Ba towards B, whereas the cumulates change in composition along DE (Figure 58b). The entry of K-felspar as a cumulus phase causes a depletion in Ba and concomittant increase in K/Ba in the melt, towards C, and the resultant K-felspar-bearing cumulates lie along FG.

The empirical data (Figure 57b) again shows a wide scatter in the K/Ba ratio for the plagioclase + quartz + biotite fractionation trend, with much less scatter in this ratio in the crystallization sequence where K-felspar is a cumulus phase.

(b) <u>The possible effects of the non-uniform distribution of biotite on the observed scatter in the empirical data</u>

It is clear that the scatter of data points in the Rb v Sr and Rb v Ba plots (Figure 54), and also in the K/Rb and K/Ba v K_2O diagrams (Figure 57), is greater than that

predicted by variations in the proportions of cumulus and intercumulus components. It will also be noted, with respect to the plagioclase + quartz + biotite fractionation trend, that the data on the Rb v Sr plot (Figure 54a) is less scattered than that on the Rb v Ba plot (Figure 54b). (Note that the relative scatter in the K/Rb and K/Ba v K_2O diagrams is subjective, as there is an order of magnitude difference between these two ratios. Whereas much of this scatter is undoubtedly analytical in origin, the different degree of scatter in the Rb v Sr and Rb v Ba plots suggests an additional source which may be related to variations in the biotite contents of the various samples. Small variations in the biotite content of the rock may markedly effect the distribution of trace elements as the latter (particularly Ba) are strongly influenced by biotite (see Table 18).

The effect of variation in the cumulus biotite content of mixed cumulus/intercumulus assemblages is illustrated in Figure 51. In this figure, point H is the composition of biotite in cumulate D and, as melt and cumulate change in composition with fractionation towards B and E respectively, this biotite changes composition towards I. With the incoming of K-felspar as a cumulus phase the biotite then changes composition towards J. Point K on this diagram represents a mixed assemblage comprising of 50% cumulate E and 50% melt B. The addition of 5% biotite (of composition I) to K results in composition L. The addition of 10% biotite results in composition M. In the Rb v Sr diagram (Figure 51a) the trend KLM, which represents the change in composition of a 50/50 cumulus/intercumulus assemblage with increasing biotite content, is broadly parallel to the plagioclase + quartz + biotite fractionation trend. However, in the Rb v Ba diagram (Figure 51b) the trend indicated by the points KLM is oblique to the plagioclase + quartz + biotite fractionation trend. Thus, variations in the amount of biotite in cumulus/intercumulus assemblages will result in an apparently greater amount of scatter on a Rb v Ba plot than on a plot of Rb v Sr. The same situation applies to the points KLM or the

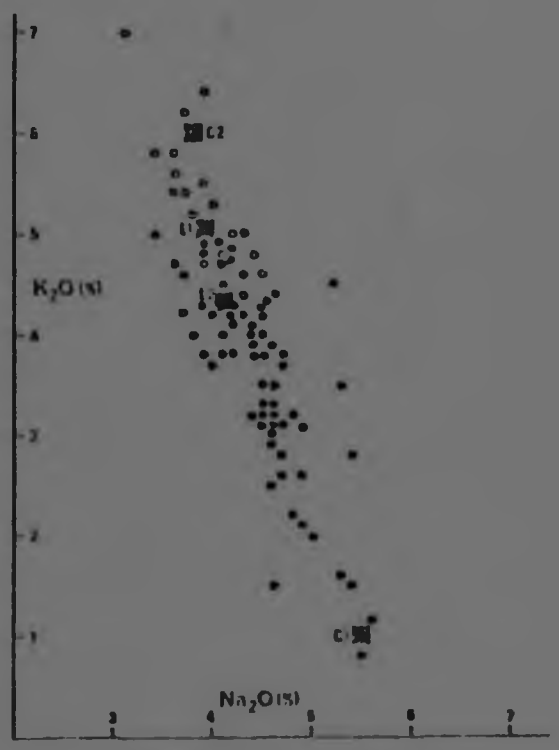

Figure 59. A plot of K_2O v Na_2O for the Nelspruit Porphyritic Granite. Closed symbols represent granites considered to have formed by plagioclase + quartz + biotite fractionation whereas open symbols represent granite thought to have formed by plagioclase + quartz + biotite + K-felspar fractionation. C1 and L1 are the calculated average cumulate and liquid (melt) compositions respectively, for the first stage of fractionation. C2 and L2 represent the average cumulate and liquid compositions for the second stage. The spread in the K_2O/Na_2O ratio between the calculated cumulate and liquid compositions, in each case, is due to variation in the proportion of cumulate and melt in the resultant rocks. Variations in the K_2O/Na_2O ratio, therefore, are not due to genetic changes in the granite type.

K/Rb and K/Ba v K_2O plots in Figure 58. Here the trend KLM, caused by increasing biotite content in a 50/50 cumulus/intercumulus assemblage, will cause a broadening in the theoretically predicted distribution of K/Rb and K/Ba. This distribution should be confined to the wedge-shaped space ABED (Figure 58) if variations in the amount of intercumulus melt present were the only factor affecting the scatter of data.

In short, it is seen that even factors such as the relative scatter of empirical data may have some bearing on the genesis and mode of crystallization of rocks undergoing fractional crystallization.

(c) The significance of the wide variation in the K_2O/Na_2O ratio in the Nelspruit Porphyritic Granite

As has been mentioned in Chapter 3, the Nelspruit Porphyritic Granite is characterized by considerable variation in its K_2O/Na_2O ratios, indicating a range in composition from tonalite through to granite(sensu stricto). The data, shown in Figure 23, is re-plotted in Figure 59 but, in this case, the data is separated into samples conforming to the plagioclase + quartz + biotite fractionation trend (dots) and to the plagioclase + quartz + biotite + K-felspar fractionation trend (open stars). This diagram shows that samples from the latter fractionation trend are clearly more potassic than those from the former trend. The composition (i.e. K_2O/Na_2O ratio) of the model cumulus assemblage (C1) for the plagioclase + quartz + biotite fractionation trend is given in Figure 59. This composition was calculated using the same proportions of cumulus minerals that were used in the calculation of the trace element model (i.e. 47% plagioclase, 49% quartz and 4% biotite). In addition it was assumed that the plagioclase contained 1,2% K_2O in solid solution. The composition of the residual liquid (L1) from which this cumulus assemblage is derived was also calculated.

(This composition L1 was calculated by assuming that an average rock, resulting from this fractionation trend, consisted of a 40/60 cumulus/intercumulus mixture). In Figure 59, the inferred solid and melt compositions (C1 and L1 respectively) straddle the observed compositional field of the samples conforming to the plagioclase + quartz + biotite fractionation trend. Therefore, variations in the relative proportions of L1 and C1 (i.e. variations in the proportion of cumulus to intercumulus component) in the rocks produced by this fractionation trend cause the wide variation in the K_2O/Na_2O ratios.

In a similiar manner the pure cumulate and melt compositions (C2 and L2), for derivitives of the plagioclase +quartz + biotite + K-felspar fractionation trend, are also shown on Figure 59, again calculated using the same proportions of cumulus mineralogy used in the trace element model (i.e. 32% plagioclase, 28% quartz, 30% K-felspar and 10% biotite). C2 and L2 also straddle the observed composition field of samples conforming to this fractionation trend, indicating that these rocks are produced by variations in the proportions of these end-member components. Significantly, the spread in K_2O/Na_2O ratio is far smaller in this case (i.e. where K-felspar is a cumulus phase) because of the much smaller difference in composition between melt and cumulate. This aspect was mentioned previously with respect to the effects of intercumulus liquid on the two fractionation trends. It should be noted that there is undoubtedly considerable uncertainty in the calculated melt and cumulate compositions (L1, L2, C1 and C2) because of the assumed 40/60 cumulus /intercumulus ratio in the average rock forming under these conditions. However, it should be noted that L1 is slightly more potassic than L2, a feature which is in accordance with experimental data of Winkler (1976) (i.e. it is expected that with the introduction of cumulus K-felspar, after 55% fractional crystallization, the K_2O content in the residual melt will decrease).

(d) The significance of the polynomial trend surface analyses on the inferred fractional crystallization of the Nelspruit Porphyritic Granite

It has been mentioned previously in this chapter that the mechanism by which fractional crystallization may have taken place in the Nelspruit Porphyritic Granite involved, not the conventional mechanism of crystal settling that is often envisaged for layered mafic rocks, but a process whereby the crystallization of successive mineral phases from the margins, towards the core regions of the magma chamber, took place. It is envisaged that while the marginal areas of the magma chamber were crystallizing the plagioclase + quartz + biotite fractionation trend was operative and that the granites formed in these areas bear only intercumulus K-felspar. Only subsequently, at a more advanced stage of crystallization (approximately 55% according to the model), when the inner portions of the magma chamber were solidifying, did the plagioclase + quartz + biotite + K-felspar fractionation trend become operative. These resultant rocks bear cumulus, and probably also intercumulus, K-felspar. Such a two-stage crystallization process should be reflected in the distribution of major, and in particular, trace elements over the area in question. The type of distribution that is anticipated would involve the enrichment of Rb, Ba and K_2O into the core regions of the magma chamber (i.e. Ba is incompatible in the first fractionation trend, Rb is incompatible in both fractionation trends) whilst Sr and Na_2O would be enriched into the marginal areas (i.e. Sr is compatible in the first fractionation trend). An examination of the polynomial trend surface analyses of K_2O, Na_2O, Rb, Sr and Ba (Figures 39-50, Chapter 4) shows that the inferred distributions determined by the nature of the crystallization mode in the Nelspruit Porphyritic Granite are generally in accordance with the empirical distributions of the data. The 2nd and 3rd degree polynomial surfaces of K_2O (Figures 40 and 41 respectively) and the 2nd degree Ba surface (Figure 50) exhibit well-defined

concentric patterns which show a concentration of these elements towards the centre of the region. The 3rd degree polynomial trend surface for Rb (Figure 46) shows a less marked, semi-concentric, surface showing a maximum concentration in the south-central portion of the study area. The 2nd degree surface for Na_2O (Figure 43) and the 2nd and 3rd degree surfaces for Sr (Figures 48 and 49 respectively) also exhibit less convincing semi-concentric surfaces, with areas of maximum depletion occurring in the south-central portions of the relevant area.

The general indications from these trend surfaces is, however, that the distribution of major and trace elements conforms with the suggestion that the Nelspruit Porphyritic Granite underwent fractional crystallization involving, initially, crystallization without cumulus K-felspar. The non-definitive distributions of Na_2O and Sr may be related to the large differences in the composition of cumulat and melt in the plagioclase + quartz + biotite fractiona trend and the consequences of small variations in the amount of intercumulus liquid on the resulting rock composition. This is a factor which has been described in detail above.

V. SUMMARY AND CONCLUSIONS

(i) The similiarity between the trace element inter-relationships shown in Figure 54, and those modelled in Figure 51, suggests that the Nelspruit Porphyritic Granite represents a cumulate whose crystallization underwent two stages :- the first stage involved the fractionation of a plagioclase + quartz + biotite assemblage and resulted in a rock bearing intercumulus K-felspar, whereas the second involved the fractionation of a plagioclase + quartz + bio + K-felspar assemblage.

(ii) During the plagioclase + quartz + biotite fractionation trend, melt and cumulate compositions were

significantly different and thus small variations in the amount of intercumulus liquid resulted in the development of rocks of varying compositions, this being reflected in their K_2O/Na_2O ratios. By contrast, during the second fractionation trend (where K-felspar is a cumulus phase) melt and cumulate compositions are very similiar and a smaller compositional variety is reflected in these rocks.

(iii) It is suggested that a component of scatter exhibited by the empirical trace element data may be due to the non-uniform distribution of biotite which is an important host for Rb and, in particular, Ba.

(iv) Polynomial trend surface analyses carried out over the study area tend to confirm the inferred fractional crystallization mode in the Nelspruit Porphyritic Granite, in that K_2O, Rb and Ba are concentrated in the core and Na_2O and Sr in the marginal areas.

(v) In conclusion, the recognition of a subtle form of fractional crystallization in the Nelspruit Porphyritic Granite is perhaps indicative of the fact that other Archaean granites may have crystallized in a similiar way and, therefore, warrant examination in this light. The conventional ideas which tend to regard granites as equilibrium products (i.e. the mineral phases are considered to grow continuously in equilibirium with the melt from which they form), may become somewhat outdated if, with accurate analyses of trace elements, a method is provided whereby a clearer understanding of the crystallization of granitic magmas may be obtained.

CHAPTER 6

THE POST-GRANITE GEOLOGY OF THE AREA BETWEEN NELSPRUIT AND BUSHBUCKRIDGE

I. INTRODUCTION

Previous workers, particularly those attached to the South African Geological Survey, have provided detailed accounts of the post-granite geology of the Barberton region as well as areas to the north of Nelspruit. These workers have focused their attention on the relative ages of dykes, sills, and other intrusives, with respect to major rock units of the Archaean and Proterozoic sequences in the eastern Transvaal.

Visser et al.. (1956) recognized four main ages of dykes in the Barberton region :-

(i) Intrusions older than the Moodies Group;
(ii) Intrusions older than the Godwan Formation;
(iii) Intrusions younger than the Transvaal Supergroup;
(iv) Dykes and sills of Karroo age.

Most of these dykes are reported to be diabasic in composition with the larger ones commonly showing evidence of differentiation into peridotitic, gabbroic,dioritic and granophyric components. The Karroo age intrusives are all doleritic.

Visser and Verwoerd (1960) have, on the other hand, recognized three ages of dykes in the area north of Nelspruit. These have been termed :-

(i) Pre-Godwan intrusions,
(ii) Post-Transvaal intrusions,
(iii) Post-Karroo dolerites.

This subdivision coincides with the types described by Visser et al., (1956) for the Barberton area, except that dykes older than the Moodies are not recognized. In the Barberton region the first two relative dyke ages are determined by their field relationships with the Transvaal Drakensberg Escarpment whereas the third variety is based upon, "...petrographical similiarity with undoubted post-Karroo dykes further to the north and to the south." (Visser and Verwoerd, 1960). The dykes in the Barberton region are generally diabasic in composition with some of the post-Transvaal intrusions being dioritic and quartz dioritic in composition. The Karroo intrusives consist predominantly of dolerites or olivine dolerites with some sills showing signs of differentiation.

Visser and Verwoerd (1960) also provide a detailed description of the shear zones that occur within the Archaean granite terrane north of Nelspruit. These are described as zones of sericitized granite which stand out as ridges of varying height and persistency by virtue of the concentration of silica within them. The above authors also documented, with the aid of chemical analyses, the change in granite composition accompanying the approach to shear zones. The analyses indicate that shearing and sericitization is accompanied by decreases in the soda and increases in the potash and alumina contents of these rocks. Evidence of a horizontal component of shear along these zones of sericitization is provided by the displacement of dykes that cross-cut them. In some instances displacements of up to 2km have been reported.

II. DYKES AND SILLS IN THE STUDY AREA

During the course of field work all dykes and sills evident on the aerial photographs were recorded and these are reproduced on a 1:150 000 map of the study area (Figure 60). These dykes and sills are described according to their relative ages, bearing in mind the classification proposed by Visser and Verwoerd (1960). In addition, brief mention

will be made of dykes which the writer considers to be older than the pre-Godwan intrusions.

(a) Very old dykes

Certain mafic bands occurring in the Nelspruit Migmatite and Gneiss Terrane bear resemblance to very ancient dykes which have possibly been affected by the events and processes responsible for the formation of the migmatites themselves. Such a feature is illustrated in Plate 8f which shows an elongate, mafic band, which may originally have been linear but has now undergone considerable contortion presumably due to the introduction of granitic material into the site which it previously occupied. This mafic band may, in the writers opinion, be indicative of a very early dyke phase which intruded the earth's granitic crust while it was still in the process of consolidation (i.e. between 3,4 and 3,0 b.y. ago). Such dyke-like features have been described previously in the Nelspruit area by Anhaeusser (1969).

(b) Pre-Godwan Intrusions

The majority of dykes in the study area (in particular the very prominent dyke swarm occupying the terrain between Hazy View and Bushbuckridge, Figure 60) are considered by Visser and Verwoerd (1960) to be pre-Godwan in age. These authors stated that, "On either side of the Sabie River dykes of this age (i.e. pre-Godwan) form a swarm with a general east- west trend". The rugged nature of this dyke swarm is illustrated in Plate 8a.

The Pre-Godwan dykes are predominantly diabasic in composition and in thin section consist essentially of plagioclase and clinopyroxene. Very rarely, however, are pristine textures observed in thin section and the plagioclase is often sericitized and the pyroxene uralitized. Chlorite and magnetite form common accessory constituents of this dyke variety. A major element analysis, confirming the

diabasic composition of this dyke-type, is presented in Table 19. The sample H.V.2, is a diabase taken from the dyke swarm in the Hazy View area.

Figure 60 shows that the prominent east-west trending Hazy View - Bushbuckridge dyke swarm extends, in a westerly direction, into extensive sheets or sills of diabasic material. The sills in this area appear to overly the granites and it is not uncommon to find that river valleys have cut through the sill capping thereby exposing the underlying granite. The continuity between dykes and sills in the Hazy View-Bushbuckridge area indicates that the dykes, which occupy essentially the eastern half of this area, may be the feeders to the sill cappings in the west. A major element analysis of a diabase sill, sampled in the region to the west of Hazy View, is presented in Table 19 (sample H.V.1) and is seen to have a composition very similiar to the diabase dyke sampled further to the east (viz. H.V.2). This tends to confirm the view that the dykes and sills in the Hazy View-Bushbuckridge area may be co-magmatic.

In some cases the pre-Codwan dykes may possess a composite texture consisting of a matrix of diabase, within which are contained inclusions of granitic material consisting essentially of felspar and quartz. This texture (Plate 8d) is perhaps indicative of the assimilation of granitic material by the invading dyke magma and its subsequent separation as an immiscible fraction. The Bushbuckridge dyke, which is the prominent northernmost dyke shown in Figure 60, shows signs of having assimilated granitic material in places along its western extremities.

(c) Post-Transvaal Intrusions

Although these dykes are extremely common on the Transvaal Drakensberg Escarpment they are relatively rare within the Archaean granite terrane. Visser and Verwoerd

(1960) have noted this fact and stated that, "... in the Archaean granite they (i.e. post-Transvaal dykes) are not as numerous as those of pre-Godwan age."

Two prominent dykes of Post-Transvaal age outcrop continuously over a strike length of approximately 50km in the study area, originating near the Mpageni Granite pluton in the southeast and trending in a northwesterly direction. At least one of these dykes was observed to cut the Transvaal sediments to the south of Sabie.

In thin section the Post-Transvaal dykes consist predominantly of orthopyroxene with lesser amounts of plagioclase. The mineral constituents, by contrast with the pre-Godwan dykes, appear relatively fresh and unaltered. A major element analysis of one of these dykes, sampled just south of White River, indicates a much higher MgO content (and correspondingly lower Al_2O_3 content) than the pre-Godwan dykes (Table 19). The orthopyroxene in this rock probably has a composition approaching the MgO-rich end of the orthopyroxene solid-solution series (i.e. enstatite).

(d) Post-Karroo dolerites

Extensive areas in the northeastern portion of the region are underlain by sills which Visser and Verwoerd (1960) have ascribed to a period of post-Karroo intrusion. Two large sills of this type occur in the northeast of the study area. One occurs due west of Mkhulu Station on the main Hazy View-Skukuza road, and the other extends over a large area in the central portions of the Cunning Moor Tonalite (Figure 60). No undoubted dyke equivalents of these Karroo-age sills have been recognized in the area, possibly due to the fact that these rocks weather very easily. This feature has been previously recognized and Visser and Verwoerd (1960) noted that, "... the dyke rock weathers easily and is poorly exposed."

TABLE 19

ANALYSES OF DYKES AND SILLS OF THREE DIFFERENT AGES FROM THE NELSPRUIT - BUSHBUCKRIDGE AREA

%	H.V.1	H.V.2	P.T.1	ODS.1
SiO_2	55,3	55,8	53,2	51,4
TiO_2	0,84	1,18	0,57	0,49
Al_2O_3	14,2	14,2	6,8	7,9
Fe_2O_3	10,6	10,4	9,6	11,2
MnO	0,14	0,14	0,16	0,18
MgO	5,0	4,1	18,9	19,6
CaO	8,5	6,2	5,1	7,1
Na_2O	3,1	4,4	1,0	1,1
K_2O	1,15	0,91	0,92	0,33
P_2O_5	0,17	0,26	0,11	0,06
H_2O^+	2,0	2,1	3,0	0,6
H_2O^-	0,05	0,0	0,0	0,0
CO_2	0,0	0,2	0,6	0,05
TOTALS	101,05	99,89	99,99	100,01

H.V.1 - Diabase sill, northwest of Hazy View (Pre-Godwan intrusion)

H.V.2 - Diabase dyke, Hazy View area (Pre-Godwan intrusion)

P.T.1 - Dolerite dyke, south of White River (Post-Transvaal intrusion)

ODS.1 - Dolerite sill, west of the Sabie Sand Reserve (Karroo intrusion)

(Analysts :- Bergstrom and Bakker).

The Karroo-age sills have been described as olivine dolerites although it has been pointed out to the writer that in some places these sills appear to be differentiated (I. Schutte, personal communication, 1976). In thin section these rocks consist predominantly of orthopyroxene and plagioclase. No olivine was seen in any of the thin sections examined, but this may be due to inadequate sampling across a sill which is most likely differentiated. Accessory amounts of zircon, chlorite and an opaque oxide mineral (magnetite?) also occur. The sills have an ophitic texture with plagioclase grains occurring as a matte of grains forming the interstitial spaces between subhedral orthopyroxene grains. Plagioclase also occurs as inclusions within larger grains of orthopyroxene.

A major element analysis of a Karroo-age sill is presented in Table 19 (sample ODS.1). Its composition is similiar to that of the post-Transvaal dolerite dykes, which have high MgO and low Al_2O_3 contents. The Karroo-age sills often have a marked effect on the texture and colour of the granitic rocks underlying the. These affected granites are commonly greenish or reddish in colour, possibly due to the effects of epidotization and iron-staining. Visser and Verwoerd (1960) reported that, "Contact metamorphism by the dolerite sills imparts a red coloration to the granite, and in some places, a pitted surface that may be ascribed to partial recrystallization."

(e) A note regarding certain structures observed in minor dyke intrusions in the study area

Features found in minor dyke intrusions may provide an indication as to the mechanisms by which mafic magma is able to intrude solid granitic material. Plate 8e shows a small dyke intrusion (approximately 15cm wide) which is characterized by a"horned" or"off-set"structure with respect to its granite host. This type of structure, often demonstrated on a small

scale, is considered by Currie and Ferguson (1970) to be indicative of the mode of emplacement of dykes in general. These authors have described in detail non-tectonic "off-set" and "horned" structures in lamprophyric dykelets from various mafic intrusions in Canada. They attribute these structures to the initial injection of low-viscosity, high-velocity volatile-rich material into a set of stepped, unconnected parallel joints or fractures. This causes the initial widening of the joint or fracture. The subsequent emplacement of the mafic magma causes further widening of the fracture system, as well as widening, in some cases, the inter-connection between two adjacent,parallel fractures. The minor dyke in Plate 8e, exhibits an off-set structure which may represent the original fracture into which the initial, volatile-rich, phase of the magma may have intruded.

Currie and Ferguson (1970) add that, "If the magma is saturated or super-saturated with water, boiling off the water during intrusion causes a low-viscosity precursor of the magma which greatly facilitates intrusion." In the light of such statements it becomes easier to understand how the large scale intrusion of dyke swarms, such as that occurring between Hazy View and Bushbuckridge, may have taken place.

(f) Suggestions regarding the state of the earth's crust in the Hazy View - Bushbuckridge area during the emplacement of the pre-Godwan dyke swarm

An examination of Figure 60 shows that there is an uneven distribution of dykes and sills in the study area. The area between Nelspruit and White River has a moderate concentration of dykes of random orientation, and no sills whatsoever. The area between White River and Hazy View contains a low concentration of dykes together with a few sills. The dykes in this area show indications of a preferred east-west strike direction. By contrast the area between Hazy View and Bushbuckridge is characterized by an east-west

trending dyke swarm in the eastern half of the area and by extensive sill cappings of associated mafic material, in the western half. In the area north of Bushbuckridge, regional reconnaissance indicates that dykes are far less numerous and, once again, randomly orientated.

The uneven dyke and sill distribution pattern may indicate that certain portions of the earth's crust may be more prone to mafic intrusion than others. The Hazy View-Bushbuckridge area might represent a portion of the earth's crust that has undergone an east-west orientated upwarp or flexure. This upwarp, or flexure, may have initiated the development of a set of deep-seated, east-west trending,tensional fractures in the area, the latter preferentially facilitating the intrusion of dykes and sills in a subsequent magmatic event.

Additional evidence for an upwarp in this area is suggested by the work of Button (1973), who showed that the lower Wolkberg sediments and volcanics thin, and eventually pinch out completely, in a region which he named the "Bosbokrand Arch". This major crustal antiform was, therefore, present in pre-Transvaal times. What produced this crustal upwarp, or flexure, is at present still unknown, but it may be related to the interference pattern of major antiformal and synformal structures which pervade the Kaapvaal Craton. The latter have largely been responsible for controlling the geological evolution of supracrustal rocks developed upon it (Pretorius, 1974; Hunter, 1975).

Another aspect of regional interest involves the abundance of pre-Godwan sills in the western half of the Hazy View - Bushbuckridge area, and the absence of such sills (except for the younger Karroo intrusions) in the eastern half of the area. It is envisaged that the sills probably covered the entire Hazy View - Bushbuckridge region and their current exposure may be related to the effects of a

PLATE 8

A. A view, looking east, of the ridges which make up part of the prominent Hazy View dyke swarm. These east-west trending dykes are truncated in the middle distance by the right lateral Hazy View Shear Zone (Figure 60). Locality, approximately 3km north of Hazy View.

B. View of the large east-west trending Bushbuckridge dyke which terminates the prominent Hazy View dyke swarm. The surrounding flat-lying terrain consists mainly of the Cunning Moor Tonalite. Locality, approximately 2km south of Bushbuckridge.

C. A view, looking east, of the hilly terrain underlain by the Nelspruit Porphyritic Granite (far distance) and the flat, low-lying countryside occupied by the Cunning Moor Tonalite (foreground). The prominent peak in the Nelspruit Porphyritic Granite is known as Legogotu (Lion's Head).

D. A composite dyke occurring in the Hazy View dyke swarm. The inclusions represent assimilated granitic material which may have formed an immiscible fraction within the mafic host.

E. "Horned"off-set structures in a small-scale dyke intrusion. Structures such as these are thought to shed light on the mechanism of intrusion of mafic dykes (see text). Locality, sample site B16. The dashed lines have been inserted to emphasize the outline of the dyke.

F. Photograph of a very early dyke, possibly affected by later granite intrusion, in the Nelspruit Migmatite and Gneiss Terrane. Locality, sample site A8, 10km east of White River.

PLATE 8

A

B

C

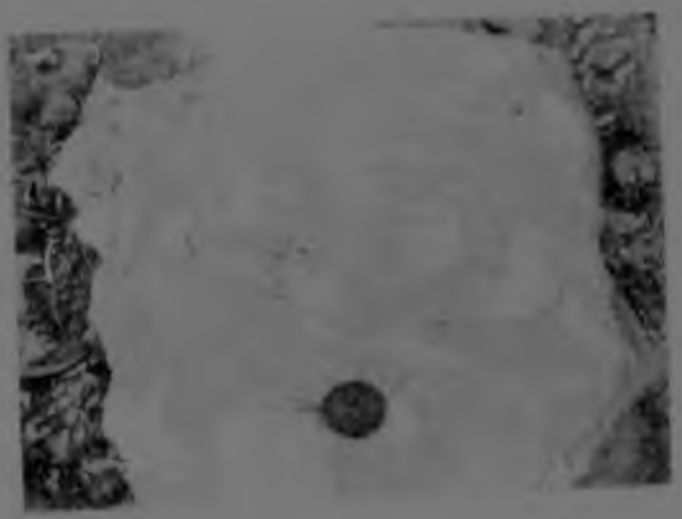

D

E

F

westerly retreating scarp face. This erosional effect is noticeable when considering the strong regional slope of topography away from the Transvaal Drakensberg Escarpment, towards the east (see, for example, the first degree polynomial trend surface for altitude; Figure 36, Chapter 4). Thus, the westerly retreating escarpment has, in retrospect, exposed the roots of the sill cappings (i.e. the dyke swarm) in the eastern half of the area.

III. SHEAR ZONES IN THE STUDY AREA

The area between Nelspruit and Bushbuckridge is characterized by numerous shear zones, ranging in size from a few hundred metres to over 70km in length. Typically, these shears are characterized by positive relief(although this feature may not necessarily be continuous along the entire strike length of the shear zones) and demarcated in the field, by white-to-greyish quartz sericite rocks. The shears are often characterized by anastomosing quartz veins which are resistant to weathering and cause the positive relief which these features exhibit (Plate 5d). Figure 60 shows that apart from numerous smaller shears, the study area is characterized by six large shears, the latter all trending in a north-northwesterly or northerly direction. The three largest shears, which occur in the central part of the study area, have been named the White River Shear, the Ngodini Shear and the Hazy View Shear (Figure 60). The Ngodini Shear is the largest of the three, being just over 70km in length. All six of these large shear zones have a right lateral displacement as is indicated by the relative displacement of dykes that intersect them. Particularly spectacular is the Hazy View Shear which displaces the dyke swarm immediately west of Hazy View. The horizontal right lateral displacement along the shear at this point is approximately 2-3km (Figure 60). The actual displacement along these shears is considered to consist of a predominantly horizontal component as is illustrated by the orientation of slickenside surfaces seen

in some of the shears (Plate 5e).

Visser and Verwoerd (1960) concluded that these shear zones have been active for a considerable period of time. Cross-cutting relationships with dykes indicate that they were active from a period pre-dating the age of the pre-Transvaal dykes up until pre-Black Reef times (the shears do not appear to fault the Black Reef Quartzite). It is also possible, however, that less pronounced movements may have taken place in post-Transvaal times (see later).

Two features intimately associated with the shear zones deserve special attention :-

(i) Hot Springs

Two hot springs are known to occur in the study area, the one being approximately 3km east of Hazy View, and the other, 2km west of Hazy View (Figure 60). The hot spring east of Hazy View is clearly associated with a shear zone but the other is not apparently related to these structures. The association of hot springs with shear zones is suggestive of the fact that the latter may still be tectonically active.

(ii) Verdite

At a number of points along the shear zones (in particular the Ngodini and Hazy View Shears) small occurrences of verdite were often noted (Figure 60). This unusual greenish mineral (or, more accurately, mineral assemblage) has been described as occurring within ultramafic rocks in the Barberton Mountain Land, but no mention has been made previously of its occurrence within the granitic terrane (Anhaeusser, 1969, 1972; Viljoen and Viljoen, 1969f). Verdite is described as a form of altered talcose serpentinite (the greenish colour probably being due to the effects of Ni) and usually occurs in ultramafic differentiated bodies, being confined to the contacts

TABLE 20

ANALYSES OF VERDITE OBTAINED FROM THE NGODINI SHEAR ZONE IN THE PEEBLES AREA, AND WILLEMSEITE FROM THE BARBERTON REGION

%	1	2
SiO_2	51,78	51,83
TiO_2	0,36	-
Al_2O_3	27,48	0,38
Fe_2O_3	0,04	2,08
Cr_2O_3	0,93	-
MnO	0,01	0,00
MgO	0,01	7,09
CaO	0,35	0,28
NiO	-	34,55
CuO	-	0,46
Na_2O	7,21	-
K_2O	10,66	-
P_2O_5	0,01	-
L.O.I.	2,96	3,66
TOTALS	101,79	100,33

Column 1 - Verdite from the farm of L. Plath, Peebles district, north of White River.

Column 2 - Willemseite from the Scotia Talc Mine area, near Sheba Siding, Barberton district.

(Analysts : Column 1 - L.J. Robb - E.X.A.M. Unit
Column 2 - after de Waal, 1970, National Institute of Metallurgy).

between harzburgitic and metagabbroic layers. The formation of the verdite is thought to be related to a stress field set up as the result of uncoupling and competency differences between these layers (Anhaeusser, 1969).

The verdite found within the shear zones in the study area appears to have formed where xenolithic pods of mafic or ultramafic material have been affected by the stress fields set up in the shear zones. A sample of verdite from the Ngodini Shear (Figure 60) has been analysed by the author (Table 20, Column 1) and shows a somewhat unusual composition. In particular, the very high Al_2O_3, K_2O and Na_2O contents are prominent, as is the very low value of MgO. The latter is surprising considering the verdite is thought to have been derived essentially from an altered ultramafic rock. It is suggested that this analysis may indicate that metasomatism has played an important role in the formation of this verdite, possibly leaching the system of MgO and enriching it in Al_2O_3, K_2O and Na_2O. It is interesting to recall that high potash values were recorded in sheared tonalite gneisses from the southern part of the study area (Table 5, Chapter 3). Sericite alteration in these affected rocks was responsible for the high potash values in the latter. In fact potash enrichment appears to be a characteristic of sheared or mylonitized granitic rocks.

At one stage it was thought that verdite mineralogy may have consisted, in part, of the recently discovered nickel silicate minerals, willemseite and nimite. These two greenish minerals were originally found in a small nickel deposit in ultramafic rocks of the Onverwacht Group, near Barberton (de Waal, 1970), and may possibly be related to the formation of verdite. However, an analysis of willemseite (Column 2, Table 20) shows a completely different composition to that of verdite from the study area (Column 1, Table 20). It is unlikely, therefore, that either willemseite or nimite (which is compositionally similiar to willemseite) occur in verdite.

Finally, brief mention is made regarding the economic significance of the shear zones. Apart from the sporadic occurrences of verdite, which is highly valued as a semi-precious,ornamental stone, unique to the Barberton region, the shear zones have, in the past, been mined for gold. The Rietfontein Reef, which is a vertically dipping, north-south trending, shear zone located 3km east of Sabie (Figure 60), was, until 1949, mined for gold, arsenopyrite, pyrite, chalcopyrite and silver (Visser and Verwoerd, 1960). At present this shear zone, which has many of the characteristics of other north-south trending shear zones in the study area, is being re-evaluated by an American exploration company, as a potential gold deposit.

IV. SUMMARY AND CONCLUSIONS

(a) The Nelspruit-Bushbuckridge area is characterized by an uneven distribution of mafic dykes and sills. In the area between Nelspruit and Hazy View, dykes occur relatively infrequently and are randomly orientated. Sills are virtually absent in this area. By contrast, the area between Hazy View and Bushbuckridge is characterized by a large number of mafic dykes which are all orientated in an east-west direction. Sills are common, particularly in the higher-lying,western half of this area.

(b) The intrusion of numerous east-west trending mafic dykes in the Hazy View-Bushbuckridge area is considered to be related to a major crustal antiform in this area. This feature pre-dates the Transvaal Supergroup as it has influenced the thickness of sedimentary units in the latter.

(c) Numerous shear zones occur throughout the Nelspruit-Bushbuckridge area. The most prominent of these

occur in an "en-echelon" type array across the study area, all orientated in a north-northwesterly-to-northerly direction. These major features all exhibit right lateral displacement which suggests that they may have all formed synchronously, in response to a single regional stress field.

(d) The shear zones contain sporadic occurrences of verdite which appear to have formed by a combination of shearing and metasomatic processes which prevail within these structures. Certain shear zones may contain gold and other precious metal mineralization. The presence of such mineralization in these features is probably related to the nature of (deep-seated?) country rocks through which they cross-cut.

CHAPTER 7

SUMMARY AND CONCLUSIONS

The following chapter presents a summary of the main conclusions that have been reached during this study of the Archaean granite-greenstone terrane between Nelspruit and Bushbuckridge :-

(1) The Barclay Vale Schist Belt is represented by an assemblage of mafic and ultramafic rocks and chemical sediments underlying an area of approximately 40km^2 and occurring approximately 25km due west of Nelspruit. The marginal areas of the schist belt consist of altered amphibolites and chlorite and talc-chlorite schists with minor serpentinites, pyroxenites and cherts. The core region of the schist belt consists of repetitive cycles of serpentinites and metapyroxenites together with pillow basalts and layers of banded iron-formation. The serpentinites and pyroxenites represent part of a layered ultramafic differentiated body which has been deformed into a synformal structure, which occupies the core region of the schist belt.

The lithological characteristics of the Barclay Vale Schist Belt are such that it can be correlated with rocks of the Lower Ultramafic Unit of the Onverwacht Group, as defined in the Barberton greenstone belt.

(2) In the Archaean granitic terrane between Nelspruit and Bushbuckridge six granite types have been recognized :-

(1) <u>The Tonalite Gneisses and Migmatites</u>

This unit is comprised essentially of tonalite gneisses which occasionally occur with migmatites. The tonalite gneisses generally occur in close proximity to greenstone belts in the southwest and southeast of the

study area, and are commonly mylonitized. These rocks are considered to be the oldest granite-type in the study area.

(ii) The Nelspruit Migmatite and Gneiss Terrane

This terrane consists of a complex suite of mixed mafic and felsic rocks which exhibit a variety of textural types and, topographically, occupies low-lying terrane in the study area. Indications are that the migmatites and gneisses probably formed as a consequence of granitic magma intruding into a pre-existing mafic and tonalitic crust. The granitic magma in question appears to have been associated with the intrusion of the Nelspruit Porphyritic Granite.

(iii) The Nelspruit Porphyritic Granite

The Nelspruit Porphyritic Granite, which occupies most of the higher-lying portions of the study area, is characterized by the almost ubiquitous appearance of large poikilitic microcline phenocrysts. This microcline is considered to have formed as a result of the in situ mobilization and recrystallization of pre-existing K-felspar. The wide range in K_2O/Na_2O and Rb/Sr ratios exhibited by this granite is indicative of a subtle crystallization history involving the fractionation of successive mineral phases in the granite system. In this light, the granite is considered to be magmatic in origin.

(iv) The Cunning Moor Tonalite

This body, of distinctively tonalitic composition, occupies the flat, low-lying terrain in the northeastern portion of the study area. The available geochronological information suggests that the Cunning Moor Tonalite post-

dates the Nelspruit Porphyritic Granite. A high initial $^{87}Sr/^{86}Sr$ ratio (i.e. R_o = 0,7034) indicates an origin related to re-working of pre-existing crustal material.

(v) The Hebron Granodiorite

The Hebron Granodiorite outcrops in two distinct forms; firstly in a unimodal outcrop area to the north-west of White River and secondly, as veins and dykelets scattered irregularly within parts of the Nelspruit Porphyritic Granite. The Hebron Granodiorite is characteristically homogenous both in the field as well as in its major and trace element chemistry. An initial $^{87}Sr/^{86}Sr$ ratio (i.e. R_o = 0,7007) suggests an uncontaminated mantle-derived origin for this rock type.

(vi) The Mpageni Granite

The Mpageni Granite appears as a small, discrete, potassium-rich pluton occurring in the southeastern portion of the study area. Previous geochronological work (De Gasparis, 1967; Oosthuyzen, 1970) indicates that it is the youngest granite in the study area. A high initial $^{87}Sr/^{86}Sr$ ratio (i.e. R_o = 0,7065) indicates, furthermore, that its origin may be related to reworking of crustal material.

(3) Comparison of empirical trace element (i.e. Rb, Sr and Ba) interrelationships with the theoretical distribution of trace elements undergoing fractional crystallization indicate that the Nelspruit Porphyritic Granite may have undergone a complex two-stage crystallization history. This appears to have involved, initially, the crystallization of a plagioclase + quartz + biotite assemblage which resulted in the development of granites in which the K-felspar present was intercumulus in nature. At an advanced stage of crystallization, after

the residual magma had become sufficiently potassic to enable the crystallization of K-felspar to take place, the assemblage plagioclase + quartz + biotite + K-felspar began crystallizing and produced a suite of rocks containing cumulus K-felspar. Rocks that formed by these two crystallization trends have distinctive trace element distributions which are statistically recognizable by means of cluster analysis.

It is envisaged, furthermore, that the Nelspruit Porphyritic Granite solidified from the margins inwards, and rocks that formed during the plagioclase + quartz + biotite fractionation, are likely to occupy areas that are peripheral to those that formed during plagioclase + quartz + biotite + K-felspar fractionation. Trend surface analyses over the study area suggest that the distribution of certain major (K_2O and Na_2O) and trace (Rb, Sr and Ba) elements are compatible with the suggested two-stage crystallization model. This model implies that the Nelspruit Porphyritic Granite is magmatic in character and that it cooled over a considerable period of time allowing the fractionation of successive mineral phases to take place.

(4) The distribution of mafic dykes and sills in the study area, and the presence of major, parallel, right-lateral shear zones, has regional tectonic implications concerning crustal movements and structure in this area. The concentration of dykes and sills in the Hazy View-Bushbuckridge area indicates the presence of an upwarped or antiformal portion of the crust, of east-west orientation. This feature may be related to the mega-fold interference pattern that occurs over the entire Kaapvaal Craton. The presence of parallel, right-lateral shear zones in the area is possibly indicative of the existence of a shear-stress in the region which may be a response to horizontal movements occuring in mobile belts on the margins of the Kaapvaal Craton.

FIGURE 61

A MODEL OF THE MAIN EVENTS THAT LED TO
THE FORMATION OF THE ARCHAEAN GRANITIC CRUST
BETWEEN NELSPRUIT AND BUSHBUCKRIDGE, EASTERN TRANSVAAL

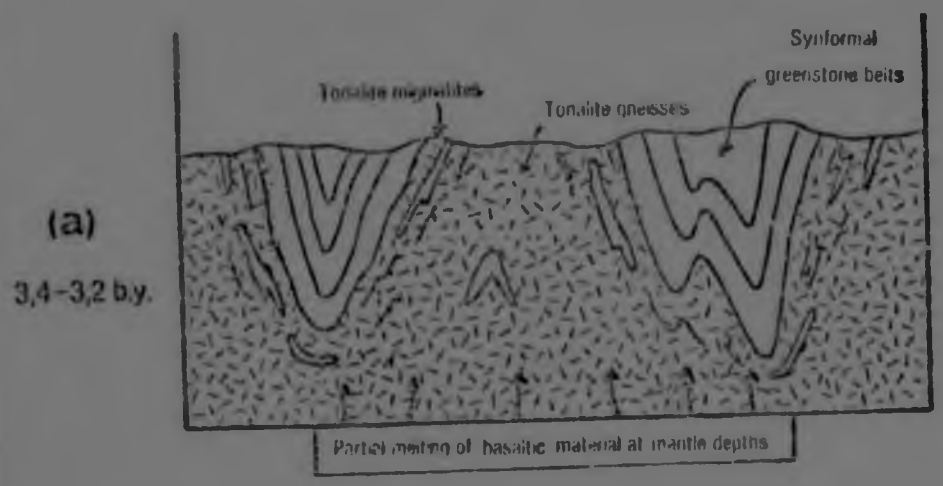

(5) In conclusion, the writer presents the following model (Figure 61) which attempts to summarize his views on the evolution of the granitic terrane between Nelspruit and Barnbuckridge, eastern Transvaal :-

(i) It is assumed, in this model, that the primordial crust was ensimatic in character in accordance with the views of Anhaeusser (1969, 1973a), Viljoen and Viljoen (1969a, 1969d) and Glikson (1976b). The remnants of this crust occur in the form of synformal greenstone belts or xenoliths, which have been intruded by various granitic phases during the subsequent development of the earth's sialic crust. The first granitic event of which there is record in the study area is believed to be represented by the Tonalite Gneisses and Migmatites, which now outcrop only in the immediate vicinity of the greenstone remnants. The tonalites are thought to have been diapirically intruded into pre-existing greenstone crust, structurally deforming the latter (Anhaeusser, 1972, 1975b). The resulting crust at this stage consisted of a suite of tonalite and trondhjemite gneisses, xenolithic greenstone remnants of varying sizes, and complex tonalitic migmatites. The migmatites developed where interaction between tonalites and greenstones took place. Classic exposures of this type of terrane occur southwest of the Barberton Mountain Land, in the Badplaas area (Figures 1 and 2). It is envisaged that this terrane reflects the likely nature of the crust in the study area approximately 3,4 - 3,2 b.y. ago (Figure 61a).

(ii) Approximately 3,2 b.y. ago the crust was intruded by a widespread potassic magma, which cooled very slowly, allowing fractionation to take place and resulting in a granite of variable composition. This magma was probably mantle derived by virtue of its low initial $^{87}Sr/^{86}Sr$ ratio. The intrusion of this granite body obliterated most of the pre-existing granitic crustal material with the exception of

its margins where potassic migmatites and gneisses now form remnants of the interaction between the invading magma and the pre-existing crust (Figure 61b). A second granodioritic intrusion (i.e. the Hebron Granodiorite), also apparently mantle derived by virtue of its low initial $^{87}Sr/^{86}Sr$ ratio, synchronously accompanied the widespread intrusive event responsible for the Nelspruit Porphyritic Granite (Figure 61b).

(iii) During the period between 2,8 and 2,6 b.y. ago further additions were made to the sialic crust in the study area (Figure 61c). These intrusions unlike the granites described earlier, were apparently unrelated to a mantle origin but were probably derived by re-working of crustal (possibly granitic) material. The first of these was the Cunning Moor Tonalite, which is the youngest tonalitic body in the Barberton region (emplaced approximately 2,8 b.y. ago). Subsequently the Mpageni Granite was intruded between 2,8 and 2,6 b.y. ago (De Gasparis, 1967; Oosthuyzen, 1970). This granite is considered to be the result of fractional crystallization of a granodioritic magma (Condie and Hunter, 1976).

The model described above has important implications regarding the origins of Archaean granites in general. It appears as though older granites (i.e. those greater than 3,2 b.y. old) such as the tonalite gneisses and migmatites, the Nelspruit Porphyritic Granite and the Hebron Granodiorite are mantle derivatives, formed as the result of partial melting and subsequent differentiation of mafic and ultramafic material characteristic of the mantle. However, younger Archaean granites, such as the Cunning Moor Tonalite and the Mpageni Granite appear to be derived from within the crust itself, as the result of partial melting and fractional crystallization of felsic material. The evidence from the

Nelspruit-Bushbuckridge granitic terrane, indicates that the formation of the earth's early granitic crust may have involved distinct processes resulting in granites whose ultimate origins and modes of formation may be quite unrelated, both in time and space.

* * * * * * * * * * *

LIST OF REFERENCES

Allsopp, H.L., Roberts, H.R., Schreiner, G.D.L., and Hunter, D.R. 1962. Rb-Sr age measurements on various Swaziland granites. J. geophys. Res., 67(13): 5307-5313.

Allsopp, H.L., Davies, R.D., De Gasparis, A.A.A., and Nicolaysen, L.O. 1969. Review of Rb-Sr age measurements from the early Precambrian terrain in the south-eastern Transvaal and Swaziland. Spec. Publ. geol. Soc. S.Afr., 2: 433-444.

Anhaeusser, C.R. 1969. The stratigraphy, structure and gold mineralization of the Jamestown and Sheba Hills areas of the Barberton Mountain Land. Unpub. Ph.D. thesis, Univ. Witwatersrand, Johannesburg. 332pp.

Anhaeusser, C.R. 1972. The geology of the Jamestown Hills area of the Barberton Mountain Land, South Africa. Trans. geol. Soc. S.Afr., 75 (3): 225-263.

Anhaeusser, C.R. 1973a. The evolution of the early Precambrian crust of southern Africa. Phil. Trans. R. Soc. Lond., A; 273; 359-388.

Anhaeusser, C.R. 1973b. The geology and geochemistry of the Archaean granites and gneisses of the Johannesburg-Pretoria dome. in : Lister, L.A. (ed.) : Symposium on Granites, Gneisses and related rocks. Spec. Publ. geol. Soc. S.Afr., 3: 361-385.

Anhaeusser, C.R. 1975a. The geological evolution of the primitive earth: evidence from the Barberton Mountain Land. Inform. Circ. econ. Geol. Res. Unit, Univ. Witwatersrand, Johannesburg. 98: 22pp.

Anhaeusser, C.R. 1975b. Precambrian tectonic environments. in. Donath, F.A. (ed.) : Ann. Rev. Earth Planet. Sci. Annual Reviews Inc., California, 3: 31-53.

Anhaeusser, C.R. 1976a. The nature of chrysotile asbestos occurrences in southern Africa : A review. Econ. Geol., 71(1) : 96-116.

Anhaeusser, C.R. 1976b. Geological and geochemical investigations of the Roodekrans ultramafic complex and surrounding Archaean volcanic rocks, Krugersdorp district. Inform. Circ. econ. Geol. Res. Unit, Univ. Witwatersrand, Johannesburg. 103 : 16pp.

Anhaeusser, C.R., Mason, R., Viljoen, M.J., and Viljoen, R.P. 1969. A reappraisal of some aspects of Precambrian shield geology. Bull. geol. Soc. Amer., 80:2175-2200.

Augustithis, S.S. 1973. "Atlas of the Textural Patterns of Granites, Gneisses and Associated Rock Types." Elsevier, New York: 378pp.

Barker, F., Friedman, I., Hunter, D.R., and Gleason, J.D. 1976. Oxygen isotopes of some trondhjemites, siliceous gneisses, and associated mafic rocks. Precambrian Res., 3:547-557.

Beach, A. and Fyfe, W.S. 1972. Fluid transport and shear zones at Scourie, Sutherland : Evidence of overthrusting? Contrib. Mineral. Petrol., 36:175-180.

Booth, B. 1968. Petrogenetic significance of alkali felspar megacrysts and their inclusions in Cornubian granites. Nature, 217:1036-1038.

Button, A. 1973. A regional study of the stratigraphy and development of the Transvaal Basin in the eastern and northeastern Transvaal. Unpub. Ph.D. thesis, Univ. Witwatersrand, Johannesburg. 352pp.

Condie, K.C. and Hunter, D.R. 1976. Trace element geochemistry of Archaean granitic rocks from the Barberton region, South Africa. Earth Planet. Sci. Lett., 29:389-400.

Currie, K.L. and Ferguson, J. 1970. The mechanism of intrusion of lamprophyre dykes indicated by "offsetting" of dykes. Tectonophy., 9: 525-535.

Davies, R.D. 1971. Geochronology and isotopic evolution of the early Precambrian crustal rocks in Swaziland. Unpub. Ph.D. thesis, Univ. Witwatersrand, Johannesburg.

Davis, J.C. 1973. "Statistics and Data Analysis in Geology." John Wiley and Sons, Inc., New York. 550pp.

De Gasparis, A.A.A. 19[illegible]. Rubidium-strontium studies relating to problems of geochronology on the Nelspruit and Mpageni granites. Unpub. M.Sc. thesis, Univ. Witwatersrand, Johannesburg.

De Waal, S.A. 1970. Nickel minerals from Barberton, South Africa: III. Willemseite, a nickel-rich talc. Amer. Miner., 55:31-42.

Dietrich, R.V. 1962. K-felspar structural states as petrogenetic indicators. Norsk geol. Tidssk., 42: 394-414.

Du Toit, A.L. 1926. "The Geology of South Africa." Oliver and Boyd, Edinburgh. 463pp.

Emeleus, C.H. 1963. Structural and petrographic observations on layered granites from southern Greenland. Mineral Soc. Amer., Spec. Paper, 1: 22-29.

Flanagan, F.J. 1969. U.S. Geological Survey standards - II. First compilation of data for the new U.S.G.S. rocks. Geochim. Cosmochim. Acta, 33:81-120.

Glikson, A.Y. 1976a. Trace element geochemistry and origin of early Precambrian id igneous series, Barberton Mountain Land, Trans . Geochim.Cosmochim. Acta, 40: 1261-1280.

Glikson, A.Y. 1976b. Archean to early Proterozoic shield elements : Relevance of plate tectonics. Geol. Assoc. Canada, Spec. Paper No. 14: 489-516.

Goldsmith, J.R. and Laves, F. 1954. The microcline-sanidine stability relations. Geochim. Cosmochim. Acta, 5 : 1-19.

Greenland, L.P. 1970. An equation for trace element distribution during magmat c crystallization. Amer. Miner., 55:455-465.

Grobler, N.J. 1972. The geology of the Pietersburg greenstone belt. Unpub. D. Sc. thesis, Univ. Orange Free State, Bloemfontein. 156pp.

Hall, A.L. 1912. The geology of the Murchison Range and district. Mem. geol. Surv. S.Afr., 6:185pp.

Hall, A.L. 1918. The geology of the Barberton gold mining district. Mem. geol. Surv. S. Afr., 9:347pp.

Harpum, J.R. 1963. Petrographic classification of granitic rocks in Tanganyika by partial chemical analyses. Rec. geol. Surv. Tanganyika, 10 : 80-88.

Heier, K.S. 1957. Phase relations of potash felspar in metamorphism. J. Geol.,65:468-480.

Heinrich, E.Wm. 1965. "Microscopic Identification of Minerals." McGraw-Hill Book Company, New York. 414pp.

Hunter, D.R. 1973a. The granitic rocks of the Precambrian in Swaziland. in : Lister, L.A. (ed.) : Symposium on Granites, Gneisses and Related Rocks. Spec. Publ. geol. Soc. S. Afr., 3 : 131-145.

Hunter, D.R. 1973b. Notes on some potassium feldspars in the Precambrian granitic rocks of Swaziland. Trans. geol. Soc. S. Afr.,76 (1) : 63-73.

Hunter, D.R. 1974. Crustal development in the Kaapvaal Craton, I. The Archaean. Precambrian Res., 1 : 259-294.

Hunter, D.R. 1975. The regional geological setting of the Bushveld Complex (An adjunct to the Provisional Tectonic Map of the Bushveld Complex). Wainwright, E.H. (ed.). Econ. Geol. Res. Unit, Univ. Witwatersrand, Johannesburg : 18pp.

Hurley, P.M., Pinson, W.H., Nagy, B., and Teska, T.M. 1972. Ancient age of the Middle Marker Horizon, Onverwacht Group, Swaziland Sequence, South Africa. Earth Planet. Sci. Lett., 14: 360-366.

Jahn, B. and Shih, C. 1974. On the age of the Onverwacht Group, Swaziland Sequence, South Africa. Geochim. Cosmochim. Acta , 38(6) : 873-885.

Kolbe, P. 1966. Geochemical investigations of the Cape Granite, southwest Cape Province, South Africa. Trans. geol. Soc. S. Afr., 69 : 161-199.

Lowman, P.D. 1965. Non-anatectic migmatites in Gilpin County, Colorado. Bull. geol. Soc. Am., 76 : 1061-1064.

McCarthy, T.S. and Hasty, R.A. 1976. Trace element distribution patterns with reference to the crystallization of granitic melts. Geochim. Cosmochim. Acta, 40 : 1351 - 1358.

Mehnert, K.R. 1968. "Migmatites and the Origin of Granitic Rocks." Elsevier, London. 393pp.

Minnitt, R.C.A. 1975. The geology of the eastern portion of the Murchison Range between the Quagga Camp area and the Kruger National Park. Unpub. M.Sc. thes s, Univ. Witwatersrand, Johannesburg. 171pp.

Newmann, H., Mead, J., and Vitaliano, C.J. 1954. Trace element variation during fractional crystallization as calculated from the distribution law. Geochim. Cosmochim. Acta, 6 : 90-99.

Nockolds, S.R. 1933. Some theoretical aspects of contamination in acid magmas. J. Geol., 41 : 561-589.

Oosthuyzen, E.J. 1970. The geochronology of a suite of rocks from the granitic terrain surrounding the Barberton Mountain Land. Unpub. Ph.D. thesis, Univ. Witwatersrand, Johannesburg.

Parslow, G.R. 1971. Variations in mineralogy and major elements in the Cairnsmore of Fleet granite, southwest Scotland. Lithos, 4 : 43-55.

Pretorius, D.A. 1974. The structural boundary between the Kaapvaal and Sonama crustal provinces. Inform. Circ. econ. Geol. Res. Unit, Univ. Witwatersrand, Johannesburg. 88 : 27pp.

Read, H.H. 1957. "The Granite Controversy." Thomas Murby and Co., London. 430pp.

San Miguel, A. 1969. The aplite-pegmatite association and its petrogenetic interpretation. Lithos, 2 : 25-37.

Shaw, D.M. 1976. Development of the early continental crust, Part 2. Prearchean, protoarchean and later eras. in Windley, B.F. (ed.) : "The Early History of the Earth." John Wiley and Sons, New York, pp.33-53.

Smith, T.E. 1974. The geochemistry of granitic rocks of Halifax County, Nova Scotia. Can. J. Earth Sci., 11 : 650-657.

Smith, T.E. 1975. Layered granitic rocks at Chebucto Head, Halifax County, Nova Scotia. Can. J. Earth Sci., 12 : 456-463.

Stone, M.and Austin, G.C. 1961. The metasomatic origin of the potash felspar megacrysts in the granites of southwest England. J. Geol., 69 : 464-472.

Stowe, C.W. 1971. Summary of the tectonic development of the Rhodesian Archaean craton. Spec. Publ. geol. Soc. Aust., 3 : 377-'83.

Taylor, W.P. 1976. Intrusion and differentiation of granitic magma at a high level in the crust: the Puscao pluton, Lima Province, Peru. J. Petrol., 17 : 194-219.

____ 1975. The Geodynamics Project in South Africa. Interim report on the South African National Programme presented to the Inter-Union Commission on Geodynamics.

Van Eeden, O.R. 1941. Die geologie van die Sheba rante en omstreke, Distrik Barberton. Unpub. D.Sc. thesis, Univ. Stellenbosch, Stellenbosch.

Van Eeden, O.R. and Marshall, C.G.A. 1965. The granitic rocks of the Barberton Mountain Land in the Transvaal. Unpub. Paper presented at the 8th Congr. geol. Soc. S. Afr., Johannesburg.

Van Niekerk, C.B. and Burger, A.J. 1969. A note on the minimum age of the acid lava of the Onverwacht Series of the Swaziland System. Trans. geol. Soc. S. Afr., 72 : 9-21.

Viljoen, M.J. 1963. The geology of the Lily syncline and portion of the Eureka syncline between the Consort Mine and Joe's Luck siding, Barberton Mountain Land. Unpub. M.Sc. thesis, Univ. Witwatersrand, Johannesburg. 131pp.

Viljoen, M.J. and Viljoen, R.P. 1969(a). The geology and geochemistry of the lower ultramafic unit of the Onverwacht Group and a proposed new class of igneous rocks. Spec. Publ. geol. Soc. S. Afr., 2: 55-85.

Viljoen, M.J. and Viljoen, R.P. 1969 (b). A proposed new classification of the granitic rocks of the Barberton region. Spec. Publ. geol. Soc. S. Afr., 2 : 153-180.

Viljoen, M.J. and Viljoen, R.P. 1969(c). The geochemical evolution of the granitic rocks of the Barberton region. Spec. Publ. geol. Soc. S. Afr., 2 : 189-219.

Viljoen, M.J. and Viljoen, R.P. 1969(d). A reappraisal of granite-greenstone terrains of shield areas based on the Barberton model. Spec. Publ. geol. Soc. S. Afr., 2 : 245-273.

Viljoen, M.J. and Viljoen, R.P. 1969(e). An introduction to the geology of the Barberton granite-greenstone terrain. Spec. Publ. geol. Soc. S. Afr., 2 : 9-28.

Viljoen, R.P. and Viljoen, M.J. 1969(f). The relationship between mafic and ultramafic magma derived from the upper mantle and the ore deposits of the Barberton region. Spec. Publ. geol. Soc. S.Afr., 2 :221-244.

Viljoen, R.P. and Viljoen, M.J. 1969(g).The geological and geochemical significance of the upper formations of the Onverwacht Group. Spec. Publ. geol. Soc. S. Afr., 2 :113-151.

Viljoen, R.P. and Viljoen, M.J. 1970. The geology and geochemistry of the layered ultramafic bodies of the Kaapmuiden area, Barberton Mountain Land. Spec. Publ. geol. Soc. S. Afr., 1 : 661-688.

Visser, D.J.L. (compiler). 1956. The geology of the Barberton area. (An explanation of the geological map of the Barberton area). Spec. Publ. geol. Surv. S. Afr., 15 : 253pp.

Visser, H.N. and Verwoerd, W.J. (compilers). 1960. The geology of the country north of Nelspruit. Expln. Sheet 22, Geol. Surv. S.Afr., 22 : 128pp.

Windley, B.F. 1973. Crustal development in the Precambrian. Phil. Trans. R. Soc. Lond., A.273 : 321-341.

Winkler, H.G.F. 1976. "Petrogenesis of Metamorphic Rocks." Springer-Verlag, New York. 320pp.

Winkler, H.G.F. and Von Platen, H. 1961. Experimentelle gesteinsmetamorphose - V. Geochim. Cosmochim. Acta , 24 : 250-259.

White, A.J.R. 1966. Genesis of migmatites from the Palmer region of South Australia. Chem. Geol., 1 : 165-200.

Whitten, E.H.T. 1961. Quantitative areal modal analysis of granitic complexes. Bull. geol. Soc. Amer., 72 : 1331 - 1360.

Whitmore, D.R.E., Berry, L.T., and Hawley, J.E. 1946. Chrome Micas. Amer. Miner., 31 : 1-21.

Wolhuter, L.E. 1973. Major and trace elements in the Opemisca Lake granite pluton, Quebec, Canada. Spec. Publ. geol. Soc. S.Afr.,3 : 387 - 410.

APPENDIX 1

ANALYTICAL PROCEDURES

1. INTRODUCTION

A total of 322 samples were analysed for the purposes of this dissertation. These analyses can be divided into two groups :-

(a) Full silicate analyses were carried out on 91 samples. These were carried out on the E.X.A.M. (Energy dispersive X-ray Analys of Minerals) unit of the Geological Survey in Pretoria and the results of these are listed in Tables 2 - 15 in the text.

(b) Partial analyses of 231 samples for K_2O, Na_2O, Rb, Sr and Ba were carried out on the Philips PW 1140/00/60 X-ray Spectrometer in the Department of Geology at the University of the Witwatersrand. Rb, Sr and Ba analyses were also obtained on this instrument for the 91 samples mentioned in section (a) above. The results of the partial analyses are presented in Tables 23-28 in Appendix 2.

2. SAMPLE PREPARATION

The crushing of all samples analysed was carried out by the sample preparation staff of the Geological Survey in Pretoria. These samples were crushed initially in a jaw-crusher and then pulverized to approximately -300 mesh using a Siebtechnik pulverizer. X-ray pellet making was carried out in two stages. The Geological Survey's E.X.A.M. unit required a metal-backed pressed pellet, and these were prepared at the Geological Survey in Pretoria. The partial analyses, carried out on the X-ray Spectrometer, required a standard

bakelite-boric acid pressed pellet and these were made in the Department of Geology at the University of the Witwatersrand.

3. ANALYTICAL PROCEDURE

(a) Full silicate analyses using the Geological Survey's E.X.A.M. unit

The E.X.A.M. unit, which operates on the principle of the energy dispersive analysis of X-rays, is a high-speed analytical technique which is advantageous if a large number of full silicate analyses are required. The instrument has the added advantage of requiring only a pressed powder pellet (and not a Norrish fusion disc such as is needed when using an X-ray Spectrometer), and hence sample preparation is greatly facilitated. Sample running time is very short (only 100 seconds for a full silicate analysis, in comparison to over half an hour on an X-ray Spectrometer) and results are printed out by means of an on-line computer-printer.

However, the nature of energy-dispersive analysis, short running times, variations in grain-size of the pellets, and even minor temperature fluctuations affect the accuracy and precision of results obtained by this technique. As a result consideration was given to the reliability of analyses obtained on the E.X.A.M. unit by running duplicate analyses on the X-ray Spectrometer (the technique of analysis by X-ray fluorescence is known to be more accurate than that of the energy-dispersive analysis of X-rays).

While calibrating the E.X.A.M. unit (using recognized international standards) it was noticed on the calibration curves that the lighter elements (noticeably Na, Mg and P) showed marked discrepancies relative to the heavier elements (i.e. Al, Si, K, Ca, Ti, Mn and Fe). A comparison of duplicated data (Table 21) shows that analyses of Na_2O and K_2O carried

TABLE 21

COMPARISON OF ANALYSES OF Na_2O AND K_2O CARRIED OUT ON THE GEOLOGICAL SURVEY'S E.X.A.M. UNIT, AND THE UNIVERSITY OF THE WITWATERSRAND'S X-RAY SPECTROMETER

ANALYSIS OF :-	NIM-G(%)	A23(i)(%)	A23(ii)(%)
Na_2O - Wits	3,60	4,62	3,67
Na_2O - Survey	3,45	4,07	3,12
K_2O - Wits	5,10	4,37	6,62
K_2O - Survey	4,95	3,84	6,52

TABLE 22

COMPARISON OF THE ACTUAL ELEMENT CONCENTRATIONS OF TWO GRANITE STANDARDS (NIM-G AND WITS-G), WITH FULL SILICATE ANALYSES OF THESE STANDARDS CARRIED OUT ON THE E.X.A.M. UNIT

	NIM-G(%)	NIM-G (E.X.A.M.)(%)	WITS-G(%)	WITS-G E.X.A.M.)(%)
SiO_2	75,59	74,61	75,34	75,46
TiO_2	0,09	0,04	0,30	0,32
Al_2O_3	12,08	11,53	11,98	10,96
Fe_2O_3	2,02	2,03	3,47	2,65
MnO	0,02	0,01	0,05	0,04
MgO	0,10	0,32	0,04	0,39
CaO	0,80	0,72	1,51	1,45
Na_2O	3,32	3,45	3,09	3,86
K_2O	4,98	4,98	4,46	4,35
P_2O_5	0,02	0,01	0,04	0,02
TOTALS	99,02	97,70	100,28	99,50

NIM-G - International granite standard
WITS-G - Local standard - Messina Granite.

out on the E.X.A.M. unit are consistently lower than those carried out on the X-ray Spectrometer. In this respect it is pertinent to note that the totals for the full silicate analyses on the E.X.A.M. unit are consistently less than 100% (by an average of approximately 2-3%). The generally low totals for the full silicate analyses obtained on the E.X.A.M. unit is indicated in Table 22, where actual element concentrations for two standards are compared with analyses of these standards carried out on the E.X.A.M. unit. This table shows a reasonable correlation between the actual values and those measured on the E.X.A.M. unit, except in the latter case where most of the element concentrations are somewhat low. For this reason it was decided to systematically increment (by approximately 2%) every element concentration obtained on the E.X.A.M. unit in order to make the totals of the full silicate analysis closer to 100%.

Finally, in all the full silicate analyses carried out on the E.X.A.M. unit, the total iron concentration is given as Fe_2O_3. In addition, the values of H_2O^+, H_2O^- and CO_2 were calculated in terms of loss on ignition (L.O.I.) by heating the sample powders to 1000^oC for five hours and determining the net mass loss.

(b) Partial analyses using the Philips X-ray Spectrometer in the Geology Department at the University of the Witwatersrand.

This instrument was used to determine all trace element concentrations (Rb, Sr and Ba) as well as the major element analyses of K_2O and Na_2O. The international standards used for calibration were G-2, GR, GK, GA, NIM-N and GSP-1, the relevant values for which were obtained from the published tables of Flanagan (1969). Standard blanks were used where no background correction factors were required. This applies to all the elements measured except Rb, Sr and Ba where background correction factors were considered. No

mass absorption corrections were made.

The concentration of K_2O was calculated by feeding the X-ray counts directly into a standard computer programme. All other concentrations (i.e. for Na_2O, Rb, Sr and Ba) were calculated by reading the concentrations directly off the relevant calibration curves. The accuracy and precision of the results is therefore dependent on that of the calibration curve and it was ensured, as a result, that the points on this curve exhibited as little scatter as possible.

APPENDIX 2

LISTS OF PARTIAL ANALYSES AND PETROLOGIC FUNCTIONS

This appendix presents the lists of partial analyses that were used, (i) in the determination of the contour and polynomial trend surfaces presented in Chapter 4, (ii) in the K_2O v Na_2O and Rb v Sr plots presented in Chapter 3 and, (iii) in determining the trace element distribution trends for the Nelspruit Porphyritic Granite, in Chapter 5. The sample localities can all be found on the Sample Locality map (Figure 11).

The partial analyses listed below were all carried out on the Philips X-ray Spectrometer in the Geology Department at the University of the Witwatersrand. Details of the analytical procedure are presented in Appendix 1.

The petrologic functions presented in Table 28 were calculated from full silicate analyses (Tables 5-15) using the standard CIPW NORM programme available for use on the IBM 370 computer, at the University of the Witwatersrand.

TABLE 23

TONALITE GNEISSES AND MIGMATITES

	%		ppm				
SAMPLE	K_2O	Na_2O	Rb	Sr	Ba	K_2O/Na_2O	K/Rb
A61A	5,91	3,93	306	87	30	1,51	193
A49	2,68	3,95	43	623	1097	0,68	623
A61	2,26	4,49	127	588	564	0,51	178
I2	1,80	5,29	64	781	279	0,34	281
I2A	4,42	4,19	126	319	177	1,03	351
I3	1,42	4,68	85	311	249	0,30	167
I3A	7,22	3,27	372	78	136	2,21	194
I8	4,45	4,24	147	299	433	1,03	298
I9	0,99	3,70	60	376	110	0,27	165
I10	5,17	3,38	339	130	313	1,52	152
I11	3,59	4,37	180	226	409	0,82	199
I12	4,16	3,29	139	115	430	1,27	299
O-MONT.	6,59	3,66	191	449	940	1,79	345

ANALYST : L.J. Robb

TABLE 24

NELSPRUIT MIGMATITE AND GNEISS TERRANE

	%		ppm				
SAMPLE	K_2O	Na_2O	Rb	Sr	Ba	K_2O/Na_2O	K/Rb
A19	4,28	3,93	165	181	335	1,09	259
A33	5,72	2,70	148	294	1139	2,12	386
A53	5,29	3,17	120	385	743	1,66	441
A31	3,68	4,03	104	350	594	0,91	354
A59	5,50	3,67	155	235	508	1,50	355
A47	3,40	4,29	28	207	383	0,79	1214
A63	3,66	4,43	79	537	665	0,83	463
A44	5,03	4,25	224	403	718	1,18	224
A57	2,88	4,73	78	415	954	0,61	369
A25	4,64	3,84	156	285	486	1,20	297
A12	3,76	4,12	56	405	507	0,91	671
A46	2,04	4,43	48	861	422	0,45	425
A24B(2)	6,41	3,15	184	216	512	2,04	348
A30	4,30	3,74	301	112	678	1,15	142
A48	4,80	3,78	100	615	1035	1,27	480
A32	2,21	4,52	85	274	211	0,49	260
A11	2,90	4,48	425	93	421	0,65	682
A36	2,23	5,79	92	450	281	0,39	242
A52	2,96	4,28	131	454	421	0,69	225
A34A	5,40	3,67	335	115	216	1,47	161
A40	3,95	4,36	94	454	540	0,90	420
A39	2,02	5,07	62	513	496	0,40	326
A51	3,69	4,26	57	653	1068	0,86	647
A6	3,92	4,67	146	291	601	0,84	268
A34	3,19	4,58	63	279	498	0,70	506
A58	3,28	4,04	62	535	794	0,31	529
A54	2,66	4,82	84	446	373	0,55	317
A37	3,07	4,78	57	356	562	0,64	538
A43A	5,40	4,06	123	274	656	1,34	444
A27	5,40	3,73	168	101	331	1,45	321
A23 (i)	4,37	4,62	156	571	952	0,95	280
A23(ii)	6,62	3,67	192	449	947	1,80	345

	%		ppm				
SAMPLE	K_2O	Na_2O	Rb	Sr	Ba	K_2O/Na_2O	K/Rb
B27	5,71	3,41	152	237	2850	1,68	376
B9	4,23	4,33	103	307	491	0,98	410
B1A	4,60	4,49	683	33	16	1,02	67
B16	5,75	3,46	136	227	759	1,66	423
B11	5,35	3,78	162	368	752	1,42	330
B25A	4,28	4,13	85	1014	1890	1,04	503
C12	5,93	3,81	126	634	1528	1,57	475
C47	5,01	3,99	118	710	1660	1,26	424
C35A	4,50	4,29	200	362	421	1,05	225
C21	5,04	3,98	121	293	824	1,27	416
C7	3,60	4,54	89	498	667	0,88	448
C12A	3,93	4,29	103	601	930	0,91	381
C36	4,78	4,30	176	368	584	1,11	271
D30	4,83	4,17	103	944	2020	1,15	469
D22	4,27	4,35	101	410	766	0,98	423
D23	4,32	4,27	68	396	898	1,01	635
E3	3,27	4,49	66	393	466	0,73	495
E12	3,81	4,28	71	460	697	0,89	537
E11	5,43	4,14	121	362	844	1,31	448
F3	2,89	4,83	61	392	424	0,60	473
F5	2,37	4,80	114	359	180	0,49	208
F2A	2,73	4,80	40	617	712	0,57	682
H2A	2,43	5,07	101	535	269	0,48	240
H11	1,89	4,54	23	489	563	0,42	821

Analyst : L.J. Robb

TABLE 25

NELSPRUIT PORPHYRITIC GRANITE

	%		ppm				
SAMPLE	K_2O	Na_2O	Rb	Sr	Ba	K_2O/Na_2O	K/Rb
A13	4,70	3,94	-	-	558	1,19	-
A3	5,43	3,71	213	426	1068	1,46	255
A12A	4,31	3,90	78	287	649	1,11	552
A41	4,55	5,20	108	400	798	0,87	421
A14	3,67	4,18	279	52	662	0,88	131
A8	2,90	4,48	88	469	614	0,65	330
A4	3,78	4,45	-	-	691	0,85	-
B14	4,66	3,67	133	455	813	1,27	350
B19	4,03	4,48	113	322	492	0,90	357
B15	4,94	4,25	177	295	514	1,16	280
B2	4,39	4,34	222	225	419	1,01	198
B24A	5,47	3,67	167	329	753	1,49	327
B22	5,33	4,05	223	223	494	1,32	241
B25	7,06	3,71	138	937	3374	1,90	511
B20	4,78	3,91	-	-	661	1,22	-
B17	5,58	3,57	133	501	944	1,56	419
B12	6,00	5,76	220	278	633	1,05	273
B18	2,80	4,60	49	486	511	0,62	571
B21	4,07	4,19	112	558	842	0,97	363
C24A	3,94	4,56	96	463	742	0,86	410
C5	3,78	4,75	80	472	567	0,80	474
C9	3,23	4,46	73	478	541	0,72	442
C20	2,17	4,83	62	602	398	0,45	350
C38	7,38	3,10	159	733	2195	2,37	464
C27	3,25	4,83	83	408	380	0,67	391
C46	3,09	4,86	97	511	689	0,64	318
C8	5,23	3,85	121	246	353	1,36	432
C40	3,76	4,54	100	541	765	0,83	376
C19	3,51	4,53	81	448	796	0,78	433
C31	4,70	4,06	145	573	1287	1,16	324
C42	4,57	4,46	140	699	985	1,02	326

	%		ppm				
SAMPLE	K_2O	Na_2O	Rb	Sr	Ba	K_2O/Na_2O	K/Rb
C2?R	4,12	4,40	100	471	743	0,94	412
C11	5,77	3,64	207	177	531	1,58	279
C28	3,06	4,67	86	508	648	0,66	356
C4A	3,14	4,48	87	536	508	0,70	361
C10	3,88	4,45	82	520	806	0,87	473
C34	4,02	4,06	101	530	897	0,99	398
C37	3,30	4,57	84	493	562	0,72	392
C1	5,53	3,90	166	879	1816	1,42	333
D18	2,99	4,64	49	547	796	0,65	610
D2	4,38	4,66	84	273	539	0,94	521
D3	3,21	4,55	97	528	673	0,71	331
D4	5,00	4,28	181	230	499	1,17	276
D11	4,83	4,10	156	599	1355	1,18	310
D14	4,76	4,43	181	386	915	1,08	263
D24	4,36	4,62	94	337	499	0,95	464
D17	4,30	4,24	86	426	913	1,02	500
D29	4,17	4,31	73	578	947	0,97	571
D32	6,40	3,90	204	215	466	1,64	314
D1	5,22	4,13	131	562	1179	1,26	398
D12	4,34	4,52	114	597	899	0,96	381
D19	4,50	4,10	76	381	753	1,10	592
D27	2,15	4,93	28	566	625	0,44	767
D21	3,76	4,28	102	769	960	0,88	368
D34	3,20	4,63	90	517	540	0,69	355
D7	4,18	3,97	119	404	627	1,05	351
D26	5,46	3,82	133	392	798	1,43	410
D9	6,22	3,72	161	481	1402	1,67	386
D25	4,81	4,07	125	461	991	1,18	385
D16	4,59	4,31	165	502	706	1,06	278
E6	2,49	4,64	37	207	559	0,54	672
E10	4,33	4,12	85	455	752	1,05	509
E14	5,74	3,63	91	473	1110	1,58	631
E13	3,73	3,90	66	580	1066	0,96	565
E22	5,07	4,06	91	465	1193	1,25	557

	%		ppm				
SAMPLE	K_2O	Na_2O	Rb	Sr	Ba	K_2O/Na_2O	K/Rb
E16	5,07	3,43	86	548	1348	1,48	589
E7	5,24	3,61	107	415	997	1,45	490
E15	1,54	5,39	23	514	348	0,29	669
E2	2,03	4,96	65	538	299	0,41	317
E24	4,04	3,77	99	386	762	1,07	408
E11A	3,09	4,63	67	654	854	0,67	461
E9	3,32	4,52	71	516	523	0,73	467
G7	5,76	3,44	203	386	946	1,67	284
G9	3,72	4,66	102	403	709	0,80	365
H1	2,61	4,88	62	456	512	0,53	421
H7	1,14	5,62	15	588	206	0,20	760
H2	4,87	3,92	117	492	1032	1,24	416
H12	3,77	4,06	106	509	663	9,81	356
H5	4,18	4,22	95	552	913	0,99	440
H13	1,65	5,26	47	416	419	0,31	351
H9	3,52	4,62	131	463	506	0,76	269

Analyst : L.J. Robb

TABLE 26

CUNNING MOOR TONALITE

	%		ppm				
SAMPLE	K_2O	Na_2O	Rb	Sr	Ba	K_2O/Na_2O	K/Rb
E17	1,96	4,92	51	423	134	0,40	384
E23	3,62	4,48	67	514	641	0,81	540
E22A	2,47	5,26	78	456	289	0,47	317
E5	2,53	4,46	57	497	1204	0,56	444
E19	2,34	5,04	45	441	381	0,46	520
E24A	2,39	5,34	58	481	484	0,45	412
E20	4,74	4,30	119	335	876	1,10	398
E21	3,02	4,68	75	468	725	0,64	403
E27	2,7	4,81	35	857	493	0,44	606
E26	1,41	4,79	36	475	218	0,30	391
F22	2,32	4,39	32	659	319	0,53	725
F16	2,36	4,64	51	474	330	0,51	462
F8A	2,89	4,64	52	486	810	0,60	556
F6	2,84	4,77	111	373	321	0,59	256
F19	3,56	4,13	66	546	737	0,86	539
F11	3,15	4,79	60	663	696	0,66	525
F18	1,66	4,92	55	604	260	0,34	302
F15	4,09	4,42	94	652	1362	0,92	435
F12A	3,06	4,56	54	568	608	0,67	567
F10	1,97	4,94	28	830	424	0,40	704
F16A	1,96	4,74	68	470	215	0,42	288
F4	4,40	4,27	110	480	698	1,03	400
F17	5,33	3,50	69	400	1582	1,52	792
F7	3,29	5,18	67	468	583	0,63	491
F7A	2,13	4,80	52	536	190	0,44	409
F5A	1,37	5,36	60	466	87	0,26	228
F2	2,22	4,99	38	659	395	0,44	584
F14A	2,02	4,69	34	596	536	0,43	594
G1	1,30	5,10	34	656	200	0,26	382
G11	3,36	4,30	106	464	708	0,78	317

	%		ppm				
SAMPLE	K_2O	Na_2O	Rb	Sr	Ba	K_2O/Na_2O	K/Rb
G5	3,54	3,96	100	315	677	0,89	354
G8	4,96	3,91	115	287	1137	1,27	431
G6	2,88	4,88	73	652	1198	0,59	394
G13	1,67	5,07	30	727	207	0,33	557
G4	2,94	4,86	119	518	534	0,60	247

Analyst : L.J. Robb

TABLE 27

HEBRON GRANODIORITE

	%		ppm				
SAMPLE	K_2O	Na_2O	Rb	Sr	Ba	K_2O/Na_2O	K/Rb
A1A	3,44	3,34	77	324	689	1,03	447
B13	5,46	3,79	136	821	1828	1,44	401
B10	4,79	4,36	193	126	224	1,09	248
B6	5,32	4,07	105	494	1541	1,31	507
B17B	4,85	3,98	106	738	1816	1,22	457
C49A	3,39	4,43	146	385	587	0,77	232
C44	4,00	4,67	119	400	640	0,86	336
C11A	4,83	3,88	92	319	1055	1,24	525
C21A	3,96	4,17	97	305	701	0,95	408
C34A	4,85	4,07	131	526	1123	1,19	370
C18	5,05	4,18	145	257	569	1,21	348
C14B	5,41	3,74	124	402	1199	1,44	436
C24	2,81	4,76	102	436	506	0,59	275
C32A	4,58	4,21	112	481	1296	1,09	409
C6	4,08	4,31	72	841	1522	0,95	567
C26	3,73	3,39	90	377	683	1,10	414
D7A	1,51	4,97	56	658	547	0,30	270
D2A	1,87	5,06	62	390	472	0,37	302
D21A	4,86	4,16	121	1130	2423	1,17	402
D4	4,52	4,40	130	318	866	1,03	348
D15	4,61	4,19	142	479	1387	1,10	325
D9A	6,13	3,52	150	359	1492	1,74	409
D34B	4,54	4,25	60	621	2034	1,07	757
E7A	5,97	3,48	114	398	1204	1,72	523
E3A	3,29	4,84	149	346	226	0,68	221
H8	3,03	4,47	119	406	381	0,68	255
H1A	2,01	4,86	58	490	175	0,41	347

Analyst : L.J. Robb

TABLE 28

PETROLOGIC FUNCTIONS (By Weight)

PEGMATITES AND APLITES	QTZ	AB	OR	FEO	MGO	ALK
A17	32,2	24,6	43,2	7,7	0,1	92,2
A28A	30,2	34,0	35,8	7,8	2,2	90,0
A38A	34,0	35,1	30,9	2,4	0,1	97,5
A31B	32,1	32,6	35,3	0,9	0,1	99,0
NELSPRUIT PORPHYRITIC GRANITE						
A16	28,4	43,8	27,8	12,1	9,3	78,6
B26	28,4	43,3	28,3	15,2	8,5	76,4
B1	26,9	49,0	24,1	19,1	19,7	61,1
B8	33,5	38,6	27,9	21,2	14,5	64,3
D28	32,7	35,6	31,7	5.2	7,2	87,6
B7	31,2	38,0	30,8	15,0	13,8	71,2
C39	34,4	39,7	25,9	9,3	6,6	84,1
E1	29,0	52,0	19,0	13,5	0,1	86,4
B28A	25,8	51,0	23,3	12,4	5,4	82,1
E4	23,3	58,8	17,8	12,5	1,5	86,0
C45	30,6	50,2	19,2	18,4	9,8	71,8
C22A	29,3	35,8	34,9	5,7	6,3	88,0
E8	38,1	50,6	11,3	15,5	10,2	74,3
H6	27,4	38,7	33,9	8,7	5,9	85,4
A3	22,9	37,8	39,3	15,4	9,9	74,7
B24A	23,7	41,9	34,5	19,6	7,3	73,1
C23B	40,7	29,9	29,4	10,3	11,6	78,1
NELSPRUIT MIGMATITE AND GNEISS TERRANE						
D28A	20,8	51,8	24,4	19,8	2,6	77,6
E4B	22,3	42,6	35,1	11,6	8,6	79,8
E8B	35,1	51,7	13,2	16,4	15,5	68,1
B28	29,8	41,3	28,9	7,3	11,1	81,6
C22	29,8	25,7	44,5	6,9	16,1	77,0
C35	33,6	35,0	31,4	13,4	9,7	76,9
A46	35,0	48,3	16,7	22,5	22,6	54,9

HEBRON GRANODIORITE	QTZ	AB	OR	FEO	MGO	ALK
C13	25,5	[illegible]	28,7	19,9	12,2	67,9
D25A	34,1	[illegible]	8,2	30,9	6,2	62,8
G2	22,1	[illegible]	26,2	12,0	23,0	65,0
C39A	36,0	41,0	23,0	10,3	9,5	80,2
C14	31,4	41,0	27,6	23,0	17,9	59,2
C49	34,1	38,6	27,3	10,3	22,7	67,0
C48	28,5	31,8	39,6	4,2	0,1	95,7
D10	21,3	49,3	29,4	18,6	23,8	57,7
CUNNING-MOOR TONALITE						
F12	35,6	56,5	7,8	20,3	0,1	79,6
F1	33.4	45,9	20,7	10,3	19,6	70,1
F8	26,3	61,6	12,2	15,9	15,0	69,1
F14	34,7	53,2	12,1	15,2	19,5	65,3
F21	25,2	59,1	15,7	11,5	4,8	83,7
F20	37,9	52,3	9,7	17,8	33,0	49,3
E25	20,5	55,4	24,1	8,3	15,7	75,9
E21A	29,3	40,1	24,6	10,6	15,2	74,1
G12	25,3	61,4	13,2	22,1	16,1	61,8
MAFIC XENOLITHS						
A33A	39,5	39,4	21,1	56,5	34,6	8,9
E4C	0,0	49,9	50,1	30,1	32,9	37,0
C28B	10,0	65,9	24,1	25,0	21,7	53,3
C22B	4,3	70,3	25,4	22,0	18,5	59,6
B25B	5,0	6,6	88,4	54,3	27,6	18,1
E26A	0,0	90,7	9,3	42,4	32,4	25,2
B16A	17,7	9,5	72,8	38,2	46,8	15,0

QTZ - Quartz
AB - Albite
OR - Orthoclase
ALK - Total alkalis

[Petrologic functions calculated with standard CIPW NORM programme]

FIG. 33

BUSHBUCKRIDGE

N

RUBIDIUM (Rb)

CONTOUR INTERVAL - 25 ppm

SCALE 1:150 000

0 KM 15

NELSPRUIT

FIG 32

BUSHBUCKRIDGE

N

SODIUM (Na_2O)

CONTOUR INTERVAL - 0,25 %

SCALE 1:150 000

0 KM 15

NEL SPRUIT

FIG. 31

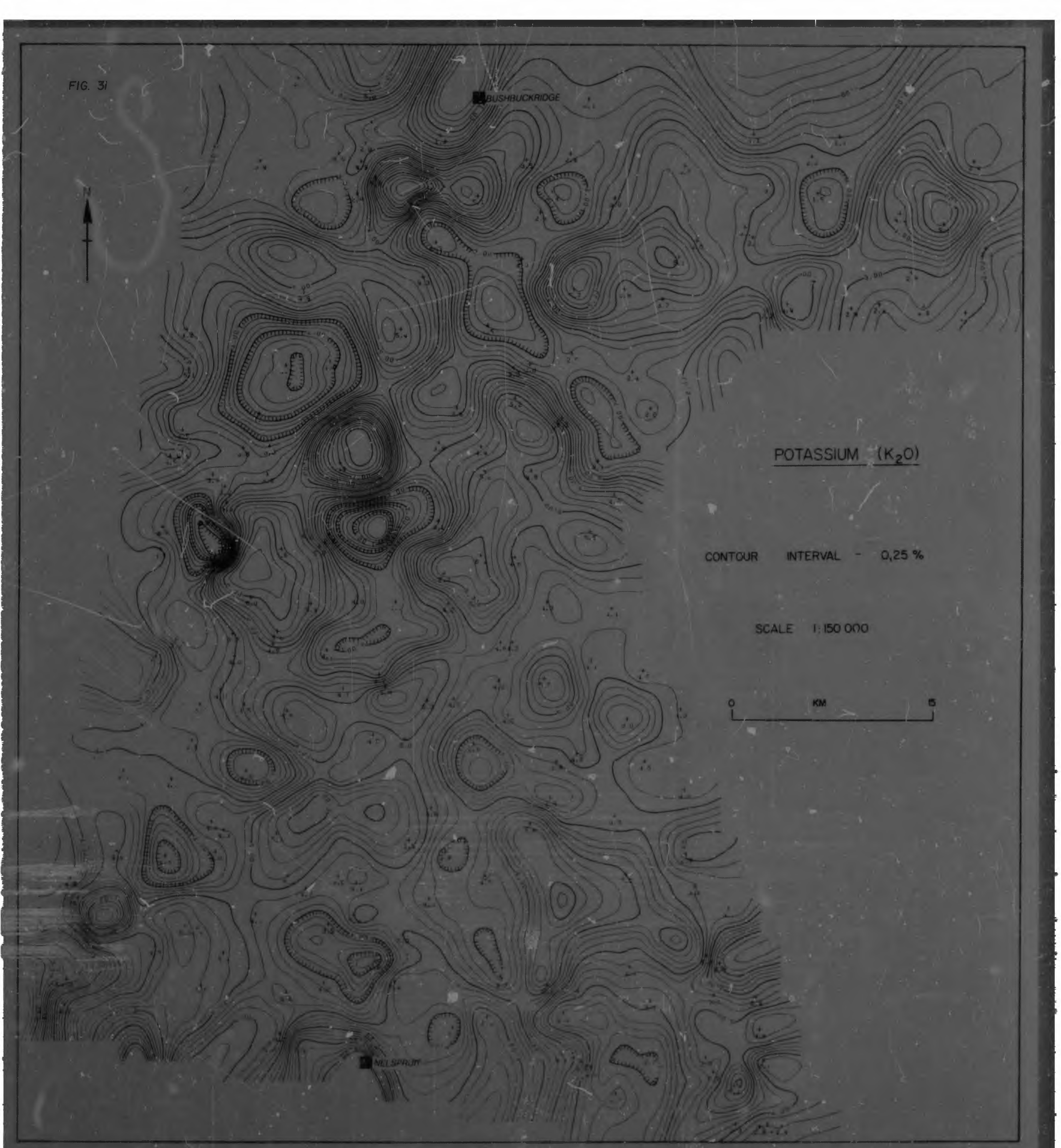

POTASSIUM (K_2O)

CONTOUR INTERVAL - 0,25 %

SCALE 1:150 000

0 KM 5

FIG. 30

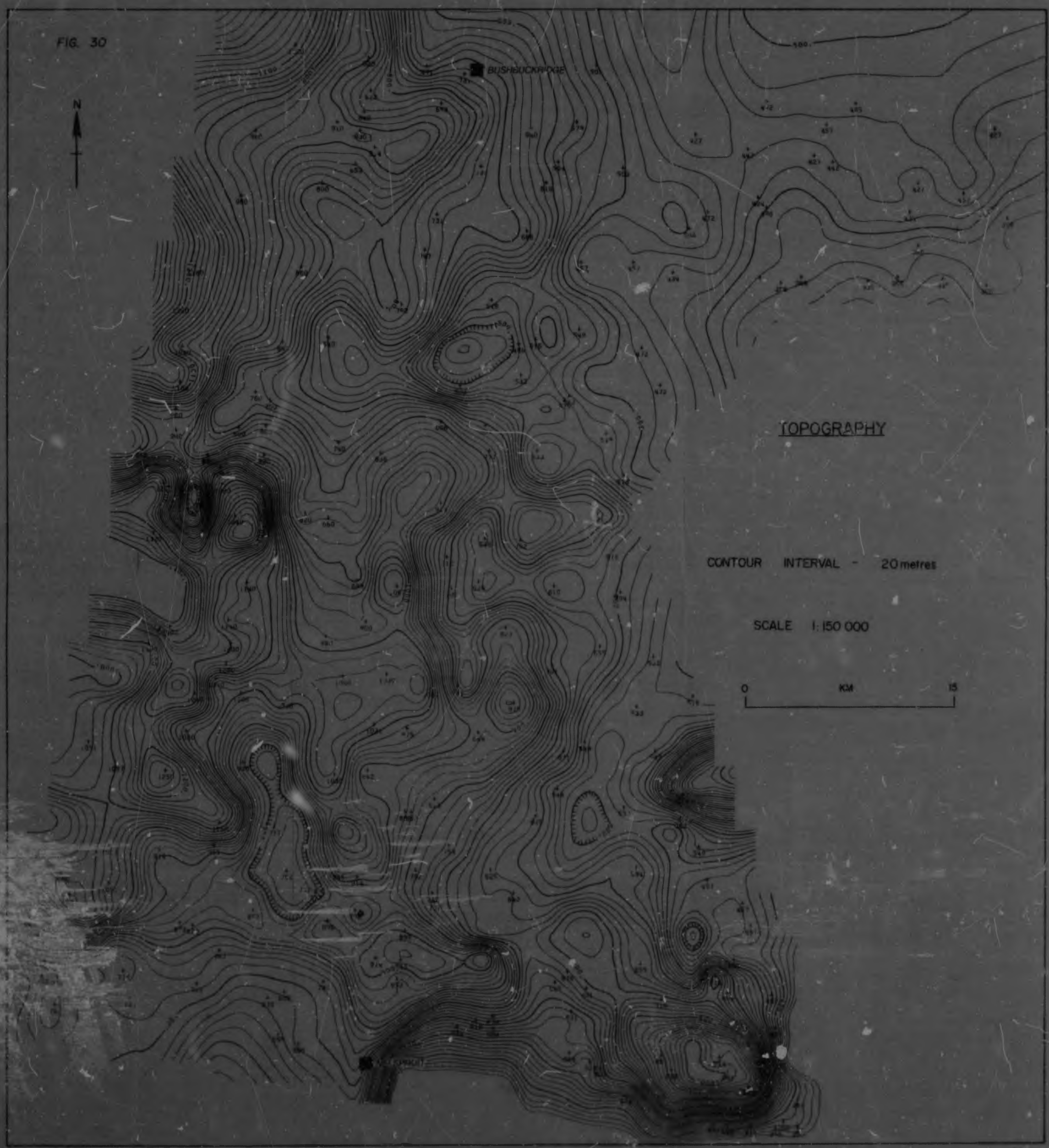

TOPOGRAPHY

CONTOUR INTERVAL - 20 metres

SCALE 1: 150 000

THE LOWVELD BETWEEN NELSPRUIT AND BUSHBUCKRIDGE

SCALE 1:150 000

FIG. 11

SAMPLE LOCALITIES

L.J. ROSS 1976

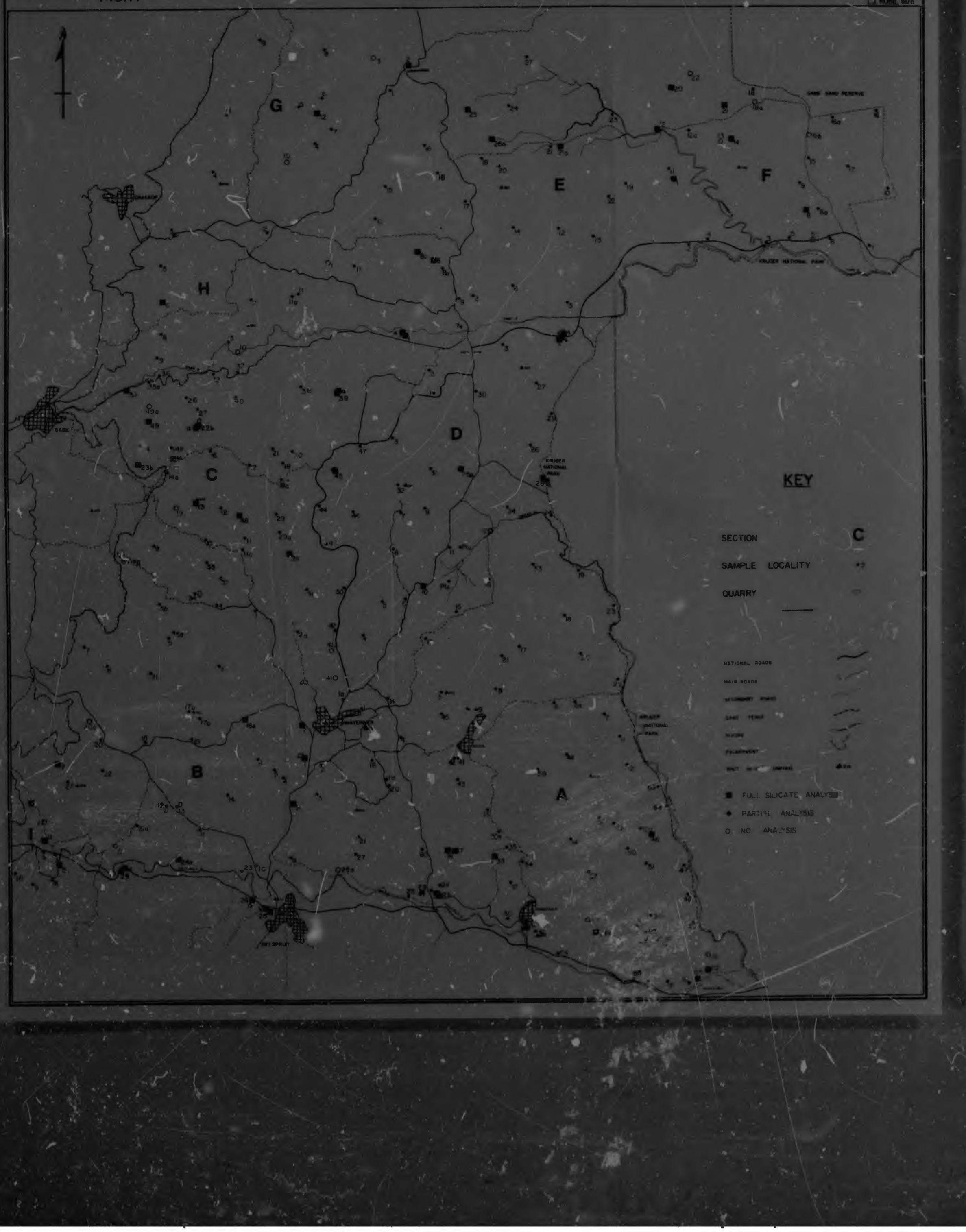

THE LOWVELD BETWEEN NELSPRUIT AND BUSHBUCKRIDGE

SCALE 1:150 000

FIG. 11

SAMPLE LOCALITIES

L.J. ROBB 1971

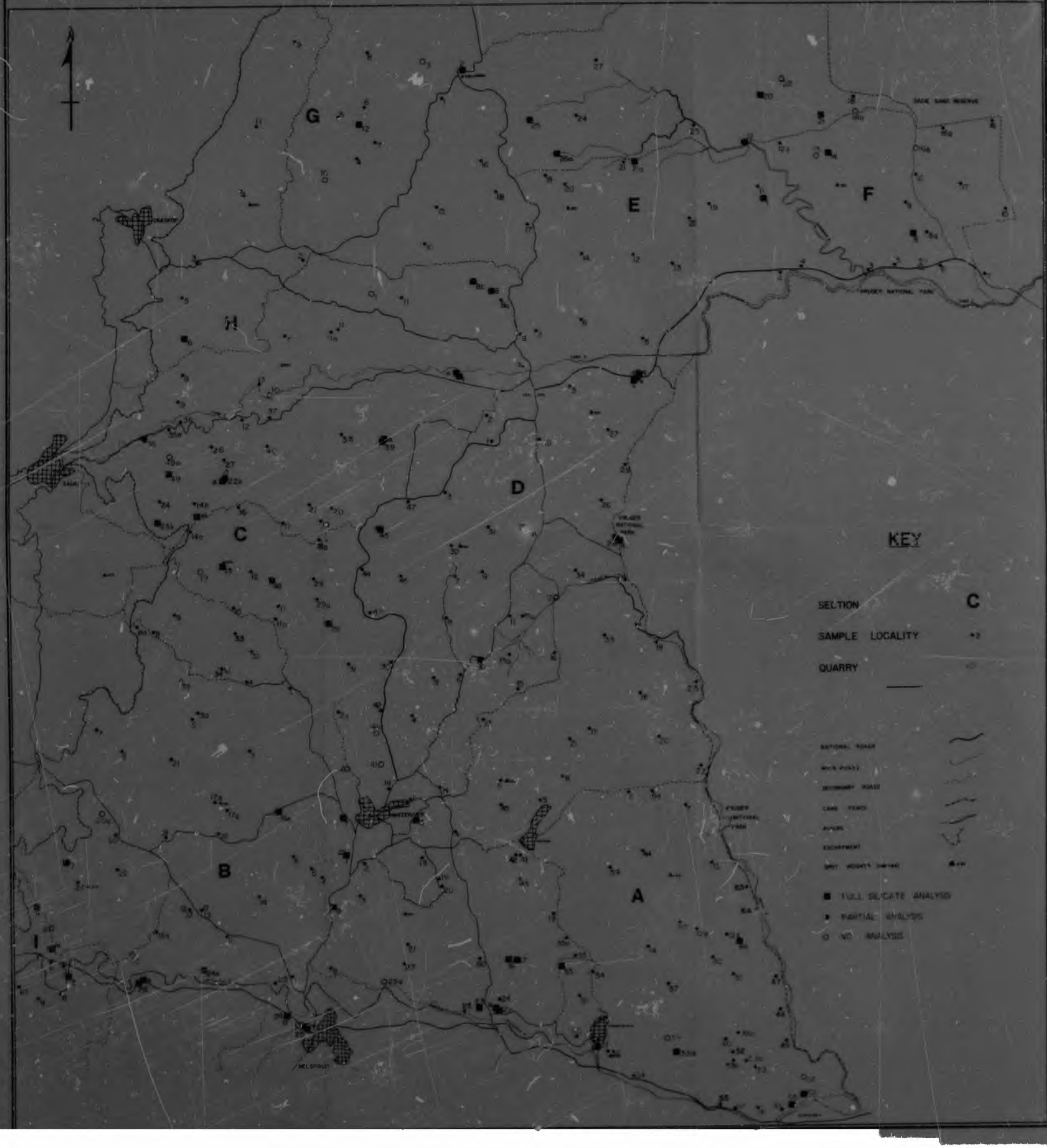

THE LOWVELD BETWEEN NELSPRUIT AND BUSHBUCKRIDGE

SCALE 1:150 000

FIG. 10

GRANITE TYPES AND TEXTURES

FIGURE 4

THE GEOLOGY OF A PORTION OF THE BARCLAY VALE SCHIST BELT ON THE FARM RICHMOND

SCALE

0 100 200 300 m.

[illegible] AUGUST 1976

KEY

Younger Cover

Dune (Blue Reef Quartzite boulders)

Intrusives

Mafic Dykes (undifferentiated)

Quartz vein

Archaean granite

Mylonitized porphyritic granite

Swartland Supergroup

Banded quartz-biotite-hornblende rock (the "contact amphibolite"

Massive amphibolite

Pyroxenite (now highly altered to tremolite)

Chlorite schist

Talc-chlorite schist

Serpentinite (sometimes a "cold-flowing" in places)

Sericite-kaolin schist

Tremolite-actinolite schist

Mafic rock with large chloritoid nodules

Fine-grained biotite schist (Tremolite-bearing)

Serpentinite (possibly originally a dunite)

Banded iron formation

Abandoned adit

Old gold mine working

Sample chemically analysed

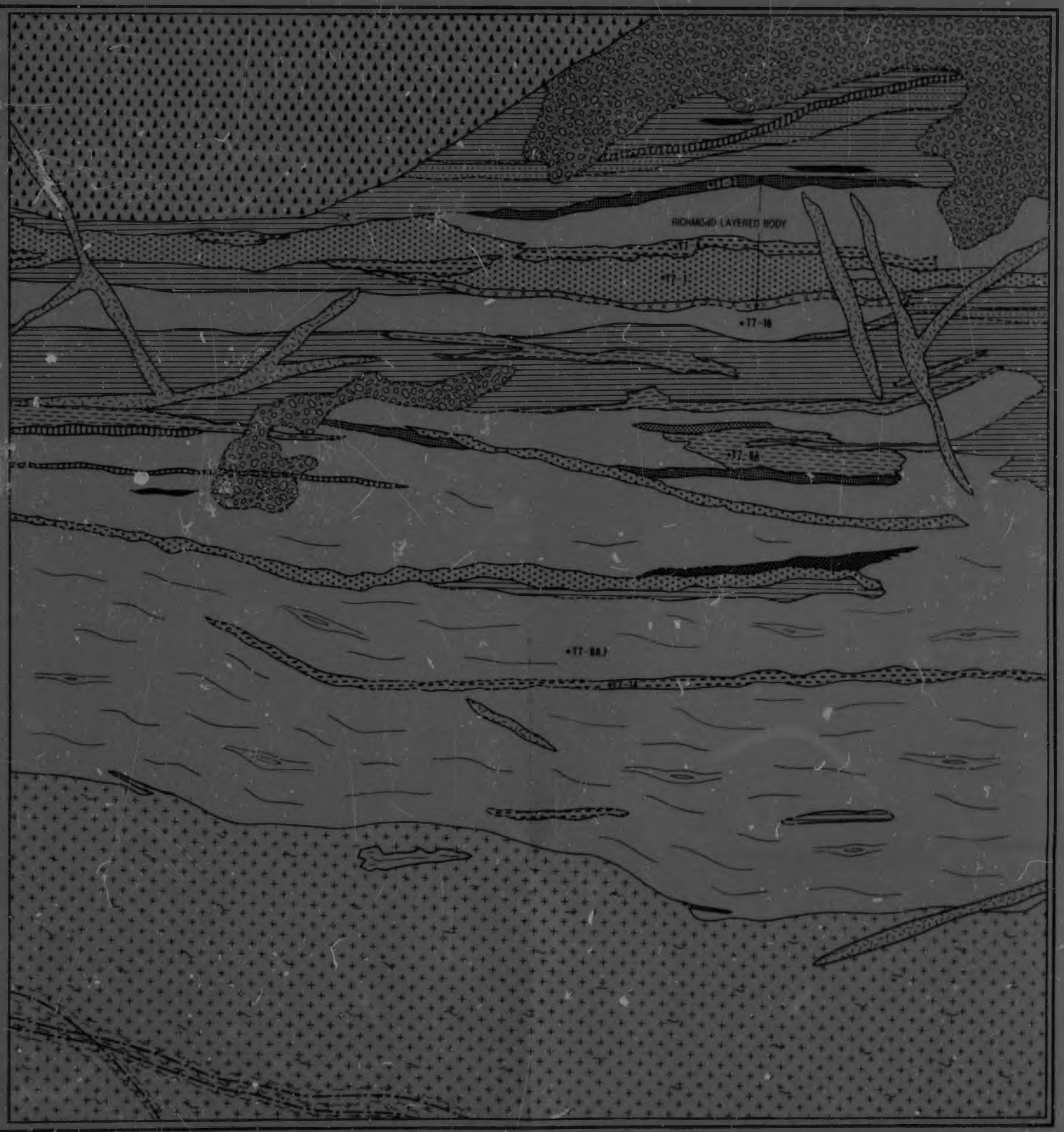

FIGURE 3

THE GEOLOGY OF THE BARCLAY VALE SCHIST BELT, EASTERN TRANSVAAL

J. RICHE AUGUST 1974

SCALE

1 0 1 kms 2

TRANSVAAL DRAKENSBURG ESCARPMENT

25°24'S

KEY

RECENT DEPOSITS

Alluvium

Transvaal Supergroup (Quartzites, conglomerates)

Scree (Black Reef Quartzite)

INTRUSIVES

Mafic dykes (Undifferentiated)

Quartz veins

ARCHAEAN GRANITE

Tonalitic gneisses, migmatites, xenomorphic granite

SWAZILAND SUPERGROUP

Serpentinite (often asbestiform)

Pyroxenite (now largely altered to hornblite)

Banded iron formation, banded cherts, banded chert

Chlorite and talc chlorite schists (in certain cases pillow structures may be preserved)

Massive and banded amphibolites

Talc tremolite schist

Pillow structures

Mylonite shears

Roads

Rivers

Peak or hill

Sample (chemically analysed)

Old gold prospect

Strike and dip of foliation or schistosity

THE LOWVELD BETWEEN NELSPRUIT AND BUSHBUCKRIDGE

SCALE 1:150 000

FIG. 60

MAFIC INTRUSIVES AND SHEAR ZONES

L.J. ROSS, 1976

KEY

SHEAR ZONES

BASIC DYKES (undifferentiated)

BASIC SILLS (" ")

QUARTZ-FELSPAR PORPHYRY DYKES

GRANITES] - ARCHAEAN

GREENSTONE REMNANTS]

THERMAL SPRINGS

VERDITE OCCURRENCES

Au RIETFONTEIN GOLD MINE

THE LOWVELD BETWEEN NELSPRUIT AND BUSHBUCKRIDGE

SCALE 1:250 000

FIG. 60

MAFIC INTRUSIVES AND SHEAR ZONES

L.J. ROBB, 1976

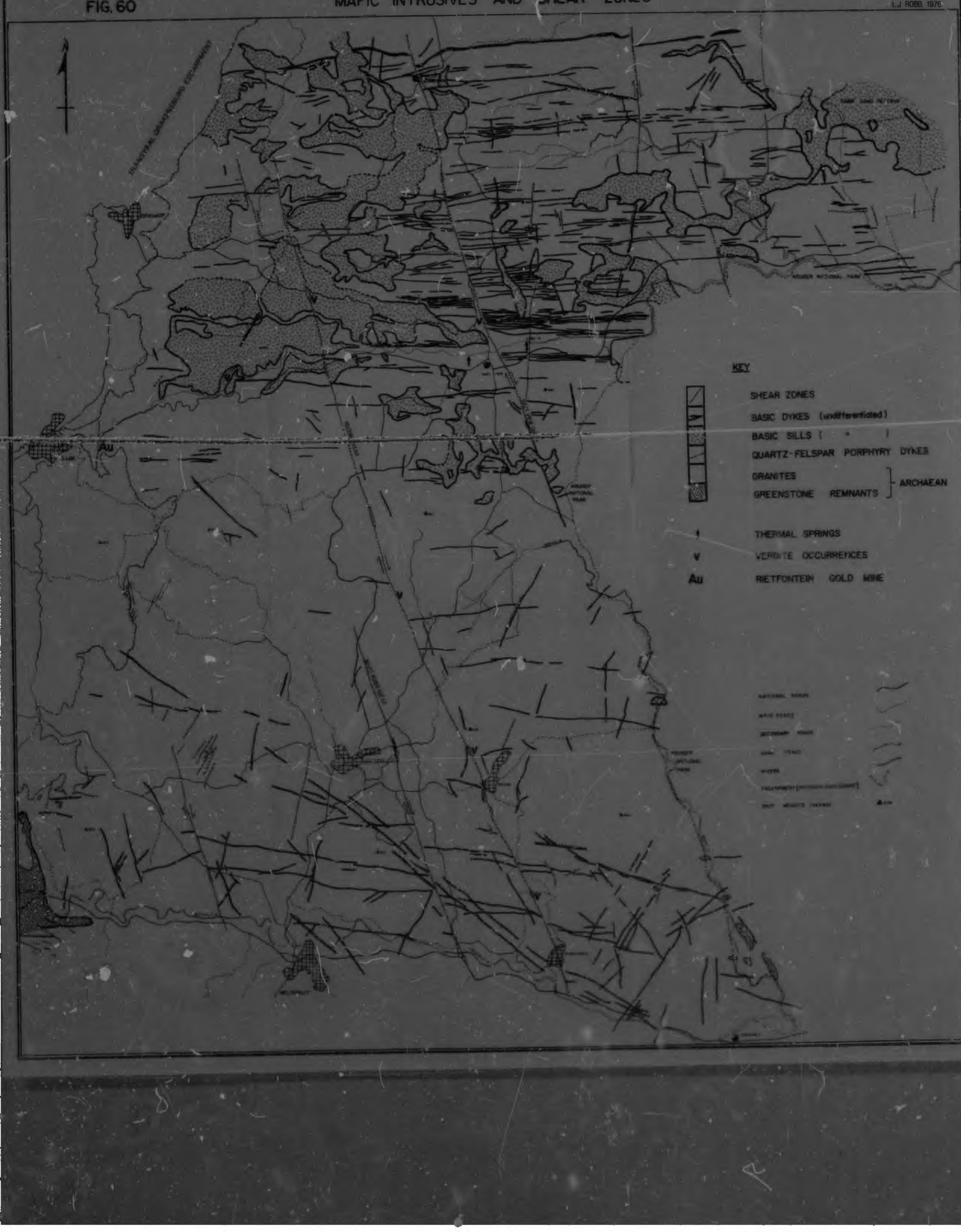

FIG. 35

BUSHBUCKRIDGE

N

BARIUM (Ba)

CONTOUR INTERVAL - 100 ppm

SCALE 1:150 000

0 KM 15

NELSPRUIT

FIG. 35

BUSHBUCKRIDGE

N

BARIUM (Ba)

CONTOUR INTERVAL - 100 ppm

SCALE 1:150 000

0 KM 15

NELSPRUIT

FIG 35

BUSHBUCKRIDGE
N
BARIUM (Ba)
CONTOUR INTERVAL - 100 ppm
SCALE 1:500 000
0
KM
15
NELSPRUIT

FIG. 34

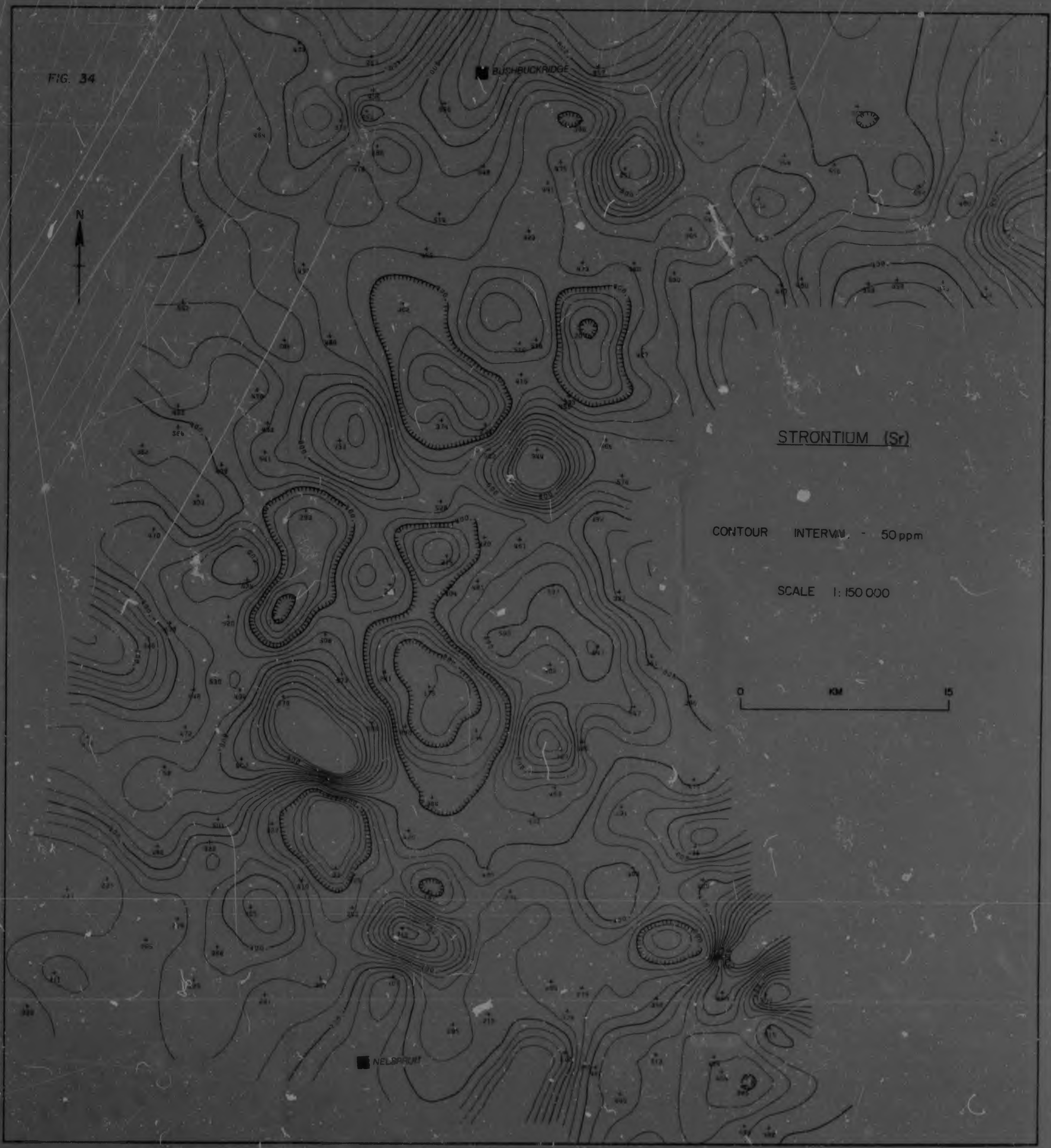

STRONTIUM (Sr)

CONTOUR INTERVAL - 50 ppm

SCALE 1: 150 000

0 KM 15

FIG. 33

BUSHBUCKRIDGE

N

RUBIDIUM (Rb)

CONTOUR INTERVAL - 25 ppm

SCALE 1:150 000

0 KM 15

NELSPRUIT